University College London

Department of Mathematics

PhD Thesis

Dynamical Systems in Dark Energy Models

Author:
Nicola Tamanini

Supervisor:
Christian G. Böhmer

Thesis submitted in fulfilment of the requirements for the degree of PhD in Applied Mathematics

October 16, 2014

I, Nicola Tamanini, confirm that the work presented in this thesis, titled "Dynamical Systems in Dark Energy Models", is my own. Where information has been derived from other sources, I confirm that this has been indicated in the thesis.

Signed: _____

Date: _____

Abstract

This PhD thesis is devoted to the study of dynamical systems appearing in theoretical models of dark energy. The quest for understanding the origin of the observed cosmic acceleration has led physicists to advance a large number of phenomenological explanations based on different fundamental theories. The best approach to analyse the background cosmological implications of all these models consists in employing dynamical systems techniques. In this thesis, after reviewing elements of dynamical systems theory and basic cosmology, several dynamical systems, which arise in dark energy models ranging from scalar fields to modified gravity, will be studied using both analytical and numerical methods. The work is organised in order to present as many details as possible for the simpler and well known models, while outlining major results and referring to the literature for the less studied ones. This choice aims at providing the reader with a complete overview and summary of dynamical systems in dark energy applications.

Contents

Preface

A PhD thesis is usually conceived as a summary and discussion of the results obtained by the student during the whole of her/his PhD journey. This PhD thesis is something a little bit different.

First of all, it is definitely not a summary of what I have achieved from the work undertaken in my PhD years. During such time I mainly studied alternative theories of gravity, focusing on mathematical and theoretical issues with very few applications of dynamical systems. I dealt with different modified gravity theories, including (extensions of) $f(R)$ gravity, $f(T)$ gravity, multi-metric gravity and others, and I have been part of a few international collaborations which produced some interesting results on these topics. I also worked on variational principles for general relativity and generalised theories of elasticity. A list of the papers I published as a PhD student can be found at the end of this preface.

From that list it is clear that no focus on dynamical systems has ever emerged during my PhD years. There are only two papers where dynamical systems applications appear, and only in one of them they constitute the main method of analysis. These two papers are given in Appendices A and B as examples from my original work where dynamical systems techniques have been employed. They however do not represent the results upon which the present work is based.

This thesis is a mixture of collected results and original calculations about dynamical systems applications to dark energy models. It is both a review and an introduction to the subject and it has been written in order to be understandable by both mathematicians and physicists. The thesis is the outcome of the last four months of my PhD time and the idea for it has been obtained from the last research work I completed; see Appendix A.

The reader may wonder why I decided to write a PhD thesis on dynamical systems applications to dark energy instead of discussing what I have obtained during my PhD. Surely, just collecting the published papers, I had enough material to write more than one PhD thesis on alternative theories of gravity, though on considerably different topics and theories. This is a question I made to myself quite a few times during these last months. I have spent a considerable amount of time and will to produce this work, when a thesis on modified theories of gravity would probably have taken me half

the time and no will at all. So why did I do it?

I think it is in my nature to prefer studying new topics and working on new problems rather than simply discussing the obtained results. I chose to write on dynamical systems applications to dark energy models mainly to expand my own knowledge, but also for whoever will be brave enough to read the outcome. Writing this thesis gave me the opportunity to learn interesting issues not only regarding dynamical systems but also about dark energy and cosmology in general. Though one of the aims of the thesis is to provide an extensive review on the designed subject and thus to be useful to the interested reader, I will certainly adopt what I gained from this experience in my future research activity.

One of the reason thus was to write something useful to both myself and the scientific community. The thesis in fact is conceived both as a review and as a work connecting mathematicians and physicists. This was a quite ambitious idea, but I like challenges and I think the present thesis well meets the desired requirements to engage readers possessing either a mathematics or physics background.

Another reason is that I wanted to write something somehow directly connected to the current progress in cosmology. Since from future astronomical observations we will hopefully obtain new insights on the nature of dark energy, I though it was useful, to both myself and the scientific community, to have a review and well explained introduction on the evolution of dark energy models analysed with dynamical systems techniques. I will use the present thesis as a references in the future, and hope other people will do the same.

Having said all this, in the end there is only one reason that really counts: the truth is that, no matter the effort, I had fun in writing this thesis. I hope the reader will enjoy the reading as I enjoyed the writing.

Acknowledgments

It is a pleasure to thank all the persons who helped me during my PhD, on whatever level they might have contributed.

In particular I owe my gratitude to my PhD supervisor Christian Böhmer who let my creativity run free during these years. His kindness and easygoing attitude allowed me to treat him more like a friend than a supervisor, though whenever needed he was always there to give experienced advices. He taught me to give always a chance to crazy ideas.

Remaining on an academical footing, I need to thank also my international collaborators whose work and expertise have been indispensable in obtaining the research results highlighted by the list of publication below. In alphabetic order they are Tomi Koivisto (Nordita), Emmanuel Saridakis (University of Athens) and Francisco Lobo (University of Lisbon).

On a different level I would like to thank all my PhD colleagues, in particular Nyein Chan, Atifah Mussa and Matthew Wright, for all the academical and non-academical discussions. I also thank all my friends in London, in particular Gianni Cara who made me play football almost every week, and all my friends in Italy, who would have made me drink beer almost every day. PhD life is already hard if you have friends, I cannot imagine how it would be without them.

I would like to express my immense gratitude to my family who supported me not only during the PhD years, but ever after since I was born. I cannot imagine better family than the one I have.

Finally my infinite love goes to Valeria who is walking the path of life with me. As ever for all the experiences we shared and for all the ones still waiting us.

Nicola Tamanini
30th of June, 2014

List of papers published during my PhD

- C. G. Böhmer, A. Mussa and N. Tamanini,
  Existence of relativistic stars in $f(T)$ gravity,
  Class. Quant. Grav. **28** (2011) 245020 [arXiv:1107.4455 [gr-qc]].

- N. Tamanini and C. G. Böhmer,
  Good and bad tetrads in $f(T)$ gravity,
  Phys. Rev. D **86** (2012) 044009 [arXiv:1204.4593 [gr-qc]].

- N. Tamanini,
  Variational approach to gravitational theories with two independent connections,
  Phys. Rev. D **86** (2012) 024004 [arXiv:1205.2511 [gr-qc]].

- C. G. Böhmer and N. Tamanini,
  A New Approach to Modifying Theories of Gravity,
  Found. Phys. **43** (2013) 1478 [arXiv:1301.5471 [gr-qc]].

- N. Tamanini and C. G. Böhmer,
  Generalized hybrid metric-Palatini gravity,
  Phys. Rev. D **87** (2013) 8, 084031 [arXiv:1302.2355 [gr-qc]].

- T. S. Koivisto and N. Tamanini,
  Ghosts in pure and hybrid formalisms of gravity theories: A unified analysis,
  Phys. Rev. D **87** (2013) 10, 104030 [arXiv:1304.3607 [gr-qc]].

- C. G. Böhmer, F. S. N. Lobo and N. Tamanini,
  Einstein static Universe in hybrid metric-Palatini gravity,
  Phys. Rev. D **88** (2013) 10, 104019 [arXiv:1305.0025 [gr-qc]].

- N. Tamanini and T. S. Koivisto,
  Consistency of nonminimally coupled $f(R)$ gravity,
  Phys. Rev. D **88** (2013) 6, 064052 [arXiv:1308.3401 [gr-qc]].

- C. G. Böhmer and N. Tamanini,
  Rotational elasticity and coupling to linear elasticity,
  Mathematics and Mechanics of Solids (2013),
  DOI: 10.1177/1081286513511093 [arXiv:1008.4005 [math-ph]].

- N. Tamanini, E. N. Saridakis and T. S. Koivisto,
  The Cosmology of Interacting Spin-2 Fields,
  JCAP **1402**, 015 (2014) [arXiv:1307.5984 [hep-th]].

- N. Tamanini,
  Dynamics of cosmological scalar fields,
  Phys. Rev. D **89** (2014) 083521 [arXiv:1401.6339 [gr-qc]].

Chapter 1

Introduction

This thesis is devoted to the study of dynamical systems applications to dark energy. In the next chapters we will define the meanings of both dynamical system and dark energy, but in order to introduce the reader to these concepts we will now provide a brief overview of what will be discussed.

1.1 Dynamical systems and cosmology

The theory of dynamical systems is a mathematical tool extremely useful to analyse special systems of first order differential equations whenever an analytical solution cannot be obtained in full generality. Its applications can be found in almost all scientific disciplines where dynamical equations must be investigated, but we will focus on physical applications only, in particular regarding cosmology. As we will see in Chapter 2, if the equations of motion of a physical system can be rewritten as a system of first order differential equations with some defined properties, then the dynamical systems machinery will determine the qualitative evolution for all possible initial conditions. This implies that instead of obtaining quantitative solutions needed to predict accurate experimental results, we will deal with qualitative analyses and global properties of the space of solutions.

The dynamical systems theory is in fact a geometrical approach which aims at describing the evolution of the system under consideration in a given geometrical space, rather than to determine analytical expressions for the solutions. It is also a powerful method when complemented by numerical computations since trajectories in the geometrical space can easily been drawn and the qualitative evolution of a physical system can sometimes be completely understood looking at just one picture.

As we mentioned above, we will deal with dynamical systems applications to cosmology and in particular to dark energy. Dark energy is a cosmological entity introduced to drive the observed accelerated expansion of the universe, which by now has been well confirmed by astronomical

data[1]. In Chapter 3 we will introduce and explain, in a rather physical and mathematical way, what we mean with "expanding universe", but for now the reader should keep in mind that the universe is a dynamically evolving quantity which can contract or expand according to some set of equations of motion. Mathematically speaking dark energy is nothing but a term in these equations of motion which implies an accelerated expansion for the universe at late times, i.e. at relatively recent cosmological times (last few billions of years).

In this thesis we will not focus on the theoretical and philosophical motivations of dark energy, but we will rather concentrate on the dynamics given by different dark energy models. Under a dynamical point of view a model of dark energy is nothing but some mechanism, derived by fundamental principles, needed to accelerate the late time expansion of the universe. Of course from a phenomenological perspective all the measured data collected by astronomical observations should be explained by any dark energy model aiming at describing our physical universe. However, as we will see through this thesis, to date there is not a model of dark energy capable of satisfying all the experimental and theoretical requirements.

But why are we focusing only on dynamical systems applications to dark energy, instead of widen the analysis to all possible cosmological or gravitational applications?

First of all it is a question of space. As the reader will notice, and probably dislike, this thesis is already quite extended only dealing with the dark energy issue. If all the cosmological applications treated with dynamical systems techniques, in particular early universe ones, were included, then this thesis would have resulted in double the size, if not more.

We have chosen to focus on dark energy mainly for two reasons. On the one hand dark energy is an important subject nowadays with forthcoming astronomical observations capable of providing more and more information on its nature. It is of great interest thus to write some sort of review on the dynamical properties of dark energy models which can be used by both theoretical physicists and mathematicians. This is indeed one of the scopes of this thesis which we will try to achieve.

On the other hand dynamical systems applications to cosmology in a broad sense have already been collected in two well known books written by Wainwright & Ellis (1997) and Coley (2003). The approach and the choices of arguments in those books are however more mathematical than the one presented in this thesis, which can be collocated in the half way between mathematics and physics, with mathematical methods employed to study only the phenomenologically relevant issues. Moreover in the books by

[1]The 2011 Nobel Prize in physics has been awarded to S. Perlmutter, B. P. Schmitd and A. G. Riess "for the discovery of the accelerating expansion of the Universe through observations of distant supernovae".

Wainwright & Ellis (1997) and Coley (2003) there is no focus on dark energy, since they collect dynamical systems results in cosmology mainly developed before the discovery of the acceleration of the universe in 1998. They also assume general relativity as the only fundamental description of gravity and thus do not treat all possible alternative theories which nowadays are extensively considered to build dark energy models. In this thesis Chapter 6 is completely dedicated to alternative theories of gravity motivated by both phenomenological ideas as well as high energy and quantum physics.

In other words the motivations for writing this thesis are to provide an overview on dynamical systems applications to cosmology which have not been reviewed nowhere else[2].

1.2 Outline and objectives

As we mentioned above one of the aims of this thesis is to provide a review on dynamical systems applications to dark energy models. An effort has been made in order to include as much literature as possible in order to refer to all the works employing dynamical systems techniques in late time cosmology. The simplest and most promising models will be analysed in detail, while for more complex models only brief discussions and references to the relevant literature will be provided. We hope that this thesis can be used in the future as a reference not only for its author, but also for other people interested in the subject. We stress that the cited references to the state of the art research in dark energy are only the ones explicitly employing dynamical systems techniques and this thesis must not be confused for a general review on dark energy phenomenology.

This thesis is however more than a simple review. The mathematical theory of dynamical systems is introduced in a rather pedagogical manner, so that almost no prerequisites are needed to understand the treated arguments. An overview of cosmology is also presented where only elementary knowledge on general relativity is required. This is mainly intended for the reader who is not familiar with the subject, but particular dynamical systems applications, which can interest the expert reader, will also appear for standard cosmological issues.

The aim for this approach is quite ambitious: this thesis is conceived as a bridge between the mathematician and the physicist. In fact the first one can have a look at applications of well known mathematical techniques in the subject of cosmology and make himself an idea of some of the problems afflicting the modern interpretation of the universe. The second one instead can learn useful mathematical tools, helped by the numerous examples appearing in the physical field of cosmology, which can eventually be applied

[2]The dynamics of dark energy has been reviewed by Copeland et al. (2006), who however did not focus only on the dynamical systems perspective as in this thesis.

to many other physical frameworks. It is the hope of the author that both the physicist and the mathematicians will find this thesis useful to broaden their general scientific knowledge.

The thesis is organized as follows. In Chapter 2 elements of the theory of dynamical systems will be treated in a rather pedagogical manner, with examples at the end of each section intended to present simple applications of the concepts just introduced. Chapter 2 will define all the mathematical tools which will then be extensively used in the subsequent chapters. An overview and introduction to standard cosmology will be first given in Chapter 3, which will then discuss the need for dark energy to drive the late time accelerated expansion of the universe. The dynamics of the simplest model of dark energy, characterized by a cosmological constant, will then be analysed in the same chapter and the problems related to such approach will be outlined. Chapters 4 to 6 are the main core of the thesis. In Chapter 4 the cosmological dynamics of the canonical scalar field, the most employed in dynamically evolving models of dark energy, will be largely studied with detailed dynamical systems analysis for the simplest examples and relevant references for the more complicated ones. In Chapter 5 the discussion will be extended to non-canonical scalar field models and particle physics models of dark energy beyond the scalar field. Again the simplest models will be treated in full detail, while for the more involved ones only the main features and results will be presented together with extensive references to the literature. Chapter 6 will cover a similar analysis dealing with dark energy models motivated by modification of general relativity. Alternative theories of gravity based on either phenomenological ideas or quantum gravity physics will be introduced and their applications to late time cosmology will be examined using dynamical systems techniques. Finally conclusions and discussions will be drawn in the end.

1.3 Notation and conventions

An attempt has been made to keep the basic notation as standard as possible. The meaning of every symbol will always be defined at its first occurrence in the text and in all places that ambiguities may arise. In Chapter 2 boldfaced quantities will denote vectors in a general $\mathbb{R}^n$ space, while from Chapters 3 to 5 the standard general relativity notation will be employed (Weinberg, 1972; Wald, 1983). In Chapter 6 some special notation may be required for alternative theories of gravity, but it will be always clarified when needed. The signature of the metric tensor is assumed to be $(-,+,+,+)$. We set $\kappa^2 = 8\pi G/c^4$, where c is the speed of light and G the Newton's gravitational constant, throughout all the thesis unless otherwise stated. Greek indices $\alpha, \beta, \lambda, \mu, \nu, ...$ will run from 0 to 3 while the range of Latin indices $i, j, k, ...$ may vary and will be specified each time.

Chapter 2

Elements of dynamical systems theory

The present chapter provides the basic knowledge about dynamical systems which will be needed to examine cosmological models in the following part of the thesis. The mathematical theory of dynamical systems is developed in a self consistent way, introducing as many details as possible but, at the same time, excluding the non essential arguments. Proofs of theorems are never explicitly given, but detailed references are always provided. In general what follows is a collection of results obtained from several well known textbooks on dynamical systems and differential equations including Arrowsmith & Place (1990); Hirsch & Smale (1974); Lefschetz (1957); Lynch (2007); Perko (2001); Wiggins (1990). The reader interested in further expanding his knowledge on the theory of dynamical systems can refer to any of the mentioned books.

The chapter is organized in the following way. In Sec. 2.1 the basic definitions and concepts to study dynamical systems are provided. In Sec. 2.2 the important notion of critical point is introduced and linear stability theory is developed to determine the stability properties of such points. In Sec. 2.3 and 2.4 special techniques to obtain the stability of critical points when the linear approximation fails are presented. In particular, Liapunov stability theory is the argument of Sec. 2.3 while centre manifold theory is the topic of Sec. 2.4. In Sec. 2.5 important concepts related to the asymptotic behavior of dynamical systems are defined and their relevance in characterizing the global evolution is considered. Sec. 2.6 and 2.7 are then dedicated to the study of 2D (two-dimensional) dynamical systems for which specific results can be obtained and special techniques can be developed. In Sec. 2.6 the asymptotic and linear properties of 2D systems are analyzed, while in Sec. 2.7 methods to study the behavior at infinity are presented. Finally in Sec. 2.8 the use of dynamical systems theory in applications is discussed in connection with the advantages coming from numerical computations. For

the sake of clarity, at the end of some sections a simple example has been added showing how the arguments just exposed materialize in a specific case.

2.1 Basics of dynamical systems

Dynamical systems

Phase space

Generally speaking the term *dynamical system* is used to denote a given deterministic rule describing the evolution of a point in some geometrical space, called the *phase space*. This evolution is parametrized by a number t which is often referred to as *time*.

In this work the phase space will always be $\mathbb{R}^n$, while the time t will always be a real number: $t \in \mathbb{R}$. The deterministic rule will be given as a system of n *ordinary differential equations* (ODE)

$$\mathbf{x}' = \frac{d\mathbf{x}}{dt} = \mathbf{f}(\mathbf{x}, t; \mu_1, \dots, \mu_m)\,, \tag{2.1}$$

where $\mathbf{x} = (x_1, \dots, x_n) \in \mathbb{R}^n$ is called a *point* in the phase space or a *state* of the dynamical system, $\mu_1, \dots, \mu_m$ are m real parameters and an over-prime denotes differentiation with respect to the time t. The function $\mathbf{f} : \mathbb{R}^{n+m+1} \mapsto \mathbb{R}^n$ can be interpreted as a *vector field* on $\mathbb{R}^n$, $\mathbf{f} = (f_1, \dots, f_n)$, and will be assumed to be (at least) of class C^1 (differentiable with continuous derivative). All these assumptions imply that we are dealing with the theory of *continuous dynamical systems*[1].

Autonomous systems

In order to simplify the notation in what follows the dependence of $\mathbf{f}$ upon $\mu_1, \dots, \mu_m$ will not be displayed and, if present, it will be implicitly assumed. Moreover we will only deal with the so-called *autonomous systems* where the function $\mathbf{f}$ does not depend on t explicitly, but only through $\mathbf{x}$. The ODE can thus be written as

$$\mathbf{x}' = \mathbf{f}(\mathbf{x})\,, \quad \text{with} \quad \mathbf{x} \in \mathbb{R}^n\,. \tag{2.2}$$

Solution, trajectory and orbit

A *solution* or *trajectory* of the ODE (2.2) is a function $\mathbf{x}_s : \mathbb{R} \mapsto \mathbb{R}^n$ satisfying $\mathbf{x}_s'(t) = \mathbf{f}(\mathbf{x}_s(t))$ for all $t \in \mathbb{R}$. The image of a solution in $\mathbb{R}^n$ is called an *orbit* of the ODE, though with a small abuse of notation the terms solution, trajectory and orbit will be interchangeably used in this work.

Thanks to the smooth properties of the function $\mathbf{f}$, it is possible to prove basic theorems (Hirsch & Smale, 1974) that assure the existence and uniqueness of a solution with given initial conditions $\mathbf{x} = \mathbf{x}_0$ at $t = t_0$.

[1] A formal definition of dynamical system can be given in terms of the *tuple* (T, M, Φ) where T is a *monoid* (written additively), M is a set, called the *phase space*, and Φ a function $\Phi \subset T \times M \mapsto M$ with $I(x) = \{t \in T | (t, x) \in U\}$, $\Phi(0, x) = x$ and $\Phi(t_2, \Phi(t_1, x)) = \Phi(t_1 + t_2, x)$ for $t_1, t_2, t_1 + t_2 \in I(x)$; see e.g. Chueshov (1999). If $T \subset \mathbb{R}$, M is a differentiable manifold and Φ a continuous function, then (T, M, Φ) is a *continuous dynamical system*. Examples of non-continuous dynamical systems are *discrete dynamical systems*, where $T \subset \mathbb{Z}$, and *cellular automatons*, where T is a lattice.

Moreover any solution $\mathbf{x}(t)$ is defined for all $t \in \mathbb{R}$ unless $||\mathbf{x}(t)|| \to \infty$ for some finite $t_{\max}$, with $||\ ||$ the standard norm in $\mathbb{R}^n$. One can then define the *flow* of the ODE (2.2) as the one-parameter family of maps $\{\psi_t\}_{t\in\mathbb{R}}$ from $\mathbb{R}^n$ into itself such that *Flow*

$$\psi_t(\mathbf{x}_0) = \mathbf{x}_s(t;\mathbf{x}_0) \quad \text{for all} \quad \mathbf{x}_0 \in \mathbb{R}^n\,, \tag{2.3}$$

where $\mathbf{x}_s(t;\mathbf{x}_0)$ is the solution of the ODE (2.2) with initial condition $\mathbf{x}_0$ at some time $t = t_0$. At any time t, the flow ψ_t gives the state of the system $\mathbf{x} = \psi_t(\mathbf{x_0})$ for all initial states $\mathbf{x}_0$. Note that an orbit $\mathbf{x}_s(t;\mathbf{x}_0)$ passing through $\mathbf{x}_0$ can also be defined from the flow as

$$\mathbf{x}_s(t;\mathbf{x}_0) = \{\mathbf{x} \in \mathbb{R}^n \mid \mathbf{x} = \psi_t(\mathbf{x}_0)\}\,. \tag{2.4}$$

It is also possible to show that the flow of an ODE forms a group (Hirsch & Smale, 1974).

An important concept related to the flow of a dynamical system is the definition of invariant sets. A subset $S \subset \mathbb{R}^n$ is an *invariant set* of the flow ψ_t on $\mathbb{R}^n$ if for all $\mathbf{x} \in S$ and all $t \in \mathbf{R}$ then $\psi_t(\mathbf{x}) \in S$. If $\psi_t(\mathbf{x}) \in S$ only for $t > 0$ ($t < 0$) then S is called a *positively (negatively) invariant set*. Usually an invariant set identifies a region of the phase space where the evolution of the system satisfies some special properties which somehow constrain or restrict it. Another important notion deriving from the flow is the definition of periodic orbit. An orbit $\mathbf{x}_s(t;\mathbf{x}_0)$ is called a *periodic orbit* if there exists a $T > t_0$ such that $\psi_T(\mathbf{x}_0) = \mathbf{x}_0$. If in the phase space there is an orbit of period T, then the corresponding dynamical system can present oscillatory behavior of period T. *Invariant set* *Periodic orbit*

The main goal in the study of dynamical systems is not to find the analytical expressions of all the possible solutions of the ODE. In fact the function $\mathbf{f}(\mathbf{x})$ can be highly non linear and the dimension of the phase space can be quite large. This implies that finding analytical solutions is commonly a difficult, if not impossible, task. The theory of dynamical systems aims at characterizing the qualitative geometry of orbits in the phase space and, if the system depends on parameters, how these orbits change under variations of the parameters. This will allow us to determine the long time behavior of the system given any initial condition and to draw conclusions on its possible final and initial states as $t \to \pm\infty$. In other words the dynamical systems techniques that will be developed in the next sections will allow us to draw conclusions on the qualitative features of the flow of a given ODE.

2.2 Critical points and linear stability theory

The most important concept in the theory of dynamical systems is the notion of critical point. A *critical* (or *equilibrium* or *fixed*) *point* $\mathbf{x}_c \in \mathbb{R}^n$ is a point *Critical point*

in the phase space that satisfies the condition

$$\mathbf{f}(\mathbf{x}_c) = 0\,. \tag{2.5}$$

In other words the critical points of the ODE $\mathbf{x}' = \mathbf{f}(\mathbf{x})$ are the zeros of the vector field $\mathbf{f}$. A critical point can equivalently be defined as a point $\mathbf{x}_c$ that satisfies $\psi_t(\mathbf{x}_c) = \mathbf{x}_c$ for all t, where ψ_t is the flow corresponding to the given ODE.

Note that since at any critical point $\mathbf{x}_c' = 0$ the evolution of the dynamical system is frozen at that point, meaning that it will not change its state in time. In more mathematical terms the orbit through a critical point is the point itself

$$\mathbf{x}_s(t; \mathbf{x}_c) = \{\mathbf{x}_s\} \quad \text{for all} \quad t \in \mathbb{R}\,. \tag{2.6}$$

Heteroclinic and homoclinic orbits

An orbit connecting two distinct critical points is called a *heteroclinic orbit*, while an orbit connecting a critical point to itself is called a *homoclinic orbit*. Note that critical points are never part of a heteroclinic or homoclinic orbit but can only be approached as $t \to \pm\infty$.

After one identifies the critical points of a given dynamical system the properties of the flow near one of such points can be determined linearizing the system in a neighborhood of the point. This is usually the first step to identify the qualitative features of the flow in the phase space. The basic idea is to determine if trajectories in the proximity of a critical point are attracted or repelled by the point itself, or, in other words, to study the stability properties of the critical point.

Consider a Taylor expansion of the function $\mathbf{f}$ around a point $\{\mathbf{x}_0\}$. At first order in $|\mathbf{x} - \mathbf{x}_0|$ we have

$$\mathbf{f}(\mathbf{x}) \simeq \mathbf{f}(\mathbf{x}_0) + \mathbf{Df}(\mathbf{x}_0)(\mathbf{x} - \mathbf{x}_0)\,, \tag{2.7}$$

Jacobian

where $\mathbf{Df}(\mathbf{x}_0)$ is the *derivative matrix* or *Jacobian* of the function $\mathbf{f}(\mathbf{x})$ at $\mathbf{x}_0$ and in coordinates reads

$$\mathbf{Df}(\mathbf{x}_0) = \left.\frac{\partial f_i}{\partial x_j}\right|_{\mathbf{x}=\mathbf{x}_0}\,, \tag{2.8}$$

where the indices i, j run from 1 to n. If we consider the same expansion around a critical point $\mathbf{x}_c$, where $\mathbf{f}(\mathbf{x}_c) = 0$, we obtain at first order in $|\mathbf{x}-\mathbf{x}_c|$

$$\mathbf{f}(\mathbf{x}) \simeq \mathbf{Df}(\mathbf{x}_c)(\mathbf{x} - \mathbf{x}_c)\,. \tag{2.9}$$

If we define the *linearization of the ODE* (2.2) at the critical point $\mathbf{x}_c$ as $\mathbf{u} = \mathbf{x} - \mathbf{x}_c$, then, around $\mathbf{x}_c$ and at first order in $\mathbf{u}$, the ODE (2.2) can be written as

$$\mathbf{u}' = \mathbf{Df}(\mathbf{x}_c)\mathbf{u}\,. \tag{2.10}$$

inear dynamical systems

In general if the function $\mathbf{f}$ of a given ODE is linear, i.e. $\mathbf{f}(\mathbf{u}) = \mathbf{M}\,\mathbf{u}$ for some $\mathbf{u} \in \mathbb{R}^n$ and constant $n \times n$ matrix $\mathbf{M}$, the dynamical system itself is called *linear* with

$$\mathbf{u}' = \mathbf{M}\,\mathbf{u}\,. \tag{2.11}$$

Since $\mathbf{Df}(\mathbf{x}_c)$ as given in Eq. (2.8) is actually a $n \times n$ matrix with constant coefficients, the ODE (2.10) represents a linear dynamical system. For any linear dynamical system $\mathbf{u}' = \mathbf{Mu}$ a general solution $\mathbf{u}_s$ with initial condition $\mathbf{u}_s(t_0) = \mathbf{u}_0$ can be written as (see e.g. Perko (2001, p. 17))

$$\mathbf{u}_s(t) = \mathbf{u}_0 e^{\mathbf{M}(t-t_0)}\,, \tag{2.12}$$

where

$$e^{\mathbf{M}(t-t_0)} = \sum_{N=0}^{+\infty} \frac{\mathbf{M}^N (t-t_0)^N}{N!}\,, \tag{2.13}$$

is the exponential matrix of $\mathbf{M}$.

Consider now the (generally complex) eigenvalues λ_i and corresponding (generalized) eigenvectors $\mathbf{e}_i$ $(i = 1, \dots, n)$ of $\mathbf{M}$. Let us define the following subspaces of $\mathbb{R}^n$:

Stable, unstable and centre subspaces

$$\text{the } \textit{stable subspace} \qquad E^s = \text{span}(\mathbf{e}_1, \dots, \mathbf{e}_s)\,, \tag{2.14}$$

$$\text{the } \textit{unstable subspace} \qquad E^u = \text{span}(\mathbf{e}_{s+1}, \dots, \mathbf{e}_{s+u})\,, \tag{2.15}$$

$$\text{the } \textit{centre subspace} \qquad E^s = \text{span}(\mathbf{e}_{s+u+1}, \dots, \mathbf{e}_{s+u+c})\,, \tag{2.16}$$

where $\{\mathbf{e}_1, \dots, \mathbf{e}_s\}$ are the s eigenvectors of $\mathbf{M}$ corresponding to eigenvalues with *negative real part*, $\{\mathbf{e}_{s+1}, \dots, \mathbf{e}_{s+u}\}$ are the u eigenvectors of $\mathbf{M}$ corresponding to eigenvalues with *positive real part* and $\{\mathbf{e}_{s+u+1}, \dots, \mathbf{e}_{s+u+c}\}$ are the c eigenvectors of $\mathbf{M}$ corresponding to eigenvalues with *vanishing real part*. A well known result (Perko, 2001, p. 55) is that

$$E^s \oplus E^u \oplus E^c = \mathbb{R}^n\,, \quad \text{i.e.} \quad s + u + c = n\,, \tag{2.17}$$

meaning that the union of the three subspaces E^s, E^u and E^c forms the whole $\mathbb{R}^n$.

The stable, unstable and centre subspaces represent invariant sets (or subspaces) of the corresponding linear ODE and thus orbits that pass through a point $\mathbf{u}_0$ in one of them remain in the same subspace for all t. Moreover, thanks to the general solution (2.12) and the properties of the exponential matrix, we have

$$\mathbf{u}_0 \in E^s \quad \text{implies} \quad \lim_{t\to+\infty} \mathbf{u}_s(t) = \lim_{t\to+\infty} \mathbf{u}_0 e^{\mathbf{M}(t-t_0)} = \mathbf{0}\,, \tag{2.18}$$

$$\mathbf{u}_0 \in E^u \quad \text{implies} \quad \lim_{t\to-\infty} \mathbf{u}_s(t) = \lim_{t\to-\infty} \mathbf{u}_0 e^{\mathbf{M}(t-t_0)} = \mathbf{0}\,, \tag{2.19}$$

where $\mathbf{0}$ is the null vector, or origin, in $\mathbb{R}^n$. These statements concern the long term stability properties of orbits in the phase space of a linear

dynamical system. An orbit in E^s will be attracted by the the origin, while an orbit in E^u will be repelled by it. If $s = n$ (i.e. $E^s = \mathbb{R}^n$) all the the orbits will end in the origin as $t \to +\infty$ while if $u = n$ (i.e. $E^u = \mathbb{R}^n$) all the the orbits will start from the origin as $t \to -\infty$.

Stable, unstable and saddle points

It is now easy to realize how to use the linearization (2.10) around a specific critical point $\mathbf{x}_c$ to understand if orbits nearby are attracted or repelled by the point. The first step is to compute the eigenvalues of the matrix $\mathbf{Df}(\mathbf{x}_c)$. Then if all these eigenvalues have negative real part ($E^s = \mathbb{R}^n$), trajectories passing nearby $\mathbf{x}_c$ will be attracted by the critical point which is then called a *stable point* or *sink*. If instead all eigenvalues have positive real part ($E^u = \mathbb{R}^n$) trajectories nearby $\mathbf{x}_c$ will be repelled by the critical point which will then be called a *unstable point* or *source*. If all the eigenvalues have non-vanishing real part but these are both positive and negative in sign, then the critical point is called a *saddle point*.

Stable, unstable and centre manifolds

The subspaces E^s, E^u and E^c are however invariant subspaces of the linear ODE (2.10) only. For any critical point of the non-linear ODE (2.2) we can generalize these invariant subspaces to invariant sets of the full non-linear dynamical system. This requires the introduction of the following invariant sets which exist for every critical point (Wiggins, 1990, p. 21). The *stable manifold* W^s of a critical point $\mathbf{x}_c$ is the differentiable manifold whose tangent space in $\mathbf{x}_c$ coincides with E^s and such that all the orbits passing through any $\mathbf{x}_0 \in W^s$ are asymptotic to $\mathbf{x}_c$ as $t \to +\infty$. Similarly the *unstable manifold* W^u of a critical point $\mathbf{x}_c$ is the differentiable manifold whose tangent space in $\mathbf{x}_c$ coincides with E^u and such that all the orbits passing through any $\mathbf{x}_0 \in W^u$ are asymptotic to $\mathbf{x}_c$ as $t \to -\infty$. Finally, the *centre manifold* W^c of a critical point $\mathbf{x}_c$ is the differentiable manifold whose tangent space in $\mathbf{x}_c$ coincides with E^c.

Hyperbolic and non-hyperbolic points

If all the eigenvalues of $\mathbf{Df}(\mathbf{x}_c)$ have non-vanishing real part (i.e. $E^c = \{\emptyset\}$), $\mathbf{x}_c$ is called a *hyperbolic* critical point. On the contrary, if only one eigenvalue has vanishing real part the critical point is called *non-hyperbolic*. The linear stability theory discussed above works only for hyperbolic critical points. If a critical point is non-hyperbolic then the linearization techniques fail to determine the stability properties of the point. However if a non-hyperbolic critical point has at least one eigenvalue with positive real part we can still refer to it as an unstable point (in the sense defined in Sec. 2.3), since, if we are interested in only the asymptotic behavior as $t \to +\infty$, this point will never represent a stable point. To determine the full linear stability properties of non-hyperbolic critical points, i.e. the asymptotic behavior in the corresponding centre manifold W^c as $t \to \pm\infty$ when either $E^s = \{\emptyset\}$ or $E^u = \{\emptyset\}$, one has to employ either Liapunov stability theory (Sec. 2.3) or centre manifold theory (Sec. 2.4).

Critical set

A dense subset $F \subset \mathbb{R}^n$ which satisfies $\mathbf{f}(\mathbf{x}_c) = 0$ for every point $\mathbf{x}_c \in F$ is called an *equilibrium* or *critical set* and every point $\mathbf{x}_c \in F$ is called a *non-isolated* critical point. Roughly speaking the dense condition means that the

set is a union of adjoint critical points, e.g. a curve, in contrast with a union of single isolated points. In other words the set F can be seen as a manifold with dimension $m \geq 1$. The Jacobian $\mathbf{Df}(\mathbf{x}_c)$ of a point $\mathbf{x}_c$ belonging to a critical set of dimension m, has at least m zero eigenvalues (Bogoyavlensky, 1985). For example, a point $\mathbf{x}_c$ in a curve of critical points, i.e. a critical curve, will always have at least one zero eigenvalue of the matrix $\mathbf{Df}(\mathbf{x}_c)$. It follows that every critical point of a critical set is a non-hyperbolic critical point. A point of a critical set of dimension n is called *normally hyperbolic* if it has only n zero eigenvalues. Critical sets are usually overlooked in dealing with dynamical systems, however there are books, such as the one of Aulbach (1984), completely dedicated to the subject.

If we denote with λ_i the eigenvalues of $\mathbf{Df}(\mathbf{x}_c)$ we can summarize the linear properties of a hyperbolic critical point as

$$\begin{aligned} \mathbf{x}_c \text{ is a } \textit{stable} \text{ point if} \quad & \Re(\lambda_i) < 0 \quad && \text{for all } i = 1, \dots, n\,, \\ \mathbf{x}_c \text{ is an } \textit{unstable} \text{ point if} \quad & \Re(\lambda_i) > 0 \quad && \text{for all } i = 1, \dots, n\,, \\ \mathbf{x}_c \text{ is a } \textit{saddle} \text{ point if} \quad & \Re(\lambda_i)\Re(\lambda_j) < 0 \quad && \text{for some } i \neq j\,. \end{aligned}$$

For a hyperbolic saddle point $\mathbf{x}_c$ one can compute also the eigenvectors of $\mathbf{Df}(\mathbf{x}_c)$ in order to determine E^s and E^u, i.e. in what linear directions the point is attractive or repulsive.

Hartman-Grobman theorem

The importance of the linearized ODE (2.10) resides in the *Hartman-Grobman theorem* (Hartman, 1982; Perko, 2001) which states that the non linear flow ψ_t of the ODE (2.2) in the neighborhood of a hyperbolic critical point $\mathbf{x}_c$ is topologically equivalent to the flow of the linearization (2.10) of the dynamical system around $\mathbf{x}_c$. Mathematically speaking two flows are topologically equivalent if there exists a homeomorphism mapping orbits of a flow into the other flow and preserving their orientation (direction of time evolution). However as far as it concerns us, the equivalence of the Hartman-Grobman theorem can be interpreted as the two flows having the same qualitative behavior. The importance of the theorem is that it implies that the non-linear flow of the original ODE has the same (local) stability properties of the linearized system. In practice the stability of a critical point according to the linearized ODE corresponds to the stability of the full nonlinear ODE.

Example 2.2

The following example has been taken from Lynch (2007, p. 58), which is also a good reference to learn numerical techniques finalised at drawing phase spaces of dynamical systems.

Consider the following two-dimensional dynamical systems

$$x' = x\left(1 - \frac{x}{2} - y\right)\,, \tag{2.20}$$

$$y' = y\left(x - 1 - \frac{y}{2}\right)\,. \tag{2.21}$$

Note that this particular case can be rewritten as (2.2) with $\mathbf{x} = (x, y) \in \mathbb{R}^2$ and $\mathbf{f}(\mathbf{x}) = (f_1, f_2) = (x(1 - x/2 - y),\, y(x - 1 - y/2))$. In the following we want to find the critical points of the system and their linear stability properties.

To compute the critical points we must solve the system $(x', y') = (0, 0)$, i.e. the system of equations

$$\begin{cases} x\left(1 - \frac{x}{2} - y\right) = 0 \\ y\left(x - 1 - \frac{y}{2}\right) = 0\,. \end{cases} \tag{2.22}$$

There are four solutions of this system which represent the four critical points, they are

$$(0,0)\,, \quad (2,0)\,, \quad (0,-2)\,, \quad (\frac{6}{5}, \frac{2}{5})\,. \tag{2.23}$$

To find the linear stability properties of these points we need to compute the Jacobian $\mathbf{Df}$, which for the system (2.20)–(2.21) reads

$$\mathbf{Df}(\mathbf{x}) = \begin{pmatrix} \frac{\partial f_1}{\partial x} & \frac{\partial f_1}{\partial y} \\ \frac{\partial f_2}{\partial x} & \frac{\partial f_2}{\partial y} \end{pmatrix} = \begin{pmatrix} 1 - x - y & -x \\ y & -1 + x - y \end{pmatrix}. \tag{2.24}$$

At the critical points (2.23) the Jacobian becomes

$$\mathbf{Df}(0,0) = \begin{pmatrix} 1 & 0 \\ 0 & -1 \end{pmatrix}, \qquad \mathbf{Df}(2,0) = \begin{pmatrix} -1 & -2 \\ 0 & 1 \end{pmatrix}, \tag{2.25}$$

$$\mathbf{Df}(0,-2) = \begin{pmatrix} 3 & 0 \\ -2 & 1 \end{pmatrix}, \qquad \mathbf{Df}(\tfrac{6}{5}, \tfrac{2}{5}) = \begin{pmatrix} -\frac{3}{5} & -\frac{6}{5} \\ \frac{2}{5} & -\frac{1}{5} \end{pmatrix}, \tag{2.26}$$

and thus the eigenvalues of the derivative matrix at the four critical points are

$$\lambda_1 = -1\,,\ \lambda_2 = 1 \qquad \text{at} \qquad (0,0)\,, \tag{2.27}$$

$$\lambda_1 = -1\,,\ \lambda_2 = 1 \qquad \text{at} \qquad (2,0)\,, \tag{2.28}$$

$$\lambda_1 = 1\,,\ \lambda_2 = 3 \qquad \text{at} \qquad (0,-2)\,, \tag{2.29}$$

$$\lambda_{1,2} = \frac{1}{5}\left(-2 \pm i\sqrt{11}\right) \qquad \text{at} \qquad (\frac{6}{5}, \frac{2}{5})\,. \tag{2.30}$$

We can now draw our conclusion on the linear stability of the critical points. Points $(0, 0)$ and $(2, 0)$ are two saddle points having eigenvalues of $\mathbf{Df}$ (with positive real part) of different sign. Point $(0, -2)$ is an unstable point since (the real part of) its $\mathbf{Df}$-eigenvalues are all positive. Finally Point $(\frac{6}{5}, \frac{2}{5})$ represent a stable point since the real parts of the corresponding eigenvalues of the matrix $\mathbf{Df}$ are all negative, in fact we have $\Re(\lambda_{1,2}) = -2/5$.

The phase space of the system (2.20)–(2.21) has been drawn in Fig. 2.1 with the flow represented by arrowed streamlines. As one can easily understand, trajectories close to Point $(\frac{6}{5}, \frac{2}{5})$ result attracted by the point itself (this point is actually what we will call a stable spiral in Sec. 2.6). Points $(0, 0)$ and $(0, 2)$ attract the flow for some directions and repel it in some others. Looking at the flow it is easy to realize that E^s is nothing but the y-axis for the origin and the x-axis for Point $(2, 0)$. Also the unstable linear subspace E^u is the x-axis for the origin, but E^u for Point $(2, 0)$ is not aligned with the axis. Finally looking at the flow near Point $(0, -2)$ we see

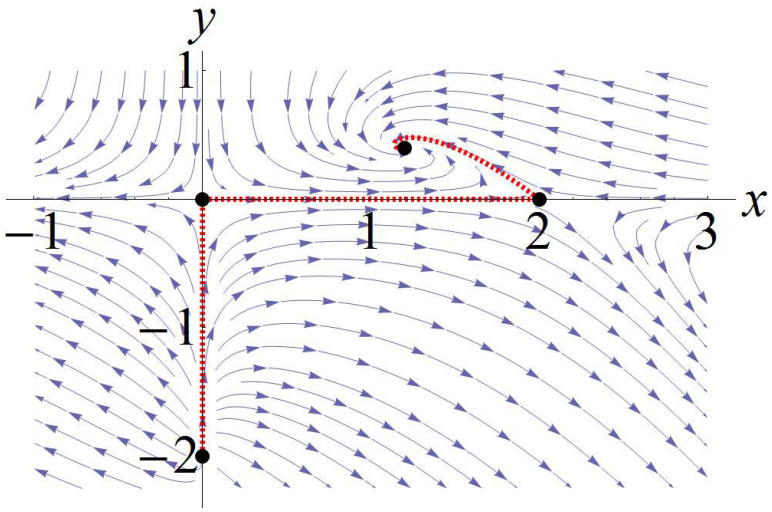

Figure 2.1: Phase space for the dynamical system (2.20)–(2.21). The red/dashed lines represent heteroclinic orbits.

that all the orbits are repelled by the point no matter in what direction they are, implying that this is indeed an unstable point.

The three possible heteroclinic orbits have been delined in Fig. 2.1 by red/dashed lines. They connect Point $(0,-2)$ to the origin $(0,0)$, the origin to Point $(2,0)$ and Point $(2,0)$ to Point $(\frac{6}{5},\frac{2}{5})$. Note that there are no orbits following the sequence $(0,-2)\to(0,0)\to(2,0)\to(\frac{6}{5},\frac{2}{5})$ since every solution passing nearby Point $(0,-2)$ will eventually diverge at infinity as $t\to+\infty$. We can read the qualitative behavior of the flow in the phase space from Fig. 2.1 as follows. Orbits in the bottom-right quadrant start at Point $(0,-2)$ as $t\to-\infty$ and diverge ($||\mathbf{x}||=\sqrt{x^2+y^2}\to\infty$) as $t\to+\infty$. Orbits in the bottom-left quadrant also start at Point $(0,-2)$ as $t\to-\infty$ and diverge as $t\to+\infty$. The same long time asymptotic behavior happens for orbits in the upper-left quadrant, but as $t\to-\infty$ these orbits diverge too. Finally orbits in the upper-right quadrant are all attracted by Point $(\frac{6}{5},\frac{2}{5})$ as $t\to+\infty$ and diverge as $t\to-\infty$. Note that the four quadrants are all invariant sets since orbits in one of them never intersect the axes.

So far we can only state if orbits diverge, i.e. if $||\mathbf{x}||\to+\infty$, as $t\to\pm\infty$. In Sec. 2.7 we will see how to describe the behavior of orbits as they diverge. In other words we will learn how to deal with critical points at infinity.

2.3 Liapunov stability theory

In Sec. 2.2 we have seen how to determine the stability properties of hyperbolic critical points. In this section we will present the methods developed by Liapunov to describe the asymptotic behavior of orbits close to a critical point, showing how one can use them to study the stability of both

hyperbolic and non-hyperbolic critical points.

Before stating the central theorem of Liapunov theory, we need to introduce the proper definitions of stability. In Sec. 2.2 a critical point of a given dynamical system was *locally* stable if the eigenvalues of its corresponding Jacobian had all negative parts. This definition is of course related to the linearization of the corresponding ODE, and it applies only to hyperbolic critical points. A more general definition can be given in the following way.

Liapunov and asymptotic stability

A critical point $\mathbf{x}_c$ of a given ODE is a *(Liapunov) stable point* if for all neighborhoods U of $\mathbf{x}_c$, there exists a neighborhood U_* of $\mathbf{x}_c$ such that if $\mathbf{x}_0 \in U_*$ at $t = t_0$ then $\psi_t(\mathbf{x}_0) \in U$ for all $t > t_0$, where ψ_t is the flow of the ODE. Moreover a critical point $\mathbf{x}_c$ is said to be *asymptotically stable* if it is stable and for all $\mathbf{x} \in U_*$, $\lim_{t\to+\infty} ||\psi_t(\mathbf{x}) - \mathbf{x}_c|| = 0$. Note that the local stability condition defined in Sec. 2.2 from the linearization of the ODE, implies the asymptotic stability of the critical point. A critical point will be called *(Liapunov) unstable* if it is not stable. Note that the local instability condition of Sec. 2.2 is now different from Liapunov instability and corresponds to what we will now call *asymptotic stability in the past* which is similarly defined considering $t \to -\infty$.

Liapunov stability theorem

We are now ready to formulate the *Liapunov stability theorem* (Perko, 2001; Wiggins, 1990). Let $\mathbf{x}_c$ be a critical point of the ODE $\mathbf{x}' = \mathbf{f}(\mathbf{x})$. Let U be a neighborhood of $\mathbf{x}_c$ and $V : \mathbb{R}^n \mapsto \mathbb{R}$ be a C^1 function such that $V(\mathbf{x}_c) = 0$, $V(\mathbf{x}) > 0$ for all $\mathbf{x} \in U - \{\mathbf{x}_c\}$. Then

1. If $\frac{d}{dt}V(\mathbf{x}) < 0$ for all $\mathbf{x} \in U - \{\mathbf{x}_c\}$, $\mathbf{x}_c$ is *asymptotically stable*;
2. If $\frac{d}{dt}V(\mathbf{x}) \leq 0$ for all $\mathbf{x} \in U - \{\mathbf{x}_c\}$, $\mathbf{x}_c$ is *stable*;
3. If $\frac{d}{dt}V(\mathbf{x}) > 0$ for all $\mathbf{x} \in U - \{\mathbf{x}_c\}$, $\mathbf{x}_c$ is *unstable*.

Liapunov function

A function V that satisfies the conditions of the theorem with $\frac{d}{dt}V(\mathbf{x}) \leq 0$ is called a *Liapunov function*. Moreover if V satisfies the condition of the theorem with $\frac{d}{dt}V(\mathbf{x}) < 0$ then it is called a *strict Liapunov function*.

To assure the stability of a critical point one then needs only to find a Liapunov function in its neighborhood. Of course in any different situation no one knows what function will work for the theorem and to find the right Liapunov function one must proceed by trial and error.

Example 2.3

The following simple example has been taken from Wiggins (1990, p. 13). Consider the following 2D dynamical system

$$x' = y\,, \tag{2.31}$$

$$y' = -x + \epsilon\, x^2 y\,, \tag{2.32}$$

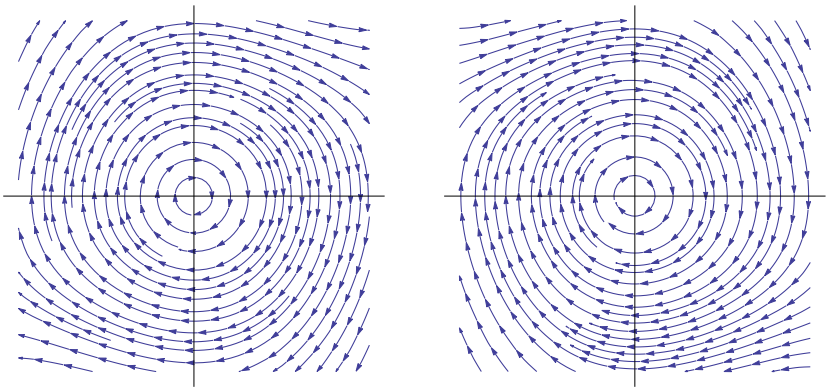

(a) $\epsilon > 0$ (b) $\epsilon < 0$

Figure 2.2: Phase space portraits near the origin for the dynamical system (2.31)–(2.32) with positive and negative ϵ. Note the highly non-linear nature of the flow.

where ϵ is a constant parameter. One can easily verify that the origin is a non-hyperbolic critical point. To determine the stability properties of the origin we can apply the Liapunov theorem. Consider the function

$$V(x, y) = \frac{1}{2}\left(x^2 + y^2\right) , \tag{2.33}$$

which clearly satisfies $V(0, 0) = 0$ and $V(x, y) > 0$ in any neighborhood of the origin. Using the chain rule and (2.31)–(2.32) we obtain

$$\frac{d}{dt}V(x, y) = \epsilon\, x^2 y^2 , \tag{2.34}$$

which, using Liapunov theorem, tells us that if $\epsilon < 0$ the origin is a stable point for the system (2.31)–(2.32). Note that if $\epsilon > 0$ we cannot conclude from the theorem that the origin is an unstable point since (2.34) is not strictly positive everywhere in its neighborhood. However, as shown in Fig. 2.2 where the flow of the system (2.31)–(2.32) has been drawn in a neighborhood of the origin, if $\epsilon < 0$ the origin is indeed attractive, while if $\epsilon > 0$ it is repulsive.

2.4 Centre manifold theory

In this section we will explain how to analyze the stability of a non-hyperbolic critical point $\mathbf{x}_c$ whose Jacobian $\mathbf{Df}(\mathbf{x}_c)$ presents at least one eigenvalue with vanishing real part. As we have seen in Sec. 2.3 a way to determine the stability of a non-hyperbolic critical point consists in finding a suitable Liapunov function. However such method works only if one is actually able to construct such a function and in some cases is practically impossible to guess the right function one needs. These situations require the use of *centre*

manifold theory explained, for example, in Wiggins (1990) or Carr (1981) (see also Boehmer et al. (2012a)). In this section we will closely follow the arguments of Wiggins (1990, Chap. 2).

Since we are interested in the long time behavior of trajectories passing nearby the critical point $\mathbf{x}_c$, i.e. in the stability properties of the critical point as defined in Sec. 2.3, our aim will be only to determine if such a point attracts or repels those orbits. We have already stated in Sec. 2.2 that if the Jacobian $\mathbf{Df}(\mathbf{x}_c)$ of a non-hyperbolic critical point $\mathbf{x}_c$ has at least one eigenvalue with positive real part, then $\mathbf{x}_c$ is always an unstable point. Even though we do not know if orbits in the centre manifold W^c of the point are attracted or repelled, we know that as $t \to +\infty$ all trajectories not belonging to the centre manifold will eventually be repelled by the point; see Wiggins (1990) for the application of centre manifold theory to saddle points.

The situation is different if all eigenvalues with non vanishing real part have negative (positive, in the $t \to -\infty$ case) real part, i.e. if $E^u = \{\emptyset\}$ ($E^s = \{\emptyset\}$). In this case we do not know if the point is a stable (stable in the past) point, and the behavior of trajectories as $t \to +\infty$ ($t \to -\infty$) cannot be determined by the linear stability theory. In what follows we will suppose that the non-hyperbolic critical point $\mathbf{x}_c$ is such that $E^u = \{\emptyset\}$. The scope will then be to determine if $\mathbf{x}_c$ is a stable point or a saddle, i.e. to determine the behavior of orbits as $t \to +\infty$. The case $E^s = \{\emptyset\}$ can be similarly treated performing the analysis as $t \to -\infty$.

For the sake of simplicity, we will consider the point $\mathbf{x}_c$ to be the origin $\mathbf{0}$. This can always be achieved with a simple coordinate transformations $\mathbf{x} \mapsto \mathbf{x} - \mathbf{x}_c$. Thanks to these assumptions a nonlinear ODE (2.2) can always be rewritten as

$$\mathbf{x_1}' = \mathbf{A}\,\mathbf{x_1} + \mathbf{f_1}(\mathbf{x_1}, \mathbf{x_2})\,, \tag{2.35}$$

$$\mathbf{x_2}' = \mathbf{B}\,\mathbf{x_2} + \mathbf{f_2}(\mathbf{x_1}, \mathbf{x_2})\,, \tag{2.36}$$

where $(\mathbf{x_1}, \mathbf{x_2}) \in \mathbb{R}^c \times \mathbb{R}^s$ (with $c = \dim E^c$ and $s = \dim E^s$) and the two functions $\mathbf{f_1}$, $\mathbf{f_2}$ satisfy the conditions

$$\mathbf{f_1}(\mathbf{0}, \mathbf{0}) = 0\,, \qquad \mathbf{Df_1}(\mathbf{0}, \mathbf{0}) = 0\,, \tag{2.37}$$

$$\mathbf{f_2}(\mathbf{0}, \mathbf{0}) = 0\,, \qquad \mathbf{Df_2}(\mathbf{0}, \mathbf{0}) = 0\,. \tag{2.38}$$

In (2.35) and (2.36), $\mathbf{A}$ is a $c \times c$ matrix with all eigenvalues having vanishing real parts, $\mathbf{B}$ is a $s \times s$ matrix with all eigenvalues having negative real parts and $\mathbf{f_1}$, $\mathbf{f_2}$ are functions of at least class C^1. The new vectors $\mathbf{x_1}$ and $\mathbf{x_2}$ represent the decomposition of $\mathbf{x}$ into the centre and stable subspaces respectively.

In our case, a centre manifold can always be characterized by a function $\mathbf{h} : \mathbb{R}^c \mapsto \mathbb{R}^s$, taking vectors of E^c into E^s. In other words the centre manifold can be defined as[2]

Centre manifold

$$W^c(\mathbf{0}) = \{(\mathbf{x_1}, \mathbf{x_2}) \in \mathbb{R}^c \times \mathbb{R}^s \,|\, \mathbf{x_2} = \mathbf{h}(\mathbf{x_1}), ||\mathbf{x_1}|| < \delta, \mathbf{h}(\mathbf{0}) = \mathbf{0}, \mathbf{Dh}(\mathbf{0}) = \mathbf{0}\}\,, \tag{2.39}$$

for $\delta \in \mathbb{R}$ sufficiently small, $\mathbf{h}$ of at least class C^2 and where $||\,||$ here denotes the (Euclidean) norm of $\mathbb{R}^c$. Of course the conditions $\mathbf{h}(\mathbf{0}) = \mathbf{0}$ and $\mathbf{Dh}(\mathbf{0}) = \mathbf{0}$ imply nothing but the fact that $W^c(\mathbf{0})$ is tangent to E^c at $\mathbf{x} = \mathbf{0}$.

In order to study the stability of orbits in the centre manifold, we will make use of three theorems taken from Carr (1981).

First theorem

The first theorem states that the dynamics of the system (2.35)–(2.36) restricted to the centre manifold $W^s(\mathbf{0})$, for $\mathbf{x_1}$ sufficiently small, is given by the following c-dimensional dynamical system

$$\mathbf{x_1}' = \mathbf{A}\,\mathbf{x_1} + \mathbf{f_1}(\mathbf{x_1}, \mathbf{h}(\mathbf{x_1}))\,, \tag{2.40}$$

where of course $\mathbf{x_1} \in \mathbb{R}^c$ (i.e. E^c).

Second theorem

The second theorem states the following two results. First if the origin $\mathbf{x_1} = \mathbf{0}$ of $\mathbb{R}^c$ is a stable (unstable) point for the dynamical system (2.40), then the origin $\mathbf{x} = \mathbf{0}$ of $\mathbb{R}^n$ is a stable (unstable) point for the dynamical system (2.35)–(2.36). Second if the origin $\mathbf{x_1} = \mathbf{0}$ of $\mathbb{R}^c$ is a stable point for the dynamical system (2.40) and $(\mathbf{x_1}(t), \mathbf{x_2}(t))$ is a solution of the dynamical system (2.35)–(2.36) with $(\mathbf{x_1}(t_0), \mathbf{x_2}(t_0))$ sufficiently small at some time t_0, then there is a solution $\mathbf{x_1^s}(t)$ of the system (2.40) such that as $t \to +\infty$

$$\mathbf{x_1}(t) = \mathbf{x_1^s}(t) + \mathcal{O}(e^{-\gamma t})\,, \tag{2.41}$$

$$\mathbf{x_2}(t) = \mathbf{h}(\mathbf{x_1^s}(t)) + \mathcal{O}(e^{-\gamma t})\,, \tag{2.42}$$

where $\gamma > 0$ is a constant.

The two theorems just exposed imply that once one knows the function $\mathbf{h}$ characterizing the centre manifold W^c then the stability restricted to W^c is given by (2.40) and moreover the orbits passing close to the origin of $\mathbb{R}^n$ approximate the orbits in W^c as $t \to +\infty$. The problem is now how to determine the function $\mathbf{h}$. This can be achieved with the following simple steps.

First of all any point $(\mathbf{x_1}, \mathbf{x_2}) \in W^c$ must satisfy $\mathbf{x_2} = \mathbf{h}(\mathbf{x_1})$; see (2.39). Differentiating with respect to time we have $\mathbf{x_2}' = \mathbf{Dh}(\mathbf{x_1})\mathbf{x_1}'$ and using (2.35)–(2.36) we obtain

$$\mathcal{N}(\mathbf{h}(\mathbf{x_1})) = \mathbf{Dh}(\mathbf{x_1})\,[\mathbf{A}\,\mathbf{x_1} + \mathbf{f_1}(\mathbf{x_1}, \mathbf{h}(\mathbf{x_1}))] - \mathbf{B}\,\mathbf{h}(\mathbf{x_1}) - \mathbf{f_2}(\mathbf{x_1}, \mathbf{h}(\mathbf{x_1})) = \mathbf{0}\,. \tag{2.43}$$

This is a quasilinear partial differential equation which $\mathbf{h}(\mathbf{x_1})$ has to satisfy in order to characterize the centre manifold W^c. Thus all one needs to do to find the centre manifold and the stability properties of non-hyperbolic points is to solve (2.43). Of course (2.43) can be difficult if not impossible to solve. Fortunately the last theorem from Carr (1981) provides us with

[2] Note that nothing assures that $\mathbf{h}$ is unique.

a method for computing an approximated solution to any desired degree of accuracy.

Third theorem

The theorem states the following: let $\mathbf{p} : \mathbb{R}^c \mapsto \mathbb{R}^s$ be a C^1 map with $\mathbf{p}(\mathbf{0}) = \mathbf{Dp}(\mathbf{0}) = 0$ such that $\mathcal{N}(\mathbf{p}(\mathbf{x_1})) = \mathcal{O}(||\mathbf{x_1}||^q)$ as $\mathbf{x_1} \to \mathbf{0}$ for some $q > 0$, then

$$||\mathbf{h}(\mathbf{x_1}) - \mathbf{p}(\mathbf{x_1})|| = \mathcal{O}(||\mathbf{x_1}||^q) \quad \text{as } \mathbf{x_1} \to \mathbf{0}\,. \tag{2.44}$$

This allow us to compute $\mathbf{h}(\mathbf{x_1})$ to any desired degree of accuracy by solving (2.43) to the same degree of accuracy. In other words what one needs to do is to approximate $\mathbf{h}(\mathbf{x_1})$ with a simple function valid up to the desired order of accuracy, usually powers series expansions work nicely, and then substitute it into (2.43) which will then give a simpler system of equations to solve. All this is clearer following an example.

Example 2.4

The following example has been taken from Wiggins (1990, p. 196). Consider the dynamical system

$$x' = x^2 y - x^5\,, \tag{2.45}$$

$$y' = -y + x^2\,, \tag{2.46}$$

where $(x, y) \in \mathbb{R}^2$. We will focus our analysis on the origin which is obviously a critical point of this system. The eigenvalues of the Jacobian at the origin are 0 and -1, meaning that the origin is a non-hyperbolic critical point and to determine its stability properties we must apply the centre manifold theory.

In this example the system (2.45)–(2.46) can be rewritten as (2.35)–(2.36) with

$$\mathbf{A} = 0\,, \quad \mathbf{B} = -1\,, \quad \mathbf{f_1}(x, y) = x^2 y - x^5\,, \quad \mathbf{f_2}(x, y) = x^2\,, \tag{2.47}$$

where now $E^c = E^s = \mathbb{R}$, $\mathbf{x_1} = x$ and $\mathbf{x_2} = y$. We need to solve (2.43) in order to find the function $\mathbf{h}(x)$ characterizing the centre manifold. We will consider $\mathbf{h}(x)$ to be of the power-law type up to the fourth order

$$\mathbf{h}(x) = ax^2 + bx^3 + \mathcal{O}(x^4)\,, \tag{2.48}$$

where a, b are constants and the linear and constant terms do not appear because of conditions $\mathbf{h}(0) = \mathbf{Dh}(0) = 0$ that $\mathbf{h}(x)$ must satisfy; see (2.39). At this point we substitute (2.48) into (2.43) which then reads

$$\mathcal{N}(\mathbf{h}(x)) = (a - 1)x^2 + bx^3 + \mathcal{O}(x^4) = 0\,. \tag{2.49}$$

In order for this equation to be valid every coefficient in the polynomial must vanish and thus we find

$$a = 1\,, \quad \text{and} \quad b = 0\,, \tag{2.50}$$

implying that

$$\mathbf{h}(x) = x^2 + \mathcal{O}(x^4)\,. \tag{2.51}$$

Thus thanks to (2.40) the vector field $\mathbf{f}(\mathbf{x})$ restricted to the centre manifold is

$$x' = x^4 + \mathcal{O}(x^5)\,, \tag{2.52}$$

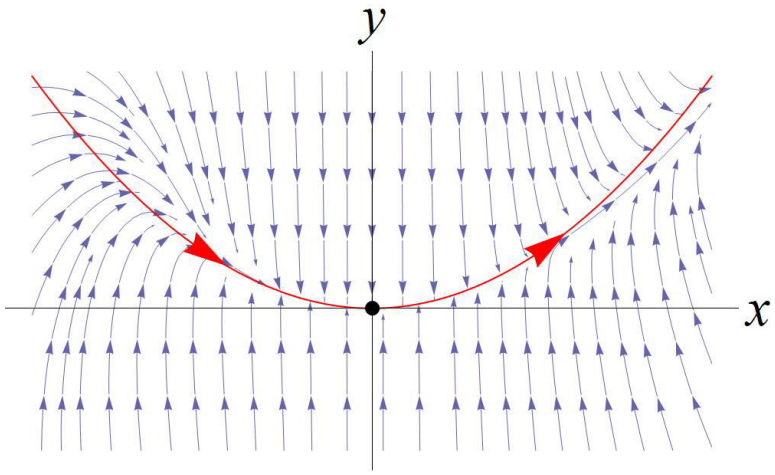

Figure 2.3: Phase space for the dynamical system (2.45)–(2.46) in a neighborhood of the origin. The red/thick line shows the centre manifold approximated by (2.51).

meaning that for x sufficiently small, the critical point $x = 0$ is an unstable point of the system restricted to the centre manifold (2.51) (this can easily be seen integrating (2.52) to find the solution $x(t)$ which will then diverge as $t \to +\infty$). Hence, by the second theorem above the origin $(x, y) = (0, 0)$ in $\mathbb{R}^2$ is an unstable point of the system (2.45)–(2.46).

In Fig. 2.3 the flow of the dynamical system (2.45)–(2.46) in the neighborhood of the origin has been drawn. The red/continuous line denotes the function $\mathbf{h}(x) = x^2$ which approximates the centre manifold W^c at small values of x. One can easily realize from Fig. 2.3 that the smaller the values of x the better $\mathbf{h}(x)$ approximates W^c as the flow is exactly attracted by the red/continuous line. The arrows on the red/continuous line identify the direction of the flow restricted to the centre manifold. As we can see, the trajectories in the centre manifold are attracted for $x < 0$ and repelled for $x > 0$ making the origin a saddle point.

This example can also be used to understand how the linear approximation fails for non-hyperbolic critical points. The idea is the following. Since E^c corresponds to the y-direction, one might expect that the y component of orbits near the origin decays exponentially fast to zero. Therefore one might be tempted to reduce the question of stability only to the x component of orbits near the origin, or, in other words, to set $y = 0$ in (2.45) obtaining

$$x' = -x^5 \,. \tag{2.53}$$

This procedure corresponds to approximate W^c with E^c, which is of course wrong. In fact from (2.53) one would arrive at the wrong result concerning the stability of $x = 0$ obtaining that it is a stable point.

2.5 Limits sets and attractors

In the previous sections we have developed useful techniques which allow us to determine the local stability properties of critical points. On the other hand we are also interest in the *asymptotic* and *global* behavior of the system, i.e. in characterizing the evolution of orbits as $t \to \pm\infty$ even if the initial conditions are far away from a critical point. This is actually one of the main goal of dynamical systems theory itself. To achieve such an aim in full generality requires the adoption of advanced methods of dynamical systems theory such as, for example, bifurcation theory. In this section we will not explain these advanced techniques since they are beyond the scope of the present work. We will limit ourself to introduce some concepts which are of fundamental importance in describing the asymptotic behavior of dynamical systems leaving the advanced material to Arrowsmith & Place (1990); Hirsch & Smale (1974); Lefschetz (1957); Perko (2001); Wiggins (1990).

ω-limit and α-limit points

The first notion we introduce is the definition of ω-limit and α-limit sets. A point $\mathbf{x}$ of the phase space $\mathbb{R}^n$ is an *ω-limit point* of $\mathbf{x}_0 \in \mathbb{R}^n$ if there exists a sequence $t_N \to +\infty$ such that

$$\lim_{N\to+\infty} \psi_{t_N}(\mathbf{x}_0) = \mathbf{x}\,, \tag{2.54}$$

ω-limit and α-limit sets

where ψ_t is the flow of a given dynamical system. The *α-limit point* is defined in a similar way using a sequence $t_N \to -\infty$. The set of all ω-limit points of $\mathbf{x}_0$ is called the *ω-limit set* of $\mathbf{x}_0$ and denoted as $\omega(\mathbf{x}_0)$. Similarly the set of all the α-limit points of $\mathbf{x}_0$ is called the *α-limit set* of $\mathbf{x}_0$ and denoted as $\alpha(\mathbf{x}_0)$. For every point $\mathbf{x}_0$ the ω-limit set $\omega(\mathbf{x}_0)$ is a closed subset of $\mathbb{R}^n$ and moreover if the positive orbits passing through $\mathbf{x}_0$ is bounded, then $\omega(\mathbf{x}_0)$ is non-empty and connected (Perko, 2001, p. 175). Of course the same is true for α-limit sets.

The ω-limit set and α-limit set of a point $\mathbf{x}_0$ describe the future and past asymptotic behavior of the orbit passing through $\mathbf{x}_0$. The simplest example of an ω-limit (α-limit) set is a critical point $\mathbf{x}_c$. In this case the orbit approaches $\mathbf{x}_c$ as $t \to +\infty$ ($t \to -\infty$). Other examples are the closure of a homoclinic orbit, a heteroclinic cycle (a sequence of critical points joined by heteroclinic orbits) and a periodic orbit.

The concepts of ω and α-limit sets depend on a point $\mathbf{x}_0$ of the phase space. To determine the asymptotic behaviour of a given dynamical system, one should then consider the ω and α-limit sets of all the points in the phase space. This considerations lead to introduce the notion of attractor[3]. The

Future and past attractors

future attractor A^+ is the smallest closed invariant set such that $\omega(\mathbf{x}_0) \subset A^+$

[3]Despite its importance, the notion of attractor has been introduced in the dynamical systems literature as recently as 1964; see Auslander et al. (1964). The definition employed in this thesis has been found useful in dynamical systems applications to cosmology (Wainwright & Ellis, 1997).

for all $\mathbf{x}_0 \in \mathbb{R}^n$ a part from a set of measure zero. The *past attractor* A^- is defined in the same way replacing the ω-limit set with the α-limit set. Sometimes the attractors $A^\pm$ can refer to a proper subset S of the phase space rather than to the whole of $\mathbb{R}^n$. In that case we will talk about attractors of the subset S. If S is compact, then each point $x \in S$ has non-empty ω and α-limit sets and then $A^\pm \neq \{\emptyset\}$.

Although the global asymptotic behavior of orbits in the phase space can be well described by the concepts of limit sets and attractors, the *intermediate behavior* is usually more difficult to characterize. The simplest situation happens when an orbit passes nearby a saddle point, first shadowing a solution in the stable manifold and then following another solution in the unstable manifold. In this case the evolution slows down since $\mathbf{x}' \simeq 0$ near the critical point and the system undergoes a period of *quasi-equilibrium* before being driven away from the critical point. In general such behavior is associated with a so-called *finite heteroclinic sequence* which is a set of N critical points $\mathbf{x}_c^0, \ldots, \mathbf{x}_c^N$ where $\mathbf{x}_c^0$ is a stable point, $\mathbf{x}_c^N$ is a local unstable point (or stable in the past) and the rest are saddle points, such that there is a heteroclinic orbit which joins $\mathbf{x}_c^{i-1}$ with $\mathbf{x}_c^i$ for $i = 1, \ldots, N$. Note however that given a finite heteroclinic sequence $\mathbf{x}_c^0, \ldots, \mathbf{x}_c^N$, the existence of an orbit connecting a neighborhood of $\mathbf{x}_c^0$ with a neighborhood of $\mathbf{x}_c^N$ is not guaranteed. If $\mathbf{x}_c^0$ is not stable in the past, or $\mathbf{x}_c^N$ is not stable, then one might still refer to a *non-finite heteroclinic sequence* or simply heteroclinic sequence.

Heteroclinic sequence

Example 2.5

Consider again Fig. 2.1 of Example 2.2. One can immediately realize that there are no global attractors since trajectories in different quadrants (taken excluding the boundaries) have different asymptotic behaviors. The ω-limit set of every orbit in the upper-right quadrant coincides with the stable point $(\frac{6}{5}, \frac{2}{5})$, while the α-limit set is empty. Trajectories in the bottom-right quadrant have always an empty ω-limit set, but their α-limit set can either be empty or Point $(0, -2)$. The α-limit set of orbits in the bottom-left quadrant is the unstable point $(0, -2)$, while the ω-limit set of these orbits is empty. In the upper-left quadrant every orbit has both the ω and α-limit sets empty. Point $(2, 0)$ is the ω-limit set of trajectories along the positive x-axis, while the origin is the ω-limit set of trajectories along the y-axis (only up to Point $(0, -2)$ in the negative direction) and the α-limit set of orbits along the x-axis (only up to Point $(2, 0)$ in the positive direction).

From all this we can say that the future attractor of the upper-right quadrant is Point $(\frac{6}{5}, \frac{2}{5})$, while the past attractor of the lower-left is Point $(0, -2)$. The other two quadrants have no attractors ($A^\pm = \{\emptyset\}$), though part of the bottom-right quadrant has Point $(0, -2)$ as A^-.

Finally, as we already noticed, the red/dashed lines in Fig. 2.1 identify the finite heteroclinic sequence $(0, -2) \to (0, 0) \to (2, 0) \to (\frac{6}{5}, \frac{2}{5})$. However, as it is clear from Fig. 2.1, there are no trajectories starting from the neighborhood of Point $(0, -2)$ and ending in Point $(\frac{6}{5}, \frac{2}{5})$.

2.6 2D dynamical systems: special theorems and linear systems

This section is dedicated to the study of dynamical systems on $\mathbb{R}^2$. Two-dimensional dynamical systems on the plane are of special importance because of several results which cannot be applied to higher dimensional systems. In what follows we will present some of these results.

Dulac's criterion

The first result is a theorem which allow one to exclude periodic orbits in some subset of $\mathbb{R}^2$ and it called the *Dulac's criterion*; see e.g. Perko (2001, p. 246). Consider the ODE $\mathbf{x}' = \mathbf{f}(\mathbf{x})$ on $\mathbb{R}^2$ with $\mathbf{x} = (x, y)$ and $\mathbf{f} = (f_1, f_2)$. If $D \subseteq \mathbb{R}^2$ is a simply connected open set and $B : \mathbb{R}^2 \mapsto \mathbb{R}$ is a C^1 function such that

$$\frac{\partial}{\partial x}(B\, f_1) + \frac{\partial}{\partial y}(B\, f_2) > 0 \quad \text{or} \quad < 0\,, \tag{2.55}$$

on D, then there are no periodic orbits on D. The function B in this case is called a *Dulac function*. Dulac's criterion is useful if one wants to exclude the possibility that there are periodic orbits in a given subset of $\mathbb{R}^2$.

Poincaré-Bendixson theorem

The following result is a well known theorem which characterize all the possible asymptotic behaviors on the plane. It is called the *Poincaré-Bendixson theorem* (Wiggins, 1990, Sec. 1.1I) and it states the following. Let P be a positively invariant region of the ODE $\mathbf{x}' = \mathbf{f}(\mathbf{x})$ on $\mathbb{R}^2$ containing a finite number of critical points. Let $\mathbf{x}_0 \in P$ and consider the ω-limit set $\omega(\mathbf{x}_0)$. Then if $\omega(\mathbf{x}_0) \neq \{\emptyset\}$, one of the following possibilities must hold:

1. $\omega(\mathbf{x}_0)$ is a *critical point*;
2. $\omega(\mathbf{x}_0)$ is a *periodic orbit*;
3. $\omega(\mathbf{x}_0)$ is a *finite heteroclinic sequence*.

Of course the same consequences are valid for α-limit sets if negatively invariant sets are considered. Note that if P is compact then $\omega(\mathbf{x}_0)$ is always non-empty and one of the three outcomes of the theorems must apply. The importance of the Poincaré-Bendixson theorem resides in the fact that it limits the asymptotic behavior of orbits in $\mathbb{R}^2$ to only four possibilities: either the orbit diverges ($||\mathbf{x}_s(t)|| \to +\infty$ as $t \to \pm\infty$) or it must converge to one of the three sets of the theorem.

2D linear dynamical systems

To conclude this section we consider *2D linear dynamical systems* whose phase space portraits can always be reduced to a finite number of qualitative behaviors. A linear dynamical system in $\mathbb{R}^2$ can be written as

$$\mathbf{x}' = \mathbf{M}\,\mathbf{x}\,, \tag{2.56}$$

where $\mathbf{x} = (x, y)$ and $\mathbf{M}$ is a 2×2 matrix. Of course the only critical point is the origin and in order to determine its stability we need first to find the eigenvalues $\lambda_{1,2}$ of $\mathbf{M}$. For a 2×2 matrix these eigenvalues can only

be given by one of the following possibilities with respective consequences (Lynch, 2007; Perko, 2001):

- If $\lambda_{1,2} \in \mathbb{R}$ with $\lambda_1 < 0$ and $\lambda_2 < 0$, then the origin is a *stable* point which is called a *simple attracting node* (*attracting focus* if $\lambda_1 = \lambda_2$) if both eigenvectors are non-vanishing (see Fig. 2.4 (a) and (b)) or a *Jordan attracting node* if one of the eigenvector is the null vector (see Fig. 2.4 (c)); *Focus, simple node and Jordan node*

- If $\lambda_{1,2} \in \mathbb{R}$ with $\lambda_1 > 0$ and $\lambda_2 > 0$, then the origin is an *unstable* point (stable in the past) which is called a *simple repelling node* (*repelling focus* if $\lambda_1 = \lambda_2$) if both eigenvectors are non-vanishing (see Fig. 2.4 (a) and (b) inverting the direction of the flow) or a *Jordan repelling node* if one of the eigenvector is the null vector (see Fig. 2.4 (c) inverting the direction of the flow);

- If $\lambda_{1,2} \in \mathbb{R}$ and $\lambda_1\lambda_2 < 0$ (opposite sign), then the origin is a *saddle* point (see Fig. 2.4 (d)); note that saddle points are (Liapunov) unstable; *Saddle*

- If $\lambda_{1,2} \in \mathbb{R}$, $\lambda_1 = 0$ and $\lambda_2 > 0$ (or $\lambda_1 > 0$ and $\lambda_2 = 0$), then the origin is an *unstable non-hyperbolic* point and there is a *repelling line* (a critical line) along the direction identified by the positive eigenvector (see Fig. 2.4 (e) inverting the direction of the flow);

- If $\lambda_{1,2} \in \mathbb{R}$, $\lambda_1 = 0$ and $\lambda_2 < 0$ (or $\lambda_1 < 0$ and $\lambda_2 = 0$), then the origin is a *non-hyperbolic* point, whose stability can be determined using centre manifold theory, and there is an *attracting line* (a critical line) along the direction identified by the negative eigenvector (see Fig. 2.4 (e));

- If $\lambda_{1,2} \in \mathbb{R}$ and $\lambda_1 = \lambda_2 = 0$ but there is a non vanishing eigenvector, then the origin is a *non-hyperbolic* point and there is a *neutral line* (a critical line) along the direction identified by the non-vanishing eigenvector (see Fig. 2.4 (f))

- If $\lambda_{1,2} \in \mathbb{C}$ with $\lambda_{1,2} = \alpha \pm i\beta$ and $\alpha < 0$ and $\beta \neq 0$, then the origin is a *stable* point and it is sometimes called a *stable spiral* (see Fig. 2.4 (g)); *Spiral*

- If $\lambda_{1,2} \in \mathbb{C}$ with $\lambda_{1,2} = \alpha \pm i\beta$ and $\alpha > 0$ and $\beta \neq 0$, then the origin is an *unstable* point (stable in the past) and it is sometimes called an *unstable spiral* (see Fig. 2.4 (g) inverting the direction of the flow);

- If $\lambda_{1,2} \in \mathbb{C}$ with $\lambda_{1,2} = \pm i\beta$ and $\beta \neq 0$, then the origin is called a *centre* and the solutions around it posses an *oscillatory behavior* (see Fig. 2.4 (h)).

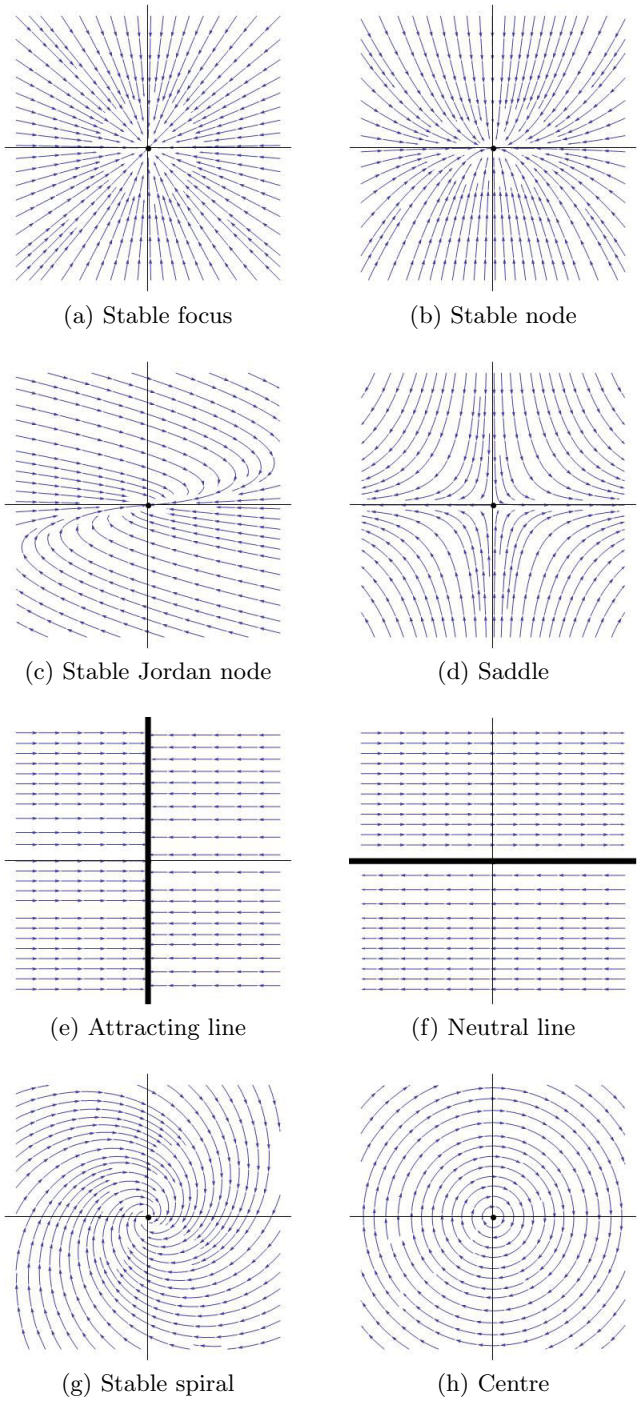

(a) Stable focus (b) Stable node

(c) Stable Jordan node (d) Saddle

(e) Attracting line (f) Neutral line

(g) Stable spiral (h) Centre

Figure 2.4: Phase space portraits near the origin for 2D stable linear dynamical systems. The axes are aligned along the eigendirections. The unstable behaviors can be visualized inverting the direction of the flow.

Of course for non-linear dynamical systems the behavior of the flow around a non-hyperbolic critical point cannot be determined by the arguments above. In fact the nonlinear terms destroy the validity of the above constructions and only centre manifold theory or Liapunov stability theory can provide a correct answer.

In any case, for hyperbolic critical points the argument above can be applied and the flow in a neighborhood of the point can indeed be described by one of the above situations. In particular, for 2D dynamical systems, we can distinguish between attracting (or repelling) spirals, nodes and focuses in order to better characterize the behavior of the flow near the critical point.

2.7 2D dynamical systems: behavior at infinity

In this section we will study the properties of the flow at infinity, i.e. when $||\mathbf{x}|| = \sqrt{x^2 + y^2} \to +\infty$, for dynamical systems on the plane. In $\mathbb{R}^2$ it is indeed possible to make use of certain projection techniques needed to analyze the behavior of the flow at infinity. If this procedure is successfully completed, then one is able to draw the *global portrait* of the phase space, including the asymptotic behavior as $||\mathbf{x}|| \to +\infty$. What follows can be found in different books treating dynamical systems such as Lefschetz (1957); Lynch (2007); Perko (2001).

In order to compactify the phase space we will consider the so-called *Poincaré sphere* which maps points at infinity onto its equator. This is defined as the unit sphere

Poincaré sphere

$$S^2 = \{(X, Y, Z) \in \mathbb{R}^3 \,|\, X^2 + Y^2 + Z^2 = 1\}\,, \tag{2.57}$$

such that its north (or south) pole is tangent to the (x, y)-plane in the origin. Then point on the (x, y)-plane can be mapped on the surface of the upper hemi-sphere by projecting lines passing by the center of the sphere. The mapping is provided by the change of variables

$$X = x\,Z\,, \qquad Y = y\,Z\,, \qquad Z = \frac{1}{\sqrt{1 + x^2 + y^2}}\,. \tag{2.58}$$

The following two theorems can be used to determine the flow at infinity. Only the statements of the theorem will be provided, but the reader interested in the details can find them in Lefschetz (1957) or Perko (2001). Consider the following dynamical systems defined in $\mathbb{R}^2$

$$x' = P(x, y)\,, \tag{2.59}$$

$$y' = Q(x, y)\,, \tag{2.60}$$

where P and Q are *polynomial* functions in x and y. Let m denote the maximum polynomial degree of the terms in P and Q and let P_m and Q_m be the

Critical points at infinity

higher terms of the corresponding polynomial functions P and Q. The *critical points at infinity* of the systems (2.59)–(2.60) lie on the points $(X, Y, 0)$ of the equator of the Poincaré sphere where $X^2 + Y^2 = 1$ and

$$X\,Q_m(X,Y) - Y\,P_m(X,Y) = 0\,, \tag{2.61}$$

or equivalently at the polar angles θ_j and $\theta_j + \pi$ satisfying

$$G_{m+1}(\theta) = \cos\theta\,Q_m(\cos\theta,\sin\theta) - \sin\theta\,P_m(\cos\theta,\sin\theta) = 0\,, \tag{2.62}$$

which, if not identically zero, has at most $m+1$ pairs θ_j and $\theta_j+\pi$. Moreover, if $G_{m+1}(\theta)$ is not identically zero, the flow on the equator of the Poincaré sphere is clockwise (counter-clockwise) at points corresponding to polar angles θ where $G_{m+1}(\theta) < 0$ ($G_{m+1}(\theta) > 0$). Note that the points at infinity of $\mathbb{R}^2$ will always come in pairs since the projective lines intersect the equator of the Poincaré sphere twice as $||x|| \to +\infty$.

Stability of critical points at infinity

The behavior of the flow near critical points at infinity, i.e. the *stability properties of critical points at infinity*, can then be described projecting the flow on the Poincaré sphere onto the two planes (x, z) and (y, z) tangent to the equator points $Y = 1$ and $X = 1$ respectively. This is summarized in the following theorem. The flow on the Poincaré sphere in the neighborhood of any critical point on the equator, except the points $(0, \pm 1, 0)$, is topologically equivalent to the flow defined by the system

$$\pm y' = y\,z^m\,P(\frac{1}{z},\frac{y}{z}) - z^m\,Q(\frac{1}{z},\frac{y}{z})\,, \tag{2.63}$$

$$\pm z' = z^{m+1}\,P(\frac{1}{z},\frac{y}{z})\,, \tag{2.64}$$

where the sign is determined by the flow on the equator of S^2 as provided by the sign of (2.62). Similarly, the flow on the Poincaré sphere in the neighborhood of any critical point on the equator, except the points $(\pm 1, 0, 0)$, is topologically equivalent to the flow defined by the system

$$\pm x' = x\,z^m\,Q(\frac{x}{z},\frac{1}{z}) - z^m\,P(\frac{x}{z},\frac{1}{z})\,, \tag{2.65}$$

$$\pm z' = z^{m+1}\,Q(\frac{x}{z},\frac{1}{z})\,, \tag{2.66}$$

where the sign is determined by the flow on the equator of S^2 as provided by the sign of (2.62). This means that if $(0, \pm 1, 0)$ is not a critical point at infinity we can use (2.63)–(2.64) to find the stability of all critical points at infinity. Similarly if $(\pm 1, 0, 0)$ is not a critical point at infinity we can use (2.65)–(2.66) to find the stability of all critical points at infinity. If both $(0, \pm 1, 0)$ and $(\pm 1, 0, 0)$ are critical points at infinity, then we must analyze both (2.63)–(2.64) and (2.65)–(2.66).

All this seems a bit abstract, but we can see how the theorems work with an example.

Example 2.7

Consider again the system (2.20)–(2.21) of Example 2.2 which we recall here for the sake of simplicity

$$x' = x\left(1 - \frac{x}{2} - y\right)\,, \tag{2.67}$$

$$y' = y\left(x - 1 - \frac{y}{2}\right)\,. \tag{2.68}$$

This can be rewritten as

$$x' = P(x,y) = P_1(x,y) + P_2(x,y)\,, \tag{2.69}$$

$$y' = Q(x,y) = Q_1(x,y) + Q_2(x,y)\,, \tag{2.70}$$

where P and Q are the polynomial functions

$$P(x,y) = x - \frac{x^2}{2} - xy \qquad \text{and} \qquad Q(x,y) = -y + xy - \frac{y^2}{2}\,, \tag{2.71}$$

and

$$P_1(x,y) = x\,, \qquad\qquad Q_1(x,y) = -y\,, \tag{2.72}$$

$$P_2(x,y) = -\frac{x^2}{2} - xy\,, \qquad\qquad Q_2(x,y) = xy - \frac{y^2}{2}\,, \tag{2.73}$$

are the coefficients of first and second degree of the corresponding polynomial. Now we can find the critical points at infinity using (2.62), which in our case reads

$$G_3(\theta) = \frac{1}{4}\sin(2\theta)\,(\sin\theta + 3\cos\theta) = 0\,. \tag{2.74}$$

The solutions in the interval $(-\pi, \pi]$ are

$$\theta = 0\,, \quad \theta = \pi\,, \quad \theta = -\frac{\pi}{2}\,, \quad \theta = \frac{\pi}{2}\,, \tag{2.75}$$

$$\theta = -\arctan(3)\,, \quad \theta = \pi - \arctan(3)\,, \tag{2.76}$$

and identify the critical points on the equator of the Poincaré sphere, i.e. the critical points at infinity. Note that, as predicted, they always come in pairs $(\theta, \theta + \pi)$.

The behavior of the flow on the equator of the Poincaré sphere can be deduced from the sign of $G_3(\theta)$. Analyzing (2.74) we can deduce that $G_3(\theta)$ is negative in the intervals $(-\pi, \pi/2)$, $(-\arctan(3), 0)$, $(\pi/2, \pi - \arctan(3))$ and positive in the intervals $(-\pi/2, -\arctan(3))$, $(0, \pi/2)$, $(\pi - \arctan(3), \pi)$. This means that in the first set of intervals the flow on the equator will be clockwise, while in the second set it will be counter-clockwise.

The stability of critical points at infinity can now be determined applying the second theorem. We will do this only for one critical point, but the computation is similar for all the other points. Consider the the critical point at infinity identified by $\theta = 0$, which corresponds to the point $(X, Y, Z) = (1, 0, 0)$. For this point we cannot use the projection (2.65)–(2.66), but we must use the projection (2.63)–(2.64) on the (y, z)-plane. In our case this reads

$$\pm y' = -\frac{1}{2}y(y - 4z + 3)\,, \tag{2.77}$$

$$\pm z' = -\frac{1}{2}z(2y - 2z + 1)\,, \tag{2.78}$$

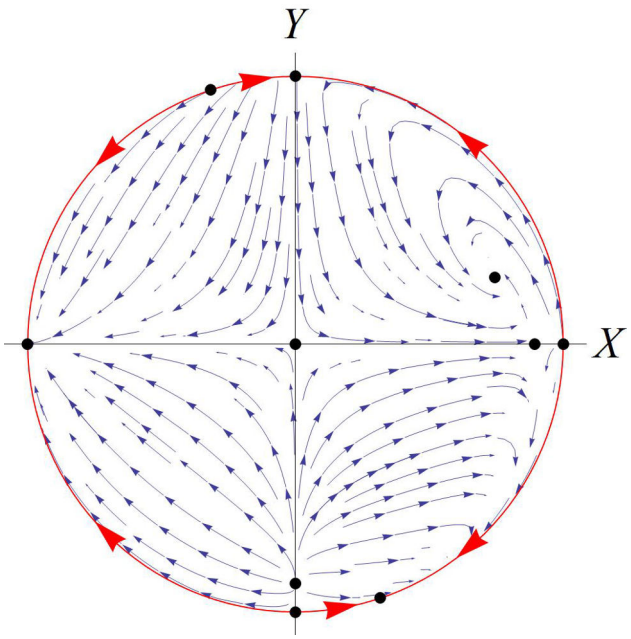

Figure 2.5: Global phase space for the dynamical system (2.67)–(2.68). The direction of the flow at infinity, i.e. on the circle, is indicated by the red/continous lines.

where the sign is determined by the direction of the flow on the equator (which corresponds to $z = 0$) near $\theta = 0$. This is counter-clockwise for $\theta > 0$ and clockwise for $\theta < 0$ meaning that on the equator $\theta = 0$ repels orbits. Then (2.77) restricted to $z = 0$ must give a local unstable point at $y = 0$, which is achieved only if the sign is negative in (2.77)–(2.78), i.e.

$$y' = \frac{1}{2} y(y - 4z + 3)\,, \tag{2.79}$$

$$z' = \frac{1}{2} z(2y - 2z + 1)\,. \tag{2.80}$$

Now we can compute the Jacobian of this system and find the eigenvalues at the origin which is the point corresponding to $\theta = 0$. These are given by $\lambda_1 = 1/2$ and $\lambda_2 = 3/2$ meaning that this is an unstable point.

The flow on the Poincaré sphere projected on the $Z = 0$ plane has been drawn in Fig. 2.5. This standard plotting is called the *global portrait of the phase space* since it includes critical points both finite and at infinity. The direction of the flow at infinity, i.e. on the equator of the Poincaré sphere, has been delineated with red/arrowed lines at the boundary of the unit disk. Note that point $(1, 0)$ is indeed an unstable point as we predicted from our calculation.

2.8 Perspectives for applications

The theory of dynamical systems can be used as a powerful tool in analyzing systems of differential equations which cannot be easily integrated. For this reason it is successfully applied to describe the qualitative dynamics of several physical systems, including, as we will see, many cosmological systems. Furthermore dynamical systems are easy to integrate numerically, which means that their theory is of particular importance if one wants to employ numerical techniques. In other words, once the dynamics of a physical system is rewritten as a dynamical system, i.e. as an ODE, then using a mixture of simple theoretical results and numerical methods it is usually quite easy to determine the qualitative evolution of the system, i.e. its phase space portrait.

2D systems

In particular, the special results of Sec. 2.6 and 2.7 for 2D dynamical systems imply that one should not only be able to determine the complete local properties of the flow near critical points, but also its global evolution computing the asymptotic properties and the behavior at infinity. Of course numerical techniques can be of help at any stage, especially to determine the evolution far from any critical point. Moreover they can effectively be used to draw the local or global dynamics of the flow on a plane. For these reasons 2D dynamical systems are not only the simplest to analyze but also the simplest to visualize. Note that if one is interested in only a compact (and possibly invariant) subset of the phase space, there is no need to find the behavior of the flow at infinity. In fact the analysis at infinity is practically never performed even if the phase space at hand is the whole $\mathbb{R}^2$. This usually happens when the interesting features of a physical system are all determined by the local dynamics of the flow near a finite set of critical points and thus the dynamics of diverging orbits is commonly neglected.

3D systems

For 3D dynamical systems we cannot make use of the special results available for 2D systems. The local behavior of the flow near critical points cannot be characterized as one can do on the plane using the results for linear systems of Sec. 2.6. Nonetheless one should be able to determine the stability properties of critical points and, even if it is not possible to describe the global behavior of the system, the qualitative evolution can be obtained with the help of numerical techniques. Of course, if it is possible, one should identify any invariant set or asymptotic limit and verify their properties against the numerical integration. Once all the available information have been collected, no matter how few, it should be anyway possible to visualize the phase space portrait, at least locally, with the help of a 3D picture. In the end, for 3D dynamical systems we still have the possibility to understand what is going on using numerical techniques and suitable plots of the phase space.

Higher-dimensional systems

Unfortunately this cannot be done for higher-dimensional ($n > 3$) systems since it is not possible to effectively visualize the phase space with a

nice plot. Of course one could project any 3D or 2D subspace of the phase space and depict the dynamics restricted to such a subspace. However in such operation some information would inevitably be lost, no matter how many projections one draws. Moreover trajectories in such a subspace would intersect because of the motion in the hidden dimensions. Usually this practice is never considered unless there is some particular motivation to restrict the analysis to one of such subspaces. For dynamical systems with dimension bigger than three it is common to only study the local properties of the flow, such as finding the critical points and describing their stability, and then to look for physically interesting behaviors such as particular heteroclinic sequences or attractors. Of course numerical techniques can be employed to verify or just strengthen any conclusion which has been achieved.

In conclusion the use of dynamical systems theory mixed with numerical techniques can be successfully adopted in many different situations. On average, we will be able to obtain more results for lower dimensional systems and only fragmented information for higher dimensional ones. Having said so, the failure or success of such methods will obviously depend on the dynamical system under consideration. For a highly nonlinear system one could struggle to find the critical points even if the dimension is low, or complications can arise in the study of the linear stability of a particular critical point. In these cases one either relies on numerical techniques to find as much of information as possible, or restrict the analysis to subsets of physical interest, for example looking for critical points or orbits satisfying certain constraints.

Chapter 3

Cosmology, dark energy and the cosmological constant

Cosmology is the study of the large scale structures and dynamics of the universe. Its primary scope is to understand the origin, the fate and the evolution of the universe as a whole. The fundamental theory used to describe the physics of such long distances is *general relativity*. In this chapter, and in the rest of the thesis, it will be assumed that the reader has a sufficient knowledge of general relativity, though no advanced concepts will be necessary. For some classics books on general relativity we refer to Schutz (1985); Wald (1983); Weinberg (1972).

The present chapter will introduce the basic concepts used in cosmology and will present the physical motivations which will lead us to the study of theoretical models of dark energy in the remaining part of the thesis. The emphasis will be on the physical motivations and phenomenological observations rather than on the mathematical technicalities. Moreover the discussion will be focused on late time cosmology, i.e. on the evolution of the universe at relatively recent times. This implies the exclusion of several important issues regarding the physics of the very early universe. The reader interested in more details and applications about the physics and mathematics of cosmology can refer to well known textbooks such as Dodelson (2003); Mukhanov (2005); Weinberg (2008).

The chapter is organized in the following way. In Sec. 3.1 the fundamental principles and equations employed in cosmology will be reviewed and discussed. Sec. 3.2 will be devoted to the description of the observed expanding universe and to the developing of the cosmological Big Bang theory. The recent discovery of cosmic acceleration and consequent introduction of dark energy is the argument of Sec. 3.3. Finally Secs. 3.4 and 3.5 focus on the concept of the cosmological constant, first showing how it can account for the observed cosmic acceleration (Sec. 3.4) and then discussing theoretical and phenomenological problems connected to its measured value (Sec. 3.5).

The physical and phenomenological issues presented in this chapter will constitute the background motivations on which the subsequent chapters will be based.

3.1 Elements of FRW cosmology

Cosmological principle

Modern cosmology is based on the so-called *cosmological principle* (sometimes *Copernican principle*) which states that at sufficiently large scales ($\sim 10^8$ light years) the universe is assumed to be homogeneous and isotropic[1]. In other words the principle asserts that the Earth does not occupy a special position in the universe. The cosmological principle is the basic assumption of cosmology and cannot be tested experimentally, at least not with the current technological possibilities. In fact, even if from the Earth's point of view the universe is observed to be highly isotropic, the homogeneity condition cannot be verified by observations obtained from a single cosmic location. It requires isotropy from two different points, separated by a cosmological distance, in order to verify the homogeneity of the universe. Nonetheless the principle is presumed to be true so that the universe can be studied within a scientific perspective, but ultimately it will be the agreement with observations which will confirm its validity.

FRW metric

The cosmological principle implies that the universe is highly symmetric. A four dimensional manifold with such symmetries must possess the maximally spatially symmetric *Friedmann-Robertson-Walker (FRW) metric* (sometimes called *FLRW metric* to include Lemaître); see Wald (1983) or Weinberg (1972). In pseudo-spherical[2] coordinates (t, r, θ, φ) centred at any point of the universe, the line element of the FRW metric reads

$$ds^2 = -dt^2 + a(t)^2 \left(\frac{dr^2}{1 - k\, r^2} + r^2 d\theta^2 + r^2 \sin\theta \, d\varphi^2 \right) , \qquad (3.1)$$

Scale factor

where $k = -1, 0, +1$ is the spatial curvature and $a(t) > 0$ is a function of the time coordinate called the *scale factor*. If $k = 1$ we say that the universe is (spatially) closed, if $k = -1$ we say that it is (spatially) open and if $k = 0$ we say it is (spatially) flat. The coordinates (r, θ, φ) are referred to as comoving coordinates: an observer at rest in these coordinates remains at rest, i.e. at constant r, θ, and φ for all time t. The scale factor $a(t)$ linearly relates to spatial lengths in the universe. For example the radial distance $(dt = d\theta = d\varphi = 0)$ between two point A and B in the universe is given by

$$L_{AB} = \int_A^B ds = a(t) \int_A^B \frac{dr}{\sqrt{1 - kr^2}} \, . \qquad (3.2)$$

[1] As seen by comoving observers; more below.

[2] The coordinates (r, θ, φ) coincides with actual spherical coordinates only for the case $k = 0$, but for $k \neq 0$ they represent a more general system of coordinates.

The last integral measures radial distances in a close, open or flat universe. In the simplest case $k = 0$ we obtain $L_{AB} = a(t)(r_B - r_A)$. Eq. (3.2) shows how the separation between two points in the universe evolves in time due to the presence of the scale factor. In other words, the larger is the scale factor the further away will be points in the universe.

The dynamics of the metric tensor $g_{\mu\nu}$, i.e. of the gravitational potential, at cosmological scales is described by the *Einstein field equations*

Einstein field equations

$$R_{\mu\nu} - \frac{1}{2} R\, g_{\mu\nu} = \kappa^2\, T_{\mu\nu}\,, \tag{3.3}$$

where $R_{\mu\nu}$ is the *Ricci tensor*, $R = g^{\mu\nu} R_{\mu\nu}$ is the *Ricci* or *curvature scalar*, $T_{\mu\nu}$ is the *energy-momentum tensor* of matter sources and $\kappa^2 = 8\pi G/c^4$. Matter inside a homogeneous and isotropic universe can be described, at large scales and with high precision, as a *perfect fluid*. Its energy-momentum tensor is solely determined by its energy density $\rho(t)$ and isotropic (no shear nor viscosity) pressure $p(t)$:

Perfect fluid energy-momentum tensor

$$T_{\mu\nu} = p\, g_{\mu\nu} + (\rho + p)\, u_\mu u_\nu\,, \tag{3.4}$$

where the vector u^μ denotes the four-velocity of an observer comoving with the fluid and in comoving coordinates reads $u^\mu = (-1, 0, 0, 0)$. The energy density and pressure of the matter fluid are related by an *equation of state* $p = p(\rho)$ (referred to as EoS). For perfect fluids the equation of state is always a linear relation

Equation of state (EoS)

$$p = w\, \rho\,, \tag{3.5}$$

where w is called the *equation of state parameter*. For a non-relativistic (dust-like) perfect fluid $w = 0$, while for a relativistic (radiation-like) fluid $w = 1/3$. Values outside the $[0, 1/3]$ range are not permitted by the known macroscopic physics, though, as we will see, some phenomenological models rely on non-physical values of w in order to match the astronomical observations.

The *cosmological equations* arising from the Einstein field equations (3.3) with the FRW metric ansatz (3.1) consist in two coupled differential equations for the scale factor $a(t)$ and the matter variables $\rho(t)$ and $p(t)$. The *Friedmann equation* (or *Friedmann constraint*) follows from the time-time component of the Einstein field equation and can be written as

Friedmann equation

$$\frac{k}{a^2} + H^2 = \frac{\kappa^2}{3}\rho\,, \tag{3.6}$$

where the *Hubble rate* (or *parameter*) is defined as

$$H = \frac{\dot{a}}{a}\,, \tag{3.7}$$

with an over-dot denoting differentiation with respect to t. On the other hand, from the spatial (diagonal) components of the Einstein field equations we obtain the *acceleration equation*

$$\frac{k}{a^2} + 2\dot{H} + 3H^2 = -\kappa^2 p\,. \tag{3.8}$$

The cosmological equations (3.6) and (3.8) determine the evolution of the scale factor $a(t)$ once an equation of state relating ρ and p has been assumed.

Acceleration equation

Using the Friedmann equation (3.6), the acceleration equation (3.8) can be rewritten as

$$\frac{\ddot{a}}{a} = -\frac{\kappa^2}{6}\left(\rho + 3p\right)\,, \tag{3.9}$$

which is sometimes called the *Raychaudhuri equation*. Note that from (3.9) we can obtain a condition on the matter variables that discriminates between an accelerating and a decelerating universe depending on the sign of $\ddot{a}$. If $\rho + 3p > 0$ the universe is decelerating, while if $\rho + 3p < 0$ the universe is accelerating. If the linear equation of state (3.5) holds, the condition can be transferred to the equation of state parameter implying $w > -1/3$ for deceleration and $w < -1/3$ for acceleration. The matter physically meaningful values included between 0 and 1/3 always describe a decelerating universe.

Energy conservation equation

From the conservation of the energy-momentum tensor $\nabla_\mu T^{\mu\nu}$, or equivalently from equations (3.6) and (3.8), we can derive the *energy conservation equation* for the matter fluid

$$\dot{\rho} + 3H\left(\rho + p\right) = 0\,, \tag{3.10}$$

expressing the conservation of energy through the evolution of the universe. If a linear equation of state (3.5) is assumed, the conservation equation (3.10) provides the following solution of ρ in terms of a:

$$\rho \propto a^{-3(w+1)}\,. \tag{3.11}$$

For a dust-like fluid, usually referred to as simply *matter fluid*, we have $p_m = 0$ and thus

$$\rho_m \propto a^{-3} \qquad \text{for } \textit{matter}\,, \tag{3.12}$$

while for a radiation-like fluid $p_r = \rho_r/3$ and thus

$$\rho_r \propto a^{-4} \qquad \text{for } \textit{radiation}\,. \tag{3.13}$$

Note that the energy density of non-relativistic matter scales as the comoving three-dimensional volume of the universe: $\rho_m \propto a^{-3} = \mathrm{Vol}^{-1}$. To find the expression of a in time, one has to substitute these solutions into (3.6) and solve the resulting first order differential equation for a. In Sec. 3.2 we will obtain the solutions for a flat universe.

To conclude this section we discuss the possibility of multiple fluids sourcing the cosmological equations. If the total energy-momentum tensor $T_{\mu\nu}$ in the Einstein field equations (3.3) is composed by more than one matter component, e.g. $T_{\mu\nu} = T^{(1)}_{\mu\nu} + T^{(2)}_{\mu\nu}$, the conservation equation $\nabla^\mu T_{\mu\nu} = 0$ will only imply the conservation of the total energy and momentum of the fluids. The energy and momentum of a single fluid component might not be conserved due to possible interactions with the other fluid components. For two fluids $T^{(1)}_{\mu\nu}$ and $T^{(2)}_{\mu\nu}$ sourcing the Einstein field equations we can generally write

$$\nabla^\mu T^{(1)}_{\mu\nu} = Q_\nu \quad \text{and} \quad \nabla^\mu T^{(2)}_{\mu\nu} = -Q_\nu \,, \tag{3.14}$$

where Q_ν denotes the energy-momentum exchanged between the two fluids. If $Q_\nu = 0$ there is no exchange between the two fluids and they evolve without interacting. The specification of Q_ν is an assumption regarding the physical properties of the two fluids that must be taken into account in order to solve the field equations. Without this assumption the dynamics of the single components of the fluid cannot be found from the Einstein field equations only. Note that the total energy-momentum is always conserved

$$\nabla^\mu T_{\mu\nu} = \nabla^\mu \left(T^{(1)}_{\mu\nu} + T^{(2)}_{\mu\nu} \right) = 0 \,. \tag{3.15}$$

Of course if there are more than two fluids sourcing the Einstein field equations we will need more than one exchange vector Q_ν. In general if there are n fluids we must specify $n-1$ exchange vectors in order to fully determine the dynamics of the system.

3.2 The expanding universe: the Big Bang theory

Throughout the 20th century a number of observations have been collected in favor of a current expanding dynamics of the universe; see e.g. Weinberg (2008). Nowadays we know for sure that at the present time $\dot{a} > 0$, or equivalently $H > 0$. From these observations we can immediately draw an important conclusion regarding the origin of our universe. In fact assuming that the universe is filled only with standard (baryonic) matter satisfying the $\rho + 3p > 0$ constraint at all times, then from (3.9) we obtain that the universe must have been expanded for all its past history and at some point in the past the condition $a = 0$ must have occurred.

In order to prove this statement, consider Eq. (3.9). If the condition $\rho + 3p > 0$ holds for all $t < t_0$ with t_0 the present cosmological time, then also the condition $\ddot{a}(t) < 0$ must hold for $t < t_0$. Integrating the latter condition we find

$$\int_t^{t_0} \ddot{a}(t')dt' = \dot{a}(t_0) - \dot{a}(t) < 0 \,, \tag{3.16}$$

which implies

$$\dot{a}(t) > \dot{a}(t_0) > 0 \qquad \forall\, t < t_0\,. \tag{3.17}$$

This tells us that since $\dot{a} > 0$ today, then $\dot{a}(t) > 0$ always in the past. If we now integrate again Eq. (3.16) we find

$$\int_t^{t_0} \left[\dot{a}(t_0) - \dot{a}(t')\right] dt' = \dot{a}(t_0)\,(t_0 - t) - a(t_0) + a(t) < 0\,, \tag{3.18}$$

implying

$$a(t) < a(t_0) + \dot{a}(t_0)\,(t - t_0) \qquad \forall\, t < t_0\,. \tag{3.19}$$

This last constraint tells us that at a time $t_* = t_0 - a(t_0)/\dot{a}(t_0) = t_0 - 1/H_0$, $a(t_*)$ is negative. Moreover $t_* < t_0$, since both $a(t_0)$ and $\dot{a}(t_0)$ (i.e. H_0) are positive. Hence at some time t_{BB} between t_* (where $a(t_*) < 0$) and t_0 (where $a(t_0) > 0$) the function $a(t)$ must achieve the condition $a(t_{BB}) = 0$, which proves our statement.

Big Bang theory

The time when the condition $a = 0$ happened is called the *Big Bang* and the theory describing the universe as generating from that moment is known as the *Big Bang theory*. Note that if distances were really small in the past, then all the matter and energy content of the universe were constrained into a small amount of space and consequently the mean energy (or temperature) was much more higher than the mean energy observed today. This not only allows for the light elements (hydrogen, helium, ...) to be created but also, as the universe cooled down and gravity began to dominate, for the formation of cosmological structures (galaxies, stars, ...). The Big Bang theory is indeed in astonishing agreement with observations and it is considered a perfectly good model of our universe for times ranging from few fractions of a second to billion of years (i.e. today) after the Big Bang.

On the other hand, from recent astronomical observations[3] strong constraints on the measured value of the spatial curvature k has been collected, implying that today $k \simeq 0$. From the Friedmann equation (3.6) we can then conclude that k has been always near zero through all the history of the universe. The argument goes as follows. Rewriting the Friedmann constraint as

$$\frac{\kappa^2 \rho}{3H^2} - 1 = \Omega - 1 = \frac{k}{\dot{a}^2}\,, \tag{3.20}$$

the condition $k \simeq 0$ translates to the condition $\Omega \simeq 1$, which is actually what we measure from the observations. However since $\dot{a}$ is always decreasing with time, then the right hand side of (3.20) is always increasing meaning that if at some moment in the history of the universe $\Omega \simeq 1$, then before that moment Ω will result even closer to 1. This implies that if the observed

[3] Mostly CMB measurements: the recent WMAP (Hinshaw et al., 2013) and Planck (Ade et al., 2013) missions constrain k to be zero within an error of the order of 10^{-3}.

value of Ω today is basically one, in the past it was much closer to 1 and thus we can safely assume that $k = 0$ from the Big Bang to now[4].

With this in mind we can now find the evolution of the scale factor a for the matter and radiation dominated universes, which represent the two fluid components we can directly observe in the universe. Substituting (3.12) and (3.13) into the Friedmann equation (3.6) and then solving for $a(t)$ yields

$$a(t) \propto t^{2/3} \quad \text{for } \textit{matter}, \tag{3.21}$$

$$a(t) \propto t^{1/2} \quad \text{for } \textit{radiation}. \tag{3.22}$$

A matter dominated universe expands faster than a radiation dominated universe, but for both of them $\ddot{a} < 0$ at any time meaning that the expansion is always decelerating. More generally for any matter fluid with a linear equation of state $\rho = wp$, substituting (3.11) into the Friedmann equation (3.6) with $k = 0$ leads to the solution

$$a(t) \propto t^{\frac{2}{3(w+1)}}, \tag{3.23}$$

which of course reduces to (3.21) or (3.22) if $w = 0$ or $w = 1/3$, respectively.

The standard Big Bang theory requires a radiation dominated epoch followed by a matter dominated phase because at high energies the radiation component dominates over the matter one, but at low energies it is the other way around. Indeed, as can be seen from (3.12) and (3.13), the energy density of radiation decays faster than the matter one as a expands. At some point, called the radiation to matter transition, in the history of the universe, the matter energy will eventually be higher than the radiation energy and will remain so thereafter. The model assumes that no appreciable interaction occurs between the radiation and matter fluids, or, in terms of (3.14), that $Q_\mu = 0$. Solving such a system of equations will always lead to (3.12) and (3.13) but the scale factor will now evolve in time following first (3.21) and then (3.22).

We can understand this with a simple application of dynamical system theory. Consider the dimensionless variables

$$x = \Omega_m = \frac{\kappa^2 \rho_m}{3H^2} \quad \text{and} \quad y = \Omega_r = \frac{\kappa^2 \rho_r}{3H^2}. \tag{3.24}$$

Thanks to the physical assumptions $\rho_m > 0$ and $\rho_r > 0$, we obtain the constraint $x > 0$ and $y > 0$ which restrict the physical phase space in the (x, y)-plane. Moreover the Friedmann equation (3.6) now reads

$$1 = x + y, \tag{3.25}$$

[4]The origin of the observed flatness of the universe can be explained by taking into account an *inflationary phase* in the very early universe; see e.g. Bassett et al. (2006); Riotto (2002); Linde (1990); Mukhanov (2005).

meaning that the two variables are not independent and that the analysis can be reduced to a 1D dynamical system. Note also that since $x > 0$ and $y > 0$ the Friedmann constraint (3.25) implies $x < 1$ and $y < 1$. Thus we just need to consider one of the two variables, say x, in the physical domain $x \in [0, 1]$.

To find the differential equation governing the dynamical system, we derive the variable x with respect to $\eta = \log a$ (i.e. $d\eta = Hdt$):

$$\frac{dx}{d\eta} = \frac{1}{H}\frac{dx}{dt} = \frac{\kappa^2\dot{\rho}_m}{3H^3} - \frac{2\rho_m}{3H^2}\frac{\dot{H}}{H}\,. \tag{3.26}$$

The terms $\dot{\rho}_m$ and $\dot{H}/H^2$ can be found from Eq. (3.8) and the relation (3.12) respectively as

$$\dot{\rho}_m = -3H\rho_m\,, \quad \text{and} \quad \frac{\dot{H}}{H^2} = -\frac{3}{2} - \frac{\kappa^2\rho_r}{6H^2} = -\frac{3}{2} - \frac{y}{2}\,, \tag{3.27}$$

where the assumption $p = p_r = \rho_r/3$ has been used. Inserting these back into Eq. (3.26) yields

$$\begin{aligned}\frac{dx}{d\eta} &= -3\frac{\kappa^2\rho_m}{3H^2} - 2\frac{\kappa^2\rho_m}{3H^2}\left(-\frac{3}{2} - \frac{\kappa^2\rho_r}{6H^2}\right) \\ &= -3x + 2x\left(\frac{3}{2} + \frac{y}{2}\right)\,,\end{aligned} \tag{3.28}$$

which thanks to the Friedmann constraint $y = 1 - x$ gives the following 1D dynamical system

$$x' = f(x) = -x\,(1 - x)\,, \tag{3.29}$$

where a prime denotes differentiation with respect to η.

A solution of this dynamical system gives us the evolution of x, or in other words of the relative energy density of matter. The time parameter η is a dimensionless measure of time which measure the universe expansion in logarithmic units. A solution $x(\eta)$ of (3.29) will give us the evolution of Ω_m in terms of a. The complete solution in terms of t will depend on the initial condition of the universe and in general it is difficult to find analytically. However note that at any critical point x_c, the acceleration equation (3.8) will give us

$$\frac{\dot{H}}{H^2} = \frac{x_c - 4}{2}\,. \tag{3.30}$$

Since x_c is constant we can solve this equation and obtain $H = 2/[(4 - x_c)(t - t_0)]$ with t_0 a constant of integration. Finally from $H = \dot{a}/a$ we find

$$a(t) \propto (t - t_0)^{\frac{2}{4 - x_c}}\,, \tag{3.31}$$

where $t_0 = 0$ if the Big Bang initial condition $a(0) = 0$ is enforced. This implies that at any critical point the universe is expanding according to

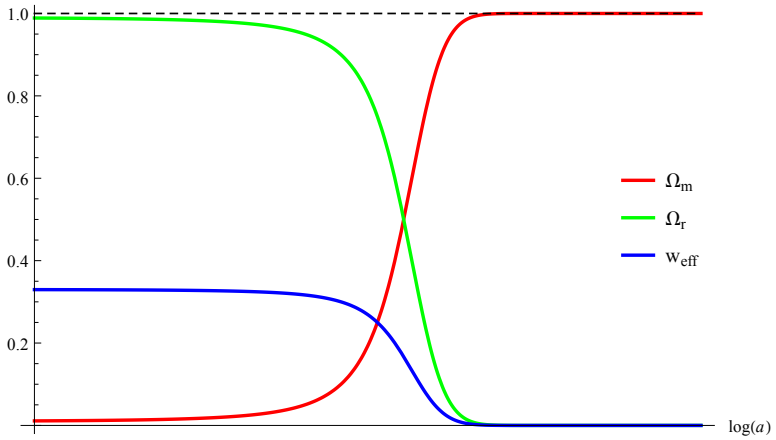

Figure 3.1: Evolution of the relative energy density of matter (Ω_m) and radiation (Ω_r) together with the effective equation of state parameter (w_{eff}) of a universe filled with radiation and matter fluids.

the power-law evolution given by (3.31). We may not find the complete evolution of the universe at any t, but we will certainly know its asymptotic states, since these are given by critical points of the system (3.29).

The only two critical points of the dynamical system (3.29) are obviously $x = 0$ and $x = 1$. The first one is an unstable point ($f'(0) = 1$), while the second one is a stable point ($f'(1) = -1$) and constitutes the future attractor of the physical phase space. Of course $x = 0$ corresponds to a radiation dominated universe ($y = 1$), while $x = 1$ corresponds to a matter dominated universe ($y = 0$). This can also be understood form (3.31) which gives (3.21) for $x = 1$ and (3.22) for $x = 0$. The evolution in the physical phase space always starts ($a \to 0$) from a radiation dominated universe ($\Omega_m = 0$ and $\Omega_r = 1$) and ends ($a \to +\infty$) in a matter dominated universe ($\Omega_m = 1$ and $\Omega_r = 0$) as shown in Fig. 3.1. The effective equation of state parameter of the universe defined as $w_{\text{eff}} = w_m\Omega_m + w_r\Omega_r = \Omega_r/3 = y/3$ will then start from a value of $1/3$ and then drops to zero as the matter component begins to dominate; see Fig. 3.1. Note that the value of w_{eff} in terms of x can also be found comparing (3.31) with (3.23), which clearly agrees with the one just defined.

3.3 The accelerating universe: dark energy and dark matter

With the standard picture of the universe coming from the Big Bang theory described in Sec. 3.2, one should expect to measure a current deceleration of the universe, i.e. to observe $\ddot{a} < 0$. In 1998 however it was surprisingly dis-

covered, first with supernovae surveys (Riess et al., 1998; Perlmutter et al., 1999) and subsequently with other observations (see Astier & Pain (2012) for a review), that the universe is actually *accelerating*. This unexpected observation led to a number of speculations regarding the physical mechanisms needed to explain the phenomenon.

From (3.9) we can immediately realize that for the universe to accelerate, $\ddot{a} > 0$, there must be a cosmological fluid satisfying $\rho + 3p < 0$. A type of matter with such properties has never been observed in experiments involving only standard (baryonic) matter. In other words it is impossible to build a macroscopic form of matter behaving such that $\rho + 3p < 0$ considering only particles of the Standard Model, which constitute the fundamental blocks of all the matter we detected so far. There must be some other fluid component in the universe which cannot be directly observed in nowadays experiments and such that it allows the universe to accelerate at late, i.e. relatively recent, times. This entity has been named *dark energy*.

Dark energy

Dark energy does not interact with the nuclear and electromagnetic fields and does not cluster, i.e. it does not form any structure under the influence of gravity. This implies that rather than being some new particle or type of matter, dark energy is much probably due to new fundamental physics which has still to be discovered. This is something which it does not share with another cosmological matter component which has yet to be directly observed: *dark matter*.

Dark matter

Dark matter is a (yet) undetected kind of matter which must be present at galactic and cosmological scales in order to fit the astronomical data; see e.g. Ade et al. (2013); Clowe et al. (2006); Weinberg (2008). Specifically the rotation curves of galaxies and bigger clusters are not in agreement with the theoretical predictions derived from Newtonian mechanics. More mass is needed in order for these curves to have the observed behavior, but this mass cannot be detected with electromagnetic interaction since it seems to neither emit nor absorb light.

Considering the whole picture we obtain from cosmological and astrophysical observations, there are (at least) two invisible components, dark matter and dark energy, which constitutes part of the total energy density of the universe. They represent around 95% of the total matter present in the universe: $\sim 30\%$ is dark matter and $\sim 65\%$ is dark energy (Ade et al., 2013), with the remaining 5% being standard (baryonic) matter; see Fig. 3.2. These two new form of matter and energy do not or weakly interact with the electromagnetic field and thus it is extremely difficult to observe them directly. On one hand dark matter seems to cluster and behaving as dust (pressure-less matter) suggesting that it may be given by yet undetected particles beyond the Standard Model. On the other hand dark energy does not cluster and must satisfy the constraint $\rho + 3p < 0$ which, assuming the energy to be always positive, requires the introduction of some kind of *negative pressure*. This seems to call for new physics in order to explain the

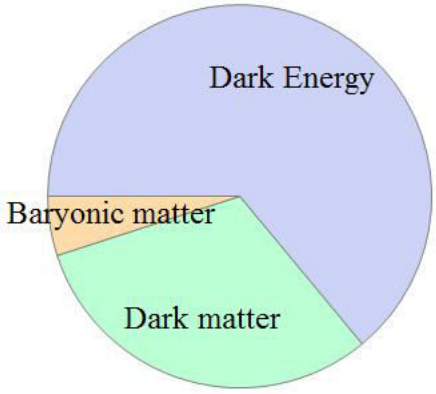

Figure 3.2: Present distribution of matter and energy in the universe: dark energy ($\sim 65\%$), dark matter ($\sim 31\%$) and baryonic matter (atoms) ($\sim 5\%$).

mystery of dark energy.

There are three major approaches to account for dark energy: the *cosmological constant*, *particle physics* and *modified gravity*. The cosmological constant approach represents the simplest model of dark energy where the introduction of a single parameter is enough to fit all the astronomical data. The cosmological constant will be reviewed in details in Secs. 3.4 and 3.5. The other two explanations consider a much more complicated dynamics at cosmological scales. The particle physics approach assumes the existence of a new particle, usually a scalar field[5], responsible for accelerating the universe at late times. On the other hand the modified gravity idea suggests that the gravitational interaction at cosmological distances is not well described by general relativity and that a new gravitational theory is needed in order to explain the acceleration of the universe. Since the cosmological dynamics for both the particle physics and modified gravity approaches is quite complicated, they represent perfect subjects for the applications of dynamical systems. Their analysis will then be left for the remaining chapters of this thesis.

3.4 The cosmological constant

The concept of cosmological constant was first introduced by Einstein himself in order to construct a cosmological model for a static universe. After the discovery of the expansion of the universe, the cosmological constant

[5]Note that fundamental scalar fields have never been observed before the recent discovery of the Higgs boson which lead to the award of the 2013 Nobel Prize for physics.

has been almost forgotten due to the fact that its contribution is not necessary to achieve a dynamical expansion in FRW cosmology; see Secs. 3.1 and 3.2. However after the 1998 observation that the universe is accelerating, the cosmological constant has been revived as a model of dark energy. In what follows we review the dynamics of a universe with a non vanishing cosmological constant. For more details on the physics of the cosmological constant we refer the reader to Carroll (2001) or Martin (2012).

The cosmological constant is introduced as a new term in the Einstein field equations (3.3), which now read

$$R_{\mu\nu} - \frac{1}{2} R\, g_{\mu\nu} + \Lambda\, g_{\mu\nu} = \kappa^2\, T_{\mu\nu}\,, \tag{3.32}$$

Cosmological constant

where Λ is indeed the *cosmological constant*. Note that unless the value of Λ is really small, practically unmeasurable at solar system scales, the Einstein field equations (3.32) do not possess the right Newtonian limit[6]. However the value of Λ needed to match the cosmological observations is of the order

$$\Lambda \simeq 10^{-52}\,\mathrm{m}^{-2}\,, \tag{3.33}$$

which is in any case sufficiently small to be safely neglected at solar system distances. Note that, according to (3.33), the cosmological constant has a positive value which is the sign needed to drive a late time accelerating phase in the universe, as we are now going to see.

Considering again the FRW metric (3.1) with vanishing spatial curvature ($k = 0$), from the new field equations (3.32) we obtain the following cosmological equations

$$3H^2 = \kappa^2 \rho + \Lambda\,, \tag{3.34}$$

$$2\dot{H} + 3H^2 = -\kappa^2 p + \Lambda\,, \tag{3.35}$$

which generalize the Friedmann equation (3.6) and the acceleration equation (3.8). Note that from these equations we can equally see the contribution of the cosmological constant as a constant energy fluid with $\rho_\Lambda = \Lambda/\kappa^2$ and $p_\Lambda = -\rho_\Lambda$. The EoS parameter of the cosmological constant has thus the constant value $w_\Lambda = -1$. From these considerations the cosmological constant can be seen as a matter cosmological component (dark energy) with constant energy density and negative pressure. The physical motivations and implications of this new matter component will be briefly discussed in Sec. 3.5. For the moment we will focus on the dynamics arising from a universe with a non vanishing Λ.

If the cosmological constant completely dominates in the evolution equations (3.34) and (3.35), meaning that the other matter contributions can be

[6] One can immediately realize this noting that the Minkowski metric is no longer a solution of (3.32).

neglected ($\rho = 0$ and $p = 0$), then one immediately obtain the solution

$$a(t) \propto e^{Ht} \quad \text{with} \quad H = \sqrt{\frac{\Lambda}{3}}\,, \tag{3.36}$$

which is known as the *de Sitter solution*[7]. In such a universe we have that the scale factor expands exponentially, meaning that the condition $\ddot{a} > 0$ is always satisfied and there is a never-ending accelerating phase. Of course this solution cannot be used as a realistic model for our universe, since we know that at early times a radiation and then matter dominated phases must have occurred. However it can be used as an asymptotic solution at late times. A universe evolving according to the Big Bang theory for a sufficiently long time and then switching to a de Sitter expansion could be an accurate description for the observed dynamics at cosmological scales.

de Sitter solution

For this reason we will now solve the cosmological equations (3.34) and 3.35) for a non vanishing matter contribution with a linear equation of state ($\rho > 0$ and $p = w\rho$). There are two ways to solve these equations. The first strategy is to rely on the conservation equation (3.10) which again follows combining (3.34) and (3.35). The solution of ρ in terms of a is thus given again by (3.11), i.e.

$$\rho \propto a^{-3(1+w)}\,. \tag{3.37}$$

Plugging this back into (3.34) will provide a differential equation for a which must be solved in order to find the solution. The second way consists in eliminating ρ from equations (3.34)–(3.35) and then solve the resulting differential equation for H. Once the solution of H in terms of t has been found, one can obtain the evolution of a solving $H = \dot{a}/a$.

No matter what way one follows, the physical solution (no negative energies and $a(0) = 0$) for the scale factor will eventually be

$$a(t) \propto \left[\sinh\left(Ct\right)\right]^{\frac{2}{3(w+1)}}\,, \tag{3.38}$$

where C is a constant. Note that at early and late times this solution has the right asymptotic behavior expected from matter and cosmological constant domination, respectively. In more mathematical terms we have that

$$a(t) \propto t^{\frac{2}{3(w+1)}} \qquad \text{as} \quad t \to 0\,, \tag{3.39}$$

$$a(t) \propto \exp\left[\frac{2Ct}{3(w+1)}\right] \qquad \text{as} \quad t \to +\infty\,, \tag{3.40}$$

which correspond, respectively, to the perfect fluid solution (3.23) and to the cosmological constant solution (3.36), with the identification $H = 2C/(3(w+1))$. Solution (3.38) can thus well describe the observed universe which must

[7] The de Sitter solution is actually a *static* solution, i.e. invariant under time translations $t \mapsto t + t_0$, as can be shown with a suitable coordinate transformation.

decelerate at early times and accelerate at late times. This means that a universe filled with a cosmological constant and some matter fluid represents a well motivated model which is able to agree with the observations.

Note that in (3.38) the matter EoS parameter has been left arbitrary. We can choose to have an early universe dominated by matter ($w = 0$), radiation ($w = 1/3$) or any other kind of fluid. Usually w is set to zero in order to have a matter dominated phase followed by a dark energy dominated epoch, which aims at characterizing the late time behavior of our universe. It is not possible to describe a two fluid universe with the solution (3.38) and in fact the radiation to matter transition happening at early times is overlooked in this model. However using dynamical system techniques we are able to analyze a cosmological constant universe filled with both matter and radiation. This is a simple and elegant generalization of what we have done in Sec. 3.2 as we are going to explain.

Consider the cosmological equations (3.34) and (3.35) with both matter ($p_m = 0$) and radiation ($p_r = \rho_r/3$):

$$3H^2 = \kappa^2\rho_m + \kappa^2\rho_r + \Lambda\,, \tag{3.41}$$

$$2\dot{H} + 3H^2 = -\frac{\kappa^2}{3}\rho_r + \Lambda\,. \tag{3.42}$$

Employing again the x and y variables first defined in (3.24), we can rewrite the Friedmann equation (3.41) as

$$1 = x + y + \Omega_\Lambda\,. \tag{3.43}$$

where $\Omega_\Lambda = \Lambda/(3H^2)$ is the relative energy density of the cosmological constant, i.e. of dark energy. Given that we are assuming a positive Λ, this equation implies that the constraint $x + y \leq 1$ must hold. Adding the fact that $x \geq 0$ and $y \geq 0$, the physically meaningful dynamics in the (x, y)-plane happens inside the triangle with vertices the origin $(0, 0)$, Point $(1, 0)$ and Point $(0, 1)$; see Fig. 3.3. Now, due to the presence of the cosmological constant term, the Friedmann constraint (3.43) does not reduce the phase space from two to one dimensions, but it only restricts it to the triangle just described. This triangle constitutes an invariant set of the whole phase space which will be called the *physical invariant set* or simply the *physical phase space*.

Physical phase space

To obtain the dynamical system, we derive the variable x and y with respect to $\eta = \log a$ ($d\eta = H dt$):

$$x' = \frac{dx}{d\eta} = \frac{1}{H}\frac{dx}{dt} = \frac{\kappa^2\dot{\rho}_m}{3H^3} - \frac{2\kappa^2\rho_m}{3H^2}\frac{\dot{H}}{H}\,, \tag{3.44}$$

$$y' = \frac{dy}{d\eta} = \frac{1}{H}\frac{dy}{dt} = \frac{\kappa^2\dot{\rho}_r}{3H^3} - \frac{2\kappa^2\rho_r}{3H^2}\frac{\dot{H}}{H}\,. \tag{3.45}$$

Point	x	y	w_{eff}	Eigenvalues	Stability
O	0	0	-1	$\{-4,-3\}$	Stable point
R	0	1	1/3	$\{1,4\}$	Unstable point
M	1	0	0	$\{-1,3\}$	Saddle point

Table 3.1: Critical points of the dynamical system (3.49)–(3.50) and their properties.

Assuming again that matter and radiation do not interact ($Q_\nu = 0$), from the conservation equation (3.10) for the two fluids we obtain

$$\dot{\rho}_m + 3H\rho_m = 0 \quad \rightarrow \quad \dot{\rho}_m = -3H\rho_m \,, \tag{3.46}$$

$$\dot{\rho}_r + 4H\rho_r = 0 \quad \rightarrow \quad \dot{\rho}_r = -4H\rho_r \,, \tag{3.47}$$

where the assumptions $p_m = 0$ and $p_r = 1/3$ have been considered. The acceleration equation (3.42) yields instead

$$\frac{\dot{H}}{H^2} = -\frac{3}{2} - \frac{\kappa^2\rho_r}{6H^2} + \frac{\Lambda}{2H^2} = -\frac{1}{2}\left(3 - y - 3\Omega_\Lambda\right) . \tag{3.48}$$

Substituting these results into (3.44)–(3.45) and using the Friedmann constraint (3.43) produces the following 2D dynamical system[8]

$$x' = x\left(3x + 4y - 3\right) , \tag{3.49}$$

$$y' = y\left(3x + 4y - 4\right) , \tag{3.50}$$

where a prime means again differentiation with respect to $\eta = \log a$.

There are three critical points: $O = (0,0)$, $R = (0,1)$ and $M = (1,0)$. Performing the linear stability analysis near the critical point we find that the eigenvalues of the Jacobian are $\{-4,-3\}$ at O, $\{1,4\}$ at R and $\{-1,3\}$ at M. This implies that the origin is a stable point (simple attracting node), R is an unstable point (simple repelling node) and M is a saddle point. The effective EoS parameter $w_{\text{eff}} = \Omega_r/3 - \Omega_\Lambda = -1 + x + 4y/3$ takes the values -1 in O, $1/3$ in R and 0 in M, meaning that these points correspond to a cosmological constant (dark energy) dominated universe, a radiation dominated universe and a matter dominated universe, respectively. For the sake of simplicity all the properties of the critical points have been summarized in Table 3.1.

The physical phase space for the system (3.49)–(3.50) has been plotted in Fig. 3.3. Point R is clearly the past attractor while the origin represents

[8]Note that equations (3.49)–(3.50) represent nothing but a simple Lokta-Volterra system. Perez et al. (2013) generalised this analysis to non-flat universes filled by general barotropic fluids showing that cyclic orbits and chaos can arise in the presence of interaction between the fluids.

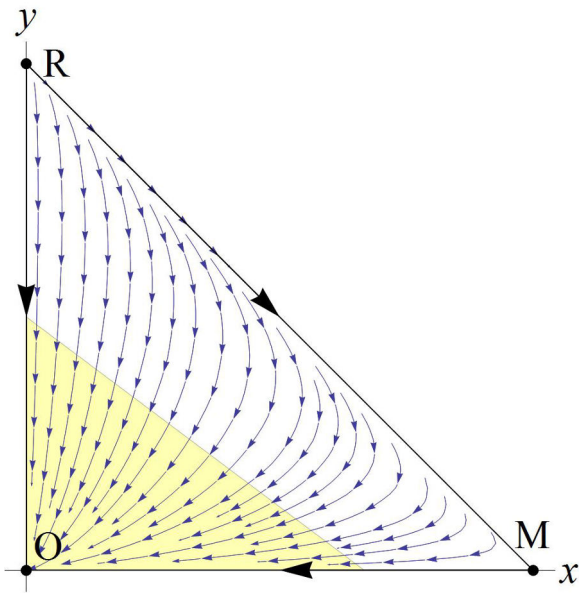

Figure 3.3: Phase space portrait of the dynamical system (3.49)–(3.50). The yellow/shaded area denotes the region of the phase space where the universe is accelerating.

the future attractor. Every solution is thus a heteroclinic orbit starting from R as $\eta \to -\infty$ and ending in O as $\eta \to +\infty$. The only exceptions are the heteroclinic orbits on the x-axis and the $y = 1 - x$ line, which connect M to O and R to M, respectively. However these trajectories correspond to either a vanishing cosmological constant or to a universe without a radiation contribution. From Fig. 3.3 it is clear that for every initial conditions in the physical phase space, the universe was radiation dominated as $a \to 0$ and dark energy dominated as $a \to +\infty$. The yellow/shaded region in Fig. 3.3 denotes the area of the phase space where $w_{\text{eff}} < -1/3$, i.e. where the universe undergoes an accelerated expansion[9]. All the trajectories will eventually enter this region so that the radiation (or matter) to dark energy transition always happens at some moment in the history of the universe.

Note that there is also an heteroclinic sequence connecting $R \to M \to O$. This heteroclinic sequence is of fundamental importance since it is the path our universe follows. We can understand it with the following reasoning. In Fig. 3.3 the line corresponding to a vanishing cosmological constant is the $y = 1 - x$ line connecting R with M. Since the measured value of the cosmological constant is actually positive but extremely small (see (3.33)), we

[9]The effective EoS parameter is connected to the acceleration equation (3.9) as $\ddot{a}/a = -\kappa^2\rho(1 + 3w_{\text{eff}})/6$ where $\rho = \rho_m + \rho_r + \Lambda/\kappa^2$ is the total energy density. It is then clear that whenever $w_{\text{eff}} < -1/3$ the universe undergoes accelerated expansion ($\ddot{a} > 0$).

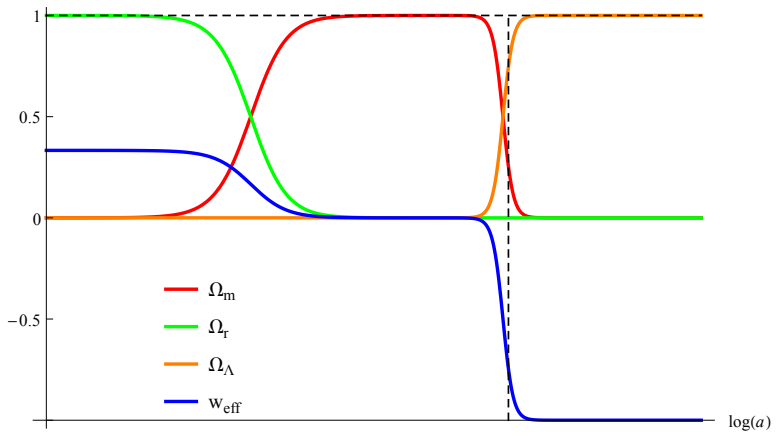

Figure 3.4: Evolution of the relative energy density of dark matter (Ω_m), radiation (Ω_r) and dark energy (Ω_Λ), together with the effective EoS parameter (w_{eff}) in the ΛCDM model. The vertical dashed line indicates the present cosmological time.

expect that the evolution of our universe corresponds to a trajectory passing exceptionally close to the $y = 1 - x$ line. Such a solution will nothing but shadow the heteroclinic orbit $R \to M \to O$, implying a universe which undergoes first a radiation, then a matter and finally a dark energy dominated phase. This is exactly the expected behavior of the observed universe which is well modeled by a universe filled with radiation, dark matter and a small positive cosmological constant. Such a theoretical description of the universe in known as the *ΛCDM model* after the cosmological constant Λ and the cold (non relativistic) dark matter fluid.

ΛCDM model

The relative energy densities of dark matter, radiation and dark energy ($\Omega_\Lambda = \Lambda/(3H^2)$) have been plotted in Fig 3.4, together with the effective EoS of the universe (w_{eff}), for a solution shadowing the $R \to M \to O$ heteroclinic orbit. As we can see from the picture, at early times radiation dominates, then there is a transient period of dark matter domination and eventually the universe becomes dominated by the cosmological constant. Note the vertical dashed line denoting the present cosmological time. As suggested by the observations, today we are in the transition period between dark matter and dark energy domination. The relative energy density of dark energy is indeed around 0.7, while the remaining 0.3 is composed by dark (and baryonic) matter. The effective EoS parameter start from the radiation value of 1/3, drops to 0 during the matter dominated era and eventually reaches -1 as the effects of dark energy becomes important. Finally we can compare Fig. 3.4 with Fig. 3.1. The non vanishing contribution of the cosmological constant introduces a new late time phase of accelerated expansion on top of the Big Bang theory evolution. Fig. 3.4 indeed represents an extension

of Fig. 3.1 with a different dynamics at late time which better matches the astronomical observations. The ΛCDM model can thus be seen as an extension of the Big Bang theory which takes into account the late time accelerated expansion.

To conclude we have seen in this section that adding a simple cosmological constant term to the Einstein field equations lead to the desired cosmological acceleration at late times. However it is questionable why such a constant must possess its extremely small measured value. From Fig. 3.4 one can immediately notice that a slightly greater value for Λ, corresponding to trajectories more distant from the $y = 1 - x$ line, would immediately lead to a fast transition from radiation to dark energy domination without allowing the intermediate matter epoch to happen. This would result in a completely different universe where all the cosmological structure, and thus also life as we know it, would be absent. The problem with the observed value of the cosmological constant, as we are going to understand in the next section, is indeed an issue which has not yet been solved under the theoretical point of view.

3.5 Problems with the cosmological constant

The extremely small value (3.33) of the cosmological constant is at odds with theoretical predictions. Even before the 1998 discovery of accelerated expansion of the universe, it was well known that a non vanishing cosmological constant implies some theoretical and philosophical problems at both the classical and quantum level. All this comes from the identification of the cosmological constant term in the Einstein field equation (3.32) with the vacuum energy of (quantum) fields. In what follows we will briefly review the major problems that follows from a positive cosmological constant. For more details we refer the reader to Carroll (2001); Martin (2012); Weinberg (1989, 2000).

As we have noticed in Sec. 3.4 the cosmological constant term in the Einstein equations (3.32) can be seen as a matter fluid contribution with constant energy density ρ_Λ and negative pressure $p_\Lambda = -\rho_\Lambda$. The same type of contribution to the right hand side of the Einstein field equations arises from the *vacuum energy* of matter fields. The energy-momentum tensor of a field in its vacuum state $|0\rangle$ is given by

Vacuum energy

$$\langle 0|T_{\mu\nu}|0\rangle = -\rho_{\rm vac}\, g_{\mu\nu}\,, \tag{3.51}$$

where $\rho_{\rm vac}$ is the *constant* energy density of the vacuum. This can be derived from both classical and quantum mechanical considerations. From the classical point of view the term (3.51) can be identified with the value of matter fields when they rest in their minimal energy state, i.e. the vacuum state. However at the quantum level the Heisenberg uncertainty principle prevents

the kinetic and potential energies to vanish at the same time. In fact taking into account the quantum mechanical fluctuations form the zero point energy of quantum fields, gives another source of energy which contributes to the Einstein equations with a term of the form (3.51). There are thus two different contributions of the form (3.51) coming from considerations on the vacuum state of matter fields: one is classical and the other quantum mechanical. We will first deal with the classical considerations and then with the quantum ones.

The classical cosmological constant problem

The so-called *classical cosmological constant problem* can be understood making a simple example with a scalar field. The energy-momentum tensor of a scalar field ϕ is given by

$$T^{(\phi)}_{\mu\nu} = \partial_\mu\phi\partial_\nu\phi - g_{\mu\nu}\left[g^{\alpha\beta}\partial_\alpha\phi\partial_\beta\phi + V(\phi)\right] , \tag{3.52}$$

where $V(\phi)$ is the self-interacting potential of the scalar field. At the classical level the vacuum state corresponds to the state of minimum energy where the kinetic energy of the field vanishes and the potential takes its minimum value $V_{\rm min}$. This means that in the vacuum state the energy momentum tensor (3.52) takes the form

$$\langle 0|\, T^{(\phi)}_{\mu\nu}\, |0\rangle = -V_{\rm min}\, g_{\mu\nu} , \tag{3.53}$$

which indeed matches (3.51) since $V_{\rm min}$ is constant. Every matter field whose vacuum energy does not vanish will source the Einstein field equations with a term of the form (3.53). In the Standard Model of particle physics a non vanishing value of the vacuum energy is present after (or before) a *(symmetry breaking) phase transition*. Without going into the details we mention that in the Standard Model there are two of such possible phase transitions: the Electro-Weak phase transition and the QCD phase transition. The first one leads to a value of the (Higgs field's) vacuum energy density of

$$\rho^{\rm EW}_{\rm vac} \simeq 10^8\,{\rm GeV}^4 , \tag{3.54}$$

while the vacuum energy coming from QCD is

$$\rho^{\rm QCD}_{\rm vac} \simeq 10^{-2}\,{\rm GeV}^4 . \tag{3.55}$$

These two values should be added and compared with the measured value of ρ_Λ, which, in GeV units, is

$$\rho_\Lambda \simeq 10^{-47}\,{\rm GeV}^4 . \tag{3.56}$$

Comparing (3.54) and (3.55) with the measured value (3.56) immediately gives the severity of the problem we are facing with. The observed value of ρ_Λ is 55 and 45 orders of magnitude away from the numbers predicted by the Electro-Weak and QCD transitions, respectively. Theoretically this is

a catastrophe since the predicted vacuum energy is so high that it should have been observed long time ago. The problem does not ameliorate if also quantum considerations are included.

The quantum cosmological constant problem

As we mentioned before the quantum fluctuations in the vacuum state of matter fields contribute with a sourcing term of the form (3.51) in the Einstein field equations. Thus also this effect should be added in evaluating the value of the cosmological constant. The contribution arising from these quantum fluctuations leads to what is called the *quantum cosmological constant problem*. Again we will explain the problem using a scalar field as example. Consider a massive ($V = m^2\phi^2/2$) scalar field in Minkowski spacetime. From quantum-mechanical considerations, the energy density of the field in its vacuum state is given by

$$\rho_{\text{vac}}^{\text{QM}} = \langle 0| \rho_\phi |0\rangle = \frac{1}{2(2\pi)^3} \int d^3k \sqrt{k^2 + m^2}\,, \tag{3.57}$$

with the integral performed over all 3-dimensional momentum space. Clearly the integral diverges and the energy result infinite. This is however the kind of divergence that in quantum field theory can be handled with the concept of *renormalization*. There are various techniques that can be employed to regularize the integral (3.57), but the one working properly in our case is *dimensional regularization*[10]. Without going into the details, this procedure gives the result

$$\rho_{\text{vac}}^{\text{QM}} = \frac{m^2}{64\pi^2} \log\left(\frac{m^2}{\mu^2}\right)\,, \tag{3.58}$$

where μ is a constant scale introduced to fix the dimensionality of the equation. All massive matter fields in the universe contributes with a term similar to (3.58) in the vacuum energy. Summing the contribution from all the particles of the Standard Model, and choosing a suitable value for μ (Martin, 2012), gives the number

$$\rho_{\text{vac}}^{\text{QM}} \simeq -10^8\,\text{GeV}^4\,, \tag{3.59}$$

which, regardless of the sign, is still 55 order of magnitude away from the measured value (3.56). So from the quantum side of matter fields we predict another contribution which completely disagrees with observations.

Of course, since physically and mathematically nothing prevents it, one can also suppose that a *bare* cosmological constant Λ_{B} is present in the Einstein field equations and it adds its energy contribution ρ_{B} to the vacuum energies we have just computed. This implies that in general the total vacuum energy will be given by

$$\rho_\Lambda = \rho_{\text{B}} + \rho_{\text{vac}}^{\text{QM}} + \rho_{\text{vac}}^{\text{EW}} + \rho_{\text{vac}}^{\text{QCD}} + \dots\,, \tag{3.60}$$

[10] Introducing a cut-off at some higher energy breaks Lorentz invariance and thus leads to a wrong result (Martin, 2012).

where for completeness every contribution from either unknown phase transitions or quantum fluctuations of particles beyond the Standard Model should be added. We know the measured value of ρ_Λ and have estimated the values of all the other vacuum energy appearing on the right hand side of (3.60) but for ρ_B. According to quantum field theory, the value of ρ_B cannot be evaluated from theoretical arguments and it is a number that must be chosen in order to renormalize ρ_Λ to let it agree with experiments. In our case this means that ρ_B must possess the right value that cancels all the vacuum energy contributions on the right hand side of (3.60) leaving exactly the small measured value on the left hand side. This is clearly absurd since one should adjust ρ_B up to fifty orders of magnitude or more. In these terms the cosmological constant problem is nothing but a problem of *fine tuning*. It makes no sense to assume that the bare cosmological constant is exactly the one needed to cancel all the vacuum energy sources giving only the small amount we need to match the observations.

The issues related to the vacuum energy of matter fields are not the only problems plaguing the cosmological constant. As we have seen in Sec. 3.4, even if we put aside all the theoretical explanations for Λ, an extremely small value of the cosmological constant is needed in order to have a sufficiently long period of matter domination during the history of the universe. A slightly bigger value of Λ would means a direct transition from radiation to dark energy domination preventing in this way the formation of galaxies, stars and all the other cosmic structures. Moreover the observed value of the cosmological constant is the right one needed for the transition from dark matter to dark energy to happen exactly today, i.e. during the relatively small time when humanity has evolved. This is known as the *cosmic coincidence problem*. It can equivalently formulated as follows: how is it possible that we are observing the universe exactly when the relative energy density of dark energy is of the same order of the dark matter one? If we take a look back to Fig. 3.4 it is easy to realize that the present cosmological time, denoted by the vertical dashed line, could be placed anywhere[11] in the history of the universe and there is no apparent reason for it to be exactly where the transition from matter to dark energy domination happens. If the cosmological constant dominated phase is the final state of our universe, it was much more likely that we would have lived during a period of dark energy domination rather than matter domination, or even less probably, exactly during the transition phase. This rather philosophical problem is not specific of the cosmological constant, though, as we will see in the next chapters, in other models of dark energy it could be relaxed.

The cosmic coincidence problem

In conclusion we have seen that theoretical considerations fail to explain the observed value of the cosmological constant which not only seems to

[11] Of course Life as we know it needs an Earth-like planet to prosper and thus the human race could have appeared only after (dark) matter dominated for a sufficiently long time.

be abnormally small, but also to be the right one needed for a dark matter to dark energy transition to happen at the present cosmological time. Nevertheless, even taking into account these unsolved problems, the ΛCDM model with a positive small value of the cosmological constant remains the simplest model capable of fitting all the present astronomical data. In the remaining part of this thesis we will deal with different approaches to model dark energy, which, though with a more complicated cosmological dynamics, are able to introduce new theoretical features and to provide new interesting phenomenology, which can in principle better reconcile with philosophical issues and accommodate the observational data.

Chapter 4

Quintessence: canonical scalar field models of dark energy

As discussed in Chapter 3 the observed acceleration of the universe can be successfully explained by the effect of a small cosmological constant. Nevertheless, as pointed out in Sec. 3.5, from a particle physics perspective the cosmological constant seems to suffer from some fundamental problems. If one fully embraces the, so far rather successful, particle physics approach to describe dark energy, it seems more natural to assume a vanishing cosmological constant and to attribute the late-time cosmic acceleration to some yet unknown particles. Dark energy becomes thus a dynamical quantity which in principle could help in addressing the cosmic coincidence problem or the fine tuning of initial conditions. The vacuum energy problems of particle fields, i.e. the cosmological constant problems, are of course not cured just by introducing new particles in the universe. Under this perspective, the vacuum energy is supposed to vanish due to some unknown high-energy physics, while the new particles are the manifestation of the low-energy effective reduction of this high-energy theory. The particle physics approach aims at providing a phenomenological description of dark energy at first and then, if possible, to relate this effective solution to some interesting high-energy physics.

If dark energy is regarded as a dynamically evolving entity, the simplest theoretical explanation for it is achieved introducing a canonical scalar field, i.e. a scalar particle. In this chapter we study dark energy models built from such a canonical scalar field, while in the next chapters we will deal with non-canonical scalar fields and non-scalar particles. Canonical scalar field models of dark energy are collectively known under the name of *quintessence* and were first proposed immediately after the 1998 discovery of cosmic acceleration (Caldwell et al., 1998; Zlatev et al., 1999; Wang et al., 2000), though

scalar field applications in late-time cosmology were extensively studied even before 1998 (see e.g. Ratra & Peebles (1988); Peebles & Ratra (1988); Wetterich (1995); Frieman et al. (1995); Coble et al. (1997); Ferreira & Joyce (1997, 1998)). In this chapter the focus is on dynamical systems applications to dark energy rather than on physical issues. Extensive citations to dynamical systems studies will thus be provided in every section, though the reader will find only few references for more phenomenological applications. In fact a small effort has been made in order to build this chapter as a concise review on dynamical systems applications to quintessence models, knowing that reviews regarding the theory and phenomenology of quintessence can already be found in the literature (e.g. Copeland et al. (2006); Li et al. (2011)).

The chapter is organised as follows. In Sec. 4.1 we will present the main dynamical features of the background cosmology of a canonical scalar field with a self-interacting potential. The cosmological field equations will be derived from an action principle and will then be recast into a dynamical system with the introduction of suitable dimensionless variables. Secs. 4.2 and 4.3 will be devoted to the study of quintessence with an exponential and power-law potential respectively. Under a dynamical perspective, these two examples represent the most relevant canonical scalar field models of dark energy. In both Secs. 4.2 and 4.3 a complete dynamical systems analysis will be performed outlining the interesting phenomenological properties of these models at both early and late times. Sec. 4.4 will then deal with more complicated potentials, treating all of them within a unified approach which will allow us to obtain as much information as possible without specifying the actual form of the potential. In Sec. 4.5 a coupling between the scalar field and the matter sector will be considered. The different types of coupling advanced throughout the literature and studied with dynamical systems techniques will be discussed. The dynamics of the simplest and most important of such models will be analysed underlining the general benefits of the coupling between quintessence and matter. Finally in Sec. 4.6 the possibility that dark energy is composed of more than one canonical scalar field will be briefly discussed.

4.1 Dark energy as a canonical scalar field

In the context of *Lagrangian mechanics*, any consistent set of field equations can be derived varying a suitable *action functional* which is a spacetime integral depending on the various fields describing the effective degrees of freedom of the physical system at hand. The Einstein field equations (3.3) follows from the so-called *Einstein-Hilbert action*

Einstein-Hilbert action

$$S_{\rm EH} = \int d^4x\sqrt{-g}\left(\frac{R}{2\kappa^2} + \mathcal{L}_m\right) , \tag{4.1}$$

where g is the determinant of the metric, R the Ricci scalar and $\mathcal{L}_m$ is the *matter Lagrangian* which contains all the contributions of the matter fields and whose variation yields the right hand side of the Einstein field equations, i.e. the matter energy-momentum tensor $T_{\mu\nu}$ given by (3.4). The variation[1] of (4.1) with respect to the metric tensor $g_{\mu\nu}$ leads to the Einstein field equations (3.3), i.e. to

$$R_{\mu\nu} - \frac{1}{2} R\, g_{\mu\nu} = \kappa^2\, T_{\mu\nu}\,. \tag{4.2}$$

If the cosmological constant Λ is taken into account the Einstein-Hilbert action (4.1) can be modified as

$$S_{\rm EH} = \frac{1}{2\kappa^2} \int d^4x \sqrt{-g}\left(R - 2\Lambda + 2\kappa^2 \mathcal{L}_m\right)\,, \tag{4.3}$$

where the new term will give rise to the Λ contribution in the Einstein field equations (3.32).

In what follows we will set the cosmological constant to zero and consider a scalar field minimally coupled to gravity. The action which will then represent our physical system is

$$S = \int d^4x \sqrt{-g}\left(\frac{R}{2\kappa^2} + \mathcal{L}_m + \mathcal{L}_\phi\right)\,, \tag{4.4}$$

where $\mathcal{L}_\phi$ is the *canonical Lagrangian of a scalar field* ϕ uniquely given by

Canonical scalar field Lagrangian

$$\mathcal{L}_\phi = -\frac{1}{2}\partial\phi^2 - V(\phi)\,, \tag{4.5}$$

with $\partial\phi^2 = g^{\mu\nu}\partial_\mu\phi\partial_\nu\phi$ and $V(\phi)$ a general self-coupling potential for ϕ which must be positive for physically acceptable fields. Note that even if a cosmological constant was present in the action (4.4), this could be re-adsorbed into the definition of $V(\phi)$. The variation with respect to $g_{\mu\nu}$ produces the following gravitational field equations

$$R_{\mu\nu} - \frac{1}{2} g_{\mu\nu} R = \kappa^2\left(T_{\mu\nu} + T^{(\phi)}_{\mu\nu}\right)\,, \tag{4.6}$$

where

$$T^{(\phi)}_{\mu\nu} = \partial_\mu\phi\partial_\nu\phi - \frac{1}{2} g_{\mu\nu}\partial\phi^2 - g_{\mu\nu} V\,, \tag{4.7}$$

is the energy-momentum tensor of the scalar field. On the other hand, the variation with respect to ϕ gives the *Klein-Gordon equation*

Klein-Gordon equation

$$\Box\phi - V_{,\phi} = 0\,, \tag{4.8}$$

[1] For the details of the Lagrangian approach to general relativity we refer to any good book on the subject, for example Weinberg (1972); Wald (1983).

with $\Box\phi = \nabla_\mu \nabla^\mu \phi$ and $V_{,\phi} = \partial V/\partial\phi$.

Following the discussion outlined in Chapter 3, we will consider a homogeneous and isotropic universe described by a spatially flat FRW metric which in *Cartesian coordinates* reads

$$ds^2 = -dt^2 + a(t)\left(dx^2 + dy^2 + dz^2\right) , \tag{4.9}$$

with $a(t)$ the well-known scale factor (see Sec. 3.1). The energy density and pressure of matter fields will be related by a linear equation of state (EoS) $p = w\rho$ with w ranging from 0 (dust) to 1/3 (radiation). Within these assumption the gravitational field equations (4.6) produce the following Friedmann and acceleration equations

$$3H^2 = \kappa^2 \left(\rho + \frac{1}{2}\dot{\phi}^2 + V\right) , \tag{4.10}$$

$$2\dot{H} + 3H^2 = \kappa^2 \left(-w\rho - \frac{1}{2}\dot{\phi}^2 + V\right) , \tag{4.11}$$

while the Klein-Gordon equation (4.8) reduces to

$$\ddot{\phi} + 3H\dot{\phi} + V_{,\phi} = 0 . \tag{4.12}$$

Here an over-dot denotes differentiation with respect to the coordinate time t.

Note that from (4.10) and (4.11) the contribution of the scalar field ϕ can be rearranged into a perfect fluid contribution, i.e. into the form (3.4), if the energy density and pressure of ϕ are identified with

$$\rho_\phi = \frac{1}{2}\dot{\phi}^2 + V , \tag{4.13}$$

$$p_\phi = \frac{1}{2}\dot{\phi}^2 - V . \tag{4.14}$$

The EoS of the scalar field is then given by

$$w_\phi = \frac{p_\phi}{\rho_\phi} = \frac{\frac{1}{2}\dot{\phi}^2 - V}{\frac{1}{2}\dot{\phi}^2 + V} , \tag{4.15}$$

with w_ϕ a dynamically evolving EoS parameter which can take values in the range $[-1, 1]$. Whenever the potential energy V dominates over the kinetic energy $\dot{\phi}^2/2$ the EoS (4.15) becomes $w_\phi = -1$ recovering in this way a cosmological constant equation of state capable of accelerating the universe. This is the feature that renders a canonical scalar field the simplest dynamical framework for describing dark energy. Models based on a canonical scalar field for explaining the late time cosmic acceleration, are collectively denoted with the name *quintessence* and distinguished by the form of the potential V.

Quintessence

Since we are concerned with possible dynamical systems applications to such models, we need first to rewrite the cosmological equations (4.10), (4.11) and (4.12) into an autonomous system of equations. In general there are many possible way to achieve this task, but the most common one is to consider the dimensionless variables[2]

$$x = \frac{\kappa\dot{\phi}}{\sqrt{6}H} \quad \text{and} \quad y = \frac{\kappa\sqrt{V}}{\sqrt{3}H}\,. \tag{4.16}$$

The variables (4.16) are usually referred to as the *expansion normalised variables* (Wainwright & Ellis, 1997), and in what follows we will denote them as the *EN variables*. For a scalar field in the presence of barotropic matter, they were first introduced in a seminal paper by Copeland et al. (1998). Note that $y > 0$ since in an expanding universe $H > 0$ and for a physically viable scalar field potential $V > 0$.

Expansion normalised variables

Using the EN variables the Friedmann equation (4.10) can be rewritten as

$$1 = \Omega_m + x^2 + y^2\,, \tag{4.17}$$

where $\Omega_m = \kappa^2\rho/(3H^2)$ is the *relative energy density of matter*[3]. From (4.17) the meaning of the EN variables (4.16) is clear: x stands for the relative kinetic energy density of ϕ while y stands for its relative amount of potential energy density. The total relative energy density of the scalar field is given by

$$\Omega_\phi = x^2 + y^2\,, \tag{4.18}$$

while its EoS becomes

$$w_\phi = \frac{x^2 - y^2}{x^2 + y^2}\,. \tag{4.19}$$

It is now easy to see that in the limit $x \ll y$ one obtains $w_\phi \simeq -1$. From (4.18) it is also clear that the further away we are from the origin on the (x, y)-plane, the higher is the energy of the scalar field, with the origin corresponding to a completely matter dominated universe ($\Omega_m = 1$). The quantities Ω_ϕ and w_ϕ are sometimes used as dynamical variables to replace the EN ones (see e.g. Scherrer & Sen (2008); Fang et al. (2014a); Gong (2014)). The transformation $(x, y) \mapsto (\Omega_\phi, w_\phi)$ however is not convenient for mathematical and computational reasons and it is usually employed only to better parametrize the dynamical properties of dark energy when comparison with observational data is performed.

[2]For applications of dynamical systems to scalar field cosmology using different variables see e.g. Halliwell (1987); Faraoni & Protheroe (2013). The EN variables (4.16) are of physical interest since the energy densities of matter and dark energy can be easily visualised in terms of them.

[3]Relative to the critical energy density defined as $\rho_c = 3H^2/\kappa^2$.

We define the effective EoS parameter of the universe as $w_{\text{eff}} = (p + p_\phi)/(\rho + \rho_\phi) = w\Omega_m + w_\phi\Omega_\phi$ which in the EN variables reads

$$w_{\text{eff}} = x^2 - y^2 + w\left(1 - x^2 - y^2\right) . \tag{4.20}$$

The effective EoS parameter w_{eff} is of fundamental importance because it tells us whether the universe undergoes through an accelerating ($w_{\text{eff}} < -1/3$) or decelerating ($w_{\text{eff}} > -1/3$) expansion. For example, if $x = y = 0$ then $w_{\text{eff}} = w$ and the universe is matter dominated, if $x = 1$ and $y = 0$ then $w_{\text{eff}} = 1$ and the universe is dominated by the kinetic energy of the scalar field which behaves as a *stiff matter fluid* ($w = 1$), finally if $x = 0$ and $y = 1$ then $w_{\text{eff}} = -1$ and the universe is dominated by the potential energy of the scalar field which behaves as an effective cosmological constant driving an accelerated expansion.

Since the energy density of matter fields ρ is always positive, we also have that $\Omega_m > 0$. This implies that the EN variables must satisfy the constraint

$$0 \leq x^2 + y^2 = 1 - \Omega_m \leq 1 , \tag{4.21}$$

for physically viable solutions. On the (x, y)-plane the constraint (4.21) reduces the phase space of physically sensible trajectories to the unit disk centred in the origin[4]. If we add also the fact that $y > 0$ then the *physical phase space*[5] reduced to (x, y)-planes is represented by the positive y unit disk centred in the origin. Note that points on the unit circle correspond to scalar field dominated universes ($\Omega_\phi = 1$). The Friedmann constraint (4.17) can also be used to replace Ω_m in favor of x and y in the following equations, reducing in this way the dimensionality of the phase space. Furthermore from the acceleration equation (4.11) we obtain

Physical phase space

$$\frac{\dot{H}}{H^2} = \frac{3}{2}\left[(w-1)x^2 + (w+1)\left(y^2 - 1\right)\right] , \tag{4.22}$$

which at any fixed point (x_*, y_*) of the phase space can be solved for a to give

$$a \propto (t - t_0)^{\frac{2}{3[(w+1)(1-x_*^2-y_*^2)+2x_*^2]}} \tag{4.23}$$

where t_0 is a constant of integration. This corresponds to a power-law solution, i.e. a solution for which the scale factor a evolves as a power of the cosmological time t. Again if $x = 0$ and $y = 0$ the universe is matter dominated and its evolution coincides with the standard w-dependent scaling solution (3.23). If $x = 0$ and $y = 1$ the denominator of (4.23) vanishes and the universe undergoes a de Sitter expansion as can be seen from (4.22)

[4] See Roy & Banerjee (2014b) for the analysis in polar coordinates.

[5] The physical phase space is the invariant set composed by physically meaningful orbits of the phase space; see Sec. 3.4.

which forces H to be constant. Solution (4.23) shows us that at any critical point of the phase space the universe expands according to a power-law evolution. This means that even if we are not able to derive its entire evolution analytically, its asymptotic behavior, provided it is given by critical points, will always be well characterized.

Employing the EN variables (4.16), from the acceleration equation (4.11) and the scalar field equation (4.12) we can derive the following dynamical system[6]

$$x' = -\frac{3}{2}\left[2x + (w-1)x^3 + x(w+1)\left(y^2-1\right) - \frac{\sqrt{2}}{\sqrt{3}}\lambda y^2\right], \tag{4.24}$$

$$y' = -\frac{3}{2}y\left[(w-1)x^2 + (w+1)\left(y^2-1\right) + \frac{\sqrt{2}}{\sqrt{3}}\lambda x\right], \tag{4.25}$$

where a prime denotes differentiation with respect to $\eta = \log a$ and we have defined

$$\lambda = -\frac{V_{,\phi}}{\kappa V}. \tag{4.26}$$

Note that the EN variables fail to close the system of equations to an autonomous system since λ still depends upon the scalar field ϕ. In fact the EN variables were first introduced to study a scalar field with an exponential potential (Copeland et al., 1998) for which λ is indeed just a parameter and the system (4.24)–(4.25) becomes autonomous; see Sec. 4.2. In order to close the system for a general potential we can regard λ as another dynamical variable and look for an evolution equation governing its dynamics. This approach has first been considered by Steinhardt et al. (1999) and de la Macorra & Piccinelli (2000), and it has been pursued with the use of dynamical system techniques since the work of Ng et al. (2001). The equation for the variable λ follows from its definition and is given by

$$\lambda' = -\sqrt{6}\,(\Gamma - 1)\,\lambda^2 x\,, \tag{4.27}$$

where

$$\Gamma = \frac{V\,V_{,\phi\phi}}{V_{,\phi}^2}\,. \tag{4.28}$$

At first it seems that we gain nothing from this new equation since we still have a quantity (Γ) which explicitly depends on the scalar field ϕ. However since both λ and Γ are functions of ϕ, it is in principle possible to relate one to the other (Zhou, 2008; Fang et al., 2009). In other words, provided that the function $\lambda(\phi)$ is invertible so that we can obtain $\phi(\lambda)$, we can write Γ as a function of λ, i.e. $\Gamma(\phi(\lambda))$. The simplest case is the exponential

[6]The derivation of these equations can proceed as follows. First take the derivative of x and y with respect to $d\eta = H dt$, and then replace $\dot{H}$ using Eq. (4.11) and $\ddot{\phi}$ using Eq. (4.12). Finally rewrite everything in terms of the variables x, y and λ.

potential where $\Gamma = 1$ and λ is nothing but a constant. However, also the power-law potential is easily treatable since it leads to a dynamical λ but to a constant Γ. The exponential and power-law potentials will be studied in Secs. 4.2 and 4.3 respectively, while Sec. 4.4 will be devoted to more complicated potentials. Of course if the function $\lambda(\phi)$ is not invertible this approach fails to close the equations to an autonomous system. Different choices of variables, which in practice will lead to a phase space with higher dimensions, could better represent the system in these cases.

Note that all the phenomenological properties of the universe, such as the relative energy density of the scalar field (4.18), the EoS of the scalar field (4.15) and the effective EoS (4.20), are independent of λ. This means that different models of quintessence, i.e. different choices of the potential V, do not directly change the physical features of the universe. It is only through the dynamical evolution of the x and y variables that different quintessence models distinguish among each other. If two potentials lead to the same qualitative evolution of the EN variables, then the universes described by those two models will result physically indistinguishable[7].

The dynamical system (4.24)–(4.25) plus (4.27) is invariant under the transformation

$$y \mapsto -y\,, \tag{4.29}$$

so even if we drop the $V > 0$ assumption the dynamics for negative values of y would be a copy of the one for positive values. Note also that we are assuming $H > 0$ in order to describe an expanding universe. However the dynamics of a contracting universe ($H < 0$) would have the same features of our analysis in the negative y region switching the direction of time because of the symmetry (4.29). On the other hand, provided that Γ can be written as a function of λ and that $\Gamma(\lambda) = \Gamma(-\lambda)$, the dynamical system (4.24)–(4.25) plus (4.27) is also invariant under the simultaneous transformation

$$\lambda \mapsto -\lambda \quad \text{plus} \quad x \mapsto -x\,, \tag{4.30}$$

which shows that the system is parity-odd invariant if restricted to planes of constant y. In other words the dynamics for opposite values of λ is invariant after a reflection over the (y, λ)-plane. The symmetry (4.30) implies that we can fully analyse the system just taking into account positive values of λ. Negative values would give the same dynamical properties reflected over the (y, λ)-plane. If the $\Gamma(\lambda)$ is not an even function of λ, the symmetry (4.30) is broken and one must study both positive and negative values of λ. This depends on the model at hands, i.e. on the form of the potential $V(\phi)$, but, as we are going to see, for the simplest examples it is always satisfied.

[7] This is only valid at the background level. It might be that the two models give a different dynamics at the level of cosmological perturbations.

4.2 Exponential potential

In this section the self-interacting potential of the scalar field is assumed to be of the exponential kind, namely

$$V(\phi) = V_0\, e^{-\lambda\kappa\phi}\,, \tag{4.31}$$

where $V_0 > 0$ is a constant and λ is now a constant parameter which agrees with the definition (4.26). The exponential case (4.31) is the simplest example of quintessence, and can be easily justified from high-energy phenomenology.

Dynamical systems for cosmological scalar fields with an exponential potential have been studied long before the discovery of cosmic acceleration, mainly in relation with early universe inflation and high-energy physics phenomenology (see e.g. Halliwell (1987); Burd & Barrow (1988); Wands et al. (1993); Coley et al. (1997); Coley (2003)). The reference work for such a system is the well known paper by Copeland et al. (1998) where a thorough dynamical analysis is performed[8]. The arguments of this section are based on the results of that work.

The equations (4.24) and (4.25) represent now an autonomous system which defines the following 2D dynamical system

$$x' = -\frac{3}{2}\left[(w-1)x^3 + x(w+1)\left(y^2-1\right) - \frac{\sqrt{2}}{\sqrt{3}}\lambda y^2\right]\,, \tag{4.32}$$

$$y' = -\frac{3}{2}y\left[(w-1)x^2 + (w+1)\left(y^2-1\right) + \frac{\sqrt{2}}{\sqrt{3}}\lambda x\right]\,, \tag{4.33}$$

where we recall that, thanks to (4.31), λ is just a parameter and that the physical phase space, from now on referred to as simply the phase space, is the (closed) upper half unit disk in the (x, y)-plane. Since the exponential potential (4.31) reduces the phase space to two dimensions, the dynamical system (4.32)–(4.33) can be extensively analysed using the dynamical systems techniques developed in Chapter 2. As a first comment we recall that being the phase space compact it follows from the Poincaré-Bendixon theorem of Sec. 2.6 that all asymptotic states will be either critical points, periodic orbits or finite heteroclinic sequences. As we will see, numerical integration of solutions will exclude the presence of periodic orbits and all the asymptotic states will be critical points[9]. Thanks to the symmetry (4.30), which now holds trivially since $\Gamma = 1$, we only need to analyse positive values of λ since negative values would yield the same dynamics reflected over the y-axis[10].

[8] See also Urena-Lopez (2012); Tamanini (2014).

[9] Unfortunately it seems extremely complicated to find a Dulac function that excludes

Point	x	y	Existence	$w_{\rm eff}$	Accel.	Ω_ϕ	w_ϕ
O	0	0	$\forall\,\lambda, w$	w	No	0	–
$A_\pm$	± 1	0	$\forall\,\lambda, w$	1	No	1	1
B	$\frac{\sqrt{3}}{\sqrt{2}}\frac{1+w}{\lambda}$	$\sqrt{\frac{3(1-w^2)}{2\lambda^2}}$	$\lambda^2 \geq 3(1+w)$	w	No	$\frac{3(1+w)}{\lambda^2}$	w
C	$\frac{\lambda}{\sqrt{6}}$	$\sqrt{1-\frac{\lambda^2}{6}}$	$\lambda^2 < 6$	$\frac{\lambda^2}{3}-1$	$\lambda^2 < 2$	1	$\frac{\lambda^2}{3}-1$

Table 4.1: Critical points of the system (4.32)–(4.33) with existence and physical properties.

P	Eigenvalues	Eigenvectors	Stability
O	$\{\frac{3}{2}(w \pm 1)\}$	$\{\begin{pmatrix}1\\0\end{pmatrix}, \begin{pmatrix}0\\1\end{pmatrix}\}$	Saddle
A_-	$\{3-3w\,,\, 3+\frac{\sqrt{3}}{\sqrt{2}}\lambda\}$	$\{\begin{pmatrix}1\\0\end{pmatrix}, \begin{pmatrix}0\\1\end{pmatrix}\}$	Unstable node if $\lambda \geq -\sqrt{6}$ Saddle if $\lambda < -\sqrt{6}$
A_+	$\{3-3w\,,\, 3-\frac{\sqrt{3}}{\sqrt{2}}\lambda\}$	$\{\begin{pmatrix}1\\0\end{pmatrix}, \begin{pmatrix}0\\1\end{pmatrix}\}$	Unstable node if $\lambda \leq \sqrt{6}$ Saddle if $\lambda > \sqrt{6}$
B	$\{\frac{3}{4\lambda}\,[(w-1)\lambda \pm \Delta]\}$	$\{\begin{pmatrix}\frac{\lambda}{2}\frac{\sqrt{1-w}}{\sqrt{1+w}}\frac{[6(w+1)^2-\lambda\pm\Delta]}{[2(1-w^2)-\lambda^2]}\\1\end{pmatrix}\}$	Stable node if $3(w+1) < \lambda^2 < \frac{24(w+1)^2}{9w+7}$ Stable spiral if $\lambda^2 \geq \frac{24(w+1)^2}{9w+7}$
C	$\{\frac{\lambda^2}{2}-3\,,$ $\lambda^2-3w-3\}$	$\{\begin{pmatrix}\frac{\sqrt{6-\lambda^2}}{-\lambda}\\1\end{pmatrix}, \begin{pmatrix}\frac{(w-1)\lambda}{w\sqrt{6-\lambda^2}}\\1\end{pmatrix}\}$	Stable if $\lambda^2 < 3(1+w)$ Saddle if $3(1+w) \leq \lambda^2 < 6$

Table 4.2: Stability properties for the critical points of the system (4.32)–(4.33). Here $\Delta = \sqrt{(w-1)[(7+9w)\lambda^2 - 24(w+1)^2]}$.

We are now ready to find the critical points of the dynamical system (4.32)–(4.33) and to perform the stability analysis. The results are summarized in Tab. 4.1, where the existence and physical properties are outlined, and Tab. 4.2, where details of the stability analysis are exposed. There can be up to five critical points in the phase space depending on the numerical value of λ. In what follows we go through each critical point discussing its mathematical and physical features.

- *Point O.* The origin of the phase space, corresponding to a matter dominated universe ($\Omega_m = 1$), is a critical point which exists for all values of λ. This point is always a saddle point attracting trajectories

periodic orbit for the system (4.32)–(4.33) and thus we must rely on numerical techniques.

[10] In the exponential case (4.31) this symmetry is related to the invariance of the action under a sign redefinition of the scalar field: $\phi \mapsto -\phi$.

along the x-axis and repelling them towards the y-axis. Of course the effective EoS matches the matter EoS, $w_{\text{eff}} = w$, and thus for physically admissible values of w there is no acceleration. The dark EoS is undetermined in O since both its kinetic and potential energies vanish. This is in any case physically unimportant since the total energy of the scalar field, kinetic plus potential, is zero. Point O stands for the matter solution where the universe evolves according to (3.23), i.e. according to the Big Bang theory; see Sec. 3.2.

- *Points* $A_{\pm}$. In the points $(\pm 1, 0)$ the universe is dominated by the scalar field kinetic energy ($x^2 = \Omega_\phi = 1$) and thus the effective EoS reduces to a stiff fluid with $w_{\text{eff}} = w_\phi = 1$ and no acceleration. Their existence is always guaranteed and they never represent stable points. They are unstable or saddle points depending on the value of λ being greater or smaller than $\sqrt{6}$. Strictly speaking a stiff-fluid EoS cannot be viable at the classical macroscopic level, however these solutions are expected to be relevant only at early times and thus are commonly ignored in dark energy applications. According to (4.23) in Points $A_{\pm}$ the universe expands as $a \propto t^{1/3}$.

- *Point* B. This point (see Tab. 4.1 for the coordinates) represents the so-called *scaling solution* where the effective EoS matches the matter EoS. These solutions derive their name from the fact that the scalar field energy density scales proportionally to the matter energy density: $\Omega/\Omega_\phi = \lambda^2/(3w+3) - 1$. In other words we always have both $0 < \Omega_\phi = 3(1+w)/\lambda^2 < 1$ and $0 < \Omega_m = 1 - \Omega_\phi < 1$, obtaining also $w_\phi = w$. This means that the universe evolves under both the matter and scalar field influence, but it expands as if it was completely matter dominated, i.e. according to (3.23). This solution is of great physical interest for the coincidence problem since according to it a scalar field can or could be present in the universe hiding its effects on cosmological scales. However, since we have $w_{\text{eff}} = w$ there cannot be accelerated expansion. When this point exists, i.e. for $\lambda^2 \geq 3(1+w)$, it always represents a stable point attracting all the phase space trajectories. *Scaling solution*

- *Point* C. The last point stands for the cosmological solution where the universe is completely scalar field dominated (see Tab. 4.1 for the coordinates). This implies $\Omega_m = 0$ and $\Omega_\phi = x^2 + y^2 = 1$, meaning that Point C will always lie on the unit circle. It exists for $\lambda^2 < 6$ and it is a stable attractor for $\lambda^2 < 3(1+w)$ (i.e. when Point B does not appear) and a saddle point for $3(1+w) \leq \lambda^2 < 6$ (i.e. when Point B is present). The effective EoS parameter assumes the value $w_{\text{eff}} = w_\phi = \lambda^2/3 - 1$ which implies an accelerating universe for $\lambda^2 < 2$. This point represents the well-known power-law accelerated expansion driven by a sufficiently flat scalar field potential. In the limit $\lambda \to 0$ this

solution reduces to a de Sitter expansion dominated by a cosmological constant.

Before looking at the phase space portraits we make few comments on the critical points. First we mention that for Points B and C Liapunov functions can be easily constructed as shown by Boehmer et al. (2012b). However the Liapunov analysis does not lead to a conclusive result and the linear stability analysis seems to be more suited to determine the stability in this case.

On a more physical ground, if $\lambda^2 < 2$ a dark matter to dark energy transition can be achieved by a heteroclinic orbit connecting Point O with Point C. However the origin is always a saddle point meaning that it cannot be the past attractor, and the early time behavior of the universe is given by Points $A_{\pm}$. The future attractor can either be Point C (formally the heteroclinic orbit connecting Points O and C) or Point B, with the latter one never giving acceleration. The so-called scaling solution of Point B can be used to hide the presence of a scalar field in the cosmic evolution, at least at the background level. This behavior can be used at early times in order to obtain negligible effects of dark energy when matter dominates, though nucleosynthesis imposes strong constraints on the scalar field energy density ($\Omega_\phi < 0.009$ from Planck (Ade et al., 2013)). The problem is that at late times dark energy should start to dominate, but the scaling solution of Point B never gives acceleration and, being a future attractor, once the universe reaches the scaling solution it never leaves it. For this reason, even if this behavior is of great interest at early times, it cannot represent a viable model for the late time universe since it does not lead to dark energy domination. One needs a mechanism which allows to exit the scaling solution and to join the dark energy accelerating solution, but this cannot be achieved with a single canonical scalar field and more complex dynamics is required.

We can now look at the phase space portrait for different values of the parameters. Looking at Tab. 4.2, the qualitative behavior of the phase space can be divided into three regions according to the value of λ^2: 0 to $3(1+w)$, $3(1+w)$ to 6 and 6 to infinity. In what follows we will only consider positive values for λ since, as we pointed out above, the dynamics for negative values coincides with the positive one after a reflection around the y axis due to (4.30). Since we are concerned only with dark energy applications and thus late time cosmology, we will restrict the following phase space plots (Figs. 4.1, 4.2 and 4.3) to the case $w = 0$ in order to better visualize possible dark matter to dark energy transitions[11]. The yellow/shaded region in Figs. 4.1, 4.2 and 4.3 highlights the zone of the phase space where the universe undergoes an accelerated expansion, i.e. where $w_{\text{eff}} < -1/3$.

[11] Different values of w within the physically meaningful range $[0, 1/3]$ lead to the same qualitative phase space.

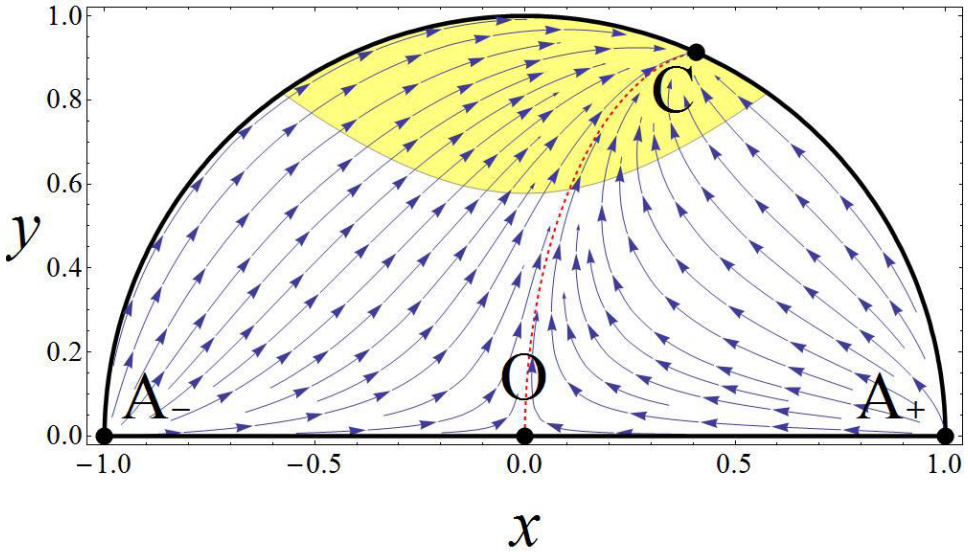

Figure 4.1: Phase space with $\lambda = 1$ and $w = 0$. The global attractor is Point C which represents an accelerating solution. For values $\lambda^2 > 2$ Point C would lie outside the acceleration region (yellow/shaded) and would not be an inflationary solution.

Range 1: If $\lambda^2 < 3(1 + w)$ there are four critical points in the phase space. Points $A_\pm$ are both unstable node, while Point O is a saddle point. The global attractor is Point C which represents an inflationary cosmological solution if $\lambda^2 < 2$. The portrait of the phase space is depicted in Fig. 4.1 where the value $\lambda = 1$ has been chosen. Point C always lies on the unit circle and it happens to be outside the yellow/shaded acceleration region if $\lambda^2 > 2$. All the trajectories in the phase space are heteroclinic orbits starting from Points $A_\pm$ and ending in Point C. The only exceptions are the orbits on the x-axis which connects Points $A_\pm$ with Point O and the orbit connecting Point O with Point C. This last trajectory divides the phase space into two invariant set: solutions on its right have Point A_+ as past attractor, while the past attractor of solutions on its left is Point A_-. There are two possible heteroclinic sequences: $A_\pm \to O \to C$. They can be used as physical models for dark matter to dark energy transition well characterizing the late time evolution of the universe with a final effective EoS given by $w_{\text{eff}} = -1 + \lambda^2/3$. However at early times we always obtain a stiff-fluid domination represented by Points $A_\pm$ which is phenomenologically disfavored.

Range 2: In the range $3(1 + w) \leq \lambda^2 < 6$ there are five critical points in the phase space. Points $A_\pm$ and O still behaves as unstable nodes and saddle point respectively. The future attractor is now Point B and Point C becomes a saddle point. The phase space portrait for $\lambda = 2$ is drawn in

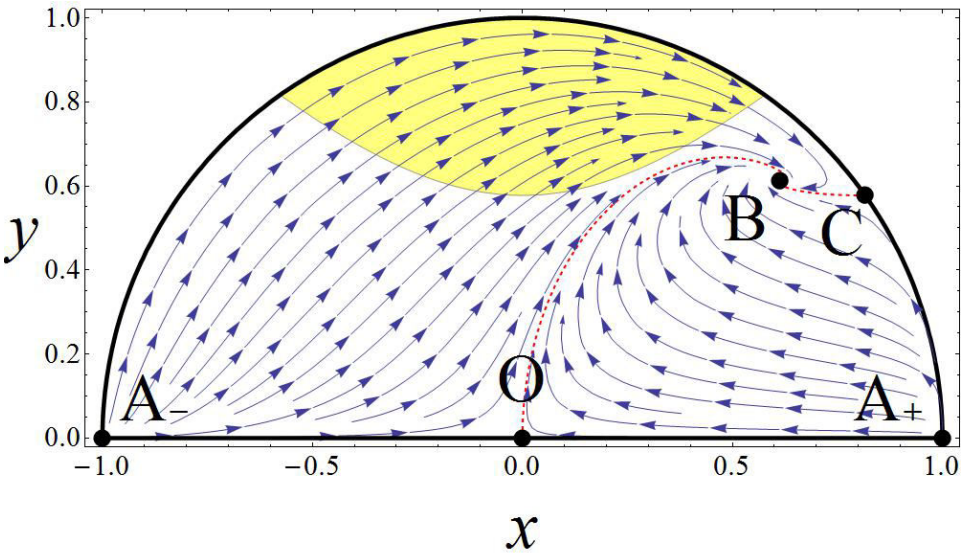

Figure 4.2: Phase space with $\lambda = 2$ and $w = 0$. The global attractor is Point B where the universe expands as it was completely matter dominated (scaling solution), while Point C is a saddle point.

Fig. 4.2. Point B always lies outside the acceleration region (yellow/shaded) and thus never describes an inflationary solution. The effective EoS parameter at this point coincides with the matter EoS parameter and thus the universe experiences a matter-like expansion even if it is not completely matter dominated (scaling solution). All the solutions are again heteroclinic orbits connecting Points $A_\pm$ to Point B. The exceptions are the orbits on the boundary of the phase space, which connect Points $A_\pm$ to either Point O or Point C, and the two heteroclinic orbits connecting Point O and Point C to Point B. These last two orbits divides the phase space into two invariant sets: one with Point A_- as past attractor and the other with Point A_+ as past attractor. The phase space depicted in Fig. 4.2 can be used for applications to transient periods of dark energy. For many trajectories (the ones passing through the yellow/shaded region) a finite period of acceleration can be achieved, and for λ sufficiently close to $\sqrt{3}$ the physically relevant heteroclinic sequence connecting the matter domination to the scaling solution experiences a transient accelerating phase.

Range 3: Finally if $\lambda^2 \geq 6$ there are again only four critical points. Point A_- is the only unstable node, while Points A_+ and O behave as saddle points. Point C does not appear anymore and the future attractor is still Point B, which again represents a scaling solution with $w_{\text{eff}} = w$. The phase space dynamics for $\lambda = 3$ is depicted in Fig. 4.3. Now all the orbits start from Point A_-, the past (global) attractor, and end in Point B, which is a simple attracting node for $3(w+1) < \lambda^2 < 24(w+1)^2/(9w+7)$

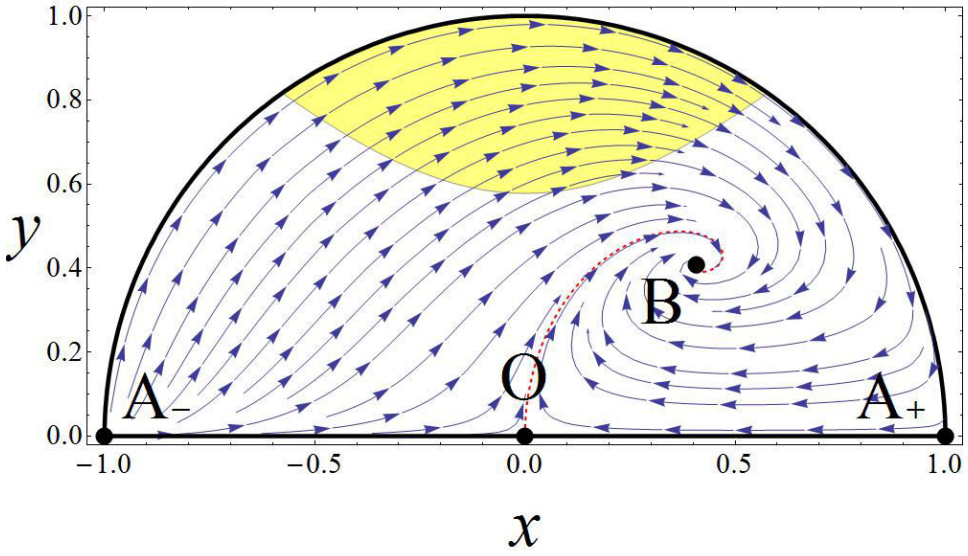

Figure 4.3: Phase space with $\lambda = 3$ and $w = 0$. Point B is the global attractor describing a scaling solution with $w_{\text{eff}} = w$.

and an attracting spiral for $\lambda^2 \geq 24(w+1)^2/(9w+7)$ as pointed out in Tab. 4.2. There are few special heteroclinic orbits connecting Point A_- to Point A_+, Points $A_\pm$ to Point O and Point O to Point B. Exactly as before, no solution of Fig. 4.3 can be used to model a dark energy dominated universe since the heteroclinic orbit connecting the origin to Point B never enters the yellow/shaded region. For increasing values of λ the qualitative dynamics of the phase space does not change while Point B lies closer to the origin. In the limit $\lambda \to +\infty$ Point B coincides with Point O.

We can now draw our conclusions on the canonical scalar field with an exponential potential.

From the mathematical perspective this model is of great interest because of its simplicity. The cosmological equations can be reduced to a 2D dynamical system with a compact phase space which is relatively easy to analyse. There are no periodic orbits and all the asymptotic behaviors are represented by critical points. All this allowed us to capture the whole dynamics of the system in the three plots of Figs. 4.1, 4.2 and 4.3.

From the physics point of view instead, the cosmological dynamics of the exponential potential is interesting because of the appearance of late time accelerated solutions which can be employed to model dark energy. For these solutions to be cosmologically viable a sufficiently flat potential ($\lambda^2 < 2$) is expected and a strong fine tuning of initial conditions is required in order for matter domination to last enough time (the solution must shadow the sequence $A_\pm \to O \to C$ in Fig. 4.1). Moreover at early times the only possible solutions are the non-physical stiff-fluid universes which cannot

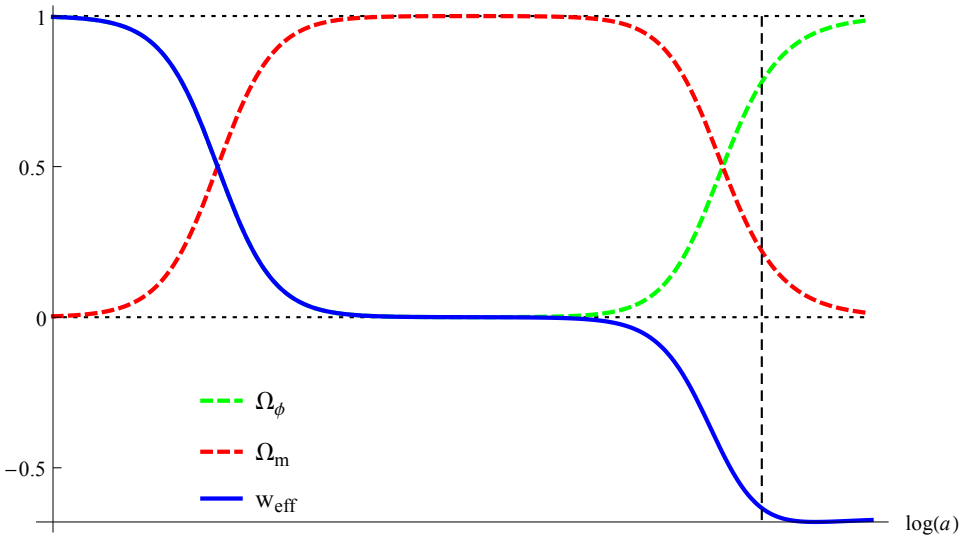

Figure 4.4: Evolution of the effective EoS parameter (w_{eff}), the matter (Ω_m) and dark energy (Ω_ϕ) relative energy densities for the quintessence model with an exponential potential. The vertical dashed line denotes the present cosmological time.

represent a viable description of the universe.

The effective EoS, together with the matter and scalar field relative energy densities, for a solution shadowing the heteroclinic sequence $A_- \to O \to C$ with $\lambda = 1$ has been plotted in Fig. 4.4. It is clear that in this model a sufficiently long period of matter domination followed by a never ending phase of dark energy domination can be achieved. Interestingly in this situation the final value of w_{eff} lies between $-1/3$ and -1 according to the value of λ. Only in the limit $\lambda \to 0$, for which the exponential potential becomes a cosmological constant, the value $w_{\text{eff}} = -1$ represent the final state of the universe. From Fig. 4.4 it is also evident that before the matter domination era a period of scalar field kinetic domination must have occurred. This period however happens at very early times when the effective description provided by the quintessence model is expected to fail since new physics, such as inflation, should come into play. For this reason the early time stiff fluid solutions are usually ignored in this model and only the late time matter to dark energy transition is considered phenomenologically interesting. Note also that the quintessence model with an exponential potential does not solve the cosmic coincidence problem since, as shown by the vertical dotted line in Fig. 4.4, the present cosmological time still lies with no explanation exactly when the dark matter to dark energy transition happens.

In our analysis we have assumed a positive potential $V > 0$ for physical reasons. However negative exponential potentials have been analysed using

dynamical systems techniques by Heard & Wands (2002). In that case a sufficiently flat potential ($\lambda^2 < 6$) always lead to a re-collapse, while with a steeper potential ($\lambda^2 > 6$) it is possible to achieve scaling solutions, but a strong dependence on initial conditions is present. Negative potentials have also been analysed by Copeland et al. (2009) who generalized the work of Heard & Wands (2002) to cosmologies with positive and negative spatial curvatures.

The scaling solutions we found in Point B are also phenomenologically important since in principle they allow the scalar field to hide its presence during the cosmological evolution. This situation can be used to postulate a scalar field which gives no contribution at early times but becomes relevant at late times. There are strong observational constraints for this situation (Ade et al., 2013) and a more complicated dynamics than the exponential potential is needed in order for the scalar field to exit the scaling solution and eventually driving the cosmic acceleration. It is impossible to achieve both the scaling and accelerating regimes with a canonical scalar field and an exponential potential, but with more complicated potentials, such as a double exponential potential (Barreiro et al., 2000), a transition from the scaling to the dark energy solution can be achieved. Furthermore we mention that scaling solutions are in general unstable in anisotropic spacetimes, though they still represent critical points which can hide the scalar field for a sufficiently long time (see Coley (2003) and references therein). Scaling solutions for scalar fields with exponential potential have also been studied in higher dimensional spacetime (Chang et al., 2005).

Finally we note that the analysis of quintessence with an exponential potential can be generalised to include both radiation and dark matter with the introduction of two barotropic fluids (Azreg-Anou, 2013). This approach breaks the degeneracy in the matter sector and the radiation to matter transition can be explicitly represented. However, except for some more complicated dynamics regarding the scaling solutions, the qualitative description of matter to dark energy transition remains unchanged.

4.3 Power-law potential

In this section we will consider quintessence with an inverse power-law type potential. Such a potential is known under the name of *Ratra-Peebles potential* (Ratra & Peebles, 1988; Peebles & Ratra, 1988) and it can be justified from supersymmetry phenomenology. Explicitly we will consider

Ratra-Peebles potential

$$V(\phi) = \frac{M^{\alpha+4}}{\phi^{\alpha}}\,, \tag{4.34}$$

where α is a dimensionless parameter and M a positive[12] constant with units of mass. Inverse power-law potentials are popular in quintessence models because of their behavior at late time which allows for a solution, or at least an alleviation, of the fine tuning of initial conditions (Zlatev et al., 1999; Liddle & Scherrer, 1999; Steinhardt et al., 1999; de la Macorra & Stephan-Otto, 2001). As we will see, models with $\alpha > 0$ are physically more interesting while scalar field potentials of the kind (4.34) with $\alpha < 0$ are less attractive for dark energy phenomenology, though they are largely used in early universe inflation[13]. In this section we will consider both positive and negative values of α, though the main discussion will focus on the $\alpha > 0$ case.

The dynamical system controlling the evolution of a universe filled by quintessence with an inverse power-law exponential potential is given by Eqs. (4.24), (4.25) and (4.27) which we recall for the sake of simplicity

$$x' = -\frac{3}{2}\left[2x + (w-1)x^3 + x(w+1)\left(y^2-1\right) - \frac{\sqrt{2}}{\sqrt{3}}\lambda y^2\right], \tag{4.35}$$

$$y' = -\frac{3}{2}y\left[(w-1)x^2 + (w+1)\left(y^2-1\right) + \frac{\sqrt{2}}{\sqrt{3}}\lambda x\right], \tag{4.36}$$

$$\lambda' = -\sqrt{6}\,(\Gamma - 1)\,\lambda^2 x\,. \tag{4.37}$$

Using the potential (4.34), from the definition (4.28) we obtain

$$\Gamma = \frac{V\,V_{,\phi\phi}}{V_{,\phi}^2} = \frac{\alpha+1}{\alpha}\,, \tag{4.38}$$

or

$$\Gamma - 1 = \frac{1}{\alpha}\,, \tag{4.39}$$

implying that Γ is in this case just a constant depending on the parameter α and equations (4.35)–(4.37) become an autonomous 3D dynamical system. Note that $\Gamma = 1$ corresponds to the exponential potential studied in Sec. 4.2 since λ becomes a constant in this case, as shown by Eq. (4.37). For this reason the value $\Gamma = 1$ will be excluded from the analysis of this section. In what follows we will apply dynamical systems methods to analyse Eqs. (4.35)–(4.37). Although all the relevant phenomenological properties of such a system have been extensively analysed with dynamical systems methods (Ng et al., 2001; Urena-Lopez, 2012; Gong, 2014; Roy & Banerjee,

[12] We will again assume a positive potential $V > 0$. For dynamical systems applications to a negative power-law potential see e.g. Felder et al. (2002).

[13] See Urena-Lopez & Reyes-Ibarra (2009) and Alho & Uggla (2014) for a dynamical systems application to the inflationary quadratic potential.

2014a), a number of achievements of this section express original results presented for the first time in this thesis[14].

Thanks to the $y \mapsto -y$ symmetry (4.29) and to the $(x, \lambda) \mapsto (-x, -\lambda)$ symmetry (4.30), which again holds trivially since Γ is a constant, the (physical) phase space of the system (4.35)–(4.37) is represented by the positive y half cylinder stretching from $\lambda = 0$ to $\lambda = +\infty$. The phase space is thus non-compact being infinite in the positive λ direction. However following Ng et al. (2001) we can compactify it defining a new variable z as

$$z = \frac{\lambda}{\lambda + 1}\,. \tag{4.40}$$

When $\lambda = 0$ we get again $z = 0$, but when $\lambda \to +\infty$ we have $z = 1$, meaning that the new variable z is bounded as $0 \leq z \leq 1$. This change of variables brings the (x, y)-plane at infinity to $z = 1$, compactifying in this way the phase space, which now becomes the half cylinder going from $z = 0$ to $z = 1$. We can invert (4.40) in order to obtain $\lambda = z/(z-1)$. The definition (4.40) holds only for $\lambda \geq 0$ since for $\lambda = -1$ a singularity would appear. This is fine in our case because we are dealing only with positive values of λ due to the symmetry (4.30). However in more general cases where also negative values of λ need to be considered, i.e. when $\Gamma(\lambda) \neq \Gamma(-\lambda)$ (see Sec. 4.4), the definition (4.40) must be generalised to $z = \lambda/(1 + |\lambda|)$, or to any other suitable change of variables leading to the compactification of the phase space without introducing new infinities.

In the new variable (4.40) the dynamical system (4.35)–(4.37) becomes

$$x' = \frac{1}{2}\left[-3(w-1)x^3 - 3x\left(w\left(y^2-1\right) + y^2 + 1\right) + \frac{\sqrt{6}y^2 z}{1-z}\right], \tag{4.41}$$

$$y' = -\frac{1}{2}y\left[3(w-1)x^2 + 3(w+1)\left(y^2-1\right) + \frac{\sqrt{6}xz}{1-z}\right], \tag{4.42}$$

$$z' = -\sqrt{6}(\Gamma - 1)xz^2\,. \tag{4.43}$$

Note that the last term in both the equations for x and y diverges as $z \to 1$. This is expected since $z \to 1$ corresponds to $\lambda \to +\infty$. In order to remove these infinities we can multiply the right hand side of (4.41)–(4.43) by $(1-z)$. This operation allows us to study the properties of the $z = 1$ plane and does not change the dynamical features of the system in the other regions of the

[14] In general an extensive dynamical systems analysis of the phenomenology of the power-law potential has never been considered in the literature. In particular the numerical analysis that lead to the figure in this section, the computation of the centre manifold around Point C and the compactification of the phase space with the study of the behaviour at infinity, all represent original work.

Point	x	y	z	Existence	$w_{\rm eff}$	Accel.	Ω_ϕ	w_ϕ
O_z	0	0	Any	$\forall\, w, \alpha$	w	No	0	-
$A_\pm$	± 1	0	0	$\forall\, w, \alpha$	1	No	1	1
B_x	Any	0	1	$\forall\, w, \alpha$	$w + x^2(1-w)$	No	x^2	1
C	0	1	0	$\forall\, w, \alpha$	-1	Yes	1	-1

Table 4.3: Critical points of the system (4.44)–(4.46) with existence and physical properties.

Point	Eigenvalues	Hyperbolicity	Stability
O_z	$\left\{0, -\frac{3}{2}(w \pm 1)(z-1)\right\}$	Non-hyperbolic	Saddle
A_+	$\{0, 3, 3(1-w)\}$	Non-hyperbolic	Saddle if $\alpha > 0$ ($\Gamma > 1$) Unstable if $\alpha < 0$ ($\Gamma < 1$)
A_-	$\{0, 3, 3(1-w)\}$	Non-hyperbolic	Unstable if $\alpha > 0$ ($\Gamma > 1$) Saddle if $\alpha < 0$ ($\Gamma < 1$)
B_x	$\left\{0, -\frac{\sqrt{3}}{\sqrt{2}}x, \sqrt{6}(\Gamma - 1)x\right\}$	Non-hyperbolic	Saddle if $x > 0$ and $\alpha > 0$ ($\Gamma > 1$) Stable if $x > 0$ and $\alpha < 0$ ($\Gamma < 1$) Saddle if $x < 0$ and $\alpha > 0$ ($\Gamma > 1$) Unstable if $x < 0$ and $\alpha < 0$ ($\Gamma < 1$)
C	$\{0, -3, -3(1+w)\}$	Non-hyperbolic	Stable if $\alpha > 0$ ($\Gamma > 1$) Saddle if $\alpha < 0$ ($\Gamma < 1$)

Table 4.4: Critical points of the system (4.44)–(4.46) with stability properties.

phase space[15] , since $(1-z)$ is always positive for $0 \leq z < 1$. After this little trick we obtain

$$x' = \frac{1}{2}(1-z)\left[-3(w-1)x^3 - 3x\left(w\left(y^2-1\right) + y^2 + 1\right)\right] + \frac{\sqrt{3}}{\sqrt{2}}y^2 z\,, \quad (4.44)$$

$$y' = -\frac{1}{2}y\,(1-z)\left[3(w-1)x^2 + 3(w+1)\left(y^2-1\right)\right] - \frac{\sqrt{3}}{\sqrt{2}}\,xyz\,, \quad (4.45)$$

$$z' = -\sqrt{6}(\Gamma - 1)(1-z)xz^2\,, \quad (4.46)$$

which is regular for $z = 1$.

We are now ready to discuss the critical points of the system (4.44)–(4.46) whose existence and phenomenological properties have been listed in Tab. 4.3, while Tab. 4.4 shows their stability properties.

[15]Strictly speaking this operation is not mathematically well-defined. However in this case we are just removing the divergent terms on the $z = 1$ plane leaving the rest of the phase space basically invariant since, in general, for any dynamical system $\mathbf{x}' = \mathbf{f}(\mathbf{x})$ the new dynamical system constructed as $\mathbf{x}' = \xi(\mathbf{x})\mathbf{f}(\mathbf{x})$ for a positive defined function $\xi(\mathbf{x}) > 0$ will present the same critical points with the same stability properties. We could have equally kept Eqs. (4.41)–(4.43) and studied the dynamics on the $z = 1$ plane only considering the diverging terms and neglecting all the others.

- *Points O_z.* The z-axis is a critical line. This means that all the points with $x = y = 0$ are critical points whose existence does not depend on the theoretical parameters w and α. Being both x and y equal to zero, the effective EoS coincides with the matter EoS and the relative energy density of the scalar field vanishes leaving w_ϕ undetermined. Since these are not isolated critical points we expect that at least one eigenvalues of the Jacobian vanishes. This is indeed the case, as one can realize from Tab. 4.4, meaning that these points are non-hyperbolic and that linear stability theory cannot be used. Moreover, since there is only one vanishing eigenvalue, the centre manifold of these points corresponds to the z-axis and the centre manifold theorem cannot apply. To determine the stability properties, from Tab. 4.4 we can see that the non vanishing eigenvalues of Points O_z are given by $-\frac{3}{2}(w \pm 1)(z - 1)$. Since $0 \leq z \leq 1$ and for physically acceptable matter fluids $0 \leq w \leq 1/3$, we obtain that one of these eigenvalues is always positive while the other is always negative. The critical lines of Points O_z is thus generally unstable, and we can also conclude that it will act as a saddle line since the non-zero eigenvalues have opposite sign. As we will see, this behavior will in fact be confirmed by numerical computations.

- *Points $A_\pm$.* The two points at $(\pm 1, 0, 0)$ are again the scalar field kinetic dominated solutions that we already encountered for the exponential potential (Sec. 4.2). They exists for all values of w and α and their phenomenological properties remain the same with $w_{\text{eff}} = w_\phi = 1$ and $\Omega_\phi = 1$, which means they represent stiff-fluid dominated solutions. From Tab. 4.4 we see that one eigenvalue of the Jacobian is zero implying that Points $A_\pm$ are isolated non-hyperbolic critical points. Since the remaining eigenvalues are both always positive, we can conclude that Points $A_\pm$ are both asymptotically unstable. However in order to understand whether they can be saddle points or past attractors we must study the flow along the centre manifold which in this case coincides with the z-direction[16], i.e. with the centre subspace (see Sec. 2.2). The flow restricted to the z-direction passing through the Points $A_\pm$ is given by $z' = \mp\sqrt{6}(1 - z)z^2(\Gamma - 1)$. Since $0 \leq z \leq 1$ the stability is determined by the parameter α through Γ. If $\Gamma > 1$ ($\alpha > 0$) then Point A_+ is a saddle point while Point A_- is asymptotically stable in the past. On the other hand, if $\Gamma < 1$ ($\alpha < 0$) then Point A_+ is a past attractor and Point A_- is a saddle point. This has been summarised in Tab. 4.4.

[16] To prove this statement one can compute the centre manifold using the methods of Sec. 2.4 and show that the function $\mathbf{h}(z)$ is zero for all z (this can be done for example by induction over the coefficients of a polynomial ansatz for $\mathbf{h}(z)$). As we will see this is confirmed by numerical computations.

- *Point B_x.* The straight line connecting Points $(\pm 1, 0, 1)$ is another critical line. Since all critical points at infinity, i.e. on the $z = 1$ plane, are points belonging to this line, Points B_x completely characterize the asymptotic behavior of trajectories as $\lambda \to +\infty$. The effective EoS at these points will depend on the scalar field relative energy $\Omega_\phi = x^2$ as $w_{\text{eff}} = w + x^2(1 - w)$. However, since the potential energy of quintessence vanishes ($y = 0$) the scalar field EoS can only be determined by its kinetic part and thus $w_\phi = 1$ with no possible acceleration for the universe ($0 \leq w_{\text{eff}} \leq 1$). As we can see in Tab. 4.4 there is only one zero eigenvalue meaning that the centre manifold for these points is nothing but the critical line itself. The only exceptions is when $x = 0$ where all the eigenvalues vanish. This is the point where the two critical lines O_z and B_x intersect and, as one can again understand from Tab. 4.4, also all the eigenvalues of Points O_z vanish at this point, i.e. at $z = 1$. Using numerical evaluations we will see that this point will in fact recall the features of a centre (see Sec. 2.6). In general the stability of the critical line B_x will depend on both the parameter α (through Γ) and the value of the coordinate x. If $\alpha > 0$ ($\Gamma > 1$) the non vanishing eigenvalues have opposite sign no matter the value of x and we can conclude that Points B_x are saddle points in this case. On the other hand if $\alpha < 0$ ($\Gamma < 1$) the non zero eigenvalues have the same sign: positive if $x < 0$ and negative if $x > 0$. As we well know linear stability theory fails in these cases, however since the centre manifold corresponds to the critical line B_x (i.e. it is flat), we can expect that orbits near B_x are perpendicularly attracted or repelled according to the sign of the non vanishing eigenvalues. Points B_x will then be attractive if $x > 0$ and repulsive if $x < 0$. As we will see with numerical techniques, this is indeed the right stability behavior.

- *Point C.* The final critical point of the system (4.44)–(4.46) is the scalar field dominated point at $(0, 1, 0)$. This corresponds to nothing but a cosmological constant-like dominated solution where the universe undergoes a de Sitter accelerated expansion. In fact Point C is dominated by the potential energy of the scalar field which is constant due to the vanishing of its kinetic energy ($x^2 = 0$). As shown in Tab. 4.4 one of the eigenvalues of the Jacobian vanishes at Point C implying that this point is an isolated non-hyperbolic critical point. Since the remaining eigenvalues are both negative, to determine the stability we must either find a Liapunov function or apply the centre manifold theorem. We will follow the second approach which will allow us also to determine the shape of the centre manifold. Here we sketch the computations leaving the details for the reader. First we must find the eigenvectors of the Jacobian at Point C which are $(1, 0, 0)$, $(0, 1, 0)$ and $(1/\sqrt{6}, 0, 1)$ with the last one corresponding to

the vanishing eigenvalues. Since the eigenvectors are not all aligned with the orthonormal axis, we need to rewrite the dynamical system with respect to the basis given by the eigenvectors themselves[17]. The corresponding change of coordinates $\mathbf{x} \mapsto \tilde{\mathbf{x}}$ is given by $x = \tilde{x} + \tilde{z}/\sqrt{6}$, $y = \tilde{y}$ and $z = \tilde{z}$. With these coordinates we can rewrite the dynamical system (4.44)–(4.46) in the form (2.35)–(2.36) and then use (2.43) to find the centre manifold. With a power-law ansatz for the centre manifold function $\mathbf{h} = (h_x, h_y)$ we obtain, up to the third order in $\tilde{z}$,

$$h_x(\tilde{z}) = \frac{\tilde{z}^2}{\sqrt{6}} + \frac{\sqrt{6}}{18}(\Gamma + 2)\,\tilde{z}^3 + O\left(\tilde{z}^4\right) , \tag{4.47}$$

$$h_y(\tilde{z}) = -\frac{\tilde{z}^2}{12} - \frac{\tilde{z}^3}{6} + O\left(\tilde{z}^4\right) . \tag{4.48}$$

These two functions determine the shape of the one dimensional centre manifold of Point C. At the smallest order in $\tilde{z}$ the dynamics along this centre manifold is given by

$$\tilde{z}' = -(\Gamma - 1)\,\tilde{z}^3 + O\left(\tilde{z}^4\right) . \tag{4.49}$$

We can thus conclude that Point C is stable if $\Gamma > 1$ ($\alpha > 0$) and a saddle if $\Gamma < 1$ ($\alpha < 0$). As we will see, numerical evaluations will not only confirm this stability behavior but will also show us how well the centre manifold (4.47)–(4.48) computed with approximation methods matches the actual one.

All the critical points we have just described are non-hyperbolic and their stability properties have not been as easy to find as in the exponential potential case of Sec. 4.2. The picture we obtained from the analysis above is that there are two possible regimes for the power-law potential (4.34) depending on the value of α being positive (inverse power-law) or negative (direct power-law), which corresponds to Γ being bigger or smaller than one. Tab. 4.4 suggests that the global future attractor of the phase space is Point C if $\Gamma > 1$ and Points B_x (with $x > 0$) if $\Gamma < 1$. As we are now going to show using numerical plotting of the phase space, this is indeed the behavior of the phase space. In what follows we will focus on the matter EoS value $w = 0$, but the results will not change for other values inside the physically meaningful interval $0 \leq w \leq 1/3$. We will mainly focus on the $\Gamma > 1$ ($\alpha > 0$) case, and then briefly discuss the $\Gamma < 1$ ($\alpha < 0$) case.

Inverse power-law potential: $\alpha > 0$ ($\Gamma > 1$)

In Fig. 4.5 the phase space for the value $\alpha = 10$, corresponding to $\Gamma = 1.1$, has been plotted. The late time global attractor is the dark energy dominated Point C, while the global past attractor is Point A_-. The red/dashed line denotes the centre manifold of Point C which in this

[17] One need to rewrite the system with respect to E^c and E^s before apply the centre manifold theorem; see Sec. 2.4

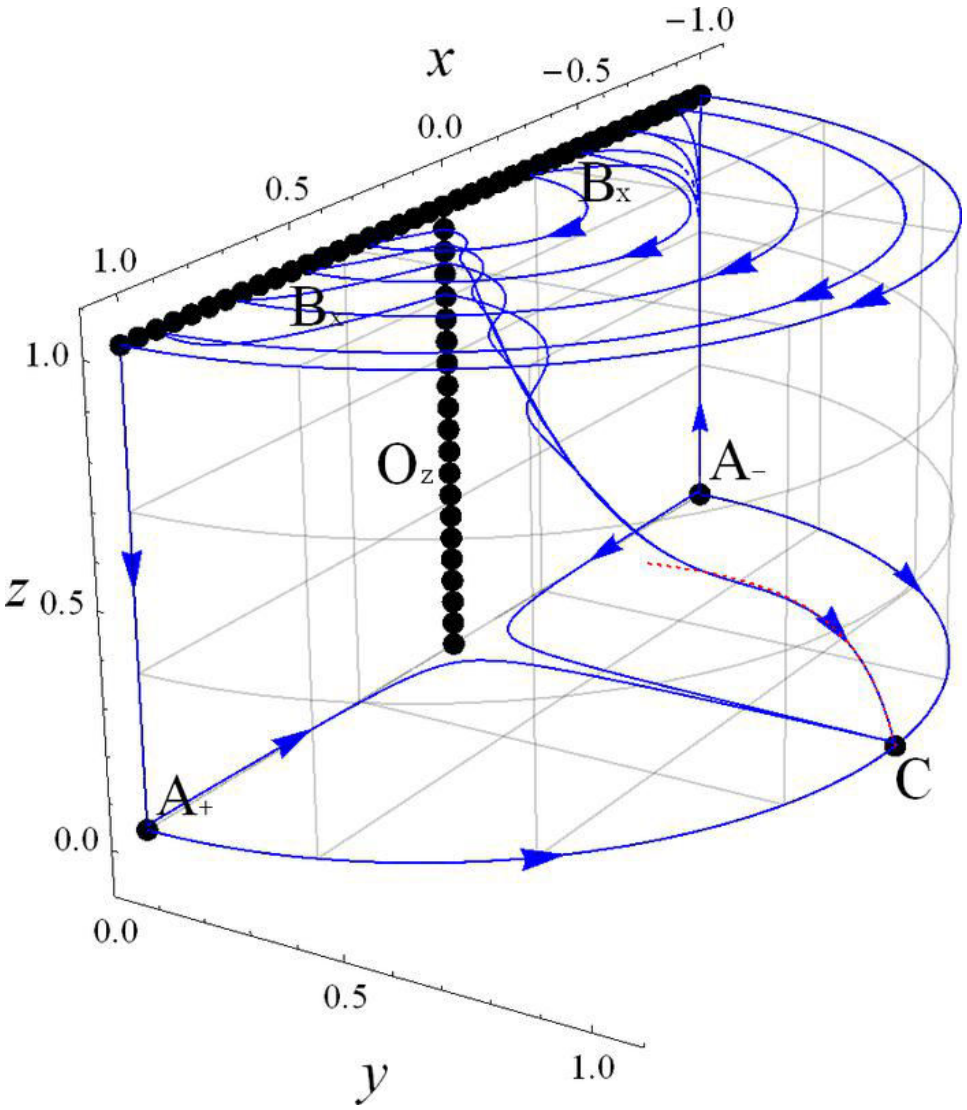

Figure 4.5: Phase space of quintessence with inverse power-law potential corresponding to the dynamical system (4.44)–(4.46). The values $w = 0$ and $\alpha = 10$ ($\Gamma = 1.1$) have been chosen. The black/thick points denotes critical points with the $x = y = 0$ line and $z = 1$ plus $y = 0$ line being critical lines. The late time attractor is the dark energy dominated Point C and orbits approaching this point are first attracted by its centre manifold approximated by the red/dashed line. In this plot the tracking behavior of solutions moving from higher to lower values of z (i.e. of λ) is particularly in evidence.

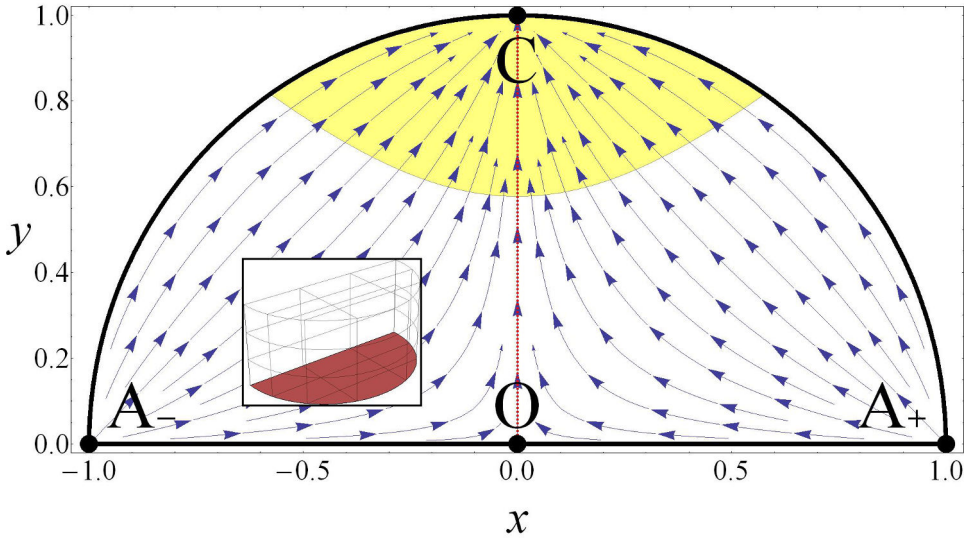

Figure 4.6: Flow of the system (4.44)–(4.46) on the $z = 0$ plane.

plot has been approximated up to the 7th order in $\tilde{z}$. The interesting phenomenological applications of quintessence with a power-law potential are all summarised in Fig. 4.5, and we will deal with them after having completely clarified the dynamics of the phase space. Numerical examples will mainly be provided for $\Gamma = 1.1$ ($\alpha = 10$), though different values do not alter the qualitative dynamical features (as long as $\Gamma > 1$).

As shown in Fig. 4.5 every orbit starts from Point A_- either remaining on the $z = 0$ plane or vertically escaping to the $z = 1$ plane. In order to better understand the behavior of these solutions we can look at the dynamics of the flow on the boundaries of the phase space. First in the $z = 0$ plane the system reduces to a universe where quintessence has a constant potential, or in other words where there is a free scalar field (no potential) and a cosmological constant. This is easy to understand since $z = 0$ implies $\lambda = 0$ which in turns corresponds to a constant potential. In fact, as shown by Fig. 4.6 the flow restricted to this plane is nothing but the exponential potential phase space of Fig. 4.1 with $\lambda = 0$. We notice that there is an heteroclinic orbit connecting the origin to Point C, which represent the matter to dark energy transition when the scalar field plays no role at all in the dynamics of the universe but the acceleration is determined by the cosmological constant.

The flow on the vertical boundaries of the phase space is drawn in Figs. 4.7 and 4.8, where the red/dashed line denotes again the centre manifold of Point C approximated to the 7th order in $\tilde{z}$. As one can realize from the pictures, the centre manifolds of Points $A_\pm$ are both linear along the z directions. The numerical results thus confirms that these centre manifold

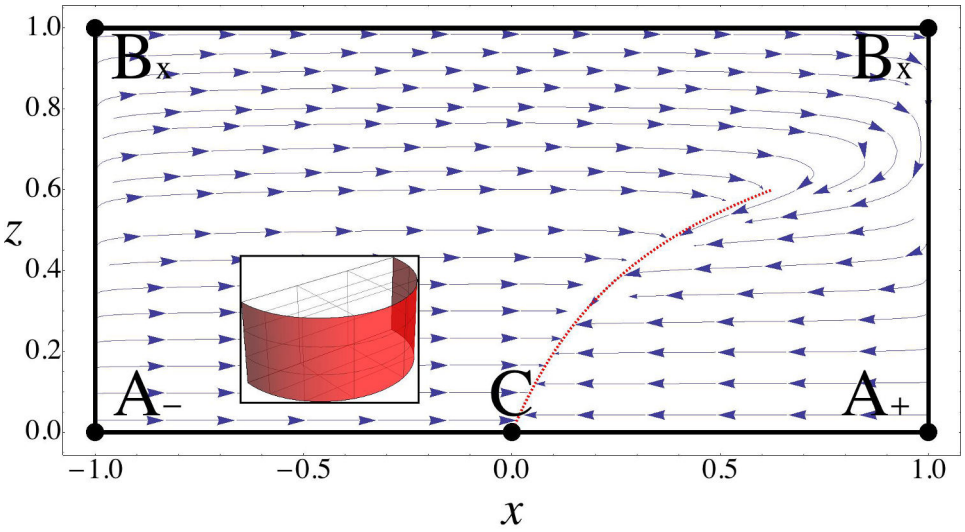

Figure 4.7: Flow of the system (4.44)–(4.46) with the values $w = 0$ and $\Gamma = 1.1$ on the $x^2 + y^2 = 1$ surface. The red/dashed line denotes the approximated (up to 7th order) centre manifold of Point C.

coincides with their corresponding centre subspaces. Furthermore the centre manifold of Point A_- is repulsive while the one of Point A_+ is attractive. This implies that while Point A_- is a past attractor, Point A_+ is a saddle point, as denoted also by the solutions plotted in Fig. 4.5. Along the curved $x^2 + y^2 = 1$ surface, where the scalar field dominates, the flow is attracted by the centre manifold of Point C. All the orbits on this surface are thus first captured by this centre manifold and eventually approach the global attractor Point C. On the other hand, a different dynamics can be found on the $y = 0$ surface of Fig 4.8. Here we have two critical lines which divide the surface into two distinct parts. On the negative x side trajectories escape from Point A_- and eventually end in either Points O_z or B_z. On the positive x side instead Points B_x are unstable and Point A_+ is a saddle. The flow can thus only end into the critical line O_z while it has as its past attractor the critical line B_x. Combining the information coming from Figs. 4.6, 4.7 and 4.8 we find that the results on the stability of Points $A_\pm$ we obtained with analytical methods are confirmed by numerical computations.

The last boundary of the phase space that remains to analyse is the $z = 1$ plane, corresponding to the original points at infinity, $\lambda \to +\infty$. The flow restricted on this surface has been drawn in Fig. 4.9. As we can see the only critical points appearing at $z = 1$ are Points B_x. For $x > 0$ their are attractive while for $x < 0$ their are repulsive on the plane. The solutions start from the negative x axis and finish into the positive x axis after a circular motion around the origin. In fact, as shown by Ng et al. (2001), the dynamical system (4.44)–(4.46) restricted on this plane can be analytically

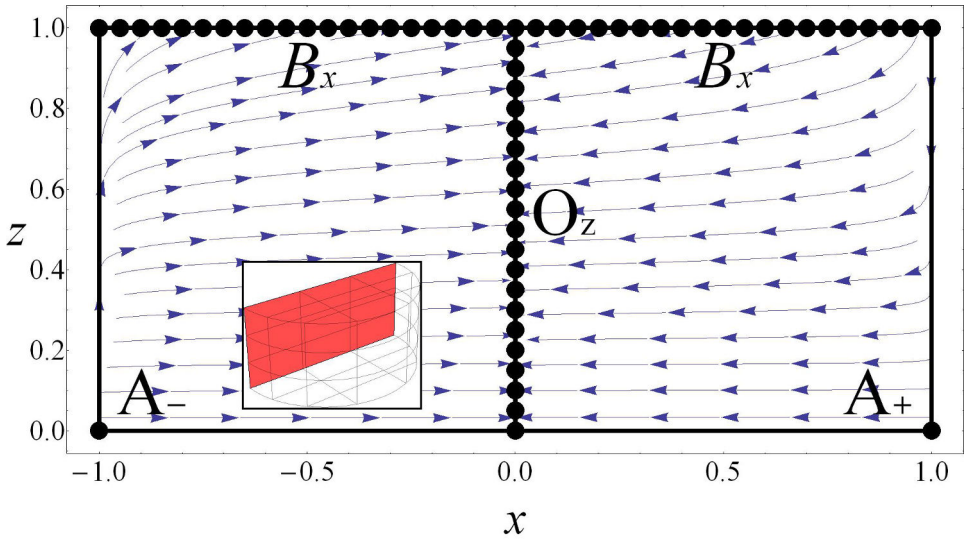

Figure 4.8: Flow of the system (4.44)–(4.46) with the values $w = 0$ and $\Gamma = 1.1$ on the $y = 0$ plane.

solved to give the solutions

$$x(\eta) = A \tanh\left[\frac{\sqrt{3}}{\sqrt{2}}(\eta - \eta_0)\right], \tag{4.50}$$

$$y(\eta) = A \operatorname{sech}\left[\frac{\sqrt{3}}{\sqrt{2}}(\eta - \eta_0)\right], \tag{4.51}$$

where A and η_0 are two constants. The flow on the $z = 1$ plane is thus composed by circular orbits and Point $(0, 0, 1)$ effectively acts as a centre. In fact, as we mentioned before, the eigenvalues of the Jacobian matrix all vanish at this point. Note that for some of these trajectories, the ones intersecting the yellow/shaded region in Fig. 4.9, a finite period of accelerated expansion can be achieved. Finally putting together the information on the flow from Figs. 4.8 and 4.9, the stability of Points B_x can be understood. We find that, in the $\Gamma > 1$ case we are currently studying, they behave as saddle points independently of the value of x. For $x < 0$ the critical line B_x attracts orbits in the $y = 0$ plane and repels them in the $z = 1$ plane. For $x > 0$ we find instead the opposite behavior: trajectories are attracted on the $z = 1$ surface and repelled in the $y = 0$ plane. These are exactly the stability properties we derived with analytical techniques.

We can now focus on the dynamics in the interior of the phase space, where the physically interesting features make their appearance. Going back to Fig. 4.5 we see that every trajectory escaping to the $z = 1$ plane, after completing the circular tour from negative to positive x, is then attracted by

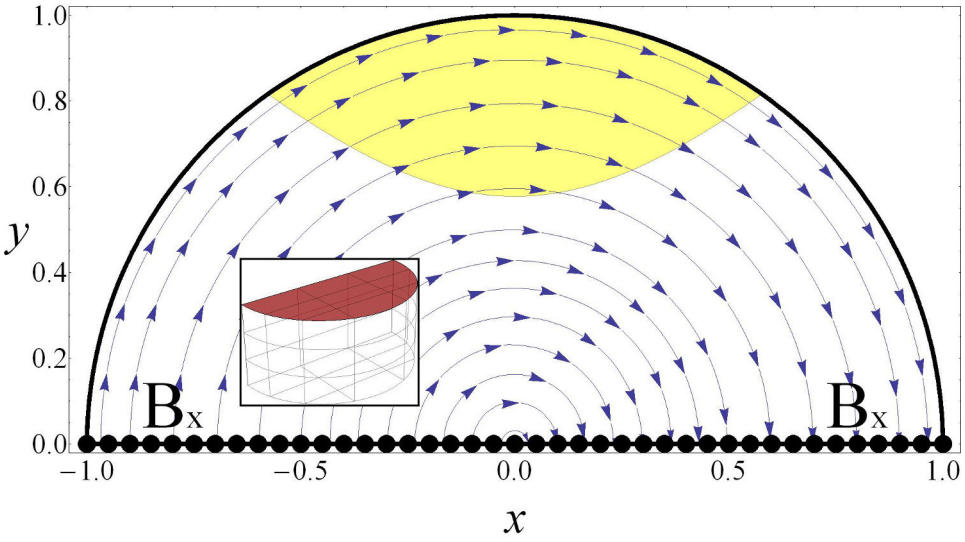

Figure 4.9: Flow of the system (4.44)–(4.46) with the values $w = 0$ and $\Gamma = 1.1$ on the $z = 1$ plane.

Points O_z, as it can be realized also looking at Fig. 4.8. More interestingly though we see that for almost all these trajectories there is a late time convergence towards a single orbit which asymptotically approaches the centre manifold of Point C. The dark matter to dark energy transition can thus be easily described by one of these orbits which always experiences a finite period of matter domination before the universe becomes dark energy dominated. This convergence behavior during the matter to dark energy transition is phenomenologically important since it can help in solving the fine tuning problems we encountered with the ΛCDM model and with the exponential potential (Zlatev et al., 1999; Steinhardt et al., 1999). We now focus our attention on this transition from Points O_z to Point C.

To better visualize what happens during this period, two projections on the (x, y)-plane have been drawn[18]. In Fig. 4.10 trajectories with different initial conditions in the case $\Gamma = 1.1$ are plotted, while in Fig. 4.11 orbits with the same initial conditions but corresponding to different values of Γ are presented. From these two pictures one can understand that as the solutions leave the matter dominated saddle Point O_z, they are first attracted by and eventually follow the red/dashed line shown in both figures. This represent the position of the attractor solution in the exponential potential case of Sec. 4.2 for all possible values of λ. The line connecting the origin to the unit circle represents the scaling solutions where the scalar field EoS matches the matter EoS, while the remaining red/dashed line on the circumference stands for the late time attracting dark energy dominating solution of the

[18]See Urena-Lopez (2012) where similar projections were considered.

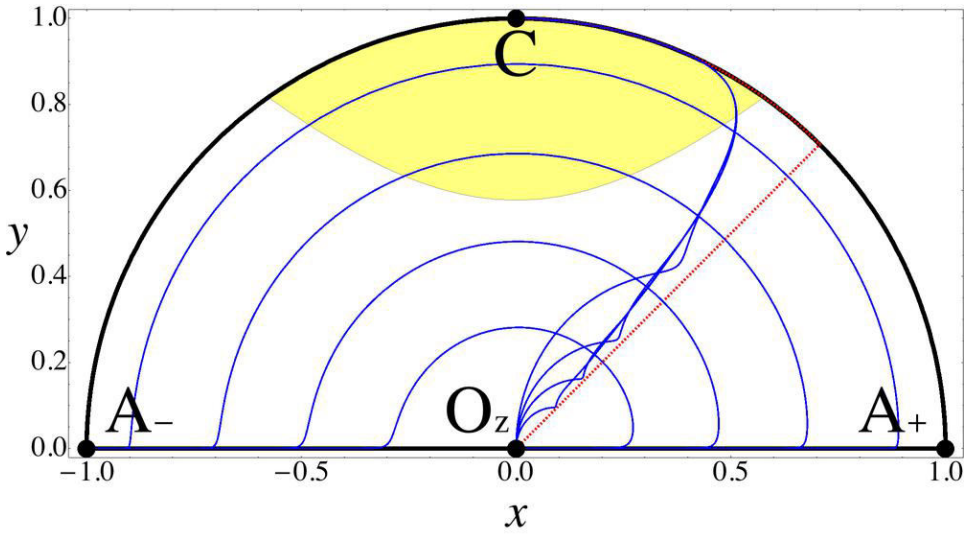

Figure 4.10: Projection onto the (x, y)-plane of solutions of the system (4.44)–(4.46) with $\Gamma = 1.1$ ($\alpha = 10$) and different initial conditions (i.e. of the trajectories in Fig. 4.5.). The tracking behavior is characterized by the orbits following the red/dashed line representing the future attractor (scaling and dark energy solutions) of the exponential potential case of Sec. 4.2 for different values of λ. Orbits whose initial circular motion on the $z = 1$ plane is closer to Points O_z eventually join the tracking behavior more rapidly.

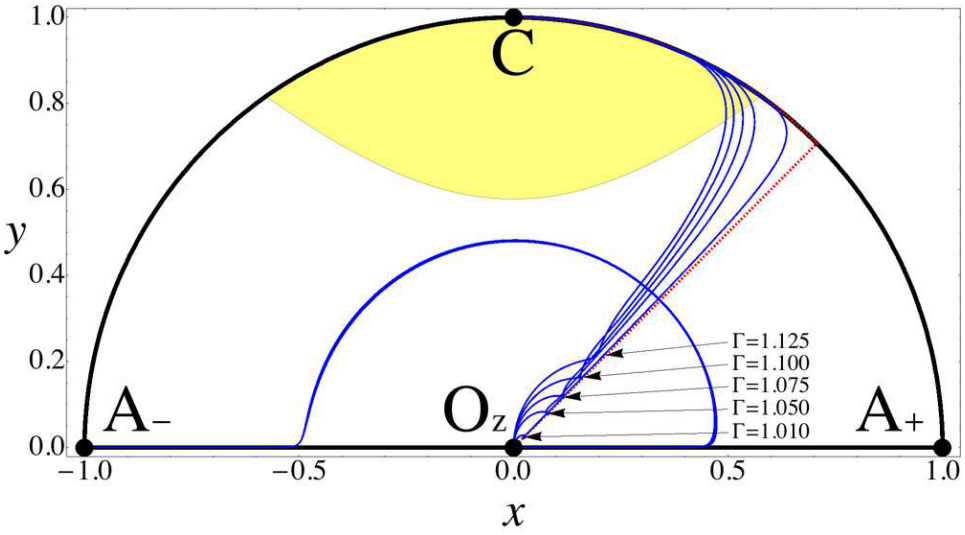

Figure 4.11: Projection onto the (x, y)-plane of solutions of the system (4.44)–(4.46) with the same initial conditions but corresponding to different values of Γ (i.e. of α). The tracking behavior is well represented by the orbits shadowing the red/dashed line, which has the same meaning as in Fig. 4.10. The more Γ is closer to one, the faster and more efficiently the solutions join the tracking behavior.

exponential potential case. The dynamics of orbits in Figs. 4.10 and 4.11 can then be understood in terms of a tracking evolution along the positions where the scaling solutions would appear. Because of this behavior these solutions are known as *tracking solutions*.

Tracking solutions

Tracking solutions are phenomenologically interesting since they allow the scalar field to follow a matter EoS for a finite period of time and then to switch to the dark energy dominated solutions. The term "tracking" refers to the ability of the scalar field to approximately follow the matter evolution in such a way that this approximation eventually fails at late time and a cosmological constant-like EoS is attained with the universe undergoing an asymptotic de Sitter expansion. Note that while the trajectories follows the scaling solutions, the energy density of the scalar field increases with the kinetic energy roughly remaining proportional to the potential energy. This is a behavior which the exponential potential scaling solutions follow exactly as λ changes. Moreover since the orbits are attracted by the positions where the scaling solutions would appear, the points on the red/dashed line of Figs. 4.10 and 4.11 are sometimes called *instantaneous critical points*, though mathematically they are not critical points.

As shown in Fig. 4.10 the closer to Points O_z the orbits take their tour on the $z = 1$ plane, the faster they join the tracking behavior. In fact the solution which is first attracted by the red/dashed line corresponds to the

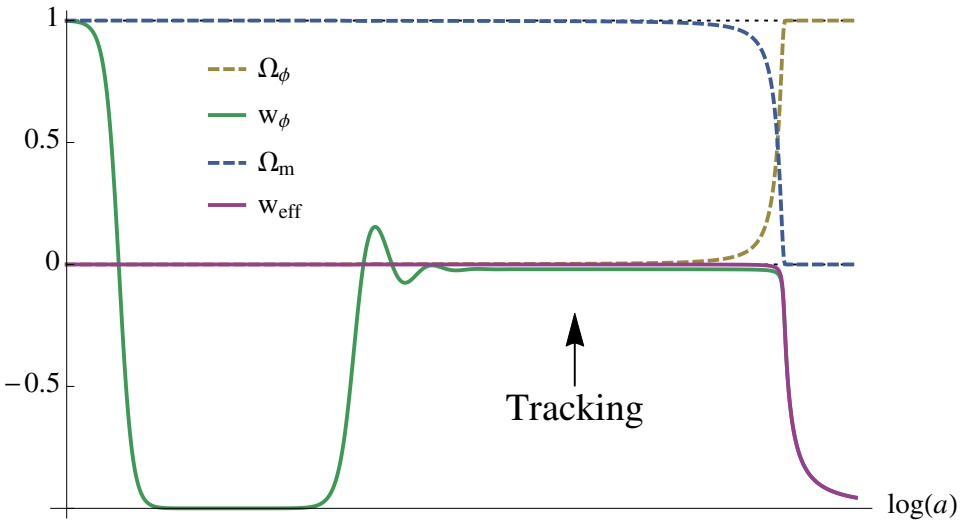

Figure 4.12: Late time evolution of the physically relevant quantities during the matter to dark energy transition of quintessence with inverse power-law potential (4.34) and $\alpha = 100$ ($\Gamma = 1.01$). Note the tracking and frozen behaviors of the scalar field (here $w = 0$).

one drawing the smaller circle, while the solution which struggle most to join the tracking behavior corresponds to the bigger circle. A similar situation happens for different values of Γ as presented in Fig. 4.11. The closer Γ is to one, the faster and more efficiently the trajectories attain the tracking nature and the more they remain near the red/dashed line. Models with larger α will lead to a better tracking behavior as can be understood comparing the $\Gamma = 1.01$ ($\alpha = 100$) with the $\Gamma = 1.125$ ($\alpha = 8$) trajectories in Fig. 4.11. The condition $\Gamma \simeq 1$ is generally known to be necessary for the achievement of a tracking solution also in models of quintessence with a dynamically changing Γ (Steinhardt et al., 1999). If Γ is effectively (but not equal to) one the orbits would accurately follow the red/dashed line in Figs. 4.10 and 4.11. In this situation the dynamics would describe an effective transition from a scaling solution to a dark energy dominated universe, which we could not obtain from the exponential potential case in Sec. 4.2. In other words the dynamics would equal the exponential potential one with a variable λ, and the relative energy of the scalar field would start dominating the universe without spoiling the matter-like evolution. We also notice that as Γ becomes closer to one, the instantaneous critical points effectively act as attracting spirals (Ng et al., 2001). This can be seen in the $\Gamma = 1.05$ and $\Gamma = 1.01$ trajectories of Fig. 4.11 where a small spiraled attraction is achieved before the tracking behavior becomes increasingly less powerful.

In order to better understand the dynamics of the scalar field during the matter to dark energy transition, in Fig. 4.12 the evolution of the phe-

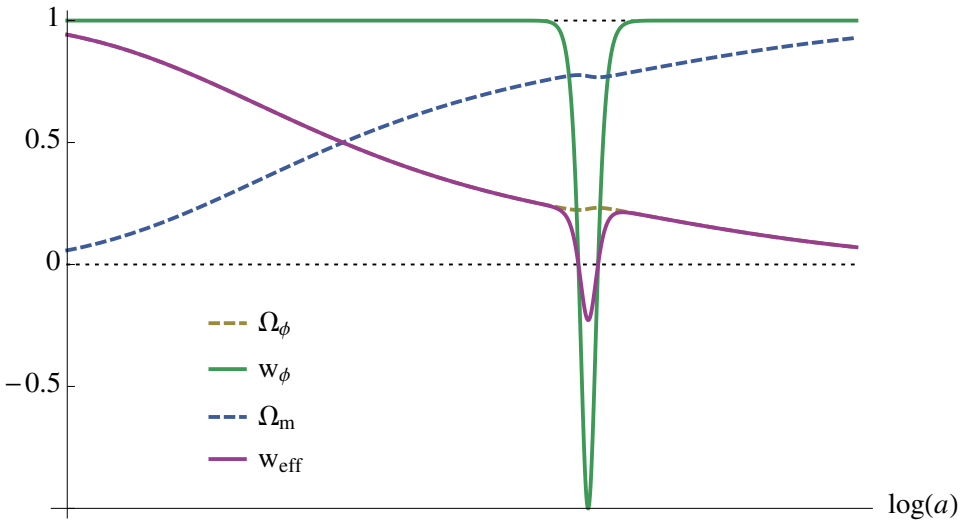

Figure 4.13: Early time evolution ($z = 1$ plane) of the physically relevant quantities of the orbits plotted in Fig. 4.11.

nomenologically interesting quantities has been plotted for the best solution of Fig. 4.11, the one with $\Gamma = 1.01$ ($\alpha = 100$) (a smaller value of α could be equivalently chosen considering different initial conditions). The tracking behavior is particularly in evidence as the quintessence EoS shadows the matter EoS before converging towards the -1 value of dark energy. Before the tracking regime we note that the scalar field EoS assumes also the cosmological constant value -1, though, being its relative energy negligible in comparison to the matter one during that period, this has no influence on the effective evolution of the universe ($w_{\text{eff}} = w$). This phase of the scalar field is known as *frozen field* epoch since the energy density of the quintessence field remains constant as the universe expand (Zlatev et al., 1999; Steinhardt et al., 1999). Note also the oscillating behavior as the field approaches the tracking regimes. This is due to the spirally attractive nature of the instantaneous critical points, whose effects are stronger for larger values of α (Γ closer to one). At the end of the tracking phase the EoS parameter of the scalar field drops from w to -1. The dynamical relation that holds between w_ϕ and Ω_ϕ during this phase predicts late time phenomenological signatures whose observation could in principle distinguish between quintessence and the cosmological constant (Zlatev et al., 1999; Gong, 2014).

At this point we spend few words regarding the early time evolutions of trajectories which will then join the tracking behavior. All these solutions start from Point A_- and are immediately attracted by the $z = 1$ plane where they perform the circular motion. As shown in Fig. 4.13, during this period the universe starts in a kinetically dominated scalar field solution ($w_{\text{eff}} = 1$) and the universe total energy slowly convert from quintessence to

matter domination. The past attractor is thus another stiff-fluid dominated solution as it is in the exponential potential case of Sec. 4.2. Though this kind of solutions are phenomenologically disfavored, they are relevant only for the dynamics of the very early universe where other physical quantities are expected to come into play (e.g. inflation). For this reason they are ignored also in quintessence models with an inverse power-law exponential and the only relevant dynamics to be considered is the late time one of Fig. 4.12. Note however that a non trivial feature appears as the orbits go through the circular motion on the $z = 1$ plane. This is represented by the sudden dropping from 1 to -1 of the quintessence EoS parameter in Fig. 4.13. What happens is that during the circular motion in the $z = 1$ plane the scalar field rapidly changes its kinetic energy into potential energy and then the other way around. This creates a dropping of the effective EoS of the universe which, for the larger circular orbits, leads to a possible finite period of acceleration in the early universe. The orbits for which this happens are exactly the ones passing throughout the yellow/shaded region in Fig. 4.9. At this point one might be tempted to identify this initial period of accelerated expansion with the early universe inflation, in such a way to have a scalar field unified model of both inflation and dark energy. Unfortunately there is no way for this finite period of acceleration to last enough time in order to describe a viable model of inflation[19]. In fact the closer to the unit circle is the orbit passing on the $z = 1$ plane the faster this period will result and for sufficiently small circles the orbits do not reach the accelerating regime. This does not depend on the parameter Γ also, as can be seen from solutions (4.50)–(4.51) where neither Γ nor α appear. The only way to achieve a sufficiently long period of steady acceleration in the universe is through the presence of a critical point in the yellow/shaded region of Fig. 4.9, which in the case of quintessence with an inverse potential is not present at early times ($z = 1$).

To conclude the analysis on the $\Gamma > 1$ case we discuss the problem of fine tuning and initial conditions. As we mentioned before trajectories entering the tracking regime can in principle solve this problem. One has to be careful that tracking solutions do not solve the cosmic coincidence problem as one can immediately realize from Fig. 4.12 where the matter to dark energy transition happens again at the present cosmological time with no apparent reason. The inverse power-law potential helps in solving another coincidence problem, namely the fine tuning problem of the initial conditions. Recall that the exponential potential quintessence model was able to describe the matter to dark energy transition only for very special initial conditions: the ones allowing for a sufficiently long period of matter domination. In the inverse power-law potential instead almost every orbit which first passes near the $z = 1$ plane, i.e. for which $\lambda \gg 1$ at early

[19] In early universe terminology it cannot last the sufficient number of e-foldings.

Tracker theorem

times, will eventually reach the tracking regime and then describe a late time transition to dark energy domination, a result known as the *tracker theorem* (Zlatev et al., 1999; Steinhardt et al., 1999; Urena-Lopez, 2012). This situation does scarcely depends on initial conditions, but how general are the solutions passing near the $z = 1$ plane? In other words, why the evolution of phenomenologically relevant trajectories should reach the $z = 1$ plane after leaving the past attractor Point A_-? To answer this question we will make two arguments: a mathematical one and a physical one.

First we recall that the unstable centre manifold of Point A_- coincides with its centre subspace which is notably parallel to the z axis. Every trajectory leaving the past attractor is immediately attracted by this centre manifold towards the increasing z direction. Considering then a random solution escaping Point A_-, it is highly probable that such a solution will travel along its centre manifold as only very particular initial conditions will force this orbit not to reach high values of z. This happens exactly because the unstable centre manifold of Point A_- is linear in the z direction. The situation is similar to the one we encountered for the future attractor Point C where all the orbits approaching the critical point are first captured by its stable centre manifold. In a similar way, if we let time travel backwards, all the orbits approaching the past attractor are first attracted by its centre manifold with the majority of them joining at high values of z near the $z = 1$ plane. This implies that given random initial conditions near the past attractor Point A_- it is highly probable to find a solution passing sufficiently near the $z = 1$ plane and thus describing the tracking behavior at late time.

The second argument is more physical and regards the value of the amplitude of the quintessence field ϕ. Recalling the definitions of λ (4.26) and of the Ratra-Peebles potential (4.34) we have

$$\lambda = -\frac{1}{\kappa}\frac{V_{,\phi}}{V} = \frac{\alpha}{\kappa\phi}\,, \quad \text{i.e.} \quad z = \frac{1}{1+\kappa\phi/\alpha}\,, \tag{4.52}$$

which implies that the amplitude of the scalar field ϕ is inversely related to λ. If we make the assumption that $\kappa\phi \ll \alpha$ at some time in the past, we automatically select trajectories near the $z = 1$ plane where $\lambda \to +\infty$. A small scalar field amplitude in the early universe is phenomenologically favored since avoids possible problems at the quantum and perturbations level. In fact it allows the effects of the scalar field to be negligible when other fields, for example the inflaton, have to drive the universe evolution. From a phenomenological perspective is thus natural to require the condition $\kappa\phi \ll \alpha$ at early time, meaning that the physically acceptable solutions in Fig. 4.5 will be the one approaching the $z = 1$ plane and converging to the tracking behavior at late time.

Direct power-law potential: $\alpha < 0$ ($\Gamma < 1$)

We turn now our discussion to the direct power-law potential case: $\alpha < 0$ ($\Gamma < 1$). In Fig. 4.14 the phase space for the values $\alpha = -10$ ($\Gamma = 0.9$) and

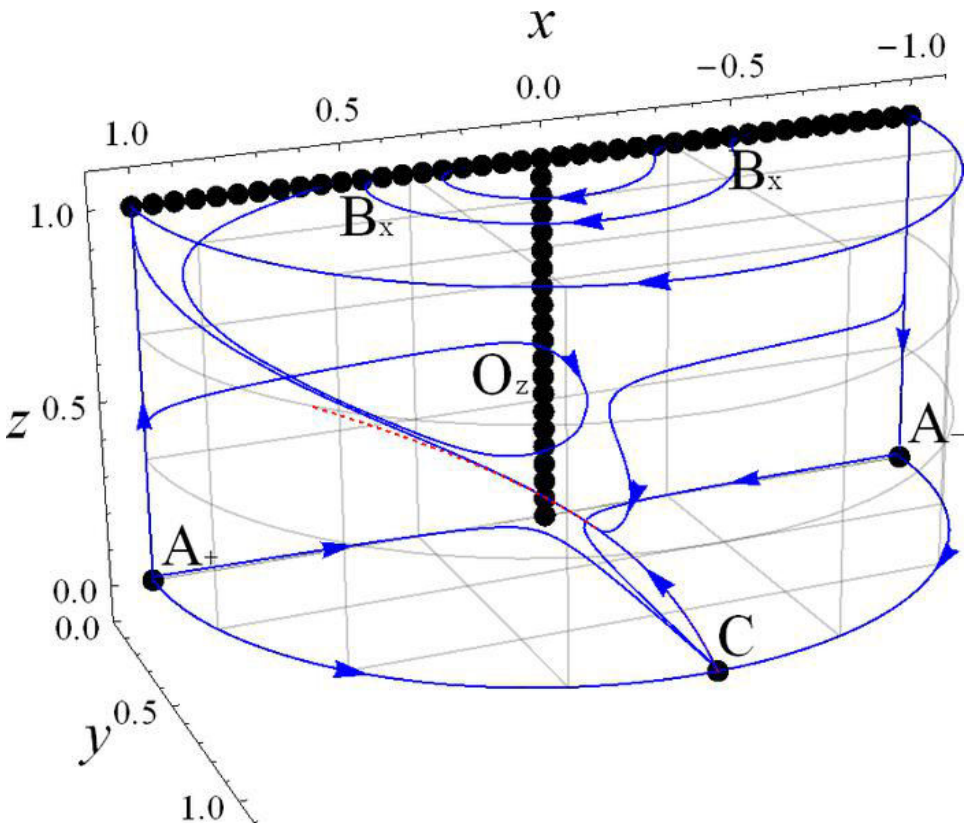

Figure 4.14: Phase space of quintessence for a direct power-law potential corresponding to the dynamical system (4.44)–(4.46). The values $w = 0$ and $\alpha = -10$ ($\Gamma = 0.9$) have been chosen. Again black/thick points denote critical points with the lines B_x and O_z being critical lines. The late time attractors are Points B_x for $x > 0$, while the past attractors are either Point A_+ or Points B_x for $x < 0$. Point C is now a saddle point attracting every solutions near the $z = 0$ plane and repelling them along its centre manifold (thawing behavior), here denoted up to 7th order in $\tilde{z}$ by the red/dashed line.

$w = 0$ has been drawn. As before we will first outline the dynamical properties of the phase space and then derive its phenomenological implications.

From Fig. 4.14 it seems that the future attractors are Points B_x for $x > 0$, while the past attractors are either Point A_+ or Points B_x for $x < 0$. This is the result we obtained before with analytical methods (see Tab. 4.4) and to confirm it we are now going to look at the flow on the boundaries of the phase space. To begin we mention that on the $z = 0$ and $z = 1$ planes the flow is the same irrespective of the value of α and thus also in the $\alpha < 0$ case it is described by Figs. 4.6 and 4.9. On the vertical boundaries however the flow is changed as shown by Figs. 4.15 and 4.16 which are different from Figs. 4.7 and 4.8. On the $x^2 + y^2 = 1$ surface there are two past attractors, Point A_+ and Point B_x for $x < 0$, which select two regions divided by the centre manifold of Point C (approximated to the 7th order in $\tilde{z}$ by the red/dashed line in Fig. 4.15). Every trajectory is first attracted by this centre manifold which eventually drives it away from Point C towards the future attractor Point B_x with $x > 0$. On the other side, the flow on the $y = 0$ plane is also divided into two parts by the critical line O_z. For positive values of x the past attractor is Point A_+ while the future attractors are either Points O_z or Points B_x. For negative values of x Point A_- is a saddle point, the past attractors are Points B_x and the future attractors are Points O_z. Combining the whole information coming from Figs. 4.15 and 4.16 together with Figs. 4.6 and 4.9, we obtain that numerical evaluation of the flow confirms our previous analytical results (Tab. 4.4) on the stability of the critical points.

We are now ready to comment about the physical implications of this model. The future possible attractors are Points B_x for $x > 0$ which, as shown in Tab. 4.3, never describe an accelerating universe. It seems thus that a direct power-law potential ($\alpha < 0$) is not suited for characterizing the late time transition from decelerated to accelerated expansion. Point C is now a saddle point which attracts solutions near the $z = 0$ plane. For some of these orbits, the ones passing close to the origin, a matter to dark energy transition can be identified by the heteroclinic orbit connecting Point O_z ($z = 0$) to Point C. This is nothing but an effective cosmological constant solution since, as we mentioned before, the dynamics on the $z = 0$ plane is given by a constant quintessence potential. Moreover the final state for these trajectories is not represented by Point C but eventually they always escape towards Point B_x ($x > 0$). Scalar field models of dark energy with an initial small value of z (i.e. of λ) are known as *thawing models*. For these solutions λ is an increasing function of time and the accelerated cosmological constant phase (Point C) never represents the final state of the universe. Though they constitute other possible models of dark energy, they cannot solve the fine tuning problem, as the tracking solutions do, since special initial conditions are required for a sufficiently long matter dominated era.

Thawing solutions

A scalar field with a direct power-law potential is commonly used in

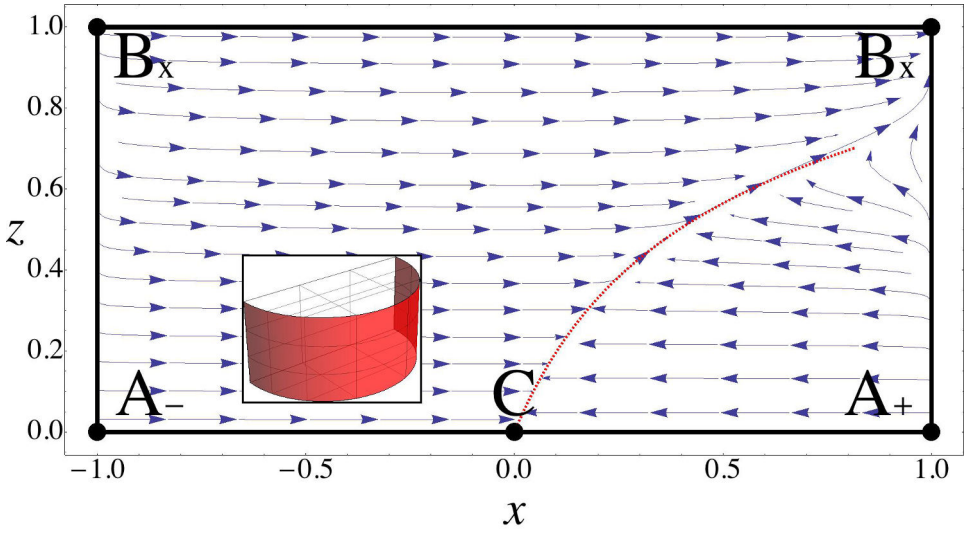

Figure 4.15: Flow of the system (4.44)–(4.46) with the values $w = 0$ and $\Gamma = 0.9$ ($\alpha = -10$) on the $x^2 + y^2 = 1$ surface. The red/dashed line denotes the approximated (up to 7th order) centre manifold of Point C.

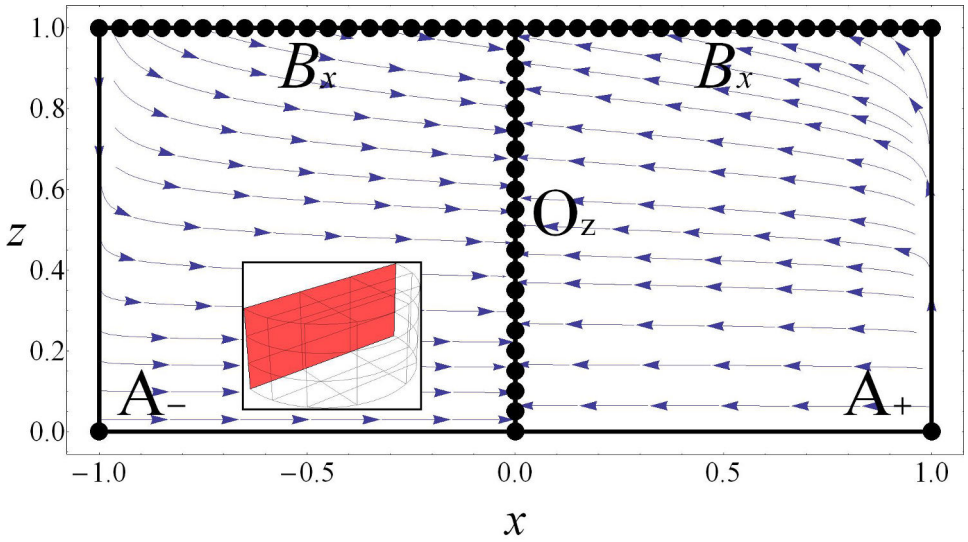

Figure 4.16: Flow of the system (4.44)–(4.46) with the values $w = 0$ and $\Gamma = 0.9$ ($\alpha = -10$) on the $y = 0$ plane.

early universe applications to obtain an inflationary solution. In this case the amplitude of the scalar field is required to be large (up to the Planck energy in some models) in order to produce appreciable quantum perturbative effects. During inflation the matter contribution is absent or ignored. This means that in our phase space the dynamics of an inflationary field is given by the flow restricted to the $x^2 + y^2 = 1$ surface of Fig. 4.15. Looking at this picture we can see that all the solutions starting near the $z = 0$ plane are immediately attracted by Point C. This implies that a sufficiently long period of de Sitter acceleration can be achieved before these orbits reach the kinetic dominated solution in Point B_x ($x > 0$). This is exactly the dynamics required for a finite inflationary period in the early universe. Note that the future attractor stiff-fluid dominated solution is usually ignored in inflation since other physical effects (e.g. reheating) are supposed to appear before this solution is attained.

To conclude this section we summarise the most important results we have obtained from quintessence with an inverse power-law potential. The direct power-law potential case $\alpha < 0$ ($\Gamma < 1$) is not suited for characterizing late time cosmic phenomenology, while the inverse power-law case $\alpha > 0$ ($\Gamma > 1$) leads to interesting features on both physical and mathematical sides. Dark energy dominated future attractors and saddle matter dominated points are present for every positive value of α. Moreover requiring λ to be large in the early universe (corresponding to ϕ being small) implies that every physically relevant trajectory reaches the so-called tracking regime at late times. This regime represents solutions which evolve shadowing the well known scaling solutions and thus determining an effective EoS of the universe which effectively matches the matter EoS. Late time transition to dark energy domination is achieved with these trajectories being attracted by the centre manifold of Point C, which stands for a cosmological constant-like solution where the universe accelerates according to a de Sitter expansion. The phenomenological importance of these tracking solutions resides in the fact that they solve the fine tuning problem of initial conditions. In other words, requiring a small scalar field amplitude at early times ($\kappa\phi \ll \alpha$) automatically assures that the tracking regime is attained for a large range of initial conditions at late times. This is in contrast with both the ΛCDM and exponential potential quintessence models where a strong fine tuning was required in order to obtain a matter to dark energy transition at late times.

Finally we note that deducing the form of the potential $V(\phi)$ from requiring Γ to be a constant in Eqs. (4.35)–(4.37), leads to a slightly more general potential than the power-law one, namely

$$V(\phi) = V_0 \left(\phi + \phi_0\right)^{\beta} , \tag{4.53}$$

with V_0, ϕ_0 and β constant parameters. However, as it as been shown by the (rather incomplete) analysis of Roy & Banerjee (2014a), since the dynamical

equations resulting from this potential are equivalent to Eqs. (4.35)–(4.37), the same results we have obtained in this section will also hold for the potential (4.53).

4.4 Other potentials

In this section we will deal with quintessence models presenting potentials more complicated than the exponential and power-law potentials studied in Secs. 4.2 and 4.3 respectively. For these models the detailed dynamical systems analysis conducted in Secs. 4.2 and 4.3 will not be performed. There are two motivations for this choice. On the one hand, complicated scalar field potentials are more difficult to treat with dynamical systems techniques and a proper analysis for every different model would probably fill a whole book by itself. On the other hand, several of these models share the same dynamics and phenomenology of the simpler exponential and power-law cases, at least on a qualitative level. There is no reason thus to analyse each model in full details when the same scaling, tracking and dark energy dominated solutions are obtained. In this section we will study all these quintessence potentials under a unified dynamical systems approach. The reader interest in a deeper dynamical systems analysis for any of the following models can refer to the reference given in Tab. 4.7.

To begin we will follow the approach first introduced by Zhou (2008), and then considered by other authors[20] (Fang et al., 2009; Matos et al., 2009; Urena-Lopez, 2012), where different forms of the potential $V(\phi)$ can be translated to different forms of the function $\Gamma(\lambda)$. As we mentioned in Sec. 4.1, if the function $\lambda(\phi)$, as defined by (4.26), is invertible then one can consider $\Gamma(\phi)$ as a function of λ and close Eqs. (4.24), (4.25) and (4.27) to an autonomous dynamical system, namely

$$x' = -\frac{3}{2}\left[2x + (w-1)x^3 + x(w+1)\left(y^2-1\right) - \frac{\sqrt{2}}{\sqrt{3}}\lambda y^2\right], \tag{4.54}$$

$$y' = -\frac{3}{2}y\left[(w-1)x^2 + (w+1)\left(y^2-1\right) + \frac{\sqrt{2}}{\sqrt{3}}\lambda x\right], \tag{4.55}$$

$$\lambda' = -\sqrt{6}f(\lambda)x\,. \tag{4.56}$$

where we have defined

$$f(\lambda) = \lambda^2[\Gamma(\lambda) - 1]\,. \tag{4.57}$$

Instead of considering a specific function $\Gamma(\lambda)$, i.e. a specific potential $V(\phi)$, in what follows we will try to obtain as much information as possible from the system (4.54)–(4.56) leaving Γ as an arbitrary function of λ. A similar approach has been considered by Fang et al. (2009). We will not assume any

[20] Some authors call this approach the *method of f-devisers* (Escobar et al., 2014).

Point	x	y	λ	Existence	$w_{\rm eff}$	Accel.	Ω_ϕ
O_λ	0	0	Any	Always	w	No	0
$A_\pm^*$	± 1	0	λ_*	$\forall\,\lambda_*$	1	No	1
B^*	$\frac{\sqrt{3}}{\sqrt{2}}\frac{1+w}{\lambda_*}$	$\sqrt{\frac{3(1-w^2)}{2\lambda_*^2}}$	λ_*	$\lambda_*^2 \geq 3(1+w)$	w	No	$\frac{3(1+w)}{\lambda_*^2}$
C^*	$\lambda_*/\sqrt{6}$	$\sqrt{1-\frac{\lambda_*^2}{6}}$	λ_*	$\lambda_*^2 < 6$	$\frac{\lambda_*^2}{3}-1$	$\lambda_*^2 < 2$	1
D	0	1	0	Always	-1	Yes	1

Table 4.5: Critical points of the system (4.54)–(4.56) with existence and physical properties. λ_* is any node of the function $f(\lambda)$ given in (4.57).

particular symmetry for the function Γ, meaning that the only symmetry of the system (4.54)–(4.56) will be the $y \mapsto -y$ reflection[21]. The (physical) phase space under consideration is thus the infinite positive y half unit cylinder stretching from $\lambda \to -\infty$ to $\lambda \to +\infty$.

First we need to find the possible critical points of the system (4.54)–(4.56). We start looking at Eq. (4.56) whose left hand side can be zero either if $x = 0$ or $f(\lambda) = 0$. In the first case ($x = 0$) we find critical points either if $y = 0$ (Points O_λ) or if $y = 1$ and $\lambda = 0$ (Point D). As long as Γ can be written as a function of λ (and $f(0)$ is finite), these two critical points are independent of the quintessence model under investigation, i.e. they are critical points for all possible potentials $V(\phi)$. The second possibility ($f(\lambda) = 0$) can be realized for more than one value of λ. If λ_* is such that $f(\lambda_*) = 0$, i.e. λ_* is a node of the function $f(\lambda)$, then the remaining two equations (4.54) and (4.55) describe exactly the exponential potential system of Sec. 4.2 and thus we will find again the same critical points of Tab. 4.1 with $\lambda = \lambda_*$. A part from the points where $x = y = 0$, which are always critical points, we find that there are up to four (depending on the value of λ_*) critical points for every node of the function $f(\lambda)$ (Points $A_\pm^*$, B^* and C^*). All these points have been listed in Tab. 4.5 with their phenomenological properties.

For every node λ_* of the function $f(\lambda)$ the number of critical points to add in the phase space depends on the value of λ_* itself. If $\lambda_* = 0$ the only two critical points to add are Points $A_\pm^*$ since in this case Point C^* coincides with Point D. If $0 < \lambda_*^2 < 3(1+w)$ we add three critical points: Points $A_\pm^*$ and Point C^*. If $3(1+w) \leq \lambda_*^2 < 6$ we add all four critical points: Points $A_\pm^*$, Point B^* and Point C^*. Finally if $\lambda_*^2 \geq 6$ we add only Points $A_\pm$ and Point B^*. In general the number of critical points in the phase space will depend on the quintessence potential through the function $f(\lambda)$. Note

[21] Remember that the $(x, \lambda) \mapsto (-x, -\lambda)$ symmetry holds only if $\Gamma(\lambda) = \Gamma(-\lambda)$.

P	Eigenvalues	Stability
O_λ	$\{0, \frac{3}{2}(w \pm 1)\}$	Saddle
A_-^*	$\{3-3w\,,\ 3+\frac{\sqrt{3}}{\sqrt{2}}\lambda_*,\ \sqrt{6}\lambda_*^2\Gamma'_*\}$	Unstable if $\lambda_* > -\sqrt{6}$ and $\Gamma'_* > 0$ Saddle if $\lambda_* < -\sqrt{6}$ or $\Gamma'_* < 0$
A_+^*	$\{3-3w\,,\ 3-\frac{\sqrt{3}}{\sqrt{2}}\lambda_*,\ -\sqrt{6}\lambda_*^2\Gamma'_*\}$	Unstable if $\lambda_* < \sqrt{6}$ and $\Gamma'_* < 0$ Saddle if $\lambda_* > \sqrt{6}$ or $\Gamma'_* > 0$
B^*	$\{\frac{3}{4\lambda_*}\left[(w-1)\lambda_* \pm \Delta\right],\ -3(w+1)\lambda_*\Gamma'_*\}$	Stable if $\lambda_*\Gamma'_* > 0$ Saddle if $\lambda_*\Gamma'_* < 0$
C^*	$\{\frac{\lambda_*^2}{2}-3\,,\ \lambda_*^2-3w-3,\ -\lambda_*^3\Gamma'_*\}$	Stable if $\lambda_*^2 < 3(1+w)$ and $\lambda_*\Gamma'_* > 0$ Saddle if $3(1+w) \leq \lambda^2 < 6$ or $\lambda_*\Gamma'_* < 0$
D	$\{-3(w+1),\ -\frac{3}{2}\left(1 \pm \sqrt{1-4f(0)/3}\right)\}$	Stable if $f(0) > 0$ Saddle if $f(0) < 0$

Table 4.6: Stability properties for the critical points of the system (4.54)–(4.56). Here Γ'_* is the derivative of $\Gamma(\lambda)$ evaluated at λ_*, $f(\lambda)$ is given by Eq. (4.57) and $\Delta = \sqrt{(w-1)[(7+9w)\lambda_*^2 - 24(w+1)^2]}$.

that the analysis we have performed is valid only if the function $f(\lambda)$ is finite for all possible values of λ. If at some λ_∞ we have $f(\lambda_\infty) = \pm\infty$, the dynamical system (4.54)–(4.56) is no longer differentiable and, in order to apply dynamical systems techniques, a change of variables must first be taken into account. In this case it is not guaranteed that the critical points will follow the scheme outlined in Tab. 4.5. Furthermore we have not considered critical points at infinity since these will depend on the specific quintessence models through the function $\Gamma(\lambda)$. In general we can state that if $\Gamma(\lambda)$ is finite as $\lambda \to \pm\infty$, the only critical points at infinity will be given by the critical line at $x = 0$, exactly as it happens in the power-law case of Sec. 4.3. However if the function $\Gamma(\lambda)$ diverges as $\lambda \to \pm\infty$ the dynamics at infinity could be more complicated and each model has to be analysed separately.

The linear stability of the critical points has been summarised in Tab. 4.6. In general this depends on the different values of λ_* and on the form the function $\Gamma(\lambda)$. Points on the critical line O_λ are always saddle points since the two non vanishing eigenvalues have opposite sign (recall that $0 \leq w \leq 1/3$). Points $A_\pm^*$ are never stable points and represent saddle or unstable point depending on the sign of Γ'_* (the function $\Gamma(\lambda)$ evaluated at λ_*) and on the value of λ_*^2 to be greater or smaller than 6. Whenever Point B^* exists, i.e. when $\lambda_*^2 \geq 3(w+1)$, it represents a stable point if $\lambda_*\Gamma'_* > 0$ and a saddle point if $\lambda_*\Gamma'_* < 0$. Point C^* is a stable point if both $\lambda_*^2 < 3(w+1)$ and $\lambda_*\Gamma'_* > 0$, while it is a saddle point if either $3(1+w) \leq \lambda^2 < 6$ or $\lambda_*\Gamma'_* < 0$. Note that in the case $\lambda_*\Gamma'_* = 0$, corresponding to $f'(0) = 0$, Points $A_\pm^*$, B^* and C^* become all non-hyperbolic and the linear theory fails to address their stability nature. This is the case of the power-law potential of Sec. 4.3.

Finally Point D is stable or a saddle depending on $f(0)$ being positive or negative respectively. If $f(0) = 0$ one of the eigenvalues vanishes and the point becomes non-hyperbolic. To address the stability in this case one can rely on the centre manifold theorem and performs a similar computation to the one we considered for Point C of Sec. 4.3. Exactly as in that case the eigenvectors of the Jacobian at this point for $f(0) = 0$ are given by $(1, 0, 0)$, $(0, 1, 0)$ and $(1/Sqrt6, 0, 1)$ with the last one corresponding to the vanishing eigenvalues. Again we have to rewrite the dynamical systems in the basis given by the eigenvectors in order to apply the centre manifold theory. The corresponding change of coordinates $\mathbf{x} \mapsto \tilde{\mathbf{x}}$ is again given by $x = \tilde{x} + \tilde{z}/\sqrt{6}$, $y = \tilde{y}$ and $z = \tilde{z}$. With a power-law ansatz for $\mathbf{h}$ the theorems of Sec. 2.4 gives the following approximation to the centre manifold

$$h_x(\tilde{z}) = \frac{\Gamma(0) - 1}{3\sqrt{6}}\tilde{z}^3 + \frac{\Gamma'(0)}{3\sqrt{6}}\tilde{z}^4 + O(\tilde{z}^5)\,, \tag{4.58}$$

$$h_y(\tilde{z}) = -\frac{1}{12}\tilde{z}^2 + \left[\frac{5}{96} - \frac{\Gamma(0)}{18}\right]\tilde{z}^4 + O(\tilde{z}^5)\,. \tag{4.59}$$

The stability along the centre manifold of Point D when $f(0) = 0$ is thus found to depend on the equation

$$\tilde{z}' = -[\Gamma(0) - 1]\tilde{z}^3 - \Gamma'(0)\tilde{z}^4 + O(\tilde{z}^5)\,, \tag{4.60}$$

where $\tilde{z}$ is the coordinate along the centre subspaces (compare this with Eq. (4.49)). If $f(0) = 0$ then Point D is stable[22] if $\Gamma(0) > 1$ and a saddle if $\Gamma(0) < 1$. If also $\Gamma(0) = 0$ the next order in $\tilde{z}$ tells us that the stability will depend on the sign of $\Gamma'(0)$.

The critical points for a general quintessence model where Γ can be written as a function of λ are repetitions of the critical points one finds with the exponential and power-law potentials. From Tab. 4.5 we can see that Points $A^*_\pm$, B^* and C^* have the same phenomenological properties of Points $A_\pm$, B and C of the exponential case in Sec. 4.2, while Points O_λ and D correspond to the critical line O_z and Point C of the power-law potential of Sec. 4.3. Of course there can be several of these points in the phase space depending on the number and values of the nodes of the function $f(\lambda)$, namely λ_*. The resulting phase space dynamics can be highly complicated and the stability of these points now depends on the properties of the function $\Gamma(\lambda)$. Multiple late time attractors can be present, as one can understand from Tab. 4.6. If none of these critical points constitutes a future attractor, periodic orbits could appear in the phase space or, as in the power-law potential case with $\alpha < 0$, the attractor can be a critical point at infinity.

[22] Note that this result is in agreement with the appendix of Fang et al. (2009), although the case $f(0) \neq 0$ was overlooked in that work.

$V(\phi)$	$\Gamma(\lambda)-1$	References
$V_1 e^{\alpha\phi} + V_2 e^{\beta\phi}$	$-(\alpha+\lambda)(\beta+\lambda)/\lambda^2$	Jarv et al. (2004); Li et al. (2005)
$V_0 \cos^2(\alpha\phi)$ or $\frac{V_0}{2}[1 \pm \cos(2\alpha\phi)]$	$-\frac{1}{2} - \frac{\alpha^2}{\lambda^2}$	Ng & Wiltshire (2001) Urena-Lopez (2012); Gong (2014)
$\exp[\alpha \exp(\beta\phi)]$	$-\beta/\lambda$	Ng et al. (2001)
$V_0 \phi^{-n} e^{\alpha\phi}$	$(1+\alpha/\lambda)^2/n$	Ng et al. (2001)
$V_0 \sinh^n(\sigma\phi)$ or $V_0 \cosh^n(\sigma\phi)$	$-\frac{1}{n} + \frac{n\sigma^2}{\lambda^2}$	Fang et al. (2009) Roy & Banerjee (2014b)
$V_0[\cosh(\sigma\phi) - 1] + \Lambda$	Eq. (4.62)	Matos et al. (2009)
$V_0 e^{\alpha\phi(\phi+\beta)/2}$	α/λ^2	Fang et al. (2009)
$V_0 e^{\alpha/\phi}$	$1/\sqrt{\alpha\lambda}$	Fang et al. (2009)
$V_0/(\eta + e^{-\alpha\phi})^\beta$	$\frac{1}{\beta} + \frac{\alpha}{\lambda}$	Zhou (2008); Fang et al. (2009)

Table 4.7: Quintessence potentials for which Γ can be related to λ. Citations to the literature refer only to dynamical systems studies.

There are only two points which are relevant for dark energy phenomenology: Point C^* and Point D. The first one represent an accelerating universe only if $\lambda_* < 2$, while the second one characterizes a cosmological constant-like dominated universe where a de Sitter expansion is guaranteed. They are important especially when representing future attractors. Note that Point D appears in every quintessence model and if $f(0) > 0$ it can always constitute a possible late time dark energy dominated solution. Moreover also the matter dominated Points O_λ are saddle points for every possible potentials. One can thus expect to find a late time matter to dark energy transition independently of the quintessence model chosen. Of course this will in general depend on initial conditions, but for some of these models also scaling solutions can be achieved whenever Point B^* appears in the phase space. If this point (or one of them if more than one are present) happens to be a saddle, then the matter to dark energy transition can be described by an heteroclinic orbit connecting Point B^* with Point D (or Point C^* for a different λ_* with $\lambda_*^2 < 2$). In this case the fine tuning problem of initial conditions can be avoided if the basin of attraction of Point B^* is sufficiently large. This situation is similar to the tracking regime we encountered for the inverse power-law case of Sec. 4.3, though in that case the scaling solutions were only instantaneous critical points. To determine which potentials are capable of yielding scaling solutions is thus an important issue in quintessence models (Nunes & Mimoso, 2000; Copeland et al., 2005b).

Now that we have gained useful information on the general behavior of quintessence models leading to a dynamical Γ, we can spend some words on few specific models. In Tab. 4.7 we have listed quintessence potentials considered in the literature for which the relation $\Gamma(\lambda)$ can be determined[23]. Some of them are motivated by well known high energy phenomenology, others by the simple relation they provide for $\Gamma(\lambda)$. Quintessence models with a pseudo-Nambu-Goldstone-boson (PNGB) potential given by cos-like expressions (see Tab. 4.7) are amongst the most studied with dynamical systems techniques (Ng & Wiltshire, 2001; Urena-Lopez, 2012; Gong, 2014). They represent thawing dark energy models with an intermediate inflationary phase and a future complicated behavior which strongly depends on the potential parameters and never gives accelerated expansion. Other well studied potentials within this approach are cosh-like potentials (Matos et al., 2009; Kiselev, 2008) which can be justified by string theory phenomenology and are employed in unified dark matter (UDM) models. For example Matos et al. (2009) considered the potential

$$V(\phi) = V_0 \left[\cosh(\sigma\phi) - 1\right] + \Lambda \,, \tag{4.61}$$

corresponding to

$$\Gamma(\lambda) - 1 = \pm \left(\frac{1}{\lambda^2} - 1\right) \frac{\sqrt{1 + \alpha(\alpha-2)\lambda^2}}{\alpha - 1 \pm \sqrt{1 + \alpha(\alpha-2)\lambda^2}} \,, \tag{4.62}$$

where $\alpha = \Lambda/V_0$ and the plus/minus sign represents different branches of the solution. The interesting phenomenological properties of these models can be found in the intermediate behavior where the scalar field acts as a dark matter candidate. The late time solution is given by a de Sitter expansion produced by a cosmological constant added to the potential. Finally one of the most studied potential (Barreiro et al., 2000; Jarv et al., 2004; Li et al., 2005) is the so-called double exponential potential

$$V(\phi) = V_1 e^{\alpha\phi} + V_2 e^{\beta\phi} \,, \tag{4.63}$$

with V_1, V_2, α and β all constant. It represents a straightforward generalisation of the exponential potential case of Sec. 4.2 and it is interesting under a phenomenological point of view since, depending on the values of the parameters, scaling and dark energy dominated solutions can appear together in the phase space. Although a simple $\Gamma(\lambda)$ relation arises in the double exponential potential case (see Tab. 4.7), for this particular model it is easier to employ EN-like variables defined as $y^2 = V_1 e^{\alpha\phi}/(3H^2)$ and $z^2 = V_2 e^{\beta\phi}/(3H^2)$ (Li et al., 2005). With these variables the physical phase space becomes automatically compact due to the Friedmann constraint which would read $x^2 + y^2 + z^2 \leq 1$.

[23] In Tab. 4.7 we have taken $\kappa = 1$ without loss of generality.

To conclude this section we recall that quintessence potentials for which the function $\Gamma(\lambda)$ cannot be obtained analytically must be analysed using another approach. In these cases different variables than the EN ones might represent a better choice to characterize the dynamics of the system (e.g. see Miritzis (2003b); Hao & Li (2003b); Faraoni & Protheroe (2013)). However, as shown in Tab. 4.7, for almost every quintessence potential considered as a viable model in literature the relation $\Gamma(\lambda)$ can easily be obtained. This provides a unified framework to analyse the isotropic[24] background dynamics of canonical scalar field models of dark energy and only highly complicated potentials will fail to enter such scheme. Note also that every potentials in Tab. 4.7 yields a function $\Gamma(\lambda)$ which is finite as $\lambda \to \pm\infty$. As we mentioned before, this implies that for all these models the dynamics at infinity will equal the one described in Sec. 4.3 for the power-law potential.

4.5 Coupled quintessence

This section is devoted to the study of quintessence interacting with matter through a non gravitational coupling[25]. As in the previous section, we will not be able to perform a detailed dynamical systems analysis for all these models. However we will discuss the basic features of the simplest and most important model and provide references for all the other ones. The presentation will of course be focused on the dynamical properties of these models[26], but the reader interested in their phenomenology can refer to the review of Bolotin et al. (2013).

As we mentioned in Sec. 3.1, the different components that source the right hand side of the Einstein field equations can in principle interact with each other. This is also the case of dark energy and dark matter whose equations of motion can be written as

$$\nabla^\mu T^{(m)}_{\mu\nu} = -Q_\nu\,, \quad \text{and} \quad \nabla^\mu T^{(\phi)}_{\mu\nu} = Q_\nu\,, \tag{4.64}$$

where $T^{(m)}_{\mu\nu}$ is the dark matter energy-momentum tensor (3.4), $T^{(\phi)}_{\mu\nu}$ is the scalar field energy-momentum tensor (4.7) and Q_ν is the *interaction vector*

[24] Anisotropic spacetimes for canonical scalar fields with complicated potentials have been studied by Fadragas et al. (2014).

[25] Strong constraints on a possible coupling between quintessence and baryonic matter arise from fifth force experiments (Will, 2014), though particular ways of avoiding these constraints have been found (Khoury & Weltman, 2004; Gubser & Khoury, 2004). The constraints on a possible coupling between dark energy and dark matter are instead not so restricting; for some recent works see Yang & Xu (2014); Wang et al. (2014); Li et al. (2014).

[26] We will also restrict the discussion to quintessence models where dark energy is assumed to be a scalar field. For dynamical systems studies of interacting dark energy as a (perfect) fluid see Olivares et al. (2008); Quartin et al. (2008); Quercellini et al. (2008); Caldera-Cabral et al. (2009); Li & Ma (2010).

which determines the coupling between the dark energy and dark matter fluids. The matter fluid $T^{(m)}_{\mu\nu}$ should represent dark matter since at cosmological scales that is the dominant matter component. However we will leave the matter sector as a simple perfect fluid with $p = w\rho$ capable of describing dark matter, baryonic matter or both of them. In this manner we will be able to study dark energy models coupled to either baryonic or dark matter within a unified framework. This will allow us to cover the majority of cosmological applications where dark energy interacts with the matter sector.

On a FRW background Eqs. (4.64) read

$$\dot{\rho} + 3H\rho(w+1) = -Q\,, \tag{4.65}$$

$$\dot{\rho}_\phi + 3H(\rho_\phi + p_\phi) = Q\,, \tag{4.66}$$

where $Q = Q_0$ is the time component of Q_μ and the scalar field energy density ρ_ϕ and pressure p_ϕ are given by (4.13) and (4.14) respectively. Note that Eq. (4.66) is equivalent to the Klein-Gordon equation (4.12) with a non vanishing source on the right hand side, namely

$$\ddot{\phi} + 3H\dot{\phi} + V_{,\phi} = \frac{Q}{\dot{\phi}}\,. \tag{4.67}$$

The sign of Q determines the direction of the energy transfer: if $Q > 0$ the matter fluid is giving energy to the scalar field, while if $Q < 0$ it is the scalar field which is releasing energy into the matter sector. In general Q is given in terms of the physical fields, i.e. the scalar and matter fields, and thus it will be a dynamical quantity depending on the cosmic time t.

The cosmological equations governing the evolution of the universe are now the Friedmann equation (4.10), the acceleration equation (4.11) and the Klein-Gordon equation (4.67). Equivalently one can consider as the independent set of equations Eqs. (4.65), (4.66) and the Friedmann equations (4.10). In order to recast these equations into a dynamical system we consider again the EN variables (4.16) and (4.26), in terms of which we obtain[27]

$$x' = \frac{1}{2}\left[2q - 3(w-1)x^3 - 3x\left(w\left(y^2-1\right) + y^2 + 1\right) + \sqrt{6}\lambda y^2\right]\,, \tag{4.68}$$

$$y' = -\frac{1}{2}y\left[3(w-1)x^2 + 3(w+1)\left(y^2-1\right) + \sqrt{6}\lambda x\right]\,, \tag{4.69}$$

$$\lambda' = -\sqrt{6}x\lambda^2[\Gamma - 1]\,, \tag{4.70}$$

where we have defined

$$q = \frac{\kappa Q}{\sqrt{6}H^2\dot{\phi}}\,. \tag{4.71}$$

[27] The derivation of these equations is equal to the derivation of Eqs. (4.24)–(4.25), a part from the q-term which will arise from the scalar field equation.

Note that only Eq. (4.68) is modified by the interaction, while Eqs. (4.69) and (4.70) are the same of Eqs. (4.25) and (4.27). As long as one chooses a quintessence model leading to a well defined $\Gamma(\lambda)$ relation (see Sec. 4.4), the only unknown quantity in Eqs. (4.68)–(4.70) is q itself. If q can be written in terms of the variables x, y and λ, then Eqs. (4.68)–(4.70) will constitute an autonomous dynamical system which in general will be three dimensional unless an exponential potential is assumed for the scalar field. The exponential potential, leading to a 2D dynamical system, is in fact the most studied in the literature of quintessence coupled to (dark) matter.

This is well explained by Tab. 4.8 where references to works considering several different coupling Q but only the scalar field exponential potential are listed[28]. Whenever possible the dimensionless quantity q in terms of x and y has been provided. For the other cases such a relation cannot be found and a new variable must be introduced increasing in this way the dynamical system to three dimensions[29]. Few works have so far considered dynamical systems applications to interacting quintessence with a non exponential potential. Leon et al. (2010) delivered a mathematical analysis for an arbitrary scalar field potential with the rather general coupling $\beta\rho\dot{\phi}\chi(\phi)$, where χ is a function of the scalar field. Such a general relation arises in Scalar-Tensor theories of gravity when described in the Einstein frame. Note that if $\lambda(\phi)$ is invertible, then one can find both $\Gamma(\lambda)$ and $\chi(\lambda)$. In such a way no new variables need to be introduced and the dynamical system remains three dimensional. Other works considering rather complicated couplings motivated by Scalar-Tensor theories are the papers by Hossain et al. (2014) and Morris et al. (2013) where the coupling $Q = \beta\rho e^{\alpha\phi}\dot{\phi}$ is studied together with a vanishing scalar field potential. Finally the coupling $Q = \beta\rho\dot{\phi}$ has been considered by Tzanni & Miritzis (2014) with a double exponential potential. Of course for more complicated couplings or potentials different variables than the EN ones might results in a simpler or more complete analysis (see e.g. Leon (2009); Fadragas & Leon (2014)).

The coupling $Q = \beta\rho\dot{\phi}$ with β a constant is probably the most important one and surely the most studied through the dynamical systems literature as the references in Tab. 4.8 confirm. This particular interaction comes from Brans-Dicke theory (once it has been rephrased into the Einstein frame), but it can also hold for more general non minimally coupled gravitational theories (see e.g. Amendola (2000); Holden & Wands (2000)). The coupling in this case is with all the matter sector (baryonic and dark). In what follows we will briefly review some of the features of this model as an example. This will show us how the interaction between dark energy and matter can affect the dynamics of the system. The reader interested in dynamical systems

[28]For the sake of simplicity $\kappa = 1$ has been taken in Tab. 4.8.

[29]In most situations such a variable is defined as $z = H_0/(H + H_0)$ with H_0 a constant (see e.g. Boehmer et al. (2008, 2010b)).

Q	q	References
$\beta\rho\dot{\phi}$	$\frac{\sqrt{3}}{\sqrt{2}}\beta(1-x^2-y^2)$	Amendola (1999, 2000) Billyard & Coley (2000) Holden & Wands (2000) Tocchini-Valentini & Amendola (2002) Gumjudpai et al. (2005) Gonzalez et al. (2006) Boehmer et al. (2008) Cicoli et al. (2012)
$\beta H\rho$	$\frac{\beta}{2}(1-x^2-y^2)/x$	Billyard & Coley (2000) Boehmer et al. (2008) Chen & Gong (2009)
$\beta\rho\dot{\phi}\phi/a^4$	–	Liu & Li (2005)
$\beta\dot{\phi}^2$	–	Mimoso et al. (2006)
$\beta H\dot{\phi}^2$	βx	Mimoso et al. (2006)
$\beta\rho$	–	Boehmer et al. (2008)
$\beta H\rho_\phi^\alpha\rho^{1-\alpha}$	$\frac{\beta}{2}x\frac{1-x^2-y^2}{[-1+1/(x^2+y^2)]^\alpha}$	Chen et al. (2008)
$\beta\rho^2/H$	–	Chen & Gong (2009)
$\beta\rho\dot{\phi}^2/H$	$3\beta x(1-x^2-y^2)$	Chen & Gong (2009)
$A\rho_\phi^2+B\rho^2+C\rho\rho_\phi$	–	Boehmer et al. (2010b)
$\beta\rho V(\phi)^n\dot{\phi}$	–	Lopez Honorez et al. (2010)
$\eta\,(\dot{\rho}_i+3\beta H\rho_i)$ with $\eta=-(1+\dot{H}/H^2)$ and $\rho_i=\rho,\,\rho_\phi,\,\rho+\rho_\phi$	–	Wei (2011a)

Table 4.8: Dark energy to (dark) matter coupling considered in the literature. The references here refer only to dynamical systems studies assuming an exponential potential for the scalar field. When q, as defined in Eq. (4.71), can be written in terms of the variables x and y, we have provided such relation.

Point	x	y	Existence	w_{eff}	Accel.
O_β	$\frac{\sqrt{3}}{\sqrt{2}}\frac{\beta}{1-w}$	0	$\beta^2 < \frac{3}{2}(w-1)^2$	$w + \frac{2\beta^3}{3(1-w)}$	No
$A_\pm$	± 1	0	$\forall\, \lambda, w$	1	No
B	$\frac{\sqrt{3}}{\sqrt{2}}\frac{1+w}{\lambda-\beta}$	$\sqrt{\frac{3(1-w^2)+2\beta(\beta-\lambda)}{2(\beta-\lambda)^2}}$	Fig. 4.17	$\frac{w\lambda+\beta}{\lambda-\beta}$	Fig. 4.17
C	$\frac{\lambda}{\sqrt{6}}$	$\sqrt{1-\frac{\lambda^2}{6}}$	$\lambda^2 < 6$	$\frac{\lambda^2}{3} - 1$	$\lambda^2 < 2$

Table 4.9: Critical points of the system (4.32)–(4.33) with existence and physical properties.

studies for this model can refer to the citations provided in Tab. 4.8.

For the coupling $Q = \beta\kappa\rho\dot{\phi}$ we can easily find that

$$q = \frac{\sqrt{3}}{\sqrt{2}}\beta\left(1 - x^2 - y^2\right) . \tag{4.72}$$

This implies that for this model there is no need to introduce new dimensions in the dynamical system. For the sake of simplicity in our example we will also consider an exponential potential for which λ is a constant in Eqs. (4.68) and (4.69), while Eq. (4.70) is automatically satisfied. Eqs. (4.68) and (4.69) constitute then an autonomous system and the phase space will be nothing but the upper half unit disk in the (x, y)-plane, i.e. the same of the uncoupled case of Sec. 4.2. Note that the presence of the coupling breaks the $(x, \lambda) \mapsto (-x, -\lambda)$ symmetry. However in this particular case this can be restored considering also a reflection on the parameter β: $(x, \lambda, \beta) \mapsto (-x, -\lambda, -\beta)$. This implies that the phase space dynamics for opposite values of λ will again be the same after a reflection over x and opposite values of β are considered. In other words, to analyse the whole dynamics of the system we just need to consider positive values of λ, though both positive and negative values for β must be taken into account[30].

The critical points of the dynamical system (4.68)–(4.69) with the coupling (4.72) are listed in Tab. 4.9. Points $A_\pm$ and C are exactly in the same position and with the same phenomenological properties of their correspondent points in the uncoupled case. This does not come as a surprise because the coupling (4.72) vanishes when the scalar field dominates, i.e. when $x^2 + y^2 = 1$. The remaining two points instead are changed by the interaction and never appear if $\lambda = \beta$. The origin is no longer a critical point and Point O_β now lies on the x-axis. It is no more a matter dominated point and its effective EoS will now depend on the parameter β, though no

[30] Of course we could consider only positive values of β if both negative and positive values of λ would have taken into account.

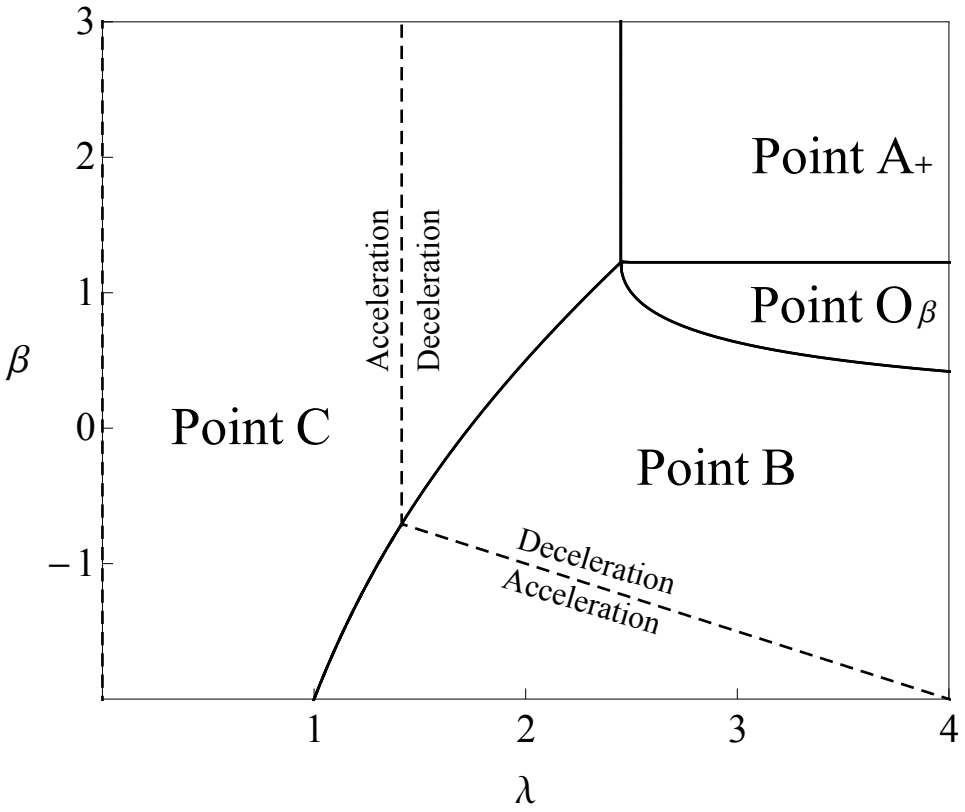

Figure 4.17: Future (global) attractors in the parameter space of the dynamical system (4.68)–(4.69) with $w = 0$ and the coupling (4.72). The dashed line delimits the region where the universe undergoes accelerated expansion at the critical point.

acceleration is possible since for this point $w \leq w_{\text{eff}} \leq 1$. The scaling solution described by Point B is also affected by the coupling. Its position and properties now depend on β, though we always have $\Omega_\phi \propto \Omega_m$ which determines the nature of the scaling solution. Interestingly the effective EoS parameter at this point now reads

$$w_{\text{eff}} = \frac{w\lambda + \beta}{\lambda - \beta}\,, \tag{4.73}$$

which implies an accelerated universe in some region of the (λ, β) parameter space, as shown in Fig. 4.17.

We will not deliver a detailed stability analysis as we did in Sec. 4.2 for each critical point of Tab. 4.9. However in Fig. 4.17 a self contained explanation on the possible future attractors of the system depending on the values of λ and β is provided. Note that with a non vanishing coupling also Points O_β and $A_\pm$ can represent future attractors. These situations are

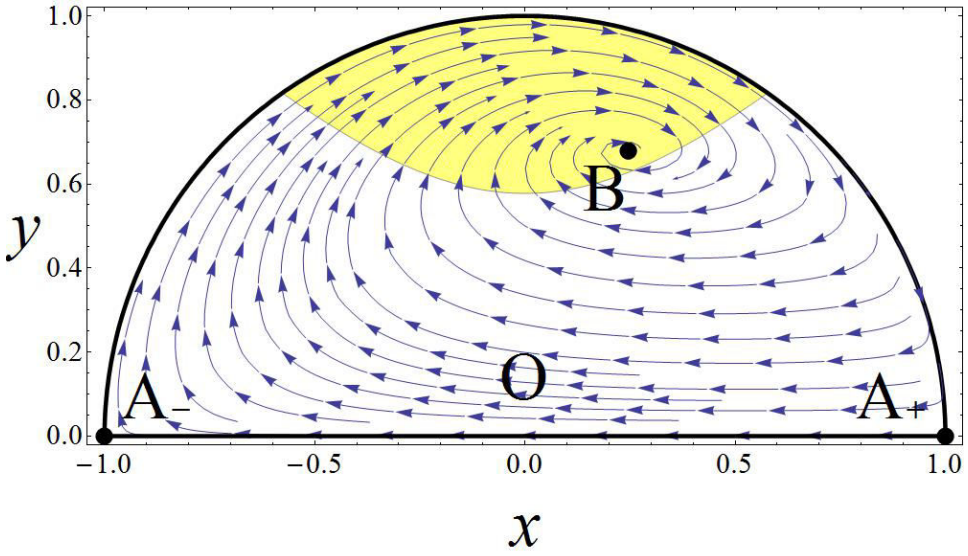

Figure 4.18: Phase space portrait of the dynamical system (4.68)–(4.69) and the coupling (4.72) with the values $w = 0$, $\lambda = 3$, $\beta = -2$. The scaling solution of Point B represents in this case an accelerating universe since lies inside the yellow/shaded region.

however not interesting for dark energy phenomenology since no accelerated expansion can be obtained at these points.

The most interesting feature of this model, and usually of all the coupled quintessence models, is that the scaling solution of Point B can now give an accelerating universe, as shown for example in the phase space portrait of Fig. 4.18. This could in principle solve the cosmic coincidence problem since an everlasting expanding solution with $\Omega_\phi \simeq 0.7$ can now be achieved. Unfortunately whenever Point B describes an accelerating solution Point O_β does not appear in the phase space. This implies the absence of a matter dominated saddle point, as shown in Fig. 4.18, and thus the expansion history of the universe cannot be fully described. Note also that unless β is very small Point O_β does not describe a matter dominated solution at all.

Although it fails to account for a matter dominated epoch, this example provides useful insights to build a suitable dark energy model capable of solving the cosmic coincidence problem. In fact it is easy to realize a slightly more complicated model where a matter dominated solution or a scaling solution with $w_{\rm eff} = w$ appear; for example with a double exponential potential (Miritzis, 2003b). If a heteroclinic orbit connecting a critical point with $w_{\rm eff} = w$ to a late time attracting scaling solution with $w_{\rm eff} < -1/3$ is present in the phase space, then a viable solution to the coincidence problem can be obtained. This suggests that introducing a coupling between quintessence and the matter sector could constitute the right way to a res-

olution of one of the cosmological problems.

To conclude this section we give a brief summary on what we have discussed. Quintessence models coupled to dark energy are well characterized by the coupling quantity Q. For sufficiently simple models the effects of the coupling Q are represented by the dimensionless variable q which can be related to the EN variables and thus does not increase the dimensionality of the phase space. Several possible coupling Q have been considered in the dynamical systems literature (see Tab. 4.8) and we have analysed the most studied one, namely $Q = \beta\kappa\rho\dot{\phi}$. This correspond to q as given by Eq. (4.72) and to a dynamical system capable of providing accelerated scaling solutions, but unable of describing a viable matter dominated cosmological era. Nevertheless this simple example suggests that quintessence models coupled to the matter sector are good candidates to solve the cosmic coincidence problem. It is expected that more complicated models could yield both a tracking regime and an accelerating scaling solution, though no such study has been performed so far. In such a situation both the fine tuning problem of initial conditions and the cosmic coincidence problem would be solved within a single theoretical dark energy model.

4.6 Multiple scalar fields

In this final section we will review the possibility that dark energy is composed by more than one scalar field. We will not present any detailed analysis but will only discuss the main features arising from multiple scalar fields and provide references to dynamical systems works.

The Lagrangian of N minimally coupled canonical scalar fields is given by

$$\mathcal{L}_{\phi_1,\dots,\phi_N} = -\sum_{i=1}^{N} \partial\phi_i^2 - V(\phi_1, \dots, \phi_N)\,, \tag{4.74}$$

where $\partial\phi_i^2 = g^{\mu\nu}\partial_\mu\phi_i\partial_\nu\phi_i$ is the kinetic term of the ith scalar field and $V(\phi_1, \dots, \phi_N)$ is a general potential for all the scalar fields. In this section Latin indices such as i, j will run from 1 to N. The whole effective action for the dynamics at cosmological scales will then be

$$S = \int d^4x\sqrt{-g}\left(\frac{R}{2\kappa} + \mathcal{L}_m + \mathcal{L}_{\phi_1,\dots,\phi_N}\right)\,, \tag{4.75}$$

where the first and second terms compose the usual Einstein-Hilbert Lagrangian plus matter (4.1).

The Friedmann and acceleration equations obtained from action (4.75)

are

$$\frac{3H^2}{\kappa^2} = \rho + \left(\sum_i \frac{\dot{\phi}_i^2}{2}\right) + V\,, \tag{4.76}$$

$$\frac{1}{\kappa^2}\left(2\dot{H} + 3H^2\right) = -p - \left(\sum_i \frac{\dot{\phi}_i^2}{2}\right) + V\,, \tag{4.77}$$

while the Klein-Gordon equation of the ith scalar field is

$$\ddot{\phi}_i + 3H\dot{\phi}_i + \frac{\partial V}{\partial \phi_i} = 0\,. \tag{4.78}$$

Note that there are N Klein-Gordon equations now, one for each scalar field. In general a coupling between one or more of the scalar fields and matter could be considered adding a right hand side term on some of Eqs. (4.78) similar to the one considered in Sec. 4.5. In our discussion however we will not consider such a possibility. Note that a coupling between the scalar fields is implicit in the potential V which is a general function of all the scalar fields. The dynamics of Eqs. (4.76)–(4.78) strongly depends on the form of the potential V and before recasting the equations into a dynamical system one is forced to choose a specific potential. In other words the choice of dimensionless variables will now depend on what potential V is assumed. In what what follows we will briefly discuss the two main potentials considered in the literature.

Assisted quintessence

The first model we consider is known as *assisted quintessence* being a late time adaptation of the *assisted inflationary model* (Liddle et al., 1998; Malik & Wands, 1999). The multifield potential is in this case given by

$$V(\phi_1, \ldots, \phi_N) = \sum_i V_i(\phi_i) = \sum_i e^{-\lambda_i \kappa \phi_i}\,, \tag{4.79}$$

where λ_i are N parameters. The potential (4.79) is nothing but the sum of N individual exponential potential for each single scalar field. Knowing the dynamics of the single quintessence model with an exponential potential, it is clear that the multifield potential (4.79) is the simplest choice one can make. In this case we can define $2N$ normalised variables as

$$x_i^2 = \frac{\kappa\dot{\phi}_i}{6H^2}\,, \quad \text{and} \quad y_i^2 = \frac{\kappa V_i}{3H^2}\,, \tag{4.80}$$

which reduce the cosmological equations to the $2N$-dimensional dynamical

system represented by[31]

$$x_i' = -3x_i + \frac{\sqrt{3}}{\sqrt{2}}\lambda_i y_i^2 + \frac{3}{2}x_i \sum_j \left[x_j^2 + (w+1)\left(1 - x_j^2 - y_j^2\right)\right] , \tag{4.81}$$

$$y_i' = -\frac{\sqrt{3}}{\sqrt{2}}\lambda_i x_i y_i + \frac{3}{2}y_i \sum_j \left[x_j^2 + (w+1)\left(1 - x_j^2 - y_j^2\right)\right] , \tag{4.82}$$

where the Friedmann constraint

$$\Omega_m + \sum_i x_i^2 + \sum_i y_i^2 = 1 \tag{4.83}$$

has been enforced.

Although it represents a simple extension of the exponential potential to more than one scalar field, the dynamics arising from this model is quite interesting. The most important feature, which was first proposed in the assisted inflationary model (Liddle et al., 1998), is that late time accelerated expansion can be achieved even if the single exponential potentials are not flat enough. In fact from Sec. 4.2 we know that for the single field exponential potential a future dark energy dominated attractor can only be obtained if $\lambda^2 < 2$. The late time dynamics of the assisted quintessence model (4.79) can however be mapped into the one of a single scalar field $\tilde{\phi}$ with potential $V(\tilde{\phi}) = V_0 \exp(-\tilde{\lambda}\kappa\tilde{\phi})$ where[32]

$$\frac{1}{\tilde{\lambda}^2} = \sum_i \frac{1}{\lambda_i^2} . \tag{4.84}$$

It is then clear how the trick of assisted quintessence works. Even if each single exponential potential V_i is such that $\lambda_i^2 > 2$, according to Eq. (4.84) the average $\tilde{\lambda}$ determining the dynamics at late times can satisfy $\tilde{\lambda}^2 < 2$. This is an interesting result especially because steep potentials are simpler to predict from high energy physics phenomenology.

The assisted inflationary and quintessence models have been analysed using dynamical systems techniques by several authors. Coley & van den Hoogen (2000) studied in detail the model with two and three scalar fields. Guo et al. (2003c) considered the case where some of the single exponential potentials V_i can be negative. Huey & Tavakol (2002) generalised the exponential potentials with a temperature (background) dependent coupling and delivered a general analysis about tracking solutions in such models. Karthauser & Saffin (2006) showed that scaling solutions for the uncoupled

[31] No summation on repeated Latin indices is considered in this section unless explicitly specified.

[32] This works for the late time attracting solution where all the scalar field achieve the same value $\phi_i = \phi$. The dynamics around this solution can be mapped into a single scalar field model by $\tilde{\phi} = N\phi$ and $\tilde{V} = NV$; see Liddle et al. (1998).

(non-interacting scalar fields) potential $V = \sum_i V_i$ appear only if the V_is are all exponential and for other kinds of potentials a coupling, such as the one motivated by string theory phenomenology that they considered, is needed. Finally Kim et al. (2005) reviewed the assisted quintessence scenario and proved that no assisted behavior arises if the V_is are all of the power-law type.

At this point we turn our attention to another well studied possibility of multi-scalar quintessence. This time we will consider the multiplicative (or cross-coupling) multifield exponential potential defined by

$$V(\phi_1, \dots, \phi_N) = \sum_i V_i(\phi_1, \dots, \phi_N) = \sum_i \Lambda_i \exp \sum_j \lambda_{ij} \phi_j \,, \tag{4.85}$$

where λ_{ij} are now $N \times N$ parameters and Λ_i are N constants. This model is sometimes called *generalised assisted quintessence* or inflation, depending if late or early time applications are respectively considered. Note that now the scalar fields are interacting with each other. Defining again $2N$ EN variables as

Generalised assisted quintessence

$$x_i^2 = \frac{\kappa \dot{\phi}_i}{6H^2} \,, \quad \text{and} \quad y_i^2 = \frac{\kappa V_i}{3H^2} \,, \tag{4.86}$$

the cosmological equations (4.76)–(4.78) can be recast into the $2N$-dimensional dynamical system

$$x_i' = -3x_i + \frac{\sqrt{3}}{\sqrt{2}} \sum_j \lambda_{ji} y_j^2 + \frac{3}{2} x_i \sum_j \left[x_j^2 + (w+1)\left(1 - x_j^2 - y_j^2\right) \right] \,, \tag{4.87}$$

$$y_i' = -\frac{\sqrt{3}}{\sqrt{2}} y_i \sum_j \lambda_{ij} x_j + \frac{3}{2} y_i \sum_j \left[x_j^2 + (w+1)\left(1 - x_j^2 - y_j^2\right) \right] \,, \tag{4.88}$$

where again the Friedmann constraint

$$\Omega_m + \sum_i x_i^2 + \sum_i y_i^2 = 1 \tag{4.89}$$

has been taken into account. Note how (4.87)–(4.88) are similar to (4.81)–(4.82) except for the λ-terms. The general system (4.87)–(4.88) has been studied by Collinucci et al. (2005) where detailed examples with two and three scalar fields were provided and useful de Sitter future attractors were found. Hartong et al. (2006) showed that such accelerated solutions can be obtained also with some negative V_is and then generalised the analysis to the case of non vanishing spatial curvature. A simpler model where all the Λ_is are equal and there are only N parameters λ_i have been considered by van den Hoogen & Filion (2000) and Guo et al. (2003a). In this case we can reduce the dimensionality of the system to $N + 1$ equations defining a single EN variable for the potential as $y^2 = \kappa V/(3H^2)$. Moreover if $\sum_i \lambda_i^2 <$

$3(w+1)$ the late time attractor is always given by a dark energy inflationary solutions (Guo et al., 2003a).

To conclude the section we mention few works considering dynamical systems arising from more complicated multifield potentials. Zhai & Zhao (2006) analysed two scalar fields with a rather complicated potential and a kinetic coupling motivated by quintessential inflation phenomenology. They showed that within this model de Sitter acceleration can be obtained both at early and late times. A kinetic coupling between the scalar fields is also present in the analysis of van de Bruck & Weller (2009) where the multifield potentials (4.79) and (4.85) are considered in such a framework. Finally Marsh et al. (2012) studied dynamical systems in the context of string theory phenomenology where a complicated two-field potential appears.

Chapter 5

Dark energy from non-canonical scalar fields

This chapter will review dynamical systems applications to dark energy models built with non-canonical scalar fields. Contrary to the canonical scalar field, whose Lagrangian is given by (4.5), the Lagrangian of a non-canonical scalar field contains a non standard kinetic term. In general non-canonical scalar fields suffer from theoretical issues which do not appear in the canonical case. They can however be easily motivated by high energy phenomenology and provide a bridge between cosmological observations and high energy physics. For these reasons the cosmological applications of non-canonical scalar fields are the subject of several works in the dark energy literature.

In this chapter a full dynamical analysis of the simplest models will be presented, while for the more complicated models brief discussions and detailed references to the dynamical systems literature will be provided.

The chapter is organised as follows. In Sec. 5.1 the dynamics of the phantom dark energy model will be reviewed in details, finding the critical points, their properties and plotting the phase space portraits. In Sec. 5.2 the quintom model, where both a phantom and a canonical scalar field appear, will be presented and discussed. Sec. 5.3 will then be devoted to k-essence and higher order scalar fields cosmology. The main features and applications of these generalised models of dark energy will be outlined and discussed. In Sec. 5.4 the cosmic dynamics of tachyons will be fully analysed with dynamical systems techniques and dark energy models built from more general Lagrangians, which can be motivated by extra dimensional theories, will be briefly treated. Finally Sec. 5.5 will present some non-scalar field models of dark energy which can be studied with dynamical systems methods.

5.1 Phantom dark energy

The first non-canonical scalar field model we study is mathematically the simplest one to deal with. Its Lagrangian is almost the same as the canonical one (4.5) with only the *sign* of the kinetic term to be the opposite of quintessence. Explicitly we have

$$\mathcal{L}_\phi = +\partial\phi^2 - V(\phi)\,, \tag{5.1}$$

where $\partial\phi^2 = \partial_\mu\phi\partial^\mu\phi$ and $V(\phi)$ is a self-interacting potential. Note the sign of the kinetic term which is the opposite with respect to (4.5).

Phantom scalar field

The scalar field defined by the Lagrangian (5.1) is known as *phantom field* since its equation of state (EoS) is capable of reaching values $w_\phi < -1$, which lie in the so-called *phantom regime* (Caldwell, 2002; Caldwell et al., 2003). A dark energy model able to produce an EoS with values below -1 is interesting under a phenomenological point of view since the phantom regime is slightly favored by astronomical observations, though not with statistical significance. The present value for the dark energy EoS parameter is measured to be roughly $w_{\rm DE} \simeq -1.1 \pm 0.2$ (Ade et al., 2013). Though the ΛCDM model with the constant value $w_\Lambda = -1$ still fits the observational results, phantom dark energy with $w_{\rm DE} < -1$ could in principle better accommodate the data. Recall that the EoS of quintessence is constrained into the interval $[-1, 1]$; see Eq. (4.15). This implies that a canonical scalar field cannot account for a dark energy EoS in the phantom regime. If future observations will exclude values $w_{\rm DE} > -1$, then we will need to rely on dark energy models where the phantom regime can be attained. For scalar field models this means to abandon the canonical formulation and to probe new non-canonical possibilities, the simplest one being the phantom field (5.1).

Unfortunately leaving the canonical paradigm means also the appearance of new theoretical problems (see e.g. Carroll et al. (2003); Cline et al. (2004)). The most evident in the case of the phantom field (5.1) is the introduction of negative energies. Flipping the sign of the kinetic energy inevitably leads to a total energy of the scalar field which is no more bounded from below. From a quantum perspective this implies the appearance of *ghosts* (modes violating unitarity) in the theory, while from a classical point of view solutions of the equations of motion are no more stable under small perturbations and the dominant energy condition is violated. For the phantom field (5.1) there is no way to cure such pathologies since a negative kinetic energy always introduce these problems. However we will consider the phantom scalar field as a simple phenomenological model capable of producing dark energy with EoS values below -1. We will ignore these theoretical problems, interpreting the model as an emergent phenomenon not to be trusted at the deepest fundamental level. This is the approach of every work whose aim is to study phantom dark energy.

A general cosmological fluid with an EoS in the phantom regime implies also a different destiny for the universe. In fact if we go back to Eq. (3.11) and assume $w < -1$, once we substitute this into the Friedmann equation (3.6), instead of obtaining Eq. (3.23), the expanding solution for the scale factor will be

$$a(t) \propto (t_0 - t)^{\frac{2}{3(w+1)}}\,, \tag{5.2}$$

where t_0 is some time in the future. Note that the exponent of $t_0 - t$ in Eq. (5.2) is negative for $w < -1$ and thus $a(t)$ is indeed expanding as t increases. The interesting feature of this solution is that at the time $t = t_0$ the scale factor diverges. This implies that at some time in the future the expansion will become so fast that everything in the universe will be ripped apart. This future singularity is known as the *big rip* (Caldwell et al., 2003) and always happens in universes which are perpetually phantom dominated. *Big rip*

At this point we start analysing the dynamics of the phantom scalar field (5.1). Assuming a flat FRW metric, the cosmological equations arising from the Lagrangian (5.1) in the presence of a matter fluid with[1] $p = w\rho$ are

$$3H^2 = \kappa^2 \left(\rho - \frac{1}{2}\dot{\phi}^2 + V\right)\,, \tag{5.3}$$

$$2\dot{H} + 3H^2 = \kappa^2 \left(-w\rho + \frac{1}{2}\dot{\phi}^2 + V\right)\,, \tag{5.4}$$

$$\ddot{\phi} + 3H\dot{\phi} - V_{,\phi} = 0\,, \tag{5.5}$$

where again a dot means differentiation with respect to the coordinate time t. Note the opposite sign with respect to Eqs. (4.10)–(4.12) in all the terms where a derivative of ϕ appears. The EoS of the scalar field is now given by

$$w_\phi = \frac{\frac{1}{2}\dot{\phi}^2 + V(\phi)}{\frac{1}{2}\dot{\phi}^2 - V(\phi)}\,, \tag{5.6}$$

while its energy density is

$$\rho_\phi = -\frac{1}{2}\dot{\phi}^2 + V(\phi)\,, \tag{5.7}$$

and is clearly negative whenever the kinetic energy is bigger than the potential energy. Moreover when the kinetic energy equals the potential energy the EoS (5.6) diverges. This can be taken as a first warning that the theoretical pathologies mentioned above can yield non physical behavior.

Since the cosmological equations (5.3)–(5.5) are almost the same as the canonical scalar field ones, the use of the expansion normalised variables (4.16) will again be of great advantage. Defining

$$x = \frac{\kappa\dot{\phi}}{\sqrt{6}H}\,, \qquad y = \frac{\kappa\sqrt{V}}{\sqrt{3}H}\,, \qquad \lambda = -\frac{V_{,\phi}}{\kappa V}\,, \tag{5.8}$$

[1]Here again $0 \leq w \leq 1/3$, not to be confused with the discussion above of $w < -1$.

the cosmological equations (5.3)–(5.5) can be rewritten as

$$x' = \frac{1}{2}\left[3(w-1)x^3 - 3x\left(w\left(y^2-1\right)+y^2+1\right) - \sqrt{6}\lambda y^2\right], \tag{5.9}$$

$$y' = -\frac{1}{2}y\left[-3(w-1)x^2 + 3(w+1)\left(y^2-1\right) + \sqrt{6}\lambda x\right], \tag{5.10}$$

$$\lambda' = -\sqrt{6}(\Gamma-1)x\lambda^2, \tag{5.11}$$

where again

$$\Gamma = \frac{VV_{,\phi\phi}}{V_{,\phi}^2}. \tag{5.12}$$

As in the quintessence scenario, Eqs. (5.9)–(5.11) do not form an autonomous system of equations unless Γ can be written as a function of λ in which case they represent a 3D autonomous dynamical system. A similar analysis for arbitrary potentials as the one conducted in Sec. 4.4 could be performed here for the phantom field and interesting potentials, such as the power-law one of Sec. 4.3, could be studied. However we will focus on the exponential case where Eqs. (5.9)–(5.10) constitute a 2D autonomous system and λ becomes a constant. This is the simplest case and also the most studied in the literature (Hao & Li, 2003a; Urena-Lopez, 2005). It will suffice in showing the most important features characterizing the phantom scalar field model of dark energy. Again, though the major dynamical and phenomenological features of a phantom scalar field with an exponential potential have extensively been analysed through the literature, some of the work presented in this section will nevertheless constitute an original contribution of this thesis[2].

In what follows we will assume

$$V(\phi) = V_0 e^{-\lambda\kappa\phi}, \tag{5.13}$$

where $V_0 > 0$ is a positive constant and λ a parameter. Eqs. (5.9)–(5.10) will form a 2D dynamical system in the variables x and y which must also satisfy the Friedmann constraint

$$\Omega_\phi = -x^2 + y^2 = 1 - \Omega_m \leq 1, \tag{5.14}$$

since Ω_m, the relative energy density of matter, is assumed to be positive. The Friedmann constraint (5.14) now fails to close the (physical) phase space to a compact set. The forbidden non-physical regions now lies above and below the hyperbolae $y = \pm\sqrt{1+x^2}$ with the physical phase space constrained between the two. The system (5.9)–(5.10) is again invariant under the transformation $y \mapsto -y$, meaning that the dynamics in the negative y half-plane will be a reflection of the one in the positive y half-plane. Having

[2]In particular the global analysis of the model with the behaviour at infinity has never been considered.

Point	x	y	Existence	w_{eff}	Accel.	Ω_ϕ	Stability
O	0	0	$\forall\, \lambda, w$	w	No	0	Saddle
C	$-\lambda/\sqrt{6}$	$\sqrt{1+\frac{\lambda^2}{6}}$	$\forall\, \lambda, w$	$-1-\lambda^2/3$	Yes	1	Stable

Table 5.1: Critical points of the system (5.9)–(5.10) with existence, physical and stability properties.

assumed $V > 0$, i.e. $y > 0$, we will only analyse the upper half-plane. Note also that the $(x, \lambda) \mapsto (-x, -\lambda)$ symmetry holds in the dynamical system (5.9)–(5.10). As in the canonical case we will thus only need to consider positive λs since negative values will lead to the same dynamics after a reflection around the y-axis. Note that the effective EoS (5.6) can now be rewritten[3] as

$$w_\phi = \frac{x^2 + y^2}{x^2 - y^2}\,, \tag{5.15}$$

which diverges whenever $x^2 = y^2$.

The critical points of the system (5.9)–(5.10) are listed, together with their existence, physical and stability properties, in Tab. 5.1. There are only two finite critical points of this system:

- *Point O.* The origin of the phase space is again a critical point representing a matter dominated universe: $\Omega_m = 1$ and $w_{\text{eff}} = w$. Its existence is independent by the values of w and λ and, as it happened in quintessence models, it always acts as a saddle point, attracting trajectories along the x-axis and repelling them towards the y-axis.

- *Point C.* The only non trivial critical point appearing in the phase space is the scalar field dominated ($\Omega_\phi = 1$) Point C (see Tab. 5.1 for the coordinates). It exists for all values of w and λ and, being scalar field dominated, it lies on the upper hyperbola $y = \sqrt{1 + x^2}$. The effective EoS at this point matches the scalar field EoS and takes the value $w_{\text{eff}} = w_\phi = -1 - \lambda^2/3$, which is in the phantom regime for every value of λ different from zero. As λ increases from zero to higher values Point C moves away from point $(0, 1)$ along the upper hyperbola. Finally Point C is always a stable point and as we will see below it always represents the future global attractor.

Although there are only two critical points, these are the right ones needed to describe a late time transition from matter to phantom domination. In fact a heteroclinic orbit connecting Point O to Point C would represent such

[3]The dynamical system for phantom scalar field in the variables (Ω_ϕ, w_ϕ) can be found in Fang et al. (2014a).

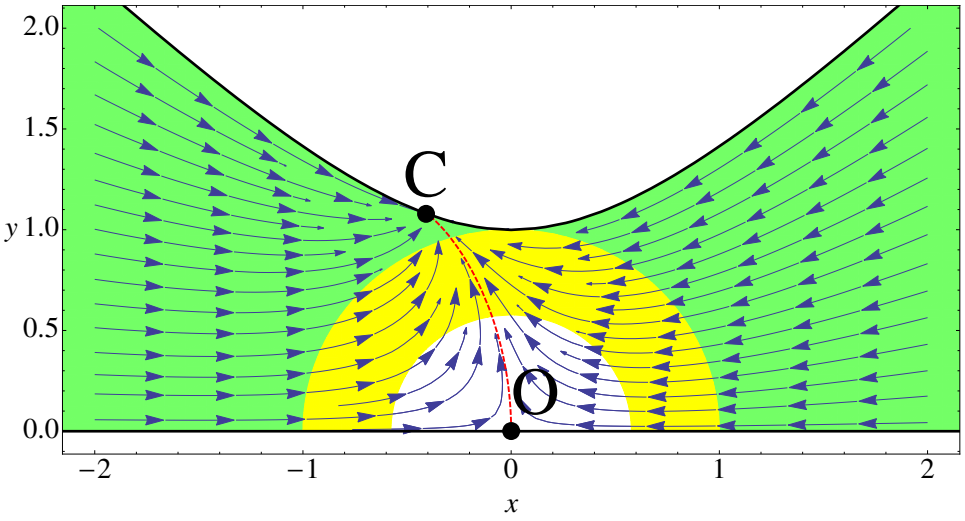

Figure 5.1: Phase space portrait near the origin of the dynamical system (5.9)–(5.10) with the values $w = 0$ and $\lambda = 1$. Point C represents a phantom dominated point, while the dashed/red line denotes the heteroclinic orbit connecting Point O to Point C and characterizing the matter to phantom transition. The external green/shaded region shows where the universe is phantom dominated ($w_{\text{eff}} < -1$), while the internal yellow/shaded region shows where the universe undergoes a standard accelerated expansion ($-1 < w_{\text{eff}} < -1/3$).

phenomenological behavior. Note that the steeper is the potential, i.e. the higher the value of λ, the more Point C will fall into the phantom regime, i.e. the lower the value of w_{eff} at Point C will be. In order to characterize the small deviation allowed by the observational data, only small values of λ should be considered in this model ($\lambda^2 \simeq 3/10$ for $w_{\text{DE}} \simeq -1.1$).

We can now have a look at the phase space portrait near the origin. This has been plotted in Fig. 5.1 for the values[4] $w = 0$ and $\lambda = 1$. The qualitative behavior of the flow in the phase space does not change for different values of λ. Point C will always constitute the global future attractor moving along the $y = \sqrt{1 + x^2}$ hyperbola as the value of λ changes, while Point O will always be a saddle point. The hyperbola $y = \sqrt{1 + x^2}$ divides the physically allowed region ($\Omega_m > 0$) of the phase space to the non physical one ($\Omega_m < 0$) above itself. The external green/shaded region in Fig. 5.2 represent the area of the phase space where the universe is phantom dominated ($w_{\text{eff}} < -1$), while the internal yellow/shaded region shows where the universe undergoes standard accelerated expansion ($-1 < w_{\text{eff}} < -1/3$). Note that outside the unit disk only phantom behavior is possible. The phase space for the

[4]Different values of w in the physically meaningful region $0 \leq w \leq 1/3$ do not alter the qualitative analysis that follows.

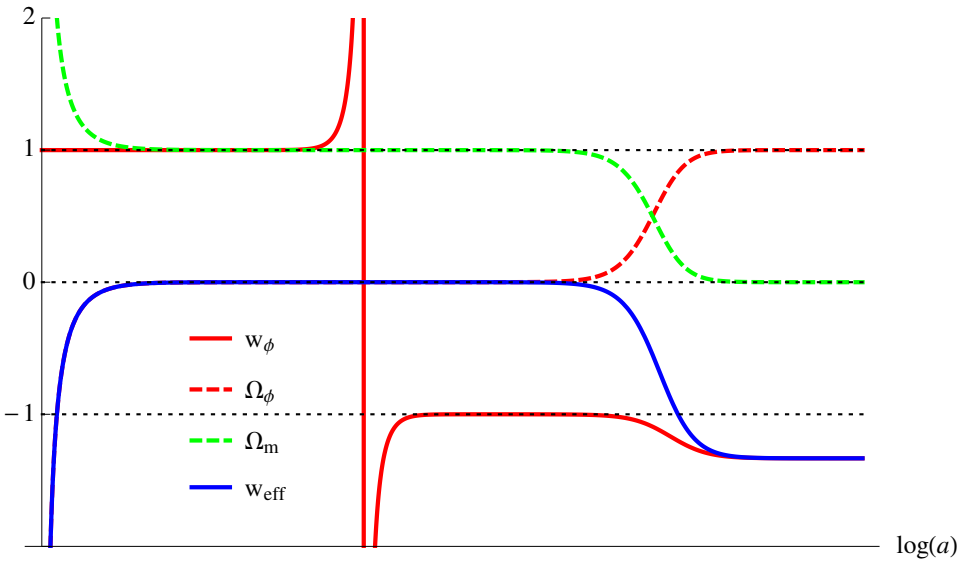

Figure 5.2: Evolution of the phenomenological quantities for an orbit shadowing the matter to phantom transition in the phantom dark energy model.

phantom scalar field is not compact and trajectories can escape at infinity. From Fig. 5.1 it is clear that the past attractors of the phase space must be represented by points at infinity.

The whole late time dynamics of the phantom scalar field model is completely self-explained by Fig. 5.1. The red/dashed line denotes the heteroclinic orbit connecting the matter dominated Point O with the phantom dominated Point C, and trajectories aiming at characterizing the late time transition from matter to phantom acceleration must shadow this orbit. In Fig. 5.2 the evolutions of the energy densities of matter (Ω_m) and the phantom field (Ω_ϕ) together with the effective EoS (w_{eff}) and the scalar field EoS (w_ϕ) have been plotted for a trajectories shadowing the heteroclinic orbit between Point O and Point C and coming from $x \to +\infty$ as $\eta \to -\infty$. The late time matter to phantom transition is well explained by the effective EoS dropping from zero to a value below -1 exactly when the scalar field start dominating. Right before the transition the scalar field acts as a negligible cosmological constant with the value $w_\phi = -1$. Nevertheless, although the late time behavior could well characterize the observed universe, the scalar field experiences non physical features during its early time evolution.

First at very early times the scalar field energy density diverges at minus infinity, while the matter energy density compensate this situation diverging at plus infinity. This non-physical behavior is independent of the trajectory coming from positive or negative values of x as $\eta \to -\infty$ since effectively $\Omega_\phi \simeq -x^2$ at early times. This implies that the scalar field will always present a negative energy in the very early universe. Its EoS during this

period is $w_\phi \simeq 1$ describing a kinetic dominated stiff fluid, while the effective EoS diverges at $-\infty$ in the past, but it stabilises around the matter value as soon as the scalar field energy density approaches zero.

At some point deep into the matter dominated era the scalar field EoS present a discontinuity diverging at $+\infty$ and emerging at $-\infty$. This always happens when $x^2 = y^2$, as noticed before in Eq. (5.15), and no orbit in the phase space can avoid such singularity[5]. Although for orbits shadowing the matter to phantom transition this discontinuity happens extremely close to Point O where the scalar field energy density is negligible, the fact that a singularity appears in the dark energy EoS represents the direct effect of the theoretical problems mentioned above. In fact the phantom scalar field model of dark energy should be trusted for phenomenological applications only after this discontinuity has occurred. Everything that comes before should be ignored, assuming that other physical mechanisms come into play and that the effective description of dark energy as a phantom scalar field ceases. This also applies to the very early unphysical behavior which for the same reason should be neglected even more. If the model is seriously considered only after the non physical behaviors have happened, then it can effectively describe the late time expansion of the universe with a distinctive signature on the dark energy EoS which could be measured by forthcoming observations.

In the final part of this section we will determine the behavior of the flow at infinity. As we mentioned above, and as it is clear from Fig. 5.1, the phase space of the system (5.9)–(5.10) is not compact. In order to analyse the flow at infinity we must employ the techniques developed in Sec. 2.7. The first step is to determine critical points at infinity using Eq. (2.62). The polynomial terms of higher order in Eqs. (5.9) and (5.10) are of the third order in x and y. If we consider only these higher terms, then Eq. (2.62) vanishes identically implying that every point at infinity is a critical point. This could be expected by the behavior of the flow in Fig. 5.1 which seems to be not attracted by any specific point as it diverges at infinity in the past.

This behavior is confirmed by numerical computation. In Fig. 5.3 the global phase space for the dynamical system (5.9)–(5.10) has been drawn. The phase space has been compactified using the projection onto the Poincaré sphere given by Eq. (2.58). Every point on the unit circle, corresponding to points at infinity, is a critical point. They lie between Points $A_\pm$ and Points $B_\pm$ which delimits the boundaries of the physical phase space. These points represent the past attractors of the system which can be split into two invariant sets: trajectories on the right of the heteroclinic orbit connecting Point O with Point C have the points between Points A_+ and B_+

[5]The singularity appears when a solution cross one of the lines $y = \pm x$. Note that before the singularity the scalar field EoS parameter is one, while after it the EoS approaches the value $w_\phi = -1$. Looking at Fig. 5.1 it is clear that every trajectory, a part from the scalar field dominated solutions on the upper hyperbola, must eventually cross one of these lines.

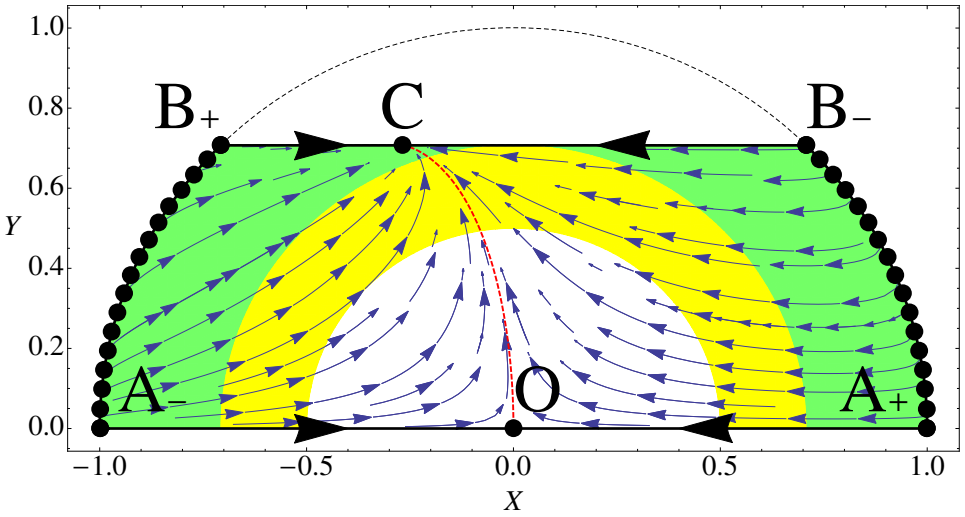

Figure 5.3: Global phase space portrait of the system (5.9)–(5.10).

as past attractors, while trajectories on the left have the points between Points A_- and B_- as their past attractors. The constant line $Y = 1/\sqrt{2}$ corresponds to the upper hyperbola $y = \sqrt{1+x^2}$ in the non compact phase space. The region of the phase space above this line, but still inside the unit disk (dashed line in Fig. 5.3) due to the compactification, stands for the physically forbidden region where the matter energy density is negative ($\Omega_m < 0$).

One might note from Fig. 5.3 that as orbits approach the critical points at infinity they are slightly attracted by Point B_+ on the right and Point A_- on the left. This behavior can be understood considering again Eq. (2.62): if we allow also the second order terms into this equations[6] we obtain

$$\sin\theta - \sin 3\theta = 0\,, \tag{5.16}$$

which gives the (physical) solutions $\theta = 0, \pi/4, 3\pi/4, \pi$ corresponding to Points $A_\pm$ and $B_\pm$ in Fig. 5.3. Moreover the function $\sin\theta - \sin 3\theta$ is always negative in the intervals $[0, \pi/4]$ and $[3\pi/4, \pi]$, implying that the flow is moving clockwise near the unit circle between the Points $A_\pm$ and $B_\pm$. In fact, as can be seen from Fig. 5.3, the flow at the right end of the compactified phase space is slightly attracted by Point A_+, while the flow at the left end is slightly attracted by Point B_-. Of course since all points at infinity are critical points and the higher order terms in Eq. (2.62) vanish, this behavior

[6]Strictly speaking, critical points at infinity, together with their stability, are only determined by the highest polynomial terms with the lower terms having no influence (Perko, 2001). However, in order to determine the qualitative behavior of the flow as infinity is reached, we can consider the highest surviving terms in this approximation and obtain some information from them.

constitutes only a higher order feature which slightly deviates the flow as it approaches infinity.

In conclusion the phantom scalar field model of dark energy can be considered as a viable description of late time cosmology capable of predicting a dark energy EoS in the phantom regime ($w_{\rm DE} < -1$). If future observations will constrain the dark energy EoS to lie in the phantom regime, then a phantom scalar field with a negative kinetic energy is certainly the simplest model which can account for such behavior. Its dynamics is extremely simple to analyse with only two finite critical points appearing in the phase space and no qualitative dependence on the theoretical parameters. The 2D phase space is mathematically simple to handle with the dynamical systems tools we developed in Chapter 2, including the behavior at infinity.

The phantom scalar field has its drawbacks. First of all its early time phenomenology presents singularities which clearly indicates the non viability of the model during this period. These infinities are the direct consequence of more fundamental problems connected with negative energies appearing in the theories. Nevertheless the model can be completely trusted as an emergent phenomenon at late times and assumed not to hold at early times where different mechanisms should come into play to cure the pathologies. Moreover the model does not solve the cosmic coincidence problem and suffer from the fine tuning of initial condition, exactly as quintessence with an exponential potential does; see Sec. 4.2. In fact the only solutions capable of well describing the late time transition from matter to acceleration, which happens at the present cosmological time with no reason, are the ones shadowing the heteroclinic orbit between Points O and C, which of course require special initial conditions.

These conclusions apply only at the phantom scalar field with an exponential potential and matter with an EoS parameter $0 \leq w \leq 1/3$. Urena-Lopez (2005) extended the analysis to matter fluids outside the $[0, 1/3]$ interval in which situation scaling solutions appear. Li & Hao (2004) instead generalised the phantom dynamics to multiple scalar fields with an $O(N)$ symmetry and found the lower bound $w_{\rm DE} > -3$ for phantom stable attractor solutions. It might also be the case that the choice of other potentials leads to the solution of some of these problems, as it happens in the quintessence case of Chapter 4. Hao & Li (2004) discussed the dynamics of the phantom field for a general potential, looking in particular at tracking, de Sitter and big rip solutions. Hao & Li (2003b) showed that de Sitter-like solutions always arises as late time attractors if the phantom scalar field potential has a non-vanishing maximum. Nojiri et al. (2005) instead classified the possible singularities appearing in general phantom dark energy models (including interactions with the matter fluid) and studied them with dynamical systems methods.

Finally several authors considered a coupling between the phantom scalar field and the matter sector. Guo et al. (2005a), Gumjudpai et al. (2005),

Chen et al. (2009) and Wei (2011a) analysed the dynamics of an exponential potential with a number of phenomenological couplings mostly of the types listed in Tab. 4.8. Leon & Saridakis (2010) studied a model where the mass of dark matter particles depends on the phantom field for both exponential and power-law potentials, and later Boehmer et al. (2012a) applied the centre manifold theorem to the same model. The common conclusion achieved by these works is that the interaction between the phantom scalar field and the matter sector cannot solve the cosmic coincidence problem, as it happens in the case of quintessence (see Sec. 4.5), because of the lack of accelerating scaling solutions constituting late time attractors.

5.2 Quintom dark energy

Before looking at other non-canonical scalar field models of dark energy, in this section we will first consider an interesting two-field model with one canonical scalar field ϕ and one phantom scalar field σ. The Lagrangian of such a model reads

$$\mathcal{L}_{\rm quintom} = -\frac{1}{2}\partial\phi^2 + \frac{1}{2}\partial\sigma^2 - V(\phi,\sigma)\,, \tag{5.17}$$

where $\partial\phi^2 = \partial_\mu\phi\partial^\mu\phi$, $\partial\sigma^2 = \partial_\mu\sigma\partial^\mu\sigma$ and $V(\phi,\sigma)$ is a general potential for both the scalar fields. Note the opposite sign of the kinetic terms implying that ϕ is a canonical scalar field and σ is a phantom scalar field. The model (5.17) has been dubbed *quintom dark energy* from the fusion of the words quintessence and phantom.

Quintom dark energy

The most interesting phenomenological feature of this model is that its dark energy EoS is capable of crossing the so-called *phantom barrier*, i.e. the cosmological constant value $w_{\rm DE} = -1$. In other words, $w_{\rm DE}$ can take values both above and below -1 with a possible dynamical transition from the standard to phantom regimes. Such behavior is important since, though astronomical observations allow for a present phantom dark energy EoS, they also favor a quintessence EoS in the past, as it was pointed out by Feng et al. (2005) who first proposed the quintom paradigm. We learned in Chapter 4 that the EoS of quintessence must satisfy $w_{\rm DE} > -1$, while in Sec. 5.1 we have seen that for phenomenologically acceptable phantom models, i.e. valid only after the early time singularities in the EoS has taken place, the scalar field EoS is constrained in the phantom regime $w_{\rm DE} < -1$. There is no way thus to cross the phantom barrier with a single canonical or phantom scalar field. This can be achieved with more general non-canonical scalar fields, but the simplest model is represented by the quintom Lagrangian (5.17).

In this section we will deal with the simplest quintom models without delivering a complete dynamical systems analysis. Detailed references to the literature for works studying quintom dark energy with dynamical systems

methods will be provided. The reader interested in the theory and phenomenology of these models can refer to the extensive review by Cai et al. (2010). Similarly to the multi-field quintessence models we encountered in Sec. 4.6, we can distinguish between interacting and non-interacting potentials for the two scalar fields ϕ and σ of the quintom scenario. We will deal first with the non-interacting case and then discuss interacting models.

The potential $V(\phi, \sigma)$ for non-interacting scalar fields can be generally written as

$$V(\phi, \sigma) = V_1(\phi) + V_2(\sigma)\,, \tag{5.18}$$

where $V_1(\phi)$ and $V_2(\sigma)$ are arbitrary self-interacting potentials for the two scalar fields ϕ and σ respectively. In this situation we have two separated scalar fields which can be treated exactly as if they were single models. The cosmological equations are given by the Friedmann and acceleration equations

$$\frac{3H^2}{\kappa} = \rho + \frac{1}{2}\dot{\phi}^2 + V_1(\phi) - \frac{1}{2}\dot{\sigma}^2 + V_2(\sigma)\,, \tag{5.19}$$

$$\frac{1}{\kappa}\left(2\dot{H} + 3H^2\right) = -w\rho - \frac{1}{2}\dot{\phi}^2 + V_1(\phi) + \frac{1}{2}\dot{\sigma}^2 + V_2(\sigma)\,, \tag{5.20}$$

and by the Klein-Gordon equations

$$\ddot{\phi} + 3H\dot{\phi} + \frac{\partial V_1(\phi)}{\partial \phi} = 0\,, \tag{5.21}$$

$$\ddot{\sigma} + 3H\dot{\sigma} - \frac{\partial V_2(\sigma)}{\partial \sigma} = 0\,. \tag{5.22}$$

In order to recast them into a dynamical system we define EN variables as

$$x_\phi = \frac{\kappa\dot{\phi}}{\sqrt{6}H}\,, \qquad y_\phi = \frac{\kappa\sqrt{V_1}}{\sqrt{3}H}\,, \qquad \lambda_\phi = -\frac{1}{\kappa V_1}\frac{\partial V_1}{\partial \phi}\,, \tag{5.23}$$

$$x_\sigma = \frac{\kappa\dot{\sigma}}{\sqrt{6}H}\,, \qquad y_\sigma = \frac{\kappa\sqrt{V_2}}{\sqrt{3}H}\,, \qquad \lambda_\sigma = -\frac{1}{\kappa V_2}\frac{\partial V_2}{\partial \sigma}\,. \tag{5.24}$$

To find the dynamical system governing the cosmological evolution, we proceed in the same way as with the quintessence and phantom field[7]. Eventu-

[7] Derive the variables x_ϕ, y_ϕ, x_σ, y_σ, λ_ϕ and λ_σ with respect to $d\eta = Hdt$, and then use Eqs. (5.19)–(5.22) to replace $\dot{H}$, $\ddot{\phi}$ and $\ddot{\sigma}$.

ally Eqs. (5.19)–(5.22) yield

$$x'_\phi = \frac{3}{2}\left[x_\phi\left[(w-1)(x_\sigma^2+1)-(w+1)(y_\phi^2+y_\sigma^2)\right]-(w-1)x_\phi^3+\frac{\sqrt{3}}{\sqrt{2}}\lambda_\phi y_\phi^2\right], \tag{5.25}$$

$$y'_\phi = -\frac{y_\phi}{2}\left[3(w-1)(x_\phi^2-x_\sigma^2)+3(w+1)\left(y_\sigma^2+y_\phi^2-1\right)+\sqrt{6}\lambda_\phi x_\phi\right], \tag{5.26}$$

$$x'_\sigma = \frac{3}{2}\left[(w-1)x_\sigma^3-x_\sigma\left[(1-w)(1-x_\phi^2)+(w+1)(y_\phi^2+y_\sigma^2)\right]-\frac{\sqrt{2}}{\sqrt{3}}\lambda_\sigma y_\sigma^2\right], \tag{5.27}$$

$$y'_\sigma = -\frac{y_\sigma}{2}\left[3(w-1)(x_\phi^2-x_\sigma^2)+3(w+1)\left(y_\sigma^2+y_\phi^2-1\right)+\sqrt{6}\lambda_\sigma x_\sigma\right], \tag{5.28}$$

$$\lambda'_\phi = -\sqrt{6}(\Gamma_\phi-1)x\lambda_\phi^2, \tag{5.29}$$

$$\lambda'_\sigma = -\sqrt{6}(\Gamma_\sigma-1)x\lambda_\sigma^2, \tag{5.30}$$

where

$$\Gamma_\phi = V_1\frac{V_{1,\phi\phi}}{V_{1,\phi}^2}, \qquad \Gamma_\sigma = V_2\frac{V_{2,\sigma\sigma}}{V_{2,\sigma}^2}, \tag{5.31}$$

and the Friedmann constraint

$$-x_\sigma^2+x_\phi^2+y_\sigma^2+y_\phi^2 = \Omega_m-1\leq 1, \tag{5.32}$$

holds. If Γ_ϕ and Γ_σ can be written as functions of λ_ϕ and λ_σ respectively, then Eqs. (5.25)–(5.30) constitute a 6D dynamical system and a similar analysis of the one we performed in Sec. 4.4 can be conducted. Such a work has recently been done in detail by Leon et al. (2014) where critical points and the stability analysis have been studied and also the specific potential $V(\phi,\sigma) = A\sinh^2(\alpha\phi)+B\cosh^2(\beta\sigma)$ has been considered as an example.

In what follow however we will briefly discuss the exponential potential case where

$$V_1(\phi) = A\,e^{-\lambda_\phi\kappa\phi} \quad \text{and} \quad V_2(\sigma) = B\,e^{-\lambda_\sigma\kappa\sigma}, \tag{5.33}$$

with A, B, λ_ϕ, λ_σ all constant. This represent the simplest situation where Eqs. (5.25)–(5.28) form an autonomous 4D dynamical system. The exponential potentials (5.33) have been analysed by Guo et al. (2005b) who found quintessence dominated solutions, phantom future attractors and scaling solutions (see also Cai et al. (2010)). We will not list here all the critical points with their properties, but limit our discussion to the interesting late time phenomenology arising from this model. The reader interested in the details may find more information in the mentioned references.

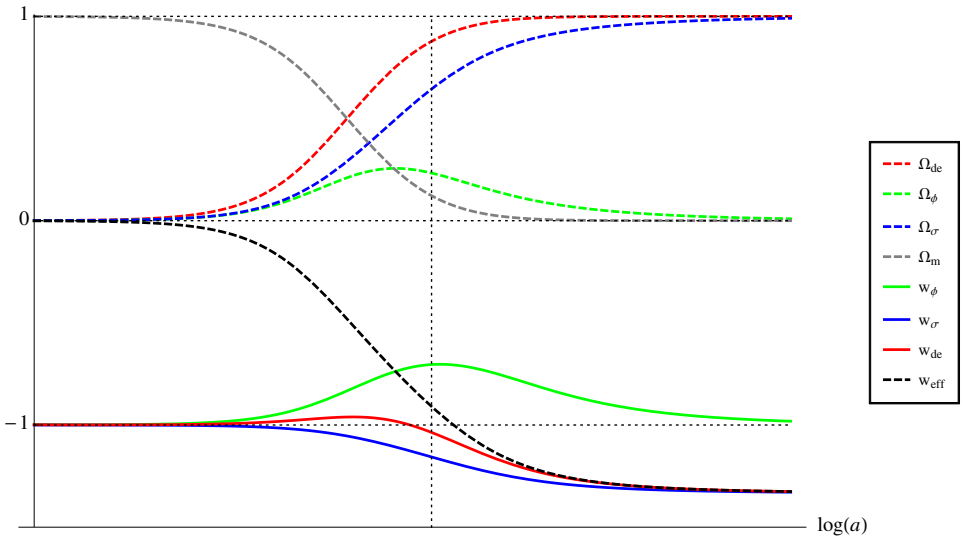

Figure 5.4: Late time evolution for the phenomenological quantities of the uncoupled quintom model with exponential potentials. The values $\lambda_\phi = 2$, $\lambda_\sigma = 1$ and $w = 0$, together with suitable initial conditions, have been chosen.

Using the variables (5.24) the energy densities and EoS of the scalar fields can be written as

$$\Omega_\phi = x_\phi^2 + y_\phi^2\,, \qquad w_\phi = \frac{x_\phi^2 - y_\phi^2}{x_\phi^2 + y_\phi^2}\,, \tag{5.34}$$

$$\Omega_\sigma = -x_\sigma^2 + y_\sigma^2\,, \qquad w_\sigma = \frac{-x_\sigma^2 - y_\sigma^2}{y_\sigma^2 - x_\sigma^2}\,, \tag{5.35}$$

while the energy density and EoS of dark energy, given by the added contributions of ϕ and σ, are

$$\Omega_{\rm DE} = -x_\sigma^2 + x_\phi^2 + y_\sigma^2 + y_\phi^2\,, \qquad w_{\rm DE} = \frac{-x_\sigma^2 + x_\phi^2 - y_\sigma^2 - y_\phi^2}{-x_\sigma^2 + x_\phi^2 + y_\sigma^2 + y_\phi^2}\,. \tag{5.36}$$

The effective EoS is instead given by

$$w_{\rm eff} = w\left(x_\sigma^2 - x_\phi^2 - y_\sigma^2 - y_\phi^2 + 1\right) - x_\sigma^2 + x_\phi^2 - y_\sigma^2 - y_\phi^2\,, \tag{5.37}$$

where one can see the separate contributions of the phantom and quintessence fields respectively.

In Fig. 5.4 the late time evolution of the phenomenological quantities (5.34)–(5.37) for the quintom uncoupled model with exponential potentials (5.33) have been plotted. The initial conditions have been chosen to highlight the characteristics of the quintom paradigm while the values $\lambda_\phi = 2$,

$\lambda_\sigma = 1$ and $w = 0$ have been considered. Only the late time evolution is shown when the singularities associated with the phantom field have already taken place and the effective field approach applies (see Sec. 5.1). In the example of Fig. 5.4 the phantom field asymptotically dominates in the future, with the quintessence field never completely dominating during its evolution. The matter to dark energy transition begins with both the scalar field energies raising from negligible values to an order of magnitude comparable with the matter energy density. However before dark energy start dominating the quintessence energy decreases again while the phantom energy begins its domination.

The interesting features happen in the EoS parameters during the matter to dark energy transition (solid lines below zero in Fig. 5.4). As one can see from Fig. 5.4, w_ϕ (green line) always lies above the phantom barrier, while w_σ (blue line) always stays below -1. Their effective contribution however, denoted by $w_{\rm de}$ (red line), is able to cross the phantom barrier being greater than -1 before the matter to dark energy transition and below -1 thereafter. The EoS of dark energy is thus above -1 in the past and below -1 at both the present and future times. Note that the effective EoS is still in the quintessence region at the present time (denoted by the vertical dotted line in Fig. 5.4) while the dark energy EoS is effectively in the phantom regime. The average evolution of the universe is not influenced by the change in nature of dark energy. Indeed the transition from matter to phantom domination for the effective EoS (black dashed line in Fig. 5.4) happens similarly as in the single phantom scalar field case of Sec. 5.1. This changes somehow for different choices of the model parameters or initial conditions, but if today the effective EoS and the dark energy EoS are constrained to be above and below -1 respectively, then the universe must evolve exactly as depicted in Fig. 5.4.

The situation described in Fig. 5.4 is the one slightly favored by observational data, though not at a statistically significant level. The quintom model with uncoupled exponential potentials is thus able to provide a dynamical crossing of the phantom barrier unifying the properties of quintessence and phantom dark energy. If future observations will constrain the dark energy EoS to be below -1 today but above -1 in the past, then the quintom scenario of Fig. 5.4 will be the simplest framework where such a situation can arise.

At this point we turn our attention to quintom models with a potential coupling the two scalar fields. As in the case of multiple quintessence fields (Sec. 4.6), the simplest and most studied of such potentials is again of the exponential type, namely

$$V(\phi, \sigma) = V_0 \, e^{-\lambda_\phi \kappa \phi - \lambda_\sigma \kappa \sigma} \, . \tag{5.38}$$

This scenario has first been studied with dynamical systems techniques by Lazkoz & Leon (2006) who found tracking, phantom and quintessence solu-

tions. Then Leon et al. (2008) employed advanced dynamical systems methods to analyse its past asymptotic dynamics and again Leon et al. (2009) generalised the investigation to spatially non-flat cosmologies, performing also the analysis at infinity.

The cosmological equations for the general coupled case are

$$\frac{3H^2}{\kappa} = \rho + \frac{1}{2}\dot{\phi}^2 - \frac{1}{2}\dot{\sigma}^2 + V(\phi,\sigma)\,, \tag{5.39}$$

$$\frac{1}{\kappa}\left(2\dot{H} + 3H^2\right) = -w\rho - \frac{1}{2}\dot{\phi}^2 + \frac{1}{2}\dot{\sigma}^2 + V(\phi,\sigma)\,, \tag{5.40}$$

and

$$\ddot{\phi} + 3H\dot{\phi} + \frac{\partial V}{\partial \phi} = 0\,, \tag{5.41}$$

$$\ddot{\sigma} + 3H\dot{\sigma} - \frac{\partial V}{\partial \sigma} = 0\,. \tag{5.42}$$

The coupled potential (5.38) is mathematically simpler to analyse than the uncoupled one (5.18), because it only requires one EN variable for the potential energy rather than two. This is a similar situation to the one we encountered in Sec. 4.6 where for multiple interacting quintessence fields with a coupling exponential potential only one EN variable was employed instead of N. In fact defining the EN variables

$$x_\phi = \frac{\kappa\dot{\phi}}{\sqrt{6}H}\,, \qquad x_\sigma = \frac{\kappa\dot{\sigma}}{\sqrt{6}H}\,, \qquad y = \frac{\kappa\sqrt{V}}{\sqrt{3}H}\,, \tag{5.43}$$

Eqs. (5.39)–(5.42) can be recast into the following 3D autonomous dynamical system

$$x'_\phi = \frac{1}{2}\left[3x_\phi\left((w-1)x_\sigma^2 - (w+1)y^2 + w - 1\right) - 3(w-1)x_\phi^3 + \sqrt{6}y^2\lambda_\phi\right]\,, \tag{5.44}$$

$$x'_\sigma = \frac{1}{2}\left[3(w-1)x_\sigma^3 - 3x_\sigma\left((w-1)x_\phi^2 + (w+1)y^2 - w + 1\right) - \sqrt{6}y^2\lambda_\sigma\right]\,, \tag{5.45}$$

$$y' = -\frac{1}{2}y\left[3(w-1)(x_\phi^2 - x_\sigma^2) + 3(w+1)\left(y^2 - 1\right) + \sqrt{6}\lambda_\sigma x_\sigma + \sqrt{6}\lambda_\phi x_\phi\right]\,, \tag{5.46}$$

where the Friedmann constraint

$$x_\phi^2 - x_\sigma^2 + y^2 = \Omega_m - 1 \leq 1\,. \tag{5.47}$$

must hold. The fact that the dynamical system of this model is three dimensional means that suitable plots of the phase space can be drawn, as for example the ones exposed by Lazkoz & Leon (2006). However we will

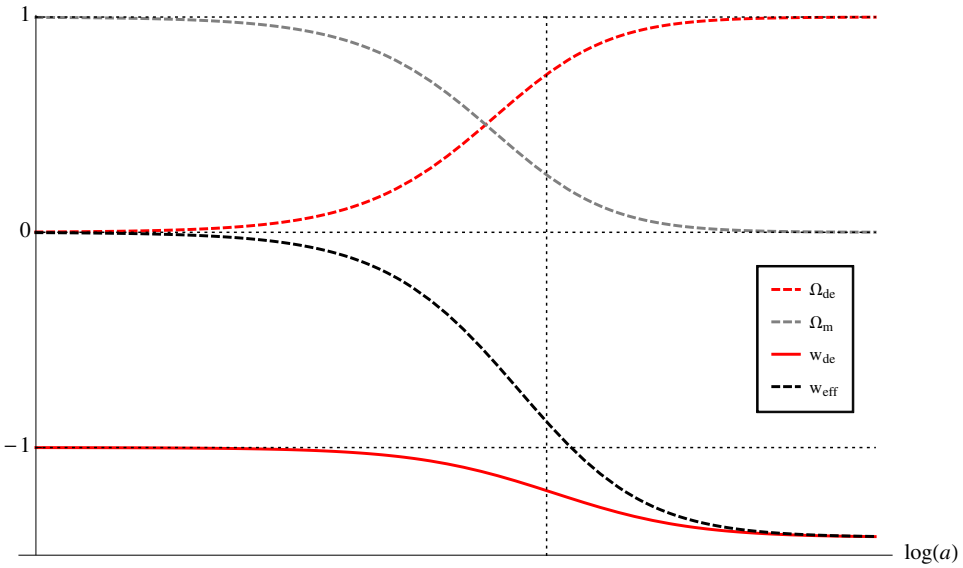

Figure 5.5: Late time evolution for the phenomenological quantities of the coupled quintom model with exponential potentials (5.38). The values $\lambda_\phi = 1$, $\lambda_\sigma = 1.5$ and $w = 0$, together with suitable initial conditions, have been chosen for the plot.

focus again on the late time phenomenology leaving the dynamical systems details to the mentioned references.

The energy density and EoS of dark energy, given by the mixed contributions of ϕ and σ, are now given by

$$\Omega_{\rm DE} = -x_\sigma^2 + x_\phi^2 + y^2\,, \qquad w_{\rm DE} = \frac{-x_\sigma^2 + x_\phi^2 - y^2}{-x_\sigma^2 + x_\phi^2 + y^2}\,. \tag{5.48}$$

while the effective EoS is

$$w_{\rm eff} = w\left(x_\sigma^2 - x_\phi^2 - y^2 + 1\right) - x_\sigma^2 + x_\phi^2 - y^2\,. \tag{5.49}$$

In Fig. 5.5 the late time evolution of these quantities have been plotted for the values $\lambda_\phi = 1$, $\lambda_\sigma = 1.5$ and $w = 0$. The initial conditions have again been chosen in order to highlight the qualities of this quintom model. For the coupled case dark energy acts as a cosmological constant during the matter dominated epoch eventually switching to phantom values during the deceleration to acceleration phase. This is clear in Fig. 5.5 where the dark energy EoS (red solid line) is constantly -1 in the past before taking values below -1. Note that also the coupled exponential potential quintom model manages to fit the best astronomical data having both $w_{\rm eff} > -1$ and $w_{\rm DE} < -1$ today (vertical dotted line in Fig. 5.5). This represents thus another viable model of dynamical crossing of the phantom barrier, even though the dark energy EoS in the past is basically -1.

Unfortunately neither the coupled nor the uncoupled quintom models with exponential potentials seem to solve the cosmic coincidence problem and the fine tuning of initial conditions. The matter to dark energy transition happens again at the present times without an apparent reason, while highly special initial conditions are required to fit the observations. It might be possible that employing potentials beyond the exponential cases will lead to a solutions of these problems, at least partially. However these models will be difficult to study with dynamical system techniques since their autonomous systems will present a minimum of six dimensions, if they can be constructed at all. For this reason few authors have considered dynamical systems applications to quintom models beyond the simple exponential potentials. Zhang et al. (2006) worked with the potential $V(\phi,\sigma) = A\exp(-\lambda_\phi\kappa\phi) + B\exp(-\lambda_\sigma\kappa\sigma) + C\exp(-\lambda_\phi\kappa\phi/2)\exp(-\lambda_\sigma\kappa\sigma/2)$ where the EN variables (5.24) can be used with the interacting term giving rise to contributions proportional to $y_\phi y_\sigma$. They also proposed a quintom model with mass varying neutrinos instead of the quintessence field. Setare & Saridakis (2008) generalised the quintom exponential case to multiple scalar fields with an $O(N)$ symmetry showing that in this case the phantom dominated solutions always represents the future attractor of the system. In general however it might be possible that different variables are better suited for the analysis of more complicated potentials. This is indeed the approach considered by some authors such as Lazkoz et al. (2007) and Setare & Saridakis (2009). Finally some people advanced models with a kinetic coupling between the scalar fields. Saridakis & Weller (2010) introduced the coupling $\partial_\mu\phi\partial^\mu\sigma$, while Wei & Cai (2005) and Alimohammadi & Mohseni Sadjadi (2006) analysed the so-called *hessence dark energy* scenario with the Lagrangian $\mathcal{L} = -\partial\phi^2/2 + \phi^2\partial\sigma^2/2 - V(\phi)$.

Hessence dark energy

5.3 k-essence and higher-order scalar fields

In this section we will briefly review dynamical systems applications to more general scalar field models characterized by Lagrangians with higher-order derivative terms. For these more complicated models dynamical systems analyses are highly involved and thus only an overview with simple discussions on the more important models will be given here. Nevertheless detailed references to the literature of dynamical systems applications, with comments on the main results, will be provided.

In order to simplify the following equations we will denote the scalar field kinetic term with

$$X = -\frac{1}{2}\partial\phi^2 = -\frac{1}{2}\partial_\mu\phi\partial^\mu\phi\,. \tag{5.50}$$

Note that for a homogeneous scalar field ($\phi = \phi(t)$) in a FRW metric (3.1)

the kinetic energy (5.50) is always positive reducing to

$$X = \frac{1}{2}\dot{\phi}^2 \,. \tag{5.51}$$

The first broad class of models we will discuss is known as *k-essence* from kinetic generalisation of quintessence. Its Lagrangian is an arbitrary function P of the kinetic term and the scalar field ϕ and can be written as

k-essence

$$\mathcal{L}_{k\text{-essence}} = P(X, \phi) \,. \tag{5.52}$$

It clearly contains as subclasses both the canonical and phantom scalar fields, but the new cosmological features of these models will mainly come from the contribution of the higher-order terms. The cosmological equations following from the scalar field Lagrangian (5.52) are

$$\frac{3H^2}{\kappa^2} = \rho + 2X\frac{\partial P}{\partial X} - P \,, \tag{5.53}$$

$$\frac{1}{\kappa^2}\left(2\dot{H} + 3H^2\right) = -p - P \,, \tag{5.54}$$

together with the scalar field equation

$$\left(\frac{\partial P}{\partial X} + 2X\frac{\partial^2 P}{\partial X^2}\right)\ddot{\phi} + 3H\frac{\partial P}{\partial X}\dot{\phi} + 2X\frac{\partial^2 P}{\partial X \partial \phi} - \frac{\partial P}{\partial \phi} = 0 \,. \tag{5.55}$$

Note that the function P plays the role of the scalar field pressure p_ϕ in Eq. (5.54), which is why the letter P has been used[8]. From Eq. (5.53) instead the scalar field energy density can be obtained as

$$\rho_\phi = 2X\frac{\partial P}{\partial X} - P \,, \tag{5.56}$$

which reduces to the usual $\rho_\phi = X + V$ in the canonical case. The EoS for the k-essence scalar field can be written as

$$w_\phi = \frac{P}{\rho_\phi} = P\left(2X\frac{\partial P}{\partial X} - P\right)^{-1} \,, \tag{5.57}$$

with the allowed range and possible singularities strongly dependent on the function $P(X, \phi)$.

As mentioned in Sec. 5.1, a non-canonical scalar field Lagrangian will in general introduce theoretical problems at both the quantum and classical levels. In order to avoid these instabilities, at least at the classical level, the k-essence Lagrangian (5.52) must satisfy some consistency conditions, which

[8] In literature the common convention is to use the lower case letter p for the Lagrangian (5.52). We will however use the upper case P in order to not create confusion with the matter pressure.

come from the requirement that solutions of the theory must be stable under small perturbations. These conditions can be translated into two constraints over the energy density and *speed of sound* of the scalar field which are required to be positive. In quantitative terms the constraints

$$\rho_\phi \geq 0 \quad \text{and} \quad c_s^2 \geq 0\,, \tag{5.58}$$

where the scalar field energy density ρ_ϕ is given by in Eq. (5.56) and the speed of sound of adiabatic perturbations is defined as

$$c_s^2 = \frac{\partial P}{\partial X} \Big/ \frac{\partial \rho_\phi}{\partial X}\,, \tag{5.59}$$

must hold (see Garriga & Mukhanov (1999) for more details).

The k-essence scalar field has first been considered as a model of dark energy by Chiba et al. (2000) and Armendariz-Picon et al. (2000, 2001) who found that tracking behavior is possible in these general models and late time accelerated solutions are easy to obtain. Eqs. (5.53)–(5.55) are however too complicated to directly study with dynamical systems techniques due to the unknown dependence upon the arbitrary function $P(X, \phi)$. For a deep dynamical analysis some assumptions to reduce the general function P must first be taken into account. Through the literature several different forms of the k-essence Lagrangian have been considered, however for dynamical systems applications we can broadly divide them into three subclasses.

The first subclass of k-essence Lagrangian we will discuss considers the function

$$P(X, \phi) = X g(X e^{\lambda \kappa \phi})\,, \tag{5.60}$$

where g is an arbitrary function and λ a constant. For these models the EN variables (4.16) are well suited for studying the dynamics since the argument of the function g becomes proportional to x^2/y^2. The reason why the Lagrangian (5.60) is important is its connection with scaling solutions. More precisely Piazza & Tsujikawa (2004) (see also Tsujikawa & Sami (2004); Gong et al. (2006)) proved that scaling solutions appear in k-essence models only if a Lagrangian of the type (5.60) is assumed. As we known from Chapter 4, scaling solutions are of great relevance for the cosmic coincidence problem since stable accelerated scaling solutions could completely solve this issue. Tsujikawa (2006) showed that for the general class (5.60), even in the presence of a coupling to the matter sector, the dark energy late time solutions are always unstable in the presence of a scaling solution unless they are of the phantom type. Subsequently Amendola et al. (2006) generalised this analysis to a matter to dark energy coupling dependent on ϕ and found that the Lagrangian (5.60) can be generalised to $P = Q^2(\phi) X g(X Q^2(\phi) e^{\lambda \kappa \phi})$ where $Q(\phi)$ is the coupling function. They also performed a dynamical systems analysis finding critical points corresponding to scaling, quintessence

and phantom dominated solutions. Remarkably they showed that a dynamical sequence with one early time matter scaling solution and one late time dark energy scaling solution never occurs in such models.

If the Lagrangian (5.60) is well known to give rise to scaling solutions, in the second subclass of k-essence we consider tracking solutions are the dominant feature. The function $P(X, \phi)$ for this category can be generally written as the factorised product

$$P(X, \phi) = K(\phi)\tilde{P}(X)\,, \tag{5.61}$$

where $K(\phi)$ and $\tilde{P}(X)$ are arbitrary functions of ϕ and X respectively. Lagrangians of this kind has been proposed in the first models of k-essence. Chiba et al. (2000) (see also Yang & Xiang-Ting (2011); Fang et al. (2014b)) considered square kinetic corrections as $P(X, \phi) = f(\phi)(-X + X^2)$ with f a general function of ϕ (usually of the power-law type) and showed that tracking behavior, as well as quintessence and phantom attractors, arise in such models. Then Armendariz-Picon et al. (2000, 2001) showed that tracking solutions naturally appear for the models (5.61) during the radiation dominated era, with the scalar field EoS reducing to -1 (cosmological constant) during the matter dominated era and driving the late time accelerated expansion as effective quintessence. Although these tracking solutions could solve the fine tuning problem of initial conditions, Malquarti et al. (2003a) showed that the basin of attraction of the k-essence tracking solutions is smaller than the quintessence one, implying that canonical scalar field models are still better candidate to address this issue.

Models of k-essence of the type (5.61) plus a self-interacting potential for the scalar field have also been studied. Malquarti et al. (2003b) demonstrated that for such models, which include (5.61), if the scalar field is approximately constant during some period of its cosmic evolution, then the theory effectively reduces to quintessence for that period of time. Piazza & Tsujikawa (2004) (see also Gumjudpai et al. (2005)) studied Lagrangians of the type $P = -X + Ae^{\lambda_1\kappa\phi}X^2 - Be^{-\lambda_2\kappa\phi}$ which can easily be motivated by string theory phenomenology. They also considered a coupling between the matter fluid and the scalar field and performed a dynamical analysis of the model $\lambda_1 = \lambda_2 = \lambda$. This last model naturally yields scaling solutions as it can be rewritten into the form (5.60) with the function $g(Y) = -1 + AY - B/Y$.

A complete dynamical systems analysis of such model has been recently delivered by the author of this thesis[9] (Tamanini, 2014). The late time dynamics of the system results similar to the late time dynamics of the canonical quintessence case with the appearance of dark energy and scaling solutions. However the early time dynamics is completely different from the canonical one. In particular the scalar field kinetic dominated solutions no

[9]See Appendix A.

longer appear in the phase space of this model. The early time behaviour is now characterized by a matter dominated solution, which is better in agreement with a radiation or dark matter dominated epoch as required by observations. The model can thus be used to describe a universe where dark energy becomes important only at late times while dark matter dominates at early times. In the same paper the case $g(Y) = -1 - B/Y + \xi\sqrt{1/Y}$ has also been considered. The background dynamics of this model presents a richer phenomenology with respect to the canonical case. The early time behaviour results similar to the canonical one, though super-stiff ($w_{\rm eff} > 1$) transient regions always appear in the phase space. What changes more is the late time evolution where phantom dominated solutions, dynamical crossings of the phantom barrier and new scaling solutions emerge in the phase space. This model can thus be used to describe a late time dark energy dominated universe capable of dynamically crossing the phantom barrier as the astronomical observations slightly favour. Moreover we can achieve transient periods of super-acceleration ($\dot{H} > 0$) where the universe expands only for a finite amount of time. These solutions can be employed to build phantom models of inflation. The drawbacks of such model arise at the level of perturbations where instabilities of the scalar field always appear.

Finally another interesting subclass of k-essence models is represented by the Lagrangian

$$P = F(X) - V(\phi)\,, \tag{5.62}$$

where a non canonical kinetic term appears together with a standard self-interacting potential for the scalar field. As shown by De-Santiago et al. (2013) (see also De-Santiago & Cervantes-Cota (2014)), who also considered bouncing solutions[10], a detailed dynamical systems analysis can be performed introducing the variables

$$x = \frac{\kappa}{\sqrt{3}H}\sqrt{2X\,F_X - F} \quad \text{and} \quad y = \frac{\kappa V}{\sqrt{3}H}\,, \tag{5.63}$$

where F_X denotes the derivative of F with respect to X. Note that for the canonical case $F = X$ these reduce to the EN variables (4.16). Besides late time accelerated solutions, De-Santiago et al. (2013) found also that scaling solutions are possible for some special functions F and V of the model (5.62), even if this cannot be written in the form (5.60).

Some authors have also consider theories of multiple non-canonical scalar fields with higher-order terms. Tsujikawa (2006) and Ohashi & Tsujikawa (2009) proved that for multiple k-essence scalar fields, each one with a Lagrangian $P_i = X_i g(X_i e^{\lambda_i \kappa \phi_i})$, assisted behavior is possible; see Sec. 4.6. More recently Chiba et al. (2014) studied scaling solutions in the same model

[10]Solutions where the universe passes from expansion to contraction (or the other way around).

with interactions to the matter sector, showing that accelerated scaling solutions can be obtained and that the cosmic coincidence problem could be avoided.

At this point we turn our discussion from k-essence models to other higher-order scalar field models. Some of them are motivated by high energy physics, some by phenomenological insights and some even by theoretical issues such as the avoidance of ghosts in the higher order scalar field terms. Gao et al. (2010) considered the direct insertion of a kinetic term in the energy-momentum tensor of the scalar field, completely bypassing the Lagrangian set up. They used this model for a unified approach to both dark matter and dark energy with the scalar field behaving as matter (dust) at early times. Leon & Saridakis (2013) delivered a detailed dynamical systems analysis for generalised *Galileon cosmologies* where the higher order terms of the scalar field satisfy the Galilean symmetry $\phi \mapsto \phi + c$ and $\partial\phi \mapsto \partial\phi + b_\mu$ with c and b_μ constant. They showed that in this model the higher order contributions do not influence the late time cosmological dynamics where the evolution is governed by an effective canonical scalar field. Finally Gomes & Amendola (2014) recently studied scaling solutions for general higher order Lagrangians of the *Horndeski* type where the equation of motion remain of the second order (no ghosts). They found matter dominated solutions followed by an accelerating scaling solution, sequence which could not be obtained with simpler scalar fields. This particular late time evolution can in principle solve the cosmic coincidence problem and provide a viable cosmic history for the observed universe.

Galileons

Horndeski Lagrangians

In conclusion higher-order scalar fields are interesting since they can provide a dynamical evolution mixing features of different canonical and phantom scalar fields. Late time tracking, scaling, quintessence and phantom behavior is possible with viable attempts at solving the fine tuning and cosmic coincidence problems. Unfortunately the rather complicated equations of motion arising in these theories prevent simple applications of dynamical systems theories and rather involved analysis are required, often dealing with non-compact high-dimensional autonomous systems.

5.4 Tachyons and DBI scalar fields

Some particular models of k-essence which deserve more attention, are the ones known under the names of *tachyonic and DBI dark energy*. In this section a detailed dynamical analysis for the simplest tachyonic theory will be delivered, while dynamical systems references and discussions will be provided for more complicated tachyonic and DBI models.

Tachyons are particles predicted by *string theory* in its low-energy effective field theory description (Mazumdar et al., 2001; Sen, 2002a,c,b). Applications of tachyonic scalar fields to late time cosmology were considered soon

Tachyons

after they arose from high-energy physics (Padmanabhan, 2002; Gibbons, 2002, 2003; Bagla et al., 2003; Gorini et al., 2004). They can be defined by the *Dirac-Born-Infeld (DBI) Lagrangian*[11]

DBI tachyonic Lagrangian

$$\mathcal{L}_{\rm tachyons} = V(\phi)\sqrt{1+\partial\phi^2}\,, \tag{5.64}$$

where again $\partial\phi^2 = g^{\mu\nu}\partial_\mu\phi\partial_\nu\phi$ and V is a general function of ϕ which is generally called the scalar field potential, though it does not correspond to the potential energy. Note that in order for the Lagrangian to be mathematically consistent, i.e. to be real, the assumption $1+\partial\phi^2 \geq 0$ must be made a priori. Also the dimensionality of the scalar field, i.e. its physical units, is now taken in order to render $\partial\phi^2$ dimensionless.

The flat FRW cosmological equations derived from the Lagrangian (5.64) minimally coupled to general relativity are

$$\frac{3H^2}{\kappa^2} = \rho + \frac{V}{\sqrt{1-\dot\phi^2}}\,, \tag{5.65}$$

$$\frac{2\dot H}{\kappa^2} = -(w+1)\rho - \frac{\dot\phi^2 V}{\sqrt{1-\dot\phi^2}}\,, \tag{5.66}$$

and the scalar field equation

$$\frac{\ddot\phi}{1-\dot\phi^2} + 3H\dot\phi + \frac{V_{,\phi}}{V} = 0\,, \tag{5.67}$$

where again $V_{,\phi}$ denotes the derivative of V with respect to ϕ. The assumption $1+\partial\phi^2 \geq 0$ now translates into $\dot\phi^2 \leq 1$ which implies the consistency of Eqs. (5.65)–(5.67). The scalar field energy density and pressure can be written as

$$\rho_\phi = \frac{V}{\sqrt{1-\dot\phi^2}} \quad \text{and} \quad p_\phi = -V\sqrt{1-\dot\phi^2}\,, \tag{5.68}$$

and its EoS becomes

$$w_\phi = \frac{p_\phi}{\rho_\phi} = -1 + \dot\phi^2\,. \tag{5.69}$$

Note that whenever the scalar field kinetic energy vanishes the EoS takes the cosmological constant value -1.

In order to convert Eqs. (5.65)–(5.67) into a dynamical system, we need to define suitable dimensionless variables. Following Copeland et al. (2005a) we introduce the variables

$$x = \dot\phi \quad \text{and} \quad y = \frac{\kappa\sqrt{V}}{\sqrt{3}H}\,. \tag{5.70}$$

[11] Sometimes the tachyonic Lagrangian $\mathcal{L}_{\rm tachyons} = -V(\phi)\sqrt{-\det(g_{\mu\nu}+\partial_\mu\phi\partial_\nu\phi)}$ is assumed instead of (5.64); see e.g. Copeland et al. (2005a). Nevertheless the cosmological equations (5.65)–(5.67) can be equally derived from both the Lagrangians.

Note that x is dimensionless due to the non standard units of ϕ (mass^{-1}). The cosmological equations (5.65)–(5.67) can now be rewritten as

$$x' = \left(x^2 - 1\right)\left(3x - \sqrt{3}\lambda y\right) , \tag{5.71}$$

$$y' = -\frac{1}{2}y\left[\frac{3y^2\left(w - x^2 + 1\right)}{\sqrt{1-x^2}} - 3(w+1) + \sqrt{3}\lambda xy\right] , \tag{5.72}$$

$$\lambda' = \sqrt{3}\left(\Gamma - \frac{3}{2}\right) xy\lambda^2 , \tag{5.73}$$

where we have defined

$$\lambda = -\frac{V_{,\phi}}{\kappa V^{3/2}} \quad \text{and} \quad \Gamma = \frac{VV_{,\phi\phi}}{V_{,\phi}^2} , \tag{5.74}$$

and the Friedmann constraint

$$\frac{y^2}{\sqrt{1-x^2}} = 1 - \Omega_m \leq 1 , \tag{5.75}$$

must be satisfied. Eqs. (5.71)–(5.73) are consistent in the range $x^2 \leq 1$ which follow from the constraint $\dot{\phi}^2 \leq 1$. The limit $x \to \pm 1$ must be handled with care but, as we will see, only the points $(x, y) = (\pm 1, 0)$ will be part of the phase space due to the Friedmann constraint (5.75).

Note the difference in the definition of λ with respect to the canonical case (4.26) where V appeared linearly in the denominator. The function $V(\phi)$ corresponding to a constant λ is the inverse square potential

$$V(\phi) = \frac{M^2}{\phi^2} , \tag{5.76}$$

where M is a constant with units of mass which relates to λ as $M = 2/(\kappa\lambda)$. The simplest case of tachyonic dark energy is thus characterized by the inverse square potential and not by the exponential potential as in canonical quintessence.

Eqs. (5.71)–(5.73) do not represent an autonomous system due to the appearance of Γ which is still a function of ϕ. However, exactly as in the quintessence models (Sec. 4.4), both λ and Γ are functions of ϕ implying that for suitable $\lambda(\phi)$ Γ can be written as a function of λ, namely $\Gamma(\lambda)$. In this case Eqs. (5.71)–(5.73) close to a 3D autonomous dynamical system and a general analysis similar to the one we considered for quintessence in Sec. 4.1 can be performed (Fang & Lu, 2010). We will however focus on the $\Gamma = 3/2$ case corresponding to the potential (5.76) and to a constant λ. References and discussions for other potentials $V(\phi)$ will follow.

For the inverse square potential (5.76) Eqs. (5.71)–(5.72) constitute an autonomous 2D dynamical system which has been studied by Copeland

Point	x	y	Existence	$w_{\rm eff}$	w_ϕ	Ω_ϕ	Stability
O	0	0	$\forall\,\lambda, w$	w	-1	0	Saddle
$A_\pm$	± 1	0	$\forall\,\lambda, w$	0	0	–	Unstable
B	$y_B\,\lambda/\sqrt{3}$	y_B	$\forall\,\lambda, w$	$-1+y_B^2\,\lambda^2/3$	$-1+y_B^2\,\lambda^2/3$	1	Stable

Table 5.2: Critical points of the system (5.71)–(5.72) with existence, physical and stability properties. The coordinate y_B is given in Eq. (5.79).

et al. (2005a) (for a similar dynamical analysis see also Aguirregabiria & Lazkoz (2004)). The variables x and y must satisfy the Friedmann constraint (5.75) which renders the phase space compact. Moreover the system (5.71)–(5.72) is odd-parity invariant, i.e. it is invariant under the mapping $(x, y) \mapsto (-x, -y)$. This implies that only half of the (x, y)-space need to be analysed and we will choose the positive y half plane for convenience. Another symmetry of the dynamical system (5.71)–(5.72) is represented by the mapping $(x, \lambda) \mapsto (-x, -\lambda)$ which is the same appearing in canonical quintessence. It implies that only positive values of λ need to be considered since negative values would lead to the same dynamics after a reflection over the y-axis. From all this information we learn that the phase space for the tachyonic potential (5.76) is compact and constrained in the region $-1 \leq x \leq 1$ and $0 \leq y \leq 1$. Its exact shape depends on the Friedmann constraint and can be seen in Fig. 5.6. Note that only at the points $(\pm 1, 0)$ of the phase space the dynamical system (5.71)–(5.72) is undetermined.

The relative energy density and EoS of the tachyonic scalar field can be written as

$$\Omega_\phi = \frac{y^2}{\sqrt{1-x^2}} \quad \text{and} \quad w_\phi = -1 + x^2\,, \tag{5.77}$$

while the effective EoS of the universe is

$$w_{\rm eff} = w\left(1 - \frac{y^2}{\sqrt{1-x^2}}\right) - y^2\sqrt{1-x^2}\,. \tag{5.78}$$

Note that the tachyonic EoS is constrained in the interval $-1 \leq w_\phi \leq 0$ since $x^2 \leq 1$.

The critical points of the system (5.71)–(5.72) are listed, together with their phenomenological and stability properties, in Table 5.2. There are four critical points:

- *Point O*. The origin of the phase space is again a matter dominated point ($\Omega_m = 1$ and $w_{\rm eff} = w$) where the scalar field energy vanishes ($\Omega_\phi = 0$). It exists for every value of the parameters and always represents a saddle point attracting orbits along the x-axis and repelling

them towards the y-axis. The tachyon EoS at this point takes the value -1 meaning that the negligible scalar field freezes and acts as a cosmological constant.

- *Points* $A_\pm$. The two points $(\pm 1, 0)$ are always present in the phase space and always represent the past attractors being them the only unstable nodes. Interestingly the tachyonic EoS vanishes at these point implying that the scalar field acts as pressure-less matter (dust) in the early universe. Points $A_\pm$ are not formally part of the phase space since the dynamical system (5.71)–(5.72) is singular for $x = \pm 1$. Nevertheless they effectively act as critical points, though carefulness must be taken in dealing with them knowing that standard dynamical systems techniques cannot apply. Their properties can only be derived studying the limit of the flow in their neighborhood. For example the scalar field energy density (5.77) is undetermined and only its limit as solutions approach Point $A_\pm$ can be evaluated[12].

- *Point* B. The last point in the phase space has coordinates $(x, y) = (y_B\,\lambda/\sqrt{3}, y_B)$ where

$$y_B = \left(\frac{\sqrt{\lambda^4 + 36} - \lambda^2}{6} \right)^{1/2} . \tag{5.79}$$

  It is a scalar field dominated point ($\Omega_\phi = 1$) where the tachyonic EoS assumes the value $w_\phi = w_{\rm eff} = -1 + y_B^2\,\lambda^2/3$. It always represent the future attractor of the phase space being the only stable point and appearing for every value of the parameters w and λ. Point B denotes a late time dark energy dominated solution if $\lambda^2 < 2\sqrt{3}$ in which case $w_{\rm eff} < -1/3$ at this point.

We notice that in the standard dynamical systems literature of this tachyonic model another critical point usually is considered (Aguirregabiria & Lazkoz, 2004; Copeland et al., 2005a). This would appear at coordinates $(x, y) = (\sqrt{w+1}, \sqrt{3(w+1)}/\lambda)$ which are indeed inside the allowed phase space. However its existence requires the condition

$$w < -1 + \frac{\lambda}{18}\left(\sqrt{\lambda^4 + 36} - \lambda^2\right) , \tag{5.80}$$

which is never satisfied inside the physically meaningful range $0 \leq w \leq 1/3$ since the right hand side of (5.80) is never positive. It represents a scaling solution with $w_\phi = w$ even if the tachyon model does not seem to fall

[12] Although Points $A_\pm$ formally lie on the $\Omega_\phi = 1$ line, implying scalar field domination, at $x = \pm 1$ the dynamical system is singular and thus only the limit as trajectories approach these point is mathematically correct. In fact, as we will see, different values of Ω_ϕ are obtained approaching Points $A_\pm$ from different directions.

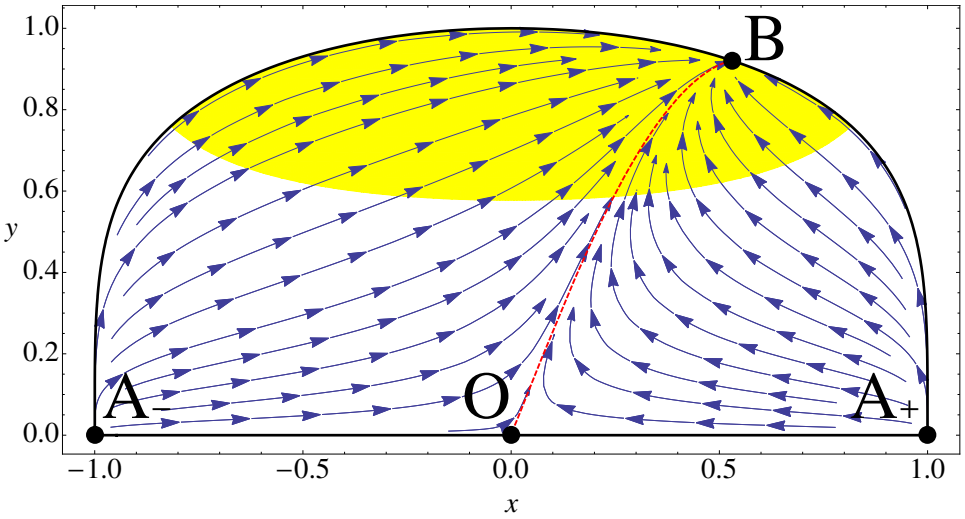

Figure 5.6: Phase space of the dynamical system (5.71)–(5.72) with the values $\lambda = 1$ and $w = 0$. The yellow/shaded region denotes the area of the phase space where the universe undergoes accelerated expansion.

into the general k-essence models (5.60) admitting scaling solutions. With a suitable field redefinition however it is possible to relate the tachyonic Lagrangian (5.64) to the k-essence Lagrangian (5.60) as shown by Copeland et al. (2005a) (see also Gumjudpai et al. (2005)). We did not consider this critical point since our focus is on dark energy models where the matter sector cannot drive the accelerated expansion. The reader interested in the analysis for non physical matter fluid can refer to Aguirregabiria & Lazkoz (2004); Copeland et al. (2005a); Gumjudpai et al. (2005).

We are now ready to look at the phase space. As it is clear from the properties of the critical points, for every admissible values of the parameters λ and w the qualitative behavior of the phase space will be the same. In Fig. 5.6 the phase space for the values $w = 0$ and $\lambda = 1$ has been plotted. The future attractor is Point B which describes a dark energy dominated solution whenever it falls inside the yellow/shaded region ($\lambda^2 < 2\sqrt{3}$), which denotes the area of the phase space where the universe undergoes acceleration. All the orbits are heteroclinic solutions connecting Points $A_\pm$, the past attractors, to Point B, except for the heteroclinic orbit between Point O and Point B (red/dashed line) and the ones between Points $A_\pm$ and Point O. The heteroclinic orbit connecting Point O to Point B divides the phase space into two invariant set with past attractors Point A_+ and Point A_- respectively.

The phase space depicted in Fig. 5.6 can be employed to characterize a late time matter to dark energy transition. Every orbit shadowing the heteroclinic solution connecting Point O to Point B will indeed describe a

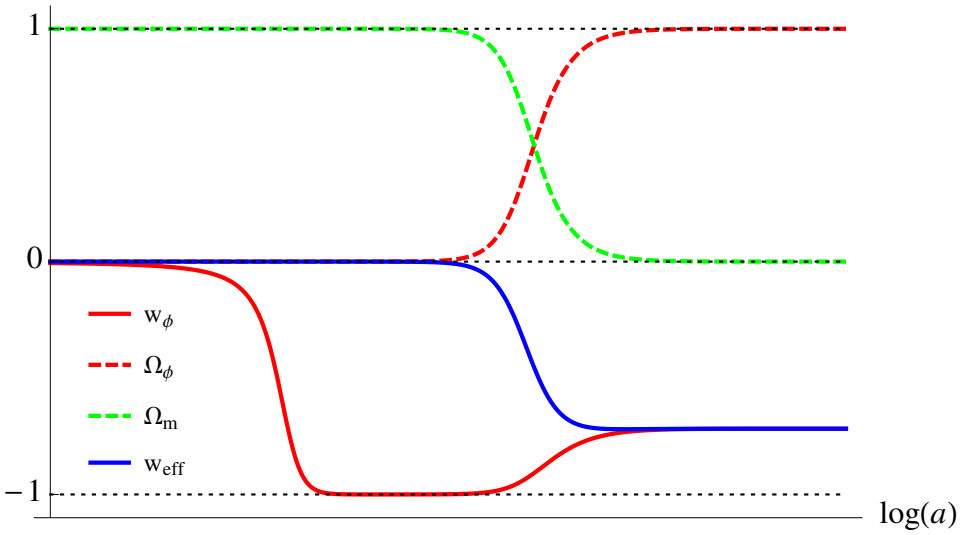

Figure 5.7: Evolution of the phenomenological quantities (5.77) and (5.78) for a solution shadowing the heteroclinic sequence $A_- \to O \to B$ in Fig. (5.6).

matter dominated era followed by never-ending accelerated expansion. The early time behavior is somehow complicated to derive since only the limit to Points $A_\pm$, the past attractors, makes sense mathematically. In any case since at Points $A_\pm$ the tachyonic EoS vanishes, the scalar field will always behave as non-relativistic matter at early times. The effective EoS of the universe will then be constrained in the range $0 \leq w_{\rm eff} \leq 1/3$ as the orbits approach Points $A_\pm$ in the past, with the precise value depending on the matter EoS parameter w and on the relative energy density of the tachyon. On the extremes if $\Omega_\phi = 0$ then $w_{\rm eff} = w$, while if $\Omega_\phi = 1$ then $w_{\rm eff} = 0$. Of course if $w = 0$ then $w_{\rm eff} = 0$ no matter the tachyonic energy Ω_ϕ as the solutions approach Points $A_\pm$.

We provide two examples of how the phenomenological quantities (5.77) and (5.78) evolve for two different trajectories in the phase space of Fig. 5.6. In Fig. 5.7 these quantities have been plotted for a trajectory shadowing the heteroclinic sequence $A_- \to O \to B$, while in Fig. 5.8 they have been plotted for a solution passing along, but not completely shadowing, the heteroclinic orbit connecting Point A_- to Point B. Both of them represent a late time matter to dark energy transition as can be realized from the dynamics of $w_{\rm eff}$ (blue/solid line) which is zero at early times and below $-1/3$ at late times[13]. The dark tachyonic EoS however behaves slightly differently in the two cases. In Fig. 5.7 it starts from zero (Point A_-), decreases to -1 during the matter domination (Point O) and finally reaches the dark energy

[13]Phantom behavior cannot be obtained in this model.

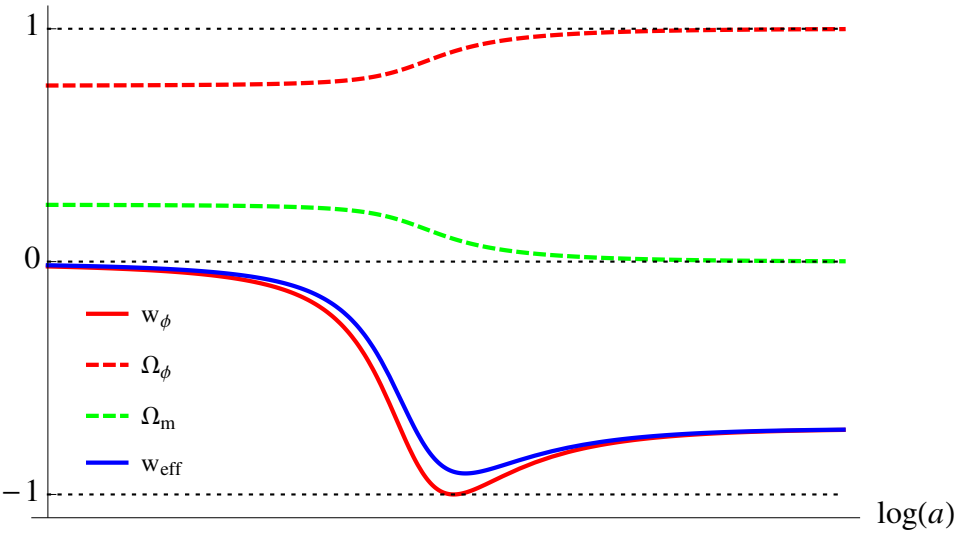

Figure 5.8: Evolution of the phenomenological quantities (5.77) and (5.78) for a solution sufficiently close to, but not completely shadowing, the heteroclinic orbit connecting Point A_- to Point B in Fig. (5.6).

negative value ($w_\phi \simeq -0.72$) at late times (Point B). In Fig. 5.8 w_ϕ starts again from zero (Point A_-) but then reaches almost immediately the dark energy value (Point B) falling for a brief moment towards -1 as the solution follow the boundary of the phase space in its transition from Point A_- to Point B.

The most important differences between Figs. 5.7 and 5.8 arise however in the evolution of the energy densities of matter and dark energy. In Fig. 5.7 the late time behavior, when matter leaves dark energy to dominate, is the expected one. At early times matter always dominates even in the neighborhood of Point A_-, since when $w_\phi \to 0$ one still find $\Omega_m = 1$. This implies that as we approach Point A_- in the past following the y-axis we find $\Omega_\phi \to 0$, as it is also evident first taking the limit $y \to 0$ of Ω_ϕ and then the $x \to \pm 1$ one. A completely different situation emerges from Fig. 5.8 where Ω_ϕ and Ω_m are of the same order of magnitude in the neighborhood of Point A_-. In fact the more an orbit shadows the boundary of the phase space in approaching Point A_-, the more dark energy dominates with $\Omega_\phi = 1$ exactly on the boundary. This is the reason why we chose a trajectory which does not follow exactly the heteroclinic orbit connecting Point A_- to Point B. Such solution would have given complete dark energy domination in the past as it approached Point A_-, while from Fig. 5.8 it is clear that a scaling behavior is possible for orbits emerging from Point A_-.

Although the evolution of the universe is practically the same at early times since $w_{\text{eff}} = 0$ for every orbit approaching Points $A_\pm$, the domination by matter or tachyons will depend on the direction of the trajectory escaping

from Points $A_{\pm}$. Note that in this tachyonic dark energy model matter domination is achieved at early times no matter the initial conditions one chooses, implying that the fine tuning problem of initial conditions does not arise in this framework. Moreover since the tachyonic field behaves as pressure-less matter at early times, and can dominate as in Fig. 5.8, this model can also be used as a dark matter unified theory, where both dark matter and dark energy are described by a single scalar field (Padmanabhan & Choudhury, 2002).

The inverse square potential (5.76) constitutes the simplest tachyonic model to study with dynamical systems techniques, but applications to other potential have also been considered in the literature. Fang & Lu (2010) performed a general analysis of the dynamical system (5.71)–(5.73) for a general function $\Gamma(\lambda)$. The same approach, with a redefinition of the tachyonic field, has been also used by Quiros et al. (2010) who studied the exponential, inverse power-law and $V(\phi) = V_0[\sinh(\lambda\phi)]^{-\alpha}$ potentials as examples. The inverse power-law potential, where Γ as given by (5.74) is constant, together with more general potentials have also been considered by Copeland et al. (2005a), while the exponential potential has been analysed also by Guo et al. (2003b). In all these models future stable accelerated attractors can be easily obtained. Hao & Li (2003b) and Chingangbam & Qureshi (2005) proved that these dark energy late time solutions always arises when the corresponding potentials admits a minimum. Li & Wu (2010) performed the dynamical analysis for tachyons in spatially curved FRW universes focusing in particular on scaling solutions and Fang et al. (2014a) rewrote the dynamical system (5.71)–(5.73) in the variables $(\Omega_\phi, w_\phi, \lambda)$ which can be directly compared with astronomical observations.

Extended tachyonic models have also appeared in the dynamical systems literature. Gumjudpai et al. (2005), Farajollahi & Salehi (2011a) and again Farajollahi et al. (2011) added a coupling between the tachyon field and the matter sector obtaining new scaling solutions. Guo & Zhang (2004) expanded the system to multiple tachyons with inverse square potentials showing that the dynamics is qualitatively similar to the single field scenario. de la Macorra & Filobello (2008) coupled instead the tachyonic field to a canonical scalar field, while Fang et al. (2014a) generalised the tachyonic Lagrangian (5.64) to the Lagrangian $\mathcal{L} = -V(\phi)(1 + \partial\phi^2)^\beta$ studying the dynamics of the cases $\beta = 1, 2$.

For phantom tachyons, where the sign of the kinetic term $\partial\phi^2$ is the opposite of the one appearing in (5.64), the condition for late time phantom stable domination is that $V(\phi)$ have a maximum (Hao & Li, 2003b). Phantom tachyons have also been studied by Fang & Lu (2010); Gumjudpai et al. (2005); Fang et al. (2014a). A quintom tachyonic model, where a standard tachyonic field is coupled to a phantom tachyon, has been proposed by Shi et al. (2009) as an alternative solution for a dynamical crossing of the phantom barrier.

In the final part of this section we will discuss non canonical scalar field models defined by a generalised DBI Lagrangians. These models are usually motivated by D-brane (higher-dimensional theories) phenomenology (see e.g. Silverstein & Tong (2004)) and can be defined by the scalar field *generalised DBI Lagrangian*

Generalised DBI models

$$\mathcal{L}_{\rm DBI} = \frac{1}{f(\phi)}\left(\sqrt{1+f(\phi)\partial\phi^2}-1\right) - V(\phi)\,, \tag{5.81}$$

where $f(\phi)$ and $V(\phi)$ are arbitrary functions of the scalar field ϕ. The cosmological equations deriving from the Lagrangian (5.81) are

$$\frac{3H^2}{\kappa^2} = \rho + \frac{\gamma^2}{\gamma+1}\dot\phi^2 + V(\phi)\,, \tag{5.82}$$

$$\ddot\phi + \frac{3H}{\gamma^2}\dot\phi + \frac{V_{,\phi}}{\gamma^3} + \frac{f_{,\phi}}{2f}\frac{(\gamma+2)(\gamma-1)}{\gamma(\gamma+1)}\dot\phi^2 = 0\,, \tag{5.83}$$

$$\dot\rho + 3H(1+w)\rho = 0\,, \tag{5.84}$$

where we have defined

$$\gamma = \frac{1}{\sqrt{1-f(\phi)\dot\phi^2}}\,. \tag{5.85}$$

Introducing the variables (Copeland et al., 2010)

$$x = \frac{\gamma\kappa\dot\phi}{\sqrt{3(\gamma+1)H}}\,, \qquad y = \frac{\kappa\sqrt{V}}{\sqrt{3}H}\,, \qquad \tilde\gamma = \frac{1}{\gamma}\,, \tag{5.86}$$

which in the limit $\gamma \to 1$ reduce to the canonical EN variables (4.16), Eqs. (5.82)–(5.84) can be conveniently rewritten in a dynamical system formulation as

$$x' = \frac{1}{2}\sqrt{3\tilde\gamma(1+\tilde\gamma)}\lambda y^2 + \frac{3}{2}x\left[(1+\tilde\gamma)(x^2-1) + (1+w)(1-x^2-y^2)\right]\,, \tag{5.87}$$

$$y' = -\frac{1}{2}\sqrt{3\tilde\gamma(1+\tilde\gamma)}\lambda xy + \frac{3}{2}y\left[(1+\tilde\gamma)x^2 + (1+w)(1-x^2-y^2)\right]\,, \tag{5.88}$$

$$\tilde\gamma' = \frac{\tilde\gamma(1-\tilde\gamma^2)}{\sqrt{1+\tilde\gamma}}\left[3\sqrt{1+\tilde\gamma} + \sqrt{3\tilde\gamma}\frac{1}{x}(\mu x^2 - \lambda y^2)\right]\,, \tag{5.89}$$

$$\lambda' = -\sqrt{3\tilde\gamma(1+\tilde\gamma)}\lambda^2(\Gamma-1)x\,, \tag{5.90}$$

$$\mu' = -\sqrt{3\tilde\gamma(1+\tilde\gamma)}\mu^2(\Xi-1)x\,, \tag{5.91}$$

where

$$\lambda = -\frac{V_{,\phi}}{\kappa V}\,, \qquad \mu = -\frac{f_{,\phi}}{\kappa V}\,, \tag{5.92}$$

and

$$\Gamma = \frac{V\,V_{,\phi\phi}}{V_{,\phi}^2}\,, \qquad \Xi = \frac{f\,f_{,\phi\phi}}{f_{,\phi}^2}\,. \tag{5.93}$$

The Friedmann constraint (5.82) imposes the condition

$$x^2 + y^2 = 1 - \Omega_m \leq 1\,, \tag{5.94}$$

which is the same arising in canonical quintessence. The dynamical system (5.87)–(5.91) seems a rather complicated extension of the ones we encountered so far. In what follows we will not perform a detailed dynamical analysis but will only discuss the main features of this model providing references to the dynamical systems literature.

The energy density and EoS of the scalar field are given by

$$\Omega_\phi = x^2 + y^2 \quad \text{and} \quad w_\phi = \frac{\tilde{\gamma}x^2 - y^2}{x^2 + y^2}\,, \tag{5.95}$$

while the effective EoS is

$$w_{\text{eff}} = \tilde{\gamma}x^2 - y^2 + w(1 - x^2 - y^2)\,. \tag{5.96}$$

Note how in this model the phenomenological quantities depend also on the new variable $\tilde{\gamma}$, which is in general constrained as $0 \leq \tilde{\gamma} \leq 1$.

In analogy with other simpler models, if the variables Γ and Ξ can be written as functions of λ and μ respectively, then Eqs. (5.87)–(5.91) would represent a 5D autonomous system. The simplest case is again determined by V and f being exponential functions where λ and μ become constant and the system reduces to three dimensions. If instead f and V are of the power-law type, then the quantity Γ and Ξ are constant and one obtain the simplest 5D system. These cases has been studied in detail by Copeland et al. (2010) where dark energy attractors and scaling solutions where properly analysed. Guo & Ohta (2008) considered the case $f \propto \phi^{-4}$ and $V \propto \phi^2$ which can be naturally justified by D-brane phenomenology. They found scaling solutions for negative (non physical) values of w in analogy to the simpler tachyonic model. A general analysis of future attractor solutions for the generalised DBI model (5.81) and different from of the functions f and V, has been performed by Ahn et al. (2010, 2009) showing that if $V(\phi)$ has a minimum then there is always a dark energy late time solution.

Finally Fang et al. (2006) studied the dynamics of the phantom case of the Lagrangian (5.81) where the sign of $\partial\phi^2$ is inverted. They found stable phantom late time attractors whenever V admits a positive maximum and then considered an example with potential $V(\phi) = V_0(1+\phi/\phi_0)\exp(-\phi/\phi_0)$. Kaeonikhom et al. (2012) instead added a coupling between the generalised DBI field and the matter sector, while Gumjudpai & Ward (2009) extended the Lagrangian (5.81) to $\mathcal{L}_{\text{DBI}} = W(\phi)/f(\phi)\sqrt{1 + f(\phi)\partial\phi^2} - 1/f(\phi) - V(\phi)$.

In conclusion the tachyonic and DBI scalar field models are strongly supported by high energy and multi-dimensional theories, but their dynamics appears to be more complicated than other dark energy models, with few exceptions as the simple tachyonic model analysed in detail in this section.

Nevertheless among all the non canonical scalar field models of dark energy they are the most studied ones since a possible observational evidence for one of them could give useful insight to physics at high energies and to possible extra dimensions.

5.5 Non-scalar models of dark energy

To conclude this chapter in this last section we briefly discuss models of dark energy beyond the scalar field approach, motivated by either particle physics or phenomenological applications. The pure gravitational sector will be given again by general relativity[14], while the matter sources will highly vary from one model to another. No detailed dynamical systems analysis will be provided in this section, but only brief discussions and references to the literature will appear. The literature regarding dark energy models beyond the scalar field paradigm is quite vast, though not extensive as the one dedicated to scalar fields[15]. In this section we will focus on models which have been analysed with dynamical systems techniques providing the due references to relevant works.

As we mentioned in Chapter 3 the particle physics approach to dark energy requires the introduction of new matter degrees of freedom needed to drive the acceleration of the universe. These degrees of freedom are usually associated with new particles yet to be discovered. The simplest case is represented by a scalar particle, i.e. a scalar field, and it is the case we considered so far in both Chapters 4 and 5. Of course the major part of the literature on the subject considers scalar fields because they are both simple to handle and able to give a low-energy effective field description of high-energy theories. Moreover the simplest way to describe unknown degrees of freedom in field theory is usually through scalar fields, unless these degrees of freedom are somehow related, for example through a (gauge) symmetry. It is thus natural to first characterize (dynamical) dark energy as a scalar field, and only if such a description fails the experimental tests more complex fields should be considered.

It might be the case however that different particle physics models of dark energy predict distinctive observational signatures or new phenomenological insights with respect to scalar field cosmology. Studying their theory and dynamics is thus important not only to build alternative routes to solve the dark energy mystery, but also to drive future experiments towards possible

[14]The dynamics of dark energy models with alternative theories of gravity will be the argument of Chapter 6.

[15]Inserting a section on non-scalar models of dark energy inside the non-canonical scalar field chapter seems quite unnatural and actually a separate chapter should be dedicated to the subject. However there are few dynamical systems applications to non-scalar models of dark energy in comparison to the large number of applications to scalar field models. A whole chapter on the subject would result quite miserable with respect to the other ones.

evidences that may differentiate between various dark energy models.

In (quantum) field theory a scalar particle is defined by having *spin-0* and thus by being invariant under *Lorentz transformations*. The first natural extension of a scalar field is represented by particles with non-zero spin[16] such as *spinors* (*spin-1/2*) and *vectors* (*spin-1*). In what follows we will first treat vector and spinor fields and then deal with other models.

Vector fields

Vector fields arise in the standard model of particle physics not only to describe the electro-magnetic interaction, but also as mediators of the nuclear forces. At the human scales the electro-magnetic field is sufficiently strong to compete with gravity, but at cosmological scales it becomes inevitably negligible with respect to the gravitational attraction. There is no way thus to render the electro-magnetic field stronger enough to obtain appreciable cosmological effects needed to drive the late time accelerated expansion.

One is thus led to postulate new vector fields, capable of modifying the large scale dynamics but undetectable at solar system distances. Introducing a new vector field however breaks the isotropy invariance of the space, since a preferred direction, the one the vector is pointing to, is automatically selected. In order to avoid this problem, which would invalidate the cosmological principle (see Chapter 3), some authors have considered a *triad* of vector fields invariant under SO(3) transformations, i.e. three dimensional rotations (Bento et al., 1993; Armendariz-Picon, 2004). A dynamical systems analysis of such model has been done by Wei & Cai (2006) who also added an interaction with the matter sector. They found that alleviations of the fine tuning and cosmic coincidence problems are possible within this framework and also phantom behavior can be attained without incurring into a big rip. Wei & Cai (2007) studied also vector fields interacting with a scalar field which can be motivated by Weyl geometry. A clear review and dynamical systems analysis on various vector field models of dark energy has been delivered by Koivisto & Mota (2008). Among other results, these authors showed that *space-like* vectors admit scaling solutions, while *time-like* vectors easily avoid anisotropies.

Yang-Mills fields

Other vector fields that appear in the standard model of particle physics are non-abelian *Yang-Mills fields* satisfying a more general gauge symmetry than the U(1) symmetry of electro-magnetism. These kind of fields where applied to dark energy modeling and studied with dynamical systems methods by Zhang et al. (2007) who, considering an interaction with both radiation and non-relativistic matter, showed that a solution of the fine tuning problem can be achieved. Zhao (2009) studied a coupling of Yang-Mills fields with the matter sector finding that phantom behavior without big rip

[16]The spin of a particle is a non-negative half-integer number. It is believed that no fundamental particles with spin higher than 2, corresponding to the *graviton*, are present in Nature.

can be obtained.

Spinor fields

Spinor fields are less employed to model dark energy than vector fields. Standard spinors, known as *Dirac spinors* and describing all the standard model fermions, are usually not used to drive the universe into an accelerated phase[17]. They are nevertheless useful to advance new models of dark matter beyond the standard model of particle physics, since are better suited to characterize non-relativistic matter.

There is a class of spinors however which has been largely considered as an alternative model of dark energy: the so-called *ELKO spinors*. They are non standard spinors[18] able to provide interesting phenomenological features in both early and late time cosmology. They can only couple directly with gravity which renders them naturally invisible to radiation and earned them the name *dark spinors*. An extensive review on the theory and cosmological applications of ELKO spinors has been compiled by Boehmer et al. (2010a). Dark energy models of ELKO spinors have been studied with dynamical systems methods by Wei (2011b) and Sadjadi (2012), who found that within this framework a solution of the fine tuning problem of initial conditions is difficult to obtain. Nevertheless Basak et al. (2013) claimed that an alleviation to the problem can be achieved, though Pereira et al. (2014) criticised the result showing that no isolated critical points appear at early times. They also found that phantom behavior is possible in such models.

Besides the dark energy models built from standard model particles, there are other approaches motivated by particle physics theory. In several high energy theories the dynamics of the physical degrees of freedom is represented by *forms*. Without going into the details, forms are geometrical objects which can be seen as generalisation of scalars (0-forms) and vectors (1-forms). In a four dimensional spacetime there can be only forms up to dimension four, but the zero and one dimensional forms correspond nothing but to scalar and vector fields, while 4-forms are never dynamical. In cosmological applications 2-forms are similar to vector fields having their same properties and problems. *Three-forms* instead lead to new phenomenology and interesting dynamics at large scales.

Three-forms

Koivisto & Nunes (2009) employed three-forms to build models of inflation and dark energy, showing that stable accelerator attractors are present in the dynamics. The dynamical systems arising from three-form cosmology present non-hyperbolic critical points and a complete analysis should make use of centre manifold theory to determine the stability, as it has been done by Boehmer et al. (2012a). Ngampitipan & Wongjun (2011) added a coupling between three-forms and dark matter, looking for solutions of the

[17] See however Ribas et al. (2005) for some cosmological accelerating solutions with Dirac fields.

[18] According to Lounesto general classification of all spinor fields, ELKO spinors belong to the class of flag-pole spinors. They have mass dimension one and obey $(CPT)^2 = -\mathbb{1}$.

cosmic coincidence problem.

Other dark energy models motivated by theoretical developments in particle physics consider the so-called *unparticle physics*. *Unparticles* are scale invariant low-energy degrees of freedom coming from effective field theories of high energy physics (see e.g. Georgi (2007)). Their cosmological dynamics has been studied with dynamical systems techniques by Chen & Jing (2009) who found scaling solutions and showed that the fine tuning problem of initial conditions can be avoided. *Unparticles*

There are also models of dark energy which are not motivated by particle physics but directly by phenomenological applications. The most famous of these models is known as *Chaplygin gas*. It is a cosmological fluid with a non standard EoS following the relation *Chaplygin gas*

$$p = -\frac{A}{\rho^{\alpha}}\,, \tag{5.97}$$

where α is a parameter and A is a constant of suitable dimensions. The first Chaplygin gas models considered the case $\alpha = 1$, but later generalisations with $\alpha \neq 1$ have been advanced.

In a cosmological context the Chaplygin gas was proposed by Kamenshchik et al. (2001) as a unified model capable of account for both dark matter and dark energy. Wu & Yu (2007) and Li et al. (2009) studied the dynamics of large scales of Chaplygin gas models interacting with dark matter, obtaining late time scaling, de Sitter and phantom attractor solutions. Then del Campo et al. (2013) coupled the Chaplygin gas to a scalar field and performed a general dynamical systems analysis using the approach we adopted in Sec. 4.4.

To conclude the section we mention some other phenomenological models of dark energy which have recently been analysed with dynamical systems techniques. Acquaviva & Beesham (2014) studied the dynamics of a dark energy model given by a viscous fluid where friction interactions modify the universe evolution. Avelino et al. (2013) (see also Cruz et al. (2014)) instead considered dark matter to be a viscous fluid and added an interaction with scalar field dark energy. In all these models dark energy late time solutions can be obtained.

Chapter 6

Dark energy beyond general relativity: modified gravity models

This chapter will deal with dark energy models motivated by modifications of general relativity. In the previous chapters we have always assumed that the gravitational interaction is well described by general relativity up to cosmological scales and that the accelerated expansion at late times is due to some field sourcing the right hand side of the Einstein field equations. However nothing assures us that general relativity provides an accurate description of Nature at cosmic distances and thus alternative theories of gravity should be equally investigated in the quest for the dark energy issue. In other words, instead of introducing some unphysical matter fluid, one changes the left hand side of the Einstein field equations, i.e. the pure gravitational sector, in order to obtain the needed late time accelerated expansion. These modifications can be equally motivated by phenomenological arguments as well as theoretical implications, such as for example the cosmological applications of quantum gravity theories.

In this chapter we will analyse alternative theories of gravity where phenomenological considerations lead to modifications of the cosmological equations. In Sec. 6.1 we will introduce Brans-Dicke theory and study it in some details with dynamical systems methods. Sec. 6.2 will then be devoted to scalar-tensor theories which generalise Brans-Dicke theory to some extent. In Sec. 6.3 modifications of the Einstein-Hilbert action given either by an arbitrary $f(R)$ function or by higher order curvature invariants will be presented. Finally in Sec. 6.4 the Palatini approach to $f(R)$ gravity and its generalisations are considered, with a particular focus on a model studied by the author in his research work.

The subject of modified theories of gravity is immensely vast, even if restricted to dark energy applications, and more than one book can easily

be filled with the topic. Moreover the cosmological dynamics arising from these models is usually much more complicated than the general relativity one and dynamical systems analyses often result in involved calculations. For these reasons, in this chapter we will avoid to present detailed dynamical systems computations, providing only qualitative calculations for the simplest models and giving references with some discussions for the more complicated ones. The result of this approach is that this chapter represents a small review on alternative dark energy models which is much more useful for a reader with already some knowledge on the subject.

6.1 Brans-Dicke theory

The first modified theory of gravity treated in this chapter introduces a scalar degree of freedom non-minimally coupled to the gravitational sector. The realization of a relativistic theory implementing Mach's principle[1] was the first motivation for the proposal of such a theory by Brans & Dicke (1961) and, among other applications, its cosmological consequences have been studied in depth since it was advanced. The theory is now known as *Brans-Dicke theory* after the authors who fathered it. The action of Brans-Dicke theory is given by

Brans-Dicke theory

$$S_{\rm BD} = \int d^4x\sqrt{-g}\left[\frac{\phi}{2}R - \frac{\omega_{\rm BD}}{2\phi}\partial\phi^2 - V(\phi) + \kappa^2\mathcal{L}_m\right], \qquad (6.1)$$

where $\partial\phi^2 = \partial_\mu\phi\partial^\mu\phi$, $V(\phi)$ is a self-interacting potential for the scalar field and $\mathcal{L}_m$ represents the matter Lagrangian. The constant $\omega_{\rm BD}$ is called the *Brans-Dicke parameter*[2]. Note the coupling between ϕ and the Ricci scalar R, implying that the scalar field is non-minimally coupled to the gravitational field.

The Brans-Dicke action (6.1) describes a modified theory of gravity with the gravitational sector no longer given by the Einstein-Hilbert Lagrangian (4.1). The left hand side of the resulting gravitational field equations will now be different from the Einstein tensor, meaning that the matter fields on the right hand side will source a more complex system of equations. Note that the scalar field ϕ replaces Newton's gravitational constant (or Planck mass) κ^2 in front of R. This implies that now the strength of the gravitational interaction depends on the amplitude of the scalar field,

[1] Mach's principle can be formulated in various ways. One of these is that the inertia of moving bodies should be related to the distribution of masses in the universe. An interesting review on Mach's principle is given in the volume edited by Barbour & Pfister (1995).

[2] Brans-Dicke theory reduces to general relativity in the limit $\omega_{\rm BD} \to \infty$ and from Solar System experiments the strong bound $\omega_{\rm BD} \gtrsim 10^3$ can be obtained (see e.g. Faraoni (2004)).

which in turn depends on the spacetime position. This was the reason why Brans-Dicke theory was first proposed as a Machian theory of gravity.

The cosmological equations following from action (6.1), derived with a spatially flat FRW metric, are (Brans & Dicke, 1961)

$$3\phi H^2 + 3H\dot{\phi} - \frac{\omega_{\rm BD}}{2}\frac{\dot{\phi}^2}{\phi} - V = \kappa^2\rho\,, \tag{6.2}$$

$$-2\phi\dot{H} + H\dot{\phi} - \omega_{\rm BD}\frac{\dot{\phi}^2}{\phi} - \ddot{\phi} = \kappa^2(1+w)\,\rho\,, \tag{6.3}$$

$$\ddot{\phi} + 3H\dot{\phi} - \frac{2}{3+2\omega_{\rm BD}}\,(2V - \phi V_{,\phi}) = \frac{\kappa^2(1-3w)}{3+2\omega_{\rm BD}}\rho\,, \tag{6.4}$$

where $V_{,\phi}$ denotes the derivatives of $V(\phi)$ with respect to ϕ and w stands for the matter EoS parameter $p = w\rho$. A coupling between the Brans-Dicke field ϕ and the matter sector is implicitly present in the theory as one can realize looking at the scalar field equations (6.4). In fact Brans-Dicke theory can be reformulated, employing conformal transformations, in the so-called *Einstein frame* where the pure gravitational sector is recovered to be the standard Einstein-Hilbert Lagrangian and a coupling between the scalar field and the matter fields arises in the matter sector. Note the special character of the coupling in the right hand side of Eq. (6.4) which vanishes for radiation ($w = 1/3$). This means that the Brans-Dicke fields does not couple to relativistic matter.

The cosmology of Brans-Dicke theory in the Einstein frame is nothing but quintessence interacting with matter and some models we mentioned in Sec. 4.5 are indeed motivated by this alternative theory of gravity. In this section however we want to study the modified gravitational dynamics derived directly from action (6.1) which is referred to as the *Jordan frame*. The analysis in the Einstein frame would be equivalent to the one we considered in Sec. 4.5.

In the Einstein frame it is also easy to understand that the value $\omega_{\rm BD} = -3/2$ reduces the theory back to general relativity since the scalar field becomes non dynamical due to the vanishing of its kinetic term. In what follows we will exclude the value $\omega_{\rm BD} = -3/2$ from our analysis which implies the consistency of Eqs. (6.2)–(6.4).

In order to recast Eqs. (6.2)–(6.4) into a dynamical system we define the dimensionless variables (Hrycyna & Szydlowski, 2013a,b)

$$x = \frac{\dot{\phi}}{H\phi}\,, \qquad y = \frac{\sqrt{V}}{\sqrt{3\phi}H}\,, \qquad \lambda = -\phi\frac{V_{,\phi}}{V}\,. \tag{6.5}$$

Note that a part from factors of ϕ these are equivalent, up to some constants, to the standards EN variables (4.16). The variable y is real only for $\phi > 0$ and in what follows we will assume this condition. If ϕ is negative then the

definition of y must be slightly changed. Note however that a negative ϕ would describe a repulsive gravitational force since it equals to flip the sign of Newton's gravitational constant. Since the equivalence principle requires an attractive only gravitational interaction, it is physically more reasonable to assume $\phi > 0$.

Thanks to the variables (6.5), the cosmological equations (6.2)–(6.4) can be rewritten as the following dynamical system

$$\begin{aligned} x' = \frac{1}{2(2\omega_{\rm BD}+3)}\Big[& x^3\omega_{\rm BD}\left(1-(w-1)\omega_{\rm BD}\right) + x^2\left((9w-7)\omega_{\rm BD}-6\right) \\ & - 6x\left(\omega_{\rm BD}\left(w\left(y^2-1\right)+y^2+1\right)+3w-\lambda y^2\right) \\ & + 6\left(y^2(2\lambda+3w+3)-3w+1\right)\Big], \end{aligned} \tag{6.6}$$

$$\begin{aligned} y' = -\frac{y}{2(2\omega_{\rm BD}+3)}\Big[& (w-1)x^2\omega_{\rm BD}^2 + 3\left(\lambda x + x - 2\lambda y^2 - 4\right) \\ & - \omega_{\rm BD}\left(2x(3w-(\lambda+2)) - 6(w+1)\left(y^2-1\right)+x^2\right)\Big], \end{aligned} \tag{6.7}$$

$$\lambda' = \lambda x\left[1-\lambda(\Gamma-1)\right], \tag{6.8}$$

where we have defined again

$$\Gamma = \frac{V\,V_{,\phi\phi}}{V_{,\phi}}\,. \tag{6.9}$$

The Friedmann constraint now reads

$$\Omega_\phi = \frac{x^2\omega_{\rm BD}}{6} - x + y^2 = 1-\Omega_m \leq 1\,, \tag{6.10}$$

where the matter relative energy density is

$$\Omega_m = \frac{\kappa^2\rho}{3\phi H}\,, \tag{6.11}$$

and is positive due to the assumptions $\rho > 0$ and $\phi > 0$. The Friedmann constraint depends on the Brans-Dicke parameter $\omega_{\rm BD}$ meaning that the physically allowed region of the phase space will in turn depend on $\omega_{\rm BD}$, being compact or non-compact according to its value.

The scalar field EoS is given by

$$\begin{aligned} w_\phi = -\frac{1}{6\left(2\omega_{\rm BD}+3\right)}\Big[& x^2\omega_{\rm BD}\left(2\omega_{\rm BD}+3w+2\right) - 2x\left(2\omega_{\rm BD}+9w\right) \\ & + 6\left(y^2\left(-2\omega_{\rm BD}+2\lambda+3w\right)-3w+1\right)\Big], \end{aligned} \tag{6.12}$$

while the effective EoS of the universe is

$$w_{\rm eff} = w\left(1-\frac{1}{6}x^2\omega_{\rm BD}+x-y^2\right) + w_\phi\Omega_\phi\,, \tag{6.13}$$

P	$\{x, y\}$	$w_{\rm eff}$	w_ϕ	Ω_ϕ
$A_\pm$	$\{\frac{3\pm\sqrt{6\omega+9}}{\omega}, 0\}$	$\frac{3\omega+6\pm2\sqrt{6\omega+9}}{-3\omega}$	$\frac{3\omega+6\pm2\sqrt{6\omega+9}}{-3\omega}$	1
B	$\{\frac{-2(\lambda+2)}{\lambda-2\omega-1}, \frac{\sqrt{(2\omega+3)(-\lambda^2-4\lambda+6\omega+5)}}{\sqrt{3}(\lambda-2\omega-1)}\}$	$\frac{2\lambda^2+9\lambda-6\omega+1}{3\lambda-6\omega-3}$	$\frac{2\lambda^2+9\lambda-6\omega+1}{3\lambda-6\omega-3}$	1
C	$\{\frac{1}{\omega+1}, 0\}$	$\frac{5\omega+6}{18(\omega+1)^3}$	$-\frac{1}{3\omega+3}$	$\frac{\lvert5\omega+6\rvert}{6(\omega+1)^2}$
D	$\{\frac{3}{\lambda}, \frac{\sqrt{-\lambda^2+5\lambda\omega+4\lambda-6\omega^2-9\omega-3}}{\lambda\sqrt{2(\lambda-2\omega-1)}}\}$	$-\frac{-7\lambda+6\omega+3}{2\lambda^3}$	$-\frac{1}{\lambda}$	$\frac{\lvert-7\lambda+6\omega+3\rvert}{2\lambda^2}$

Table 6.1: Critical points of the Brans-Dicke model with power-law potential corresponding to the dynamical system (6.6)–(6.7) with $w = 0$. Here $\omega = \omega_{\rm BD}$.

with Ω_ϕ given in Eq. (6.10).

Eqs. (6.6)–(6.8) do not form an autonomous system of equations unless Γ can be written as a function of λ. Again the situation is here similar to the one we encountered in Sec. 4.4 and an analysis for a general $\Gamma(\lambda)$ could be performed. However we will focus on the simplest model where λ becomes a constant and Eqs. (6.6)–(6.7) constitute an autonomous 2D dynamical system. Note that the potential corresponding to a constant λ now is not the exponential potential, but the power-law potential

$$V(\phi) = V_0\, \phi^{-n}\,, \tag{6.14}$$

which implies $\lambda = n$. It is easy to verify that for the potential (6.14) Eq. (6.8) vanishes identically. In what follows we will consider the potential (6.14) and analyse the dynamical system (6.6)–(6.7).

Note that Eqs. (6.6)–(6.7) are even-parity invariant in the y variable, i.e. the mapping $y \to -y$ is a symmetry of the system. We can then only study positive values of y, corresponding to expanding universes, since negative values would lead to the same qualitative dynamics. The Friedmann constraint (6.10) determines the shape of the (physical) phase space in the (x, y)-plane. If $\omega_{\rm BD}$ is negative the phase space is always non-compact, while if $\omega_{\rm BD}$ is positive the phase space is compact. We will only consider the case $\omega_{\rm BD} > 0$ in order to avoid analyses at infinities. Note that in order for the Brans-Dicke field ϕ to be non-phantom the same condition $\omega_{\rm BD} > 0$ must hold. Finally in order to simplify the analysis for the dynamical system (6.6)–(6.7), we will only focus on the case $w = 0$ corresponding to non-relativistic matter and characterizing the late time matter to dark energy transition.

The critical points of the dynamical system (6.6)–(6.7) are listed in Table 6.1 together with their phenomenological quantities. There can be up to five critical points in the phase space with phenomenological and stability properties highly dependent on the parameters $\omega_{\rm BD}$ and λ. The stability

analysis for the critical points of the system (6.6)–(6.7) is extremely complicated to compute analytically. Employing numerical techniques it is however possible to determine which point is the future (global) attractor in the phase space as we will provide in what follows; see Fig. 6.1.

- *Points* $A_{\pm}$. These two points represent scalar field dominated solutions with an EoS depending on the Brans-Dicke parameter $\omega_{\rm BD}$. Points $A_{\pm}$ are non-hyperbolic critical points and their stability is difficult to determine. However using numerical methods we can state that they never constitute stable points, but always acts either as saddle or unstable points and exist for every value of the parameters $\omega_{\rm BD}$ and λ.

- *Point* B. This is another scalar field dominated solution with EoS depending on both $\omega_{\rm BD}$ and λ. It is a hyperbolic critical point which exists only for some values of the parameters, and whenever Point D is not present in the phase space it represents the future attractor; see Fig. 6.1. Unfortunately whenever Point B is the future attractor, its EoS never allows for accelerated expansion meaning that this point cannot be used as a dark energy stable solution.

- *Point* C. This non-hyperbolic critical point exists for all the values of $\omega_{\rm BD}$ and λ. It represents the future attractor of the system in the region of the parameters space indicated by Fig. 6.1. Point C describes a scaling solution with the relative amount of dark energy and matter depending on the parameter $\omega_{\rm BD}$; see Table 6.1. Since we assumed $\omega_{\rm BD} > 0$ its EoS cannot describe acceleration but the higher the value of $\omega_{\rm BD}$, the smaller the value of $w_{\rm eff}$ meaning that for large values of $\omega_{\rm BD}$ Point C can characterize a universe evolving in an effective matter domination. Note that the scalar field EoS at this point is always in the phantom regime.

- *Point* D. The last critical point is hyperbolic and it characterizes a scaling solution with the relative energy density of matter and dark energy depending on both $\omega_{\rm BD}$ and λ. Whenever it appears in the phase space, see Fig. 6.1, Point D always acts as the future global attractor. For positive values of λ the scalar field EoS at Point D lies in the phantom regime. The effective EoS instead depends also on $\omega_{\rm BD}$ and for a narrow area of the parameter space, see Fig. 6.2, we have $w_{\rm eff} < -1/3$ implying that, depending on the parameters $\omega_{\rm BD}$ and λ, Point D can represent a solution to the late time acceleration of the universe. Moreover since Point D is a scaling solution, we can also solve the cosmic coincidence problem with a suitable choice of the theoretical parameters.

The only critical point capable of describing a late time stable accelerated solution is Point D. This happens however only in a really narrow region of

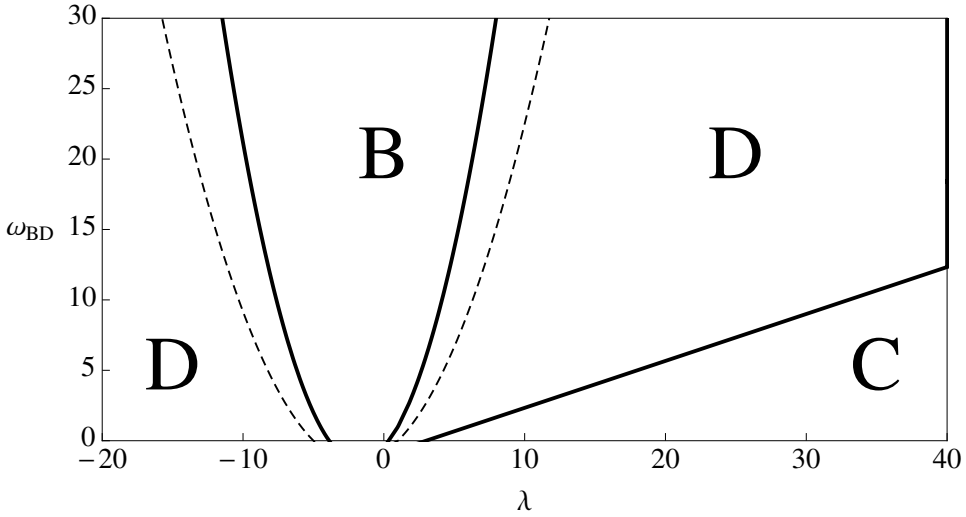

Figure 6.1: Parameter space of the Brans-Dicke model with power-law potential. The different regions denotes the global future attractor of the phase space. Points B and D exist only in the region where they are the attractors, except in the area between the dashed lines and solid lines where both of them exists and Point D is the attractor. Point C exists for every value of the parameters $\omega_{\rm BD}$ and λ.

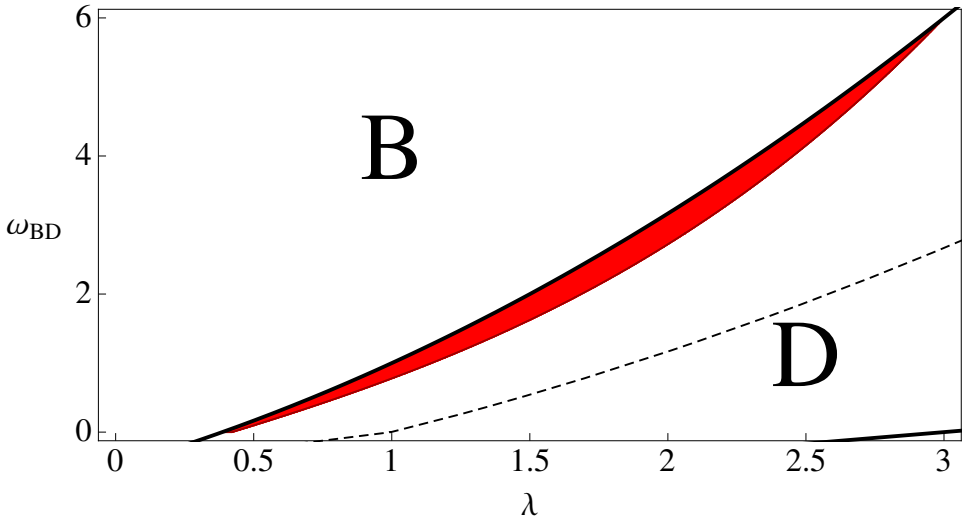

Figure 6.2: Magnification of the parameter space $(\lambda, \omega_{\rm BD})$ of Fig. 6.1 on the narrow region (red/shaded) where Point D represents an accelerated solution ($w_{\rm eff} < -1/3$).

the parameter space $(\lambda, \omega_{\rm BD})$, see Fig. 6.2, and thus highly special values of these parameters must be set to reach such behavior. The phase space for the values $w = 0$, $\omega_{\rm BD} = 0.8$ and $\lambda = 0.94$, which lie inside the acceleration region of Fig. 6.2, has been plotted in Fig. 6.3. The global future attractor is Point D which describes an accelerating solution with $w_{\rm eff} \simeq -0.7$ and consequently appears inside the yellow/shaded region. Point B acts as a phantom dominated saddle point where $w_{\rm eff} = w_\phi \simeq -1.3$. Points $A_\pm$ are the two past attractors while Point C is a saddle point characterizing a scaling solution with $w_{\rm eff} \simeq 0.1$. The values of the parameters λ and $\omega_{\rm BD}$ have been chosen in order to have $\Omega_\phi \simeq 0.69$ and $\Omega_m \simeq 0.31$ at Point D. This situation matches the late time astronomical observations with about 70% of dark energy and 30% of dark matter. Note that Point D is a scaling solution meaning that the cosmic coincidence problem can be completely solved by this model. Moreover, though the effective EoS is above -1, the dark energy EoS at Point D is $w_\phi \simeq -1.06$ implying that at late times the scalar field behaves as a phantom field. This, as pointed out in Sec. 5.1, is the situation slightly favored by observations.

It is also possible to go further. In fact for a solution shadowing the heteroclinic orbit connecting Point C to Point D, dynamical crossing of the phantom barrier can be achieved since at Point C the EoS of the scalar field is $w_\phi \simeq -0.2$. This characterizes a quintom scenario which is even more favored by astronomical observations; see Sec. 5.2. In Fig. 6.4 the late time evolution of the relative energy densities of matter and radiation and the effective and scalar field EoS for an orbit shadowing the heteroclinic sequence $A_+ \to C \to D$, has been plotted. The transition from Point C to Point D is determined by the effective EoS (blue/solid line) lowering from $\simeq 0.1$ to $\simeq -0.7$, while the scalar field EoS (red/solid line) instead crosses the phantom barrier. Apart from the wrong value of matter domination, which concretely prevent the model to be physically viable, Brans-Dicke cosmology with a power-law potential can describe dynamical crossing of the phantom barrier and thus provide the quintom scenario most favored by the observations. Note also the matter (green/dashed line) and the dark energy (red/dashed line) relative energy densities in Fig. 6.4. At early times, while Point C dominates, the first of these energies is above one while the second one is negative. This strange situation is due to the fact that Ω_ϕ is not constrained to be positive, as shown by Eq. (6.10). However the Friedmann constraint $\Omega_\phi + \Omega_m = 1$ must always hold, so if $\Omega_\phi < 0$ then $\Omega_m > 1$. After the transition from (almost) matter to dark energy domination the relative energy densities stabilize on the values $\Omega_m \simeq 0.3$ and $\Omega_\phi \simeq 0.7$. This is the exact energy content observed nowadays in the universe, as discussed in Chapter 3. Moreover since Point D is the future attractor of the phase space, once these energy contributions are attained they never change, solving in this manner the cosmic coincidence problem.

In conclusion a dark energy model based on Brans-Dicke theory with

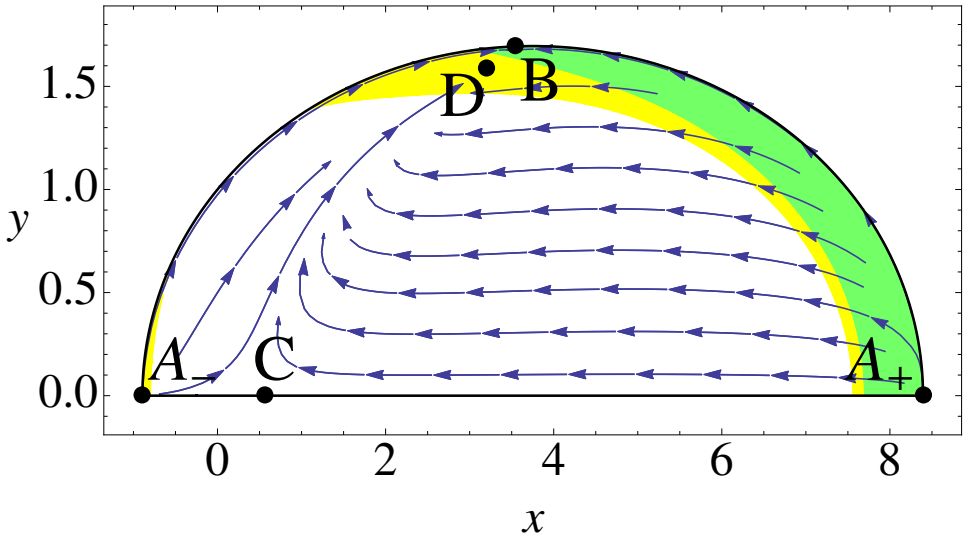

Figure 6.3: Phase space for Brans-Dicke cosmology with a power-law potential and values $w = 0$, $\lambda = 0.94$ and $\omega_{\rm BD} = 0.8$. Point D is the future attractor representing a dark energy scaling solution with $w_{\rm eff} < -1/3$ (yellow region), while Point B is a saddle point characterizing a phantom dominated solution with $w_{\rm eff} < -1$ (green region).

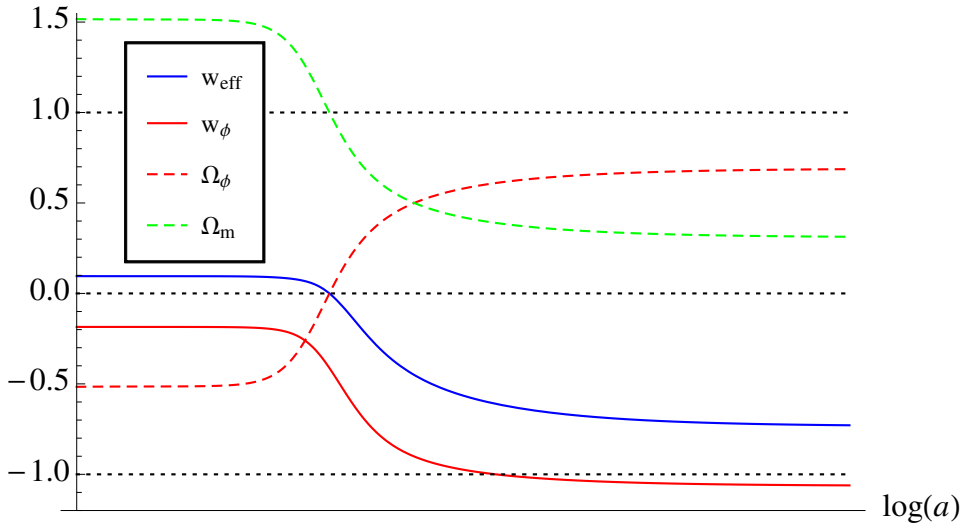

Figure 6.4: Late time evolution of the phenomenological parameters for a solution shadowing the heteroclinic orbit connecting Point C to Point D in Fig. 6.3.

a power-law potential can in principle both solve the cosmic coincidence problem and provide the quintom scenario favored by astronomical observations. Unfortunately the fine tuning problem cannot be addressed by this model and, besides particular initial conditions, also special values of the parameters $\omega_{\rm BD}$ and λ must be set in order to achieve late time dark energy domination. Furthermore the early time evolution of the universe is not described by a matter dominated solution. Only Point C can act as a matter evolving scaling solution, but for the values of Ω_ϕ and Ω_m observed at late times the effective EoS parameter $w_{\rm eff}$ at Point C is not enough small to characterize exact matter domination; see Fig. 6.4.

The analysis we have presented in this section is valid only for a power-law potential with pressure-less matter, $w = 0$. A complete study for different potentials or a general matter sector would be highly complicated and it is beyond our scopes, which only aim at providing simple working examples in as much detail as possible. A deep dynamical systems analysis for Brans-Dicke cosmology with a quadratic potential, given by (6.14) with $n = -2$, has been delivered by Hrycyna & Szydlowski (2013b). They showed that de Sitter solutions can be obtained in this special case, extended the work to non-compact phase spaces ($\omega_{\rm BD} < 0$) also performing the analysis at infinity, and considered general values of the matter EoS parameter w outside the physically allowed range $[0, 1/3]$. The same authors studied de Sitter solutions for Brans-Dicke cosmology with a general potential, performing the stability analysis (Hrycyna & Szydlowski, 2013a) and comparing the results with observational data (Hrycyna et al., 2014).

Other authors instead focused their work on the pure Brans-Dicke theory (Brans & Dicke, 1961) where no self-interacting potential for the scalar field appears. Kolitch (1996) considered this theory with a cosmological constant and found that the late time attractor is always a de Sitter solution if $\omega_{\rm BD} > 0$. Farajollahi & Salehi (2011b) and Liu et al. (2012) added a direct[3] interaction between the scalar field and the matter sector depending on H and proved the existence of late time accelerated solutions.

6.2 Scalar-Tensor theories

Scalar-tensor theories

A straightforward generalisation of Brans-Dicke theory is given by a class of gravitational theories known as *scalar-tensor theories*. The general action for these models is given by

$$S_{\rm ST} = \int d^4x\sqrt{-g}\left[\frac{F(\phi)}{2}R - \frac{\omega(\phi)}{2}\partial\phi^2 - V(\phi) + \kappa^2\mathcal{L}_m\right], \qquad (6.15)$$

where now F, ω and V are all arbitrary functions of ϕ. In this section we will briefly present the simplest way of rewriting the cosmological equations of

[3] Directly in the Jordan frame.

scalar-tensor cosmology as a dynamical system. We will not perform detailed computations, but only discuss the main features and provide references to dynamical systems literature. The reader interested in reviews on scalar-tensor theories, including their applications to cosmology, can refer to the books by Fujii & Maeda (2003) and Faraoni (2004).

Note that inside the scalar-tensor action (6.15) the function $\omega(\phi)$ can be reduced to a constant with a suitable redefinition of the scalar field ϕ. In this way the scalar field kinetic term can be recast into its canonical form. In what follows however we will keep ω as a general function of ϕ in order to directly include all possible scalar-tensor models.

The cosmological equations derived from action (6.15) with a spatially flat FRW metric are

$$3H^2F + 3H\dot{\phi}F_{,\phi} - \frac{1}{2}\omega\dot{\phi}^2 - V = \kappa^2\rho\,, \tag{6.16}$$

$$2F\dot{H} + \dot{\phi}^2F_{,\phi\phi} + (\ddot{\phi} - H\dot{\phi})F_{,\phi} + \omega\dot{\phi}^2 = -\kappa^2\rho(1+w)\,, \tag{6.17}$$

$$\ddot{\phi} + 3H\dot{\phi} + \frac{1}{\omega}\left[V_{,\phi} + \frac{\dot{\phi}^2}{2}\omega_{,\phi} - 3F_{,\phi}\left(2H^2 + \dot{H}\right)\right] = 0\,. \tag{6.18}$$

Note that if one replaces H^2 and $\dot{H}$ in Eq. (6.18) using Eqs. (6.16) and (6.17), then an explicit coupling between the scalar field and the matter sector appears. This situation is equivalent to Brans-Dicke theory (Sec. 6.1). In fact also the scalar-tensor action (6.15) can be rewritten in the Einstein frame using conformal transformations.

In order to rewrite the cosmological equations (6.16)–(6.18) as a dynamical system, we introduce the following dimensionless variables

$$x = \frac{\dot{\phi}}{H}\sqrt{\frac{\omega}{F}} \quad \text{and} \quad y = \frac{1}{H}\sqrt{\frac{V}{3F}}\,, \tag{6.19}$$

plus

$$\lambda_F = -\frac{F_{,\phi}}{F}\sqrt{\frac{F}{\omega}}\,, \qquad \lambda_V = -\frac{V_{,\phi}}{V}\sqrt{\frac{F}{\omega}}\,, \qquad \lambda_\omega = -\frac{\omega_{,\phi}}{\omega}\sqrt{\frac{F}{\omega}}\,, \tag{6.20}$$

$$\Gamma_F = \frac{F\,F_{,\phi\phi}}{F_{,\phi}^2}\,, \qquad \Gamma_V = \frac{V\,V_{,\phi\phi}}{V_{,\phi}^2}\,, \qquad \Gamma_\omega = \frac{\omega\,\omega_{,\phi\phi}}{\omega_{,\phi}^2}\,. \tag{6.21}$$

Note that these variables are well defined only if $F > 0$, $\omega > 0$ and $V > 0$. In what follows we will assume these conditions. As pointed out in Sec. 6.1, $F > 0$ is needed for an ever attractive gravitational force, $\omega > 0$ selects a non-phantom field and $V > 0$ implies a positive potential energy. From a physical perspective thus the requirements $F > 0$, $\omega > 0$ and $V > 0$ appear naturally. If one of these conditions does not hold, then the variables (6.19)–(6.21) should be defined differently.

The variables (6.19)–(6.21) have never been considered in the literature and appear for the first time in this thesis. They are however a straightforward generalisation of the variables used in Sec. 6.1. In fact if we take $F = \phi$ and $\omega = \omega_{\rm BD}/\phi$, corresponding to Brans-Dicke theory, the variables (6.19)–(6.21) reduce, up to a constant factor, to the variables (6.5). Note that in this case the variables λ_F, λ_ω, Γ_F and Γ_ω would be all constant.

The cosmological equations (6.16)–(6.18) can now be rewritten as

$$\begin{aligned} x' = \frac{1}{6\lambda_F^2+4}\Big[&+ x\lambda_F^2\left(2x^2\Gamma_F - 3\left(6w + x\lambda_\omega\right)\right) + 3\left(2\Gamma_F+1\right)\lambda_F^3 \\ &- \lambda_F\left(6xy^2\lambda_V + 9w(x^2+2y^2-2) + x^3\lambda_\omega - 7x^2 + 18y^2 + 6\right) \\ &+ x\left(-w\left(x^2+6y^2-6\right) + x^2 - 6y^2 - 6\right) + 12y^2\lambda_V\Big], \end{aligned} \tag{6.22}$$

$$\begin{aligned} y' = \frac{y}{6\lambda_F^2+4}\Big[&- \lambda_F\left(6y^2\lambda_V + x\left(6w + x\lambda_\omega - 4\right)\right) + 3x\lambda_F^3 - 2x\lambda_V \\ &+ \lambda_F^2\left(2x^2\Gamma_F - 3x\lambda_V + 12\right) - w(x^2+6y^2-6) + x^2 - 6y^2 + 6\Big], \end{aligned} \tag{6.23}$$

$$\lambda_F' = \frac{1}{2}x\lambda_F\left[\left(1-2\Gamma_F\right)\lambda_F + \lambda_\omega\right], \tag{6.24}$$

$$\lambda_V' = -\frac{1}{2}x\lambda_V\left[\lambda_F - \lambda_\omega + 2\left(\Gamma_V - 1\right)\lambda_V\right], \tag{6.25}$$

$$\lambda_\omega' = -\frac{1}{2}x\lambda_\omega\left[\left(2\Gamma_\omega - 3\right)\lambda_\omega + \lambda_F\right]. \tag{6.26}$$

with the Friedmann constraint

$$\Omega_\phi = x\lambda_F + \frac{x^2}{6} + y^2 = 1 - \Omega_m \leq 1\,, \tag{6.27}$$

where

$$\Omega_m = \frac{\kappa^2\rho}{3FH^2} \geq 0\,. \tag{6.28}$$

Eqs. (6.22)–(6.26) do not represent an autonomous system of equations unless the variables Γ_F, Γ_V and Γ_ω can be written as functions of λ_F, λ_V and λ_ω. If this is the case then Eqs. (6.22)–(6.26) will constitute an autonomous 5D dynamical system. Note that Brans-Dicke theory with a power-law potential is not the only way to reduce Eqs. (6.22)–(6.26) to a 2D dynamical system, but also with other theories this situation can be obtained. For example if $F \propto \omega$ and F, V and ω are all of the exponential type, then λ_F, λ_V and λ_ω would be all constant.

Eqs. (6.22)–(6.26) can be the starting point for a general dynamical systems study of scalar-tensor cosmology. One can either assume Γ_F, Γ_V and Γ_ω to be arbitrary functions of λ_F, λ_V and λ_ω and then carry on a similar analysis of the one we performed in Sec. 4.4, or one can postulate specific forms for the functions F, V and ω which reduce the dimensionality of the

system and then conduct a full dynamical analysis looking for interesting phenomenological applications. In this section however we will not work in these directions, but we will only provide references and discussions to the existing dynamical systems literature. These lines of research will be left for future considerations.

Dynamical systems studies of scalar-tensor cosmology have been considered by few authors in the literature and always restricted to specific models. Uzan (1999) examined scaling solutions and their stability in the model $\omega = 1/2$ with both exponential and power-law potentials. Gunzig et al. (2000) showed that chaotic behavior never arises for the non-minimal coupling $F(\phi) = 1 - \xi\phi^2$, with ξ a constant, and subsequently Faraoni et al. (2006) extended the same results to more general scalar-tensor models. The model $F = 1 - \xi\phi^2$ has also been studied by Szydlowski & Hrycyna (2009), who found new accelerated solutions for a general self-interacting scalar field potential and then presented some specific examples, and again by the same authors (Hrycyna & Szydlowski, 2010), who assumed $\omega = 1/2$ and delivered an analysis for general potentials similar to the one we carried on on Sec.4.4. They found critical points corresponding to radiation, dark matter and dark energy dominated solutions discussing the viability of this scalar-tensor theory as a dark energy model. Recently Szydlowski et al. (2014) reconsidered the same model with a general potential and performed the analysis at infinity with a geometrical interpretation of the phase space of scalar-tensor theories. The theory $F = \xi\phi^2$, $\omega = 1/2$ and $V = V_0\phi^n$ has been studied, in full detail with dynamical systems methods and including the behavior at infinity, by Carloni et al. (2008). de Souza & Saa (2005) considered instead the linear coupling $F = \phi$ plus a linear or a quadratic self interacting potential, while Jarv et al. (2010) assumed the same linear coupling but delivered a general work on potential dominated cosmological solutions. The model $F = \xi\phi^2$ and $\omega = 1/2$, which is equivalent to Brans-Dicke theory after a redefinition of the scalar field, has been studied by Maeda & Fujii (2009), who focused their discussion on future cosmological attractors, and by Cervantes-Cota et al. (2010), who analysed specific dark energy applications including interactions with the matter sector. Finally Skugoreva et al. (2014) looked at the model with power-law functions for both F and V, while Agarwal & Bean (2008) performed a general analysis of scalar-tensor cosmological dynamics in both the Jordan and Einstein frame, finding transient and stable accelerated solutions.

In conclusion the cosmological dynamics of scalar-tensor theories has never been analysed in full detail with dynamical systems techniques. As shown by the mentioned literature, only specific models have been considered so far. Starting from Eqs. (6.22)–(6.27) however a wide and general analysis of scalar-tensor cosmology can be performed. This task is beyond the scopes of this thesis and will be left for future works.

6.3 $f(R)$ gravity and higher-order theories

In this section we will consider modifications to general relativity given by general functions of the Ricci scalar which introduce higher order derivatives of the metric tensor. The general action of these theories is given by

$$S_{f(R)} = \int d^4x\sqrt{-g}\left[f(R) + 2\kappa^2\mathcal{L}_m\right] , \tag{6.29}$$

$f(R)$ gravity

where $f(R)$ is an arbitrary function of the Ricci scalar R. These theories are called $f(R)$ *theories of gravity* for obvious reasons. In what follows we will discuss the general dynamics arising from such theories without going into detailed examples. We will mainly follow the paper by Amendola et al. (2007a) who provided a dynamical study for general $f(R)$ theories, and refer to their work for more details. The reader broadly interested in the theory and applications of $f(R)$ gravity can find useful the well known reviews by Sotiriou & Faraoni (2010) and De Felice & Tsujikawa (2010).

The cosmological equations of $f(R)$ gravity, obtained varying action (6.29) with respect to the metric tensor and then assuming this to be of the FRW type, are

$$3FH^2 - \frac{1}{2}\left(RF - f\right) + 3H\dot{F} = \kappa^2\rho\,, \tag{6.30}$$

$$-2F\dot{H} - \ddot{F} + H\dot{F} = \kappa^2\rho(1+w)\,, \tag{6.31}$$

where over-dots denotes differentiation with respect to the coordinate time t and we have defined

$$F = f_{,R} = \frac{\partial f}{\partial R}\,. \tag{6.32}$$

Note that Eqs. (6.30)–(6.31) correctly reduce to the standard Friedmann and acceleration equations (3.6)–(3.8) when the general relativity limit $f(R) = R$ is applied.

The energy density and pressure of dark energy are now difficult to define properly since they are both produced by and sources of the gravitational field. However rewriting Eqs. (6.30)–(6.31) in order to have the standard gravitational terms in the left hand side, we can read off these components as

$$\rho_{\rm DE} = \frac{R}{2} - \frac{f}{R} - 3H\frac{\dot{F}}{F}\,, \tag{6.33}$$

$$p_{\rm DE} = \frac{\ddot{F}}{F} - 2H\frac{\dot{F}}{F} - \frac{R}{2} + \frac{f}{F}\,, \tag{6.34}$$

from which the dark energy EoS can easily be obtained as

$$w_{\rm DE} = \frac{\rho_{\rm DE}}{p_{\rm DE}}\,. \tag{6.35}$$

Dark energy is now given by the effects of spacetime curvature rather than an external matter source as we were used in the models we encountered so far. The effective EoS can now be generally defined as

$$w_{\rm eff} = \Omega_{\rm DE} w_{\rm DE} + \Omega_m w = -1 - \frac{2\dot{H}}{3H^2}\,. \tag{6.36}$$

In order to recast Eqs. (6.30)–(6.31) into a dynamical system, we define the following dimensionless variables (Amendola et al., 2007a)

$$x_1 = -\frac{\dot{F}}{HF}\,, \qquad x_2 = -\frac{f}{6FH^2}\,, \qquad x_3 = \frac{R}{6H^2} = \frac{\dot{H}}{H^2} + 2\,. \tag{6.37}$$

The Friedmann equation (6.30) now yields the constraint[4]

$$\Omega_{\rm DE} = x_1 + x_2 + x_3 = 1 - \Omega_m \tag{6.38}$$

where

$$\Omega_m = \frac{\kappa^2 \rho}{3FH^2}\,. \tag{6.39}$$

The cosmological equations can now be rewritten as

$$x_1' = -1 - x_3 - 3x_2 + x_1^2 - x_1 x_3\,, \tag{6.40}$$

$$x_2' = \frac{x_1 x_3}{m} - x_2\,(2x_3 - x_1 - 4)\,, \tag{6.41}$$

$$x_3' = -\frac{x_1 x_3}{m} - 2x_3\,(x_3 - 2)\,, \tag{6.42}$$

where we have defined

$$m = \frac{\partial \log F}{\partial \log R} = \frac{R\, f_{,RR}}{f_{,R}}\,. \tag{6.43}$$

Eqs. (6.40)–(6.42) do not represent an autonomous system of equations due to the presence of m, which still depends on derivatives of $f(R)$. However if we define

$$r = -\frac{\partial \log f}{\partial \log R} = -\frac{R\, f_{,R}}{f} = \frac{x_3}{x_2}\,, \tag{6.44}$$

and then, once the function $f(R)$ is known, solve for R, we can write m, which in general is a function of R, as a function of $r = x_3/x_2$ and thus close Eqs. (6.40)–(6.42) to an autonomous 3D dynamical system. This procedure is somehow similar to the one we presented in Sec. 4.4 for quintessence and it allows to study the dynamics of $f(R)$ gravity from a general perspective without specifying the form of the function $f(R)$. In what follows we will consider a general $m(r)$ and derive as much information as possible from the dynamical system (6.40)–(6.42). The simplest case, corresponding to a

[4]Note that x_1, x_2 and x_3 can also be negative, though their sum cannot exceed one.

P	$\{x_1, x_2, x_3\}$	$w_{\rm eff}$	$w_{\rm DE}$	$\Omega_{\rm DE}$
P_1	$\{0, -1, 2\}$	-1	-1	1
P_2	$\{-1, 0, 0\}$	$1/3$	$2w - \frac{1}{3}$	-1
P_3	$\{1, 0, 0\}$	$1/3$	$1/3$	1
P_4	$\{-4, 5, 0\}$	$1/3$	$1/3$	1
P_5	$\{\frac{3m}{1+m}, -\frac{1+4m}{2(1+m)^2}, \frac{1+4m}{2(1+m)}\}$	$-\frac{m}{1+m}$	$\frac{m^2(8w-2)+m(3w-2)-2w}{m(10m+7)}$	$\frac{m(7+10m)}{2(1+m)^2}$
P_6	$\{\frac{2(1-m)}{1+2m}, \frac{1-4m}{m(1+2m}, \frac{(1-4m)(1+m)}{-m(1+2m)}\}$	$\frac{2-5m-6m^2}{3m(1+2m)}$	$\frac{2-5m-6m^2}{3m(1+2m)}$	1

Table 6.2: Critical points of $f(R)$ gravity corresponding to the dynamical system (6.40)–(6.42).

constant m, is given by a simple power-law $f(R) \propto R^n$. For this choice the relation $x_3 = -nx_2$ holds and the dynamical system (6.40)–(6.42) becomes two dimensional. Unfortunately this case does not produce viable dark energy scenarios since fails to provide a sufficiently long matter dominated era (Clifton & Barrow, 2005; Amendola et al., 2007a,b).

The critical points of the system (6.40)–(6.42) with $m(r)$ has been listed, together with their phenomenological properties, in Table 6.2. In terms of the variables (6.37) the dark energy and effective EoSs are given by

$$w_{\rm DE} = \frac{1 - 2x_3 - 3w(1 - x_1 - x_2 - x_3)}{3(1 - x_1 - x_2 - x_3)}\,, \tag{6.45}$$

$$w_{\rm eff} = \frac{1}{3}\,(1 - 2x_3)\ . \tag{6.46}$$

Points P_5 and P_6 satisfy the equation

$$m(r) = -r - 1\,, \tag{6.47}$$

i.e. they are present only if such equation has at least one root. In general for each root r_i of Eq. (6.47) we obtain a pair of Points P_5 and P_6 with $m = m(r_i)$. The properties and number of these points depends on the particular $f(R)$ function one chooses to work with. On the other hand Points P_1, P_2, P_3 and P_4 appear in every $f(R)$ model with the same phenomenological properties[5].

From Table 6.2 it is clear that a de Sitter solution, Point P_1, is always present in $f(R)$ gravity and that accelerated solutions can be obtained from Points P_5 and P_6 depending on the value of m. Unfortunately the only

[5]Exceptions must be considered in the degenerate case $f(R) \propto R^n$ which reduces the system to 2D.

points capable of describing a matter era are Points P_5 and P_6 and only for special values of m. For example if $m \to 0$ at Point P_5 then we obtain a matter dominated solution. The ability of $f(R)$ gravity to provide a viable cosmological evolution will then strongly depend on the specific theoretical model one uses.

We will now briefly outline the phenomenological and stability properties of each point in Table 6.2. We will not perform a deep dynamical systems analysis for the stability and the phase space. The reader interested in more details can refer to Amendola et al. (2007a). In what follows we will denote $m_i = m(r_i)$ with r_i given by the coordinates of Point P_i.

- *Point* P_1. This is a dark energy dominated de Sitter solution capable of characterizing a late time accelerated expansion. It is a stable point if $0 \leq m_1 \leq 1$, where $r_1 = -2$, and a saddle point otherwise.

- *Point* P_2. In this point matter and dark energy coexist with constant energy densities, with the dark energy one being negative, and the universe evolves in an effective radiation solution. Point P_2 is either a saddle or stable point depending on the function $m(r)$ in a rather complicated way. Its stability can thus only be determined after a specific $f(R)$ model has been chosen.

- *Point* P_3. Similar to Point P_2 this critical point describes an effective radiation solution, but now dark energy completely dominates and the matter contribution can be neglected. Again the stability of Point P_3 strongly depends on the function $m(r)$, but in general we can state that it never represents a stable solution.

- *Point* P_4. Phenomenologically Point P_4 is similar to Point P_3 since again $w_{\rm eff} = 1/3$ and $\Omega_{\rm DE} = 1$. It is a stable point if $-1 < m_4 < 0$ and a saddle point otherwise.

- *Point* P_5. This point corresponds to a scaling solution with constant ratio $\Omega_{\rm DE}/\Omega_m$. If $m_5 \simeq 0$ then Point P_5 can describe a matter dominated era. The stability of this point depends on the particular function $m(r)$ at hand, however for $m_5 \simeq 0$ it represents a saddle point if $m_5 > 0$ and $m_5' > -1$.

- *Point* P_6. This last point is a curvature dominated solution capable of describing an accelerated expansion if $m_6 < -(1+\sqrt{3})/2$, $-1/2 < m_6 < 0$ or $m_6 > (\sqrt{3}-1)/2$. Its stability depends strongly on $m(r)$ but in general it can act as a stable point. The effective EoS at Point P_6 can also lie in the phantom regime depending on the value of m_6.

As we mentioned above only Points P_5 can describe a matter dominated solution and only if the special condition $m_5 \simeq 0$ is attained. A dark energy

$f(R)$	$m(r)$
αR^{-n}	$-1-n$
$R+\alpha R^{-n}$	$-n(1+r)/r$
$R^p(\log \alpha R)^q$	$[p^2+2pr-r(q-r+qr)]/(qr)$
$R^p \exp qR$	$-r+q/r$
$R^p \exp q/R$	$-[p+r(2+r)]/r$

Table 6.3: Form of the function $m(r)$ as given by Eq. (6.43) for different $f(R)$ models (Amendola et al., 2007a).

solution, where the universe accelerates, can instead be represented by both Points P_1 and P_6. A viable dark energy scenario can thus arise in $f(R)$ gravity only if Point P_5 is a saddle point with $m_5 \simeq 0$ and the late time attractor is given by either Point P_1 or Point P_6. This reasoning can be used to classify the various $f(R)$ theories as models of dark energy, as proposed by Amendola et al. (2007a), and then to select the ones whose dynamics should be compared against astronomical observations.

In Table 6.3 the form of the function $m(r)$ for different $f(R)$ models is presented. The function $m(r)$ can be easily obtained even for relatively complex models, and a deep dynamical systems analysis can be performed for each of these models. However the majority of authors who studied the dynamics of $f(R)$ cosmology employed different variables depending on the model under consideration.

The power-law models $f(R) \propto R^n$ are the one appearing more frequently in the literature, probably due to its simplicity. Carloni et al. (2005) studied the accelerator cosmological attractors of such models and looked for quasi-matter ($w_{\rm eff} \simeq 0$) solutions. However, as shown by Amendola et al. (2007a,b), the simple power-law model of $f(R)$ is non viable, unless the exponent is effectively one, which is the case considered by Clifton & Barrow (2005) who determined the viability conditions requiring a sufficiently long period of matter domination and then confronted the results with observational data. The power-law model $f(R) \propto R^n$ has also been examined by Goheer et al. (2008, 2009) who considered variables suited to compactify the phase space.

Other $f(R)$ theories which have been analysed with dynamical systems techniques include the function $f(R) = R + \alpha R^{-n}$, which was the case studied by Li & Barrow (2007) in full detail, including the computation of the behavior at infinity. Miritzis (2003a) considered the subclass given by $f(R) = R + \alpha R^2$ (*Starobinky model*) and performed the stability analysis

for accelerating solutions also in the presence of positive spatial curvature ($k = 1$). Sawicki & Hu (2007) showed that viable $f(R)$ cosmological models should satisfy $f_{,RR} > 0$ and then made an example with the theory $f(R) = R + \alpha/R$. Models with (inverse) power-law corrections to the Einstein-Hilbert Lagrangian were also considered by Clifton (2008) who delivered an asymptotic analysis at both early and late times.

An exponential potential model with $f(R) = \exp(-R/\Lambda)$ has instead been the subject of a work by Abdelwahab et al. (2008), who found de Sitter solutions acting as both past and future attractors and thus capable of unifying inflation with dark energy. More complicated models, including $f(R) = R \ln R$, have been studied by Guo & Frolov (2013), who provided a full dynamical systems analysis with the behavior at infinity and found late time de Sitter solutions. A DBI $f(R)$ gravity theory with $f(R) = \sqrt{1 - \alpha R}$ has been advanced by Garcia-Salcedo et al. (2010) who showed that a rich phenomenological dynamics arises at cosmological scales.

Although the majority of the works mentioned so far consider a specific function $f(R)$, some authors have examined specific features of the dynamics of general $f(R)$ theories. Amendola & Tsujikawa (2008) focused their study on phantom late time attractors and crossing of the phantom barrier for viable $f(R)$ models. A geometrical analysis for the phase space of $f(R)$ theories has been delivered by de Souza & Faraoni (2007), while Carloni et al. (2009) employed dynamical systems techniques to spatially curved $f(R)$ cosmologies, presenting also various examples. Spatially curved spacetimes have also been the subject of the work by Goheer et al. (2008, 2009).

Some authors considered also anisotropic spacetimes in the framework of $f(R)$ gravity. The model $f(R) \propto R^n$ has been studied by Leach et al. (2006) and Goheer et al. (2007, 2008, 2009), while Leon & Saridakis (2011) and again Leon & Roque (2014) analysed also general $f(R)$ anisotropic cosmologies, finding late time accelerated and bouncing solutions.

In the final part of this section we discuss other gravitational theories where higher order corrections in the metric derivatives appear in the action. These theories are generally known as *higher order theories* and differ from $f(R)$ gravity since other higher order curvature invariants are present in the gravitational action. Again we will not explain in detail the theoretical features of such theories, but will only present the main characteristics and give references to the dynamical systems literature.

Higher-order theories

The higher curvature invariants employed in these models are usually built by contractions of the Riemann tensor $R_{\mu\nu\alpha}{}^{\beta}$ with the metric tensor and itself. The most popular are the square Ricci invariant $R_{\mu\nu}R^{\mu\nu}$ and the square Riemann invariant $R_{\mu\nu\alpha\beta}R^{\mu\nu\alpha\beta}$, but also scalars formed with the Weyl tensor are often considered. A dynamical analysis of the late time cosmology of these models has been the subject of a work by Carroll et al. (2005), who considered general Lagrangians as functions of R^2, $R_{\mu\nu}R^{\mu\nu}$ and $R_{\mu\nu\alpha\beta}R^{\mu\nu\alpha\beta}$. They found general late time accelerated attractors for the-

ories with inverse power-law corrections of these higher order invariants. Another example has been given by Ishak & Moldenhauer (2009) who studied the cosmological dynamics of a theory where the higher order corrections are given by the invariant $S_{\mu\nu}S^{\mu\nu}$, where $S_{\mu\nu} = R_{\mu\nu} - g_{\mu\nu}R/4$ is the traceless part of the Ricci tensor. They obtained accelerated attractors for various more or less complicated models.

Gauss-Bonnet dark energy

The most interesting, and largely considered, higher order curvature term is perhaps the so-called *Gauss-Bonnet invariant* defined by

$$\mathcal{G} = R^2 - 4R_{\mu\nu}R^{\mu\nu} + R_{\mu\nu\alpha\beta}R^{\mu\nu\alpha\beta}\,. \tag{6.48}$$

In four dimensions this quantity is a topological invariant of the spacetime, implying that its linear contribution in the gravitational action can always be rewritten as a boundary term and thus it does not change the equation of motion in general. Nevertheless non linear terms in $\mathcal{G}$ can modify the field equations and thus give rise to new dynamics. Uddin et al. (2009) analysed such non linear contribution in the form $\mathcal{L}_{\rm grav} = R + f(\mathcal{G})$, where $\mathcal{L}_{\rm grav}$ is the gravitational Lagrangian[6]. They worked in an equivalent scalar field representation of the theory and delivered an analysis on scaling solutions. Garcia-Salcedo et al. (2010) studied instead a DBI modification of the type $\mathcal{L}_{\rm grav} = \sqrt{1 - \alpha R + \beta\mathcal{G}}$ which presents a rich phenomenology including matter and dark energy dominated solutions, scaling solutions, phantom and non-phantom late time attractors and even multiple future attractors. A general analysis on Gauss-Bonnet dark energy with the Lagrangian $\mathcal{L}_{\rm grav} = f(R, \mathcal{G})$ has been done by Alimohammadi & Ghalee (2009) who employed the quantities R and H as dynamical systems variables and studied the stability of future accelerated attractors.

Finally Koivisto (2010) considered a Gauss-Bonnet term coupled to a scalar field computing the cosmological dynamics and finding late time stable de Sitter solutions, while Kim & Kawai (2013) examined curved and anisotropic spacetimes. Tsujikawa & Sami (2007) studied instead scaling solutions for the same model with a generalised scalar field, showing that transition form the scaling regimes to dark energy domination is possible.

6.4 Palatini $f(R)$ gravity and generalisations

Besides the standard *metric approach*, where the action is varied only with respect to the metric tensor, there exists another formulation of $f(R)$ gravity which gives rise to new gravitational field equations and thus represents a physically different theory. This comes from the application of the *Palatini variational principle* in order to obtain the equations of motion from the $f(R)$ action (6.29). The variation according to the Palatini approach

Palatini $f(R)$ gravity

[6] In general the action is given by $S = \int d^4x\sqrt{-g}\mathcal{L}_{\rm grav}$.

consists in assuming the metric tensor and the spacetime *connection* to be independent fields and thus to be varied independently in the action. The $f(R)$ action (6.29) is thus generalised to[7]

$$S_{\text{Palatini}} = \int d^4x\sqrt{-g}\left[f(\tilde{R}) + 2\kappa^2\mathcal{L}_m\right] , \tag{6.49}$$

where now $\tilde{R} = g^{\mu\nu}\tilde{R}_{\mu\nu}$ with $\tilde{R}_{\mu\nu}$ the Ricci tensor formed by the independent Palatini connection $\tilde{\Gamma}^{\lambda}_{\mu\nu}$. The variation of the Palatini action (6.49) must be taken independently with respect to the metric $g_{\mu\nu}$ and the connection $\tilde{\Gamma}^{\lambda}_{\mu\nu}$. In general the $f(R)$ equations of motion obtained with this procedure differ from their corresponding metric ones, meaning that at the physical level the two approaches correspond to two different theories. In particular the dynamics at cosmological scales resulting from Palatini $f(R)$ gravity is completely different from its corresponding metric formulation. As shown by Fay et al. (2007), who considered the Palatini approach for different $f(R)$ models, a possible period of matter domination followed by dark energy domination can be obtained also for $f(R)$ cosmologies which are non viable in the metric formulation.

Hybrid metric-Palatini $f(R)$ gravity

The author of this thesis, together with his supervisor, considered a generalised *hybrid metric-Palatini formulation* of $f(R)$ gravity in order to build new models of dark energy and analysed their cosmologies with dynamical systems methods[8] (Tamanini & Boehmer, 2013). The action of this extended theory is given by

$$S_{\text{hmP}} = \int d^4x\sqrt{-g}\left[f(R,\tilde{R}) + 2\kappa^2\mathcal{L}_m\right] , \tag{6.50}$$

where now f is a general function of both the metric and Palatini Ricci scalars R and $\tilde{R}$. The equations of motion arising from the action (6.50) with an independent variation with respect to the metric and the Palatini connection are difficult to analyse with dynamical systems techniques. It is more convenient to reformulate the theory as a two-scalar field theory. In fact, in vacuum, i.e. when matter fields are neglected ($\mathcal{L}_m = 0$), the action (6.50) is dynamically equivalent to the (Einstein frame) non-minimally coupled bi-scalar field action (Tamanini & Boehmer, 2013)

$$S = \int d^4x\sqrt{-g}\left[\frac{R}{2\kappa^2} - \frac{1}{2}\partial\phi^2 - \frac{1}{2}e^{-\sqrt{2}\kappa\phi/\sqrt{3}}\partial\xi^2 - V(\phi,\xi)\right] , \tag{6.51}$$

where ϕ and ξ are two scalar fields and V is a general potential for both of them. The Palatini connection now does not appear and here R is the usual Ricci tensor in terms of the metric.

[7] Note that according to the Palatini approach the matter Lagrangian $\mathcal{L}_m$ cannot depend on the independent connection $\tilde{\Gamma}^{\lambda}_{\mu\nu}$.

[8] See Appendix B.

The cosmological equations (flat FRW metric) obtained from action (6.51), with an independent variation with respect the the metric and the two scalar fields, are

$$3H^2 = \frac{\kappa^2}{2} e^{-\sqrt{2/3}\kappa\phi} \dot{\xi}^2 + \frac{\kappa^2}{2}\dot{\phi}^2 + \kappa^2 W\,, \tag{6.52}$$

$$2\dot{H} + 3H^2 = -\frac{\kappa^2}{2} e^{-\sqrt{2/3}\kappa\phi} \dot{\xi}^2 - \frac{\kappa^2}{2}\dot{\phi}^2 + \kappa^2 W\,, \tag{6.53}$$

$$\ddot{\phi} + 3H\dot{\phi} + \frac{\kappa}{\sqrt{6}} e^{-\sqrt{2/3}\kappa\phi}\, \dot{\xi}^2 + W_\phi = 0\,, \tag{6.54}$$

$$\ddot{\xi} + 3H\dot{\xi} - \frac{\kappa\sqrt{2}}{\sqrt{3}}\, \dot{\xi}\, \dot{\phi} + e^{\sqrt{2/3}\kappa\phi}\, W_\xi = 0\,. \tag{6.55}$$

Note the coupling between the two scalar fields in the last two equations. In order to recast these equations into a dynamical system one can define the variables (Tamanini & Boehmer, 2013)

$$x^2 = \frac{\kappa^2\dot{\phi}^2}{6H^2}\,, \quad y^2 = \frac{\kappa^2 W}{3H^2}\,, \quad s^2 = \frac{\kappa^2\dot{\xi}^2}{6H^2} e^{-\sqrt{2/3}\kappa\phi}\,, \tag{6.56}$$

in terms of which the Friedmann constraint (6.52) reads

$$x^2 + y^2 = 1 - s^2\,, \tag{6.57}$$

impliying that

$$0 \leq x^2 + y^2 \leq 1\,. \tag{6.58}$$

These represent a clear generalisation of the standard EN variables with the constraint (6.57) forcing $x^2 + y^2 \leq 1$ and allowing for the substitution of s in terms of x and y. However, depending on the exact form of the potential V for the two scalar fields, it might be possible that other variables can better be employed for the dynamical systems analysis. The situation here is similar to the one of Sec. 4.5 where different variables were used according to whether the potential directly coupled the fields or not.

For the three models analysed by Tamanini & Boehmer (2013), the variables (6.56) yields 2D or 3D dynamical systems relatively easy to study. These models are characterised by the three potentials

$$W(\phi, \xi) = W_0\, e^{-\lambda\kappa\phi/\sqrt{6}}\,, \tag{6.59}$$

$$W(\phi, \xi) = W_0\, (\kappa\,\xi)^\lambda\, e^{-\lambda\kappa\phi/\sqrt{6}}\,, \tag{6.60}$$

$$W(\phi, \xi) = W_0\, e^{-\lambda\kappa\phi/\sqrt{6}} \quad \text{with matter}\,, \tag{6.61}$$

where W_0 and λ are constants and in the last model the effect of the matter sector is considered. In all these three models a behaviour similar to

the quintessence domination arises, with late time accelerated solutions and early times extended matter dominated periods. The reader interested in the dynamical systems analysis of these models can find more information in Appendix B.

Here, as an example, we provide the dynamical system obtained in the first model (the simplest), i.e. arising from the potential (6.59):

$$x' = x^2 - 3\,x\,y^2 + \frac{1}{2}(\lambda + 2)\,y^2 - 1\,, \tag{6.62}$$

$$y' = -\frac{1}{2}\,y\left(\lambda\,x + 6y^2 - 6\right)\,, \tag{6.63}$$

where a prime denotes again differentiation with respect to $\eta = \ln a$. We will not perform the full analysis of this system, which can be found in Appendix B, but limit the discussion to the physically relevant critical point $(x, y) = (\lambda/6, \sqrt{36 - \lambda^2}/6)$. For $\lambda < \sqrt{37} - 1$ this point is a stable attractor, which for $\lambda < 2\sqrt{3}$ describes an accelerating late time solution. In analogy with the exponential potential quintessence model, for a sufficiently small λ this hybrid metric-Palatini model can thus describe a universe asymptotically dominated by dark energy in the future. Although this model is similar to quintessence, the physical conclusion that we can draw is completely different. In fact, here dark energy is an effect due to the modification of the gravitational equations, rather than being due to an unknown scalar particles.

Concluding remarks

To conclude the thesis we offer a summary of what has been treated in the previous chapters, discussing the obtained results and outlining future perspectives.

Chapter 2

After the small introduction of Chapter 1, we have introduced selected topics from the foundations of dynamical systems theory in Chapter 2. These have been presented in a rather pedagogical way, without providing explicit proofs of theorems but focusing the contents on applications and examples. Only the arguments needed for the subsequent chapters have been offered, without extending the discussion to more advanced material of dynamical systems theory. The linear stability theory has been developed to analyse hyperbolic critical points, while the Liapunov and centre manifold theories have been explained to deal with non-hyperbolic critical points. The concepts of limit set and attractor have been defined and important theorems, especially regarding the compactification of the phase space, have been studied for 2D dynamical systems. Chapter 2 has been conceived as a small introduction to the theory of dynamical systems for the unfamiliar reader (usually the physicist) and as a brief review for the one possessing already an advanced knowledge on the subject (usually the mathematicians).

Chapter 3

The same approach has been maintained in the first part of Chapter 3, where basic elements of cosmology has been provided. Again the reader with already some expertise on the argument (the physicist) has probably acknowledged this part as a brief review, while for the one with less familiarity (the mathematicians) it has served as a direct introduction to cosmology. After having discussed standard homogeneous and isotropic cosmology, we have outlined the physical theory behind the dynamical behavior of the universe. In the second part of Chapter 3, dark energy and dark matter have been introduced to address the problems arising from the modern astronomical and astrophysical observations. Dark energy in particular is an entity needed to explain the late time accelerated expansion of the universe and this thesis focuses on the dynamics described by its different theoretical models. The simplest of these models is the cosmological constant, which has been largely treated in the last sections of Chapter 3. Besides its simplicity however, we have seen that some theoretical problems, in particular

the cosmic coincidence problem and the fine tuning problem of initial conditions, undermine the validity of the cosmological constant as a fundamental theory of Nature. One way of dealing with these problems is to propose dynamically evolving models of dark energy. The dynamics of such models have been the topic of the remaining chapters of the thesis.

Chapter 4 Chapter 4 has been devoted to the study of canonical scalar field models of dark energy, collectively known as quintessence. After a small introduction to scalar field cosmology, the simplest and most important quintessence models, namely the exponential and (inverse) power-law potentials, have been fully investigated with dynamical systems techniques, furnishing results from both well-known literature and new original analyses. Scaling and accelerated solutions have been examined for a cosmological scalar field with an exponential potential, while tracking behavior has been identified as the main feature of the inverse power-law potential. Scaling solutions are useful in addressing the cosmic coincidence problem, while tracking solutions can solve the fine tuning problem of initial conditions. Late time accelerated attractors can be obtained with a sufficiently flat exponential potential, while they are easier to find in the power-law potential case. The discussion has then been enlarged to more complex scalar field potentials, which have been studied under a unifying perspective. We have outlined the main features of quintessence for a general potential and provided detailed references to models considered in the dynamical systems literature. In the final part of Chapter 4, different couplings between the scalar field and the matter sector has been reviewed, with a detailed dynamical systems analysis for the simplest one and brief considerations for the other ones. In general introducing a coupling between matter and quintessence favors the presence of accelerating scaling solutions which can solve the cosmic coincidence problem. The last section of Chapter 4 has been conceived as a small overview of the multiple canonical scalar field models of dark energy. The most important feature arising from these models is the so-called assisted behavior where accelerated expansion can be achieved from the collective contribution of scalar fields with steep (exponential) potentials.

Chapter 5 In Chapter 5 we investigated non-canonical scalar field models of dark energy, where the scalar field is characterized by a non-standard kinetic term. The phantom scalar field model of dark energy, with a negative kinetic energy, has been the first one analysed. The possibility of obtaining dark energy in the phantom regime, which is slightly favored by astronomical observations, is the main result achieved in this case, though the wrong sign of the kinetic term implies incurable pathologies at the theoretical level. The phantom paradigm has then been extended to the quintom one, where the contribution of two scalar fields, one phantom and one canonical, leads to a dynamical crossing of the phantom barrier. This situation is even more in agreement with observational data, though the quintom scenario, exactly as the phantom one, can only be trusted at an effective phenomenological

level since it is plagued by theoretical problems on a more fundamental interpretation. Chapter 5 has then presented more general scalar field models characterized by higher order terms in the spacetime derivatives. The main features of these models have been discussed and a brief overview of the dynamical systems literature has been offered. The discussion has then moved on to tachyons and DBI scalar fields, which are non-canonical scalar field models predicted by high-energy physics phenomenology, in particular string theory. The dynamics of the simplest tachyonic model has been analysed finding a mix of known and new results, while more complicated models, including DBI scalar fields, have been reviewed highlighting the main properties and citing the relevant literature. The last section of Chapter 5 has been devoted to non-scalar models of dark energy, where the late time accelerated expansion is driven either by a field with non-vanishing spin or by some phenomenological matter fluid. For all these models, which span from vector and spinor fields to the Chaplygin gas, a brief introduction and references to the dynamical systems literature have been provided.

Chapter 6

Finally dark energy beyond general relativity has been studied in Chapter 6, where models of modified gravity have been considered. An original dynamical systems analysis, with the identification of possible scaling accelerated attractors capable of addressing the cosmic coincidence problem, has been performed for the cosmology of Brans-Dicke theory with a general power-law potential. The discussion has then been extended to scalar-tensor theories where new dimensionless variables for applications of dynamical systems methods have been proposed. These variables allow one to investigate the dynamics of scalar-tensor theories under a unified approach and could be employed in future works on the subject. Higher order gravitational theories, especially $f(R)$ gravity, have then constituted the following argument of Chapter 6. For $f(R)$ theories the dynamical systems literature has been reviewed following well-known papers where a collective approach has been developed to treat their dynamics. The properties of more complicated models built with higher order curvature invariants, such as for example Gauss-Bonnet dark energy, have then been presented and the due citations to the literature have been mentioned. Finally, in the last section of the chapter, the Palatini approach to $f(R)$ gravity has been discussed, introducing its main features and properties. A particular generalisation of $f(R)$ gravity, mixing both metric and Palatini approach has then been presented and some results in connection with the author's original work have been outlined.

Future perspectives

This thesis as a whole can be considered as an extensive review on dynamical systems applications to dark energy models, where not only detailed references to the literature have been furnished, but also new and original results have been obtained. It can easily be taken as a guide through the literature of the dynamics of dark energy models, though only dynamical systems applications have been considered leaving aside many more theo-

retical and phenomenological issues. It is the thought of the author that the present work is better suited to inspire future analysis on the dynamics of dark energy models rather than being a simple review of past results. Some original computations presented for the first time in this thesis could already be the starting point of future dynamical systems applications in cosmology. For example an extended and self-contained dynamical analysis on the quintessence model with power-law potential as the one we offered in Sec. 4.3 has never appeared in the literature. The results obtained in Sec. 5.4 for the simplest tachyonic scalar field model complement other ones derived in previous works and highlight new interesting phenomenological features that this model can provide. The new variables defined in Sec. 6.2 for scalar-tensor theories can be employed not only to construct a unified approach to the dynamics of such theories, but also to analyse in depth the dynamical properties of specific dark energy models. On a more general ground, this thesis can be used as a guide to dynamical systems applications to dark energy which not only presents up to date results on the subject, but also proposes new directions of research and lays the foundations for a bridge between applied mathematics and theoretical physics.

Conclusions

In conclusion we have had a long journey through the dynamics of theoretical models of dark energy. We have reviewed both mathematical and physical topics, discussed the problems afflicting modern cosmology, introduced a great number of dark energy models relying on the most different theoretical foundations and finally derived many more results on their cosmological dynamics. We have learnt that every different model of dark energy leads to interesting phenomenological features, but none of them is able to both provide a satisfactory interpretation of astronomical observations and be not plagued by any theoretical drawback. At the present time, the scientific quest for the nature of dark energy is still an open and lively issue on both the theoretical and observational sides. It is the one hope of the author that the reader, independently of her/his background, has enjoyed the journey and that she/he has found somehow useful the arguments and topics discussed. The ultimate aim of this thesis has always been to expand knowledge and inspire ideas to both the author and the reader.

Appendix A

Dynamics of cosmological scalar fields

N. Tamanini,
Dynamics of cosmological scalar fields,
Phys. Rev. D **89** (2014) 083521 [arXiv:1401.6339 [gr-qc]].

PHYSICAL REVIEW D **89,** 083521 (2014)

Dynamics of cosmological scalar fields

Nicola Tamanini*

Department of Mathematics, University College London, Gower Street, London WC1E 6BT, United Kingdom

(Received 11 February 2014; published 8 April 2014)

The background dynamical evolution of a universe filled with matter and a cosmological scalar field is analyzed employing dynamical system techniques. After the phenomenology of a canonical scalar field with exponential potential is revised, square and square root kinetic corrections to the scalar field canonical Lagrangian are considered and the resulting dynamics at cosmological distances is obtained and studied. These noncanonical cosmological models imply new interesting phenomenology including early time matter dominated solutions, cosmological scaling solutions and late time phantom dominated solutions with dynamical crossing of the phantom barrier. Stability and viability issues for these scalar fields are presented and discussed.

DOI: 10.1103/PhysRevD.89.083521 PACS numbers: 98.80.-k, 95.36.+x

I. INTRODUCTION

Since the Nobel Prize winning discovery of a current cosmological phase of accelerated expansion was made in 1998 [1,2], the theoretical models advanced to describe this phenomenon quickly multiplied in the literature. The simplest among these is the straightforward addition of a positive cosmological constant to the Einstein field equations. Although this model fits all astronomical observations, it is in tension with particle physics prediction (the cosmological constant problem [3,4]) and cosmological considerations (the coincidence problem [5]).

A way to alleviate these problems consists in letting the cosmological constant be dynamical. This implies the introduction of some cosmological field capable of reproducing the late time accelerated behavior mimicking in this way the effects of a cosmological constant. Any physical entity which at cosmic distances provides an accelerated expansion at late times is commonly called *dark energy*. The simplest field having these properties is a canonical scalar field with a potential. Dark energy models of this kind go under the name of *quintessence* and have been largely studied in the literature [6,7].

Scalar fields play an important role in cosmology since they are sufficiently simple to handle and sufficiently complicated to produce nontrivial dynamics. They are not only employed to model dark energy, but also to characterize inflation [8], dark matter [9], unified dark models [10] and other cosmological features. For dark matter phenomenology it is usually required a vanishing pressure and that the speed of sound of adiabatic perturbations is sufficiently small to allow the formation of clusters. Scalar field models proposed to unify dark matter and dark energy must thus have a dynamical equation of state evolving from dustlike to dark energy– like behavior, which can be achieved with a noncanonical scalar field [10].

Generalizations and modifications of the canonical scalar field Lagrangian can also lead to more complex cosmological predictions. Extended models where the scalar field Lagrangian is a general function of both the scalar field ϕ and its kinetic term are known as k-essence theories [11]. Within this framework it is possible to obtain not only the standard dark energy evolution but also the so-called *phantom* regime and quintessence to phantom transition, though fatal problems always arise at the level of perturbations [12–14].

A phantom scalar field is identified by an equation of state (EoS) with a negative pressure bigger than the energy density. In other words, for a scalar field EoS $p_\phi = w_\phi \rho_\phi$, the phantom regime is identified by the condition $w_\phi < -1$, which seems to be slightly favored by astronomical observations even after Planck [15,16]. The first and simplest model capable of achieving such condition consists in flipping the sign of the kinetic term of a canonical scalar field [17]. However in this model the scalar field EoS parameter is never greater than -1 creating problems at early times where dark matter with vanishing pressure must dominate. Scalar fields which can cross the phantom barrier at $w_\phi = -1$ are usually dubbed *quintom* models and imply either the use of extended Lagrangians, generally instable, or of two different scalar fields [14,18].

The present work is devoted to study the background dynamical evolution of different scalar field models. Dynamical system techniques are employed to fully determine the solutions of the cosmological equations. Suitable dimensionless variables are introduced following [19] and the phase space dynamics is analyzed using numerical methods. Canonical and noncanonical scalar field Lagrangians are presented and their cosmological implications are discussed. The complete cosmological background dynamics of two specific noncanonical scalar fields

*n.tamanini.11@ucl.ac.uk

is obtained showing that interesting phenomenology, such as early time matter dominated solutions, scaling solutions, late time phantom acceleration, superstiff and phantom transition eras, can be achieved.

The paper has the following structure. In Sec. II the canonical scalar field will be largely discussed. Its features and cosmological dynamics will be presented and analyzed in depth and the notation and conventions needed for the following sections will be introduced. In Sec. III noncanonical scalar field Lagrangians will be considered. Perturbation instabilities will be examined and the analysis will focus on models where dynamical system techniques can be successfully applied. Sections IV and V will then be dedicated to the study of square and square root kinetic corrections to the canonical scalar field Lagrangian. For these simple models the full dynamical features can be obtained and the background cosmological evolution can be determined for any initial condition. The analysis of these two sections will show that a rich phenomenology can be obtained with these extended scalar fields. Finally results and conclusions will be discussed in Sec. VI.

II. THE CANONICAL SCALAR FIELD

In this section we review the cosmological dynamics of a canonical scalar field following the analysis first performed in [19]. This will serve as an introduction to the dynamical system techniques one can apply in order to completely determine the cosmological evolution of specific models. Moreover this section will be helpful in defining notation and conventions.

The action of a minimally coupled canonical scalar field is given by

$$S = \int d^4x\sqrt{-g}\left[\frac{R}{2\kappa^2} + \mathcal{L}_\phi + \mathcal{L}_m\right], \tag{1}$$

where g is the determinant of the metric, R is the Ricci scalar, $\kappa^2 = 8\pi G/c^4$, $\mathcal{L}_m$ is the matter Lagrangian, and the scalar field Lagrangian is defined as

$$\mathcal{L}_\phi = -\frac{1}{2}\partial\phi^2 - V(\phi), \tag{2}$$

with $\partial\phi^2 = \partial_\mu\phi\partial^\mu\phi$ and V a general potential for ϕ. The variation with respect to $g_{\mu\nu}$ produces the following gravitational equations:

$$G_{\mu\nu} = \kappa^2\left(T_{\mu\nu} + \partial_\mu\phi\partial_\nu\phi - \frac{1}{2}g_{\mu\nu}\partial\phi^2 - g_{\mu\nu}V\right), \tag{3}$$

where $G_{\mu\nu} = R_{\mu\nu} - 1/2g_{\mu\nu}R$ is the Einstein tensor and $T_{\mu\nu}$ the matter energy-momentum tensor. The variation with respect to ϕ gives the Klein-Gordon equation

$$\Box\phi - \frac{\partial V}{\partial\phi} = 0, \tag{4}$$

with $\Box\phi = \nabla_\mu\nabla^\mu\phi$.

In what follows we will analyze the background cosmological evolution of this model. The metric tensor will be assumed to be of the Friedmann-Robertson-Walker (FRW) type with vanishing spatial curvature

$$g_{\mu\nu} = \mathrm{diag}(-1, a(t)^2, a(t)^2, a(t)^2), \tag{5}$$

with $a(t)$ the scale factor, while the scalar field is taken to be spatially homogeneous $\phi = \phi(t)$. The matter energy-momentum tensor will be of the perfect fluid form with $\rho(t)$ and $p(t)$ its energy density and pressure, respectively. A linear EoS $p = w\rho$, with w the EoS parameter ranging from 0 (dust) to 1/3 (radiation), will be assumed.

With these assumptions, from the gravitational equations (3) we obtain the Friedmann constraint

$$3H^2 = \kappa^2\left(\rho + \frac{1}{2}\dot\phi^2 + V\right) \tag{6}$$

and the acceleration equation

$$2\dot H + 3H^2 = -\kappa^2\left(p + \frac{1}{2}\dot\phi^2 - V\right), \tag{7}$$

where $H = \dot a/a$ is the Hubble parameter and an overdot denotes differentiation with respect to the time t. On the other hand the scalar field equation (4) gives

$$\ddot\phi + 3H\dot\phi + \frac{\partial V}{\partial\phi} = 0. \tag{8}$$

The energy density and pressure of the canonical scalar field are given, respectively, by

$$\rho_\phi = \frac{1}{2}\dot\phi^2 + V, \tag{9}$$

$$p_\phi = \frac{1}{2}\dot\phi^2 - V, \tag{10}$$

and its EoS parameter, defined as the ratio between its pressure and energy density, is

$$w_\phi = \frac{p_\phi}{\rho_\phi} = \frac{\frac{1}{2}\dot\phi^2 - V}{\frac{1}{2}\dot\phi^2 + V}. \tag{11}$$

For $V \gg \dot\phi^2$ this approaches a cosmological constant EoS with $w_\phi = -1$, while for $V \ll \dot\phi^2$ this describe a stiff fluid with $w_\phi = 1$.

At this point, following [19], we introduce new dimensionless variables as

$$x^2 = \frac{\kappa^2\dot{\phi}^2}{6H^2}, \qquad y^2 = \frac{\kappa^2 V}{3H^2}, \qquad \sigma^2 = \frac{\kappa^2\rho}{3H^2}. \quad (12)$$

These variables are largely employed in scalar field cosmology since they not only allow one to rewrite Eqs. (6)–(8) as an autonomous system of equations, but can also be generalized in different contexts such as, for example, nonminimally coupled scalar fields [20–23], tachyons [24], Galileons [25], phantom and quintom cosmology [26,27], phenomenology from higher dimensions [28–31], k essence [32,33], modified gravity [34], three-form cosmology [35,36], cosmological effective field theories [37] and dark energy models coupled to dark matter [38–40].

With the variables (12) the Friedmann constraint (6) becomes

$$1 = \Omega_m + \Omega_\phi = \sigma^2 + x^2 + y^2, \quad (13)$$

where the relative energy densities are defined as

$$\Omega_m = \frac{\kappa^2\rho}{3H^2} \quad \text{and} \quad \Omega_\phi = \frac{\kappa^2\rho_\phi}{3H^2}. \quad (14)$$

Equation (13) can be used to replace σ^2 in favor of x^2 and y^2. This implies that the only dynamical variables of the system of equations will be x and y. Also, since $\sigma^2 \geq 0$ due to the assumption $\rho \geq 0$, the constraint

$$x^2 + y^2 \leq 1 \quad (15)$$

will always hold. If in addition one assumes the potential energy V to be greater than zero, then $y \geq 0$ and the phase space of the variables (x, y) reduces to the upper-half unit disk.

At this point it is possible to convert the cosmological equations into an autonomous system of equations if one further specifies the potential V. If this is exponential, for example

$$V(\phi) = V_0 e^{-\lambda\kappa\phi}, \quad (16)$$

with $V_0 > 0$ and λ arbitrary parameters, then the phase space will remain two dimensional. If instead one chooses a power-law potential, then the phase space becomes three dimensional and the new variable

$$z = -\frac{1}{\kappa V}\frac{\partial V}{\partial\phi} \quad (17)$$

needs to be introduced [6,41], while for other potentials different variables can be better employed; see e.g. [42–45]. In this work we will only consider exponential potential of the kind (16). With this assumption the acceleration equation (7) and the scalar field equation (8) lead to the two-dimensional autonomous system

$$x' = \frac{3}{2}\left[\sqrt{\frac{2}{3}}\lambda y^2 - (w-1)x^3 - x(w+1)(y^2-1)\right], \quad (18)$$

$$y' = -\frac{3}{2}y\left[(w-1)x^2 + (w+1)(y^2-1) + \sqrt{\frac{2}{3}}\lambda x\right], \quad (19)$$

where a prime denotes differentiation with respect to $d\eta = Hdt$ and the variables x and y are functions of the dimensionless time parameter $\eta = \ln a$. Note that the dynamical system (18) and (19) is invariant under the transformation $y \mapsto -y$, so even if we drop the $V > 0$ assumption the dynamics on the negative y half-plane would be a copy of the positive y region. Note also that we are assuming $H > 0$ in order to describe an expanding universe. However the dynamics of a contracting universe ($H < 0$) would have the same features of our analysis in the negative y plane switching the direction of time because of the $y \mapsto -y$ symmetry. On the other hand the dynamical system (18) and (19) is also invariant under the simultaneous transformation

$$\lambda \mapsto -\lambda \quad \text{and} \quad x \mapsto -x, \quad (20)$$

which shows that opposite values of λ lead to the same dynamics after a reflection over the y axis.

The acceleration equation (7) gives also

$$\frac{\dot{H}}{H^2} = \frac{3}{2}[(w-1)x^2 + (w+1)(y^2-1)], \quad (21)$$

which at any fixed point (x_*, y_*) of the phase space can be solved for a to give

$$a \propto (t - t_0)^{2/[3(w+1)(1-x_*^2-y_*^2)+2x_*^2]}, \quad (22)$$

where t_0 is a constant of integration. This corresponds to a power-law solution, i.e. a solution for which the scale factor a evolves as a power of the cosmological time t. If $x = 0$ and $y = 0$, the universe is matter dominated and its evolution coincides with the standard w-dependent scaling solution. If $x = 0$ and $y = 1$, the denominator of (22) vanishes and the universe undergoes a de Sitter expansion as can be seen from (21) which forces H to be constant. An effective EoS parameter w_{eff} can now be defined rewriting (22) as[1]

$$a \propto (t - t_0)^{2/[3(1+w_{\text{eff}})]} \quad (23)$$

and corresponds to the EoS parameter of an effective fluid sourcing the gravitational equations, or in other words to an effective matter energy-momentum tensor. Comparing with (22) we find

[1]If $w_{\text{eff}} < -1$, then the physical solution for the scale factor in Eq. (22) should be $a \propto (t_0 - t)^{2/[3(1+w_{\text{eff}})]}$, which implies a big rip at $t = t_0$.

$$w_{\rm eff} = x_*^2 - y_*^2 + w(1 - x_*^2 - y_*^2). \tag{24}$$

Whenever $w_{\rm eff} < -1/3$ solution (23) describes a universe undergoing an accelerated phase of expansion. This kind of evolution is useful to model both the inflationary early universe and the late time dark energy dominated universe. We can also have a look at how w_ϕ can be rewritten in terms of the variables (12):

$$w_\phi = \frac{x^2 - y^2}{x^2 + y^2}. \tag{25}$$

This expression tells us the equation of state of the scalar field at any given point of the phase space.

The first step one should make in order to analyze the dynamical system (18) and (19) is to compute the critical or fixed points of the system. These are the phase space points (x, y) that satisfy the conditions

$$x' = 0, \qquad y' = 0. \tag{26}$$

If the system happens to be in one of these points, then there is no dynamical evolution and the universe expands according to (22). Their existence is satisfied only if their coordinates are real and lie inside the phase space, i.e. the upper unit half-disk in the present case. The stability conditions are computed linearizing the equations around the critical point under consideration which leads to the analysis of the eigenvalues of the Jacobian matrix

$$\mathcal{M} = \begin{pmatrix} \frac{\partial f_x}{\partial x} & \frac{\partial f_x}{\partial y} \\ \frac{\partial f_y}{\partial x} & \frac{\partial f_y}{\partial y} \end{pmatrix}, \tag{27}$$

evaluated at the critical point. Here $x' = f_x(x, y)$ and $y' = f_y(x, y)$ is a compact notation for the system (18) and (19). If the real part of both the eigenvalues is positive, then the point is an unstable point; if they have different signs, the point is a saddle point; and if they are both negative, the point is a stable point.

The critical points of the system (18) and (19) are shown in Table I. There can be up to five critical points according to the value of λ:

(i) *Point O*.—The origin of the phase space corresponds to a matter dominated universe ($\Omega_m = 1$) and exists for all values of λ. Of course the effective EoS matches the matter EoS, $w_{\rm eff} = w$, and thus for physically admissible values of w there is no acceleration. This point is always a saddle point attracting trajectories along the x axis and repelling in any other direction.

(ii) *Point $A_\pm$*.—In these two points the universe is dominated by the scalar field kinetic energy ($\Omega_\phi = 1$) and thus the effective EoS reduces to a stiff fluid with $w_{\rm eff} = w_\phi = 1$ and no acceleration. Their existence is always guaranteed and they never represent stable points. They are unstable or saddle points depending on the absolute value of λ being greater or smaller than $\sqrt{6}$.

(iii) *Point B*.—This point is the so-called scaling solution where the effective EoS matches the matter EoS, but the scalar field energy density does not vanish. In other words we always have both $0 < \Omega_\phi = 3(1+w)/\lambda^2 < 1$ and $0 < \Omega_m = 1 - \Omega_\phi < 1$, obtaining also $w_\phi = w$. This means that the universe evolves under both the matter and scalar field influence, but it expands as if it was completely matter dominated. This solution is of great physical interest for the coincidence problem since according to it a scalar field can or could be present in the universe hiding its effects on cosmological scales. However, since we have $w_{\rm eff} = w$ there cannot be accelerated expansion. When this point exists, i.e. for $\lambda^2 \geq 3(1 + w)$, it always represents a stable point attracting all the phase space trajectories.

(iv) *Point C*.—The last point stands for the cosmological solution where the universe is completely scalar field dominated. This implies $\Omega_m = \sigma^2 = 0$ and $\Omega_\phi = x^2 + y^2 = 1$ meaning that point C will always lie on the unit circle. It exists for $\lambda^2 < 6$ and it is a stable attractor for $\lambda^2 < 3(1 + w)$ (i.e. when point B does not appear) and a saddle point for $3(1 + w) \leq \lambda^2 < 6$. The effective EoS parameter assumes the value $w_{\rm eff} = w_\phi = \lambda^2/3 - 1$ which implies an accelerating universe for $\lambda^2 < 2$. This point represents the well-known cosmological accelerated expansion driven by a sufficiently flat scalar field potential.

TABLE I. Critical points of the system (18) and (19) and their properties.

Point	x	y	Existence	$w_{\rm eff}$	Acceleration	Ω_ϕ	Stability
O	0	0	$\forall\lambda, w$	w	No	0	Saddle
A_-	-1	0	$\forall\lambda, w$	1	No	1	Unstable if $\lambda \geq -\sqrt{6}$ Saddle if $\lambda < -\sqrt{6}$
A_+	1	0	$\forall\lambda, w$	1	No	1	Unstable if $\lambda \leq \sqrt{6}$ Saddle if $\lambda > \sqrt{6}$
B	$\sqrt{\frac{3}{2}}\frac{1+w}{\lambda}$	$\sqrt{\frac{3(1-w^2)}{2\lambda^2}}$	$\lambda^2 \geq 3(1+w)$	w	No	$\frac{3(1+w)}{\lambda^2}$	Stable
C	$\frac{\lambda}{\sqrt{6}}$	$\sqrt{1-\frac{\lambda^2}{6}}$	$\lambda^2 < 6$	$\frac{\lambda^2}{3} - 1$	$\lambda^2 < 2$	1	Stable if $\lambda^2 < 3(1+w)$ Saddle if $3(1+w) \leq \lambda^2 < 6$

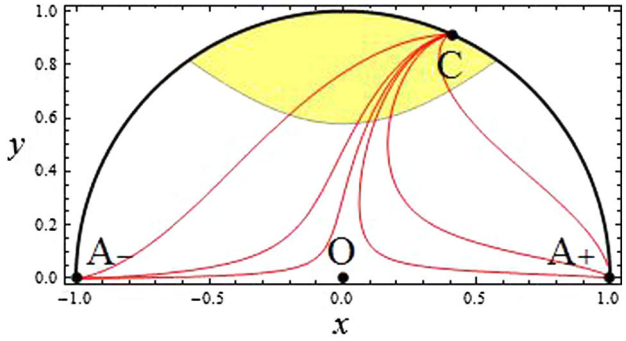

FIG. 1 (color online). Phase space with $\lambda = 1$ and $w = 0$. The global attractor is point C which represents an accelerating solution. For values $\lambda^2 > 2$ point C would lie outside the acceleration region (yellow shaded area) and would not be an inflationary solution.

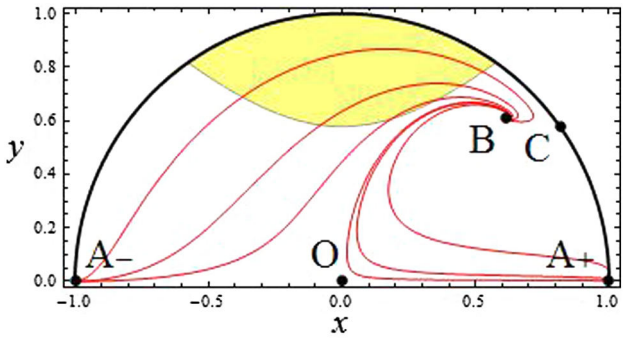

FIG. 2 (color online). Phase space with $\lambda = 2$ and $w = 0$. The global attractor is point B where the universe expands as it was completely matter dominated, while point C is a saddle point.

The physical applications abound in both the early and late time universe stages. In the limit $\lambda \to 0$ this solution reduces to a de Sitter expansion dominated by a cosmological constant.

The qualitative behavior of the phase space can be divided into three regions according to the value of λ^2. In what follows we will only consider positive values for λ. The dynamics for negative values coincides with the positive one after a reflection around the y axis because of (20).

If $\lambda^2 < 3(1+w)$, there are four critical points. Points $A_\pm$ are both unstable node, while point O is a saddle point. The global attractor is point C which represents an inflationary cosmological solution if $\lambda^2 < 2$. The portrait of the phase space is depicted in Fig. 1 where the values $\lambda = 1$ and $w = 0$ have been chosen. The yellow shaded region delimits the zone of the phase space where the universe undergoes an accelerated expansion. Point C always lies on the unit circle and it happens to be outside the acceleration region if $\lambda^2 > 2$.

In the range $3(1+w) \leq \lambda^2 < 6$ there are five critical points in the phase space. Points $A_\pm$ and O still behave as unstable nodes and saddle point, respectively. The global attractor is now point B and point C becomes a saddle point. The phase space portrait is drawn in Fig. 2. Point B always lies outside the acceleration region (yellow shaded area) and thus never describe an inflationary solution. However the effective EoS parameter at this point coincides with the matter EoS parameter and thus the universe experience a matterlike expansion even if it is not completely matter dominated. This is the so-called scaling solution where the scalar field energy density fills part of the universe but the resulting cosmological evolution still assumes the behavior of a matter dominated expansion.

Finally if $\lambda^2 \geq 6$, there are again only four critical points. Point A_- is the only unstable node, while points A_+ and O behave as saddle points. Point C does not appear anymore and the global attractor is still point B, which again represents a scaling solution with $w_{\rm eff} = w$. The phase space dynamics is depicted in Fig. 3.

The cosmological dynamics of the canonical scalar field is interesting because of the appearance of late time accelerated solutions which can be employed to model dark energy and inflation. The scaling solutions are also important since they allow a scalar field to hide its presence during the cosmological evolution. This situation can be used to postulate a scalar field which gives no contribution at early times but becomes relevant at late times. Unfortunately there are strong observational constraints from nucleosynthesis which force the parameter λ to satisfy the relation $\lambda \gtrsim 9$ at early times [46]. Since for a late time accelerating solution a sufficiently flat potential is needed ($\lambda^2 < 2$), it is impossible to achieve both the scaling and accelerating regimes with a canonical scalar field and an exponential potential.

Moreover with a canonical scalar field we always have that unstable nodes of the phase space, possibly representing very early time behaviors, are associated with scalar field kinetic dominated universe. These solutions are characterized by an effective EoS approaching the stiff regime where $w_{\rm eff} = 1$. Strictly speaking this value of $w_{\rm eff}$ is not physically viable at the classical level. However since these solutions appear to be relevant only at very early

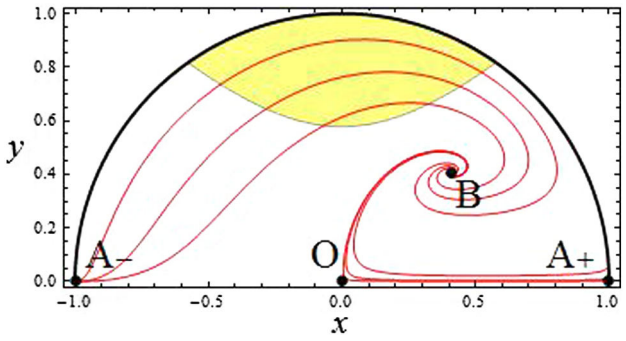

FIG. 3 (color online). Phase space with $\lambda = 3$ and $w = 0$. Point B is the global attractor describing a scaling solution with $w_{\rm eff} = w$.

times in physical applications, this feature is usually ignored. As we will see in Sec. IV, with a noncanonical scalar field an early time matter dominated solution can always be obtained.

III. THE NONCANONICAL SCALAR FIELD

In this section we will generalize the scalar field Lagrangian $\mathcal{L}_\phi$. The canonical choice for $\mathcal{L}_\phi$ has been given in (2) and its dynamics on cosmological scales has been investigated in full detail in the previous section. In order to simplify the following equations we define

$$X = -\frac{1}{2}\partial\phi^2 = -\frac{1}{2}g^{\mu\nu}\partial_\mu\phi\partial_\nu\phi. \tag{28}$$

The canonical choice for the scalar field Lagrangian corresponds then to $\mathcal{L}_\phi = X - V$. The most general Lagrangian containing X and ϕ is given by $\mathcal{L}_\phi = P(X,\phi)$, where P is an arbitrary function in both the variables. In cosmology such theories are known under the name of k essence. They received a considerable amount of attention during the last few years because of their applications to dark energy, dark matter and inflation.

In order to reduce our analysis we will focus only on scalar field Lagrangians generally defined by

$$\mathcal{L}_\phi = Vf(B) \quad \text{with} \quad B = \frac{X}{V} \tag{29}$$

and f an arbitrary function. This includes the canonical choice if one considers $f(B) = B - 1$. In [47,48] it has been shown that, within general relativity, the most general Lagrangian leading to cosmological scaling solutions with an exponential potential can be written as[2] (29). In addition the dimensionless variables (12) turn out to be of great advantage if a scalar field Lagrangian is assumed as in (29). As we will see they will permit to completely determine the cosmological dynamics of such a scalar field. As before we will only consider the exponential potential case $V = V_0\exp(-\lambda\kappa\phi)$.

The variation of the gravitational action (1) with the scalar field Lagrangian (29) leads to the gravitational equations

$$\frac{1}{\kappa^2}G_{\mu\nu} = T_{\mu\nu} + g_{\mu\nu}Vf + \frac{\partial f}{\partial B}\partial_\mu\phi\partial_\nu\phi, \tag{30}$$

while the variation with respect to the scalar field ϕ gives

$$\nabla_\mu\left(\frac{\partial f}{\partial B}\partial^\mu\phi\right) + \frac{\partial V}{\partial\phi}\left(f - \frac{\partial f}{\partial B}B\right) = 0. \tag{31}$$

[2]In [47,48] this Lagrangian was written as $\mathcal{L}_\phi = Xf(B)$; however a simple redefinition of the function f can bring this in the form (29).

Notice that these equations reduce to (3) and (4) for the canonical choice of the scalar field Lagrangian.

As before, the cosmological equations can be found employing the FRW metric (5) and assuming an homogeneous scalar field $\phi = \phi(t)$. The Friedmann constraint becomes

$$\frac{3H^2}{\kappa^2} = \rho - Vf + \frac{\partial f}{\partial B}\dot\phi^2, \tag{32}$$

while the acceleration equation generalizes to

$$2\dot H + 3H^2 = -\kappa^2(p + Vf). \tag{33}$$

On the other hand the same assumptions reduce (31) to

$$\left(\frac{\partial f}{\partial B} + 2B\frac{\partial^2 f}{\partial B^2}\right)\ddot\phi + \frac{\partial f}{\partial B}3H\dot\phi - \left(f - B\frac{\partial f}{\partial B} + 2B^2\frac{\partial^2 f}{\partial B^2}\right)\frac{\partial V}{\partial\phi} = 0, \tag{34}$$

where now $B = \dot\phi^2/(2V)$.

Some remarks can now be made on Eqs. (32)–(34). First of all we notice again that choosing $f = B - 1$ reduces these equations to (6)–(8) as expected. It is interesting to find the particular form of the function f for which the contribution of the scalar field in (32) completely disappears. This is realized for $f = \sqrt{B}$ or, in other words, for the Lagrangian $\mathcal{L}_\phi = \sqrt{XV}$. Unfortunately this particular choice also makes the first and last terms in (34) vanish. This implies that ϕ has no dynamics at all and becomes simply a constant. In any case it is worth noting that adding the $\sqrt{B}$ term to any other function f does not modify the Friedmann constraint (32) and adds a simple term $3H\sqrt{V/2}$ to the scalar field equation (34). These features will be analyzed in more detail in Sec. V. Note also that it is impossible to find a scalar field Lagrangian whose contribution in the acceleration equation (33) vanishes. This is due to the fact that $\mathcal{L}_\phi = Vf$ and thus the vanishing of the scalar field contribution in (33) would correspond to a zero scalar field Lagrangian.

At this point it is useful to see what the Friedmann constraint (32) looks like in terms of the variables (12). We obtain

$$1 = \sigma^2 - y^2 f + 2x^2\frac{\partial f}{\partial B}, \tag{35}$$

where we also have that

$$B = \frac{x^2}{y^2}. \tag{36}$$

The Friedmann constraint (35) determines the boundaries of the phase space described by the variables x and y. In the

canonical case (2) this reduces to (13) and the phase space is simply the upper-half unit circle. However if we choose a different function f the phase space arising from (35) can be considerably different from the canonical one. As a consequence we can even lose the compactness of the phase space. In the next sections we will study what happens with different choices for the function f. In particular we will look for functions for which the phase space remains compact.

The expression of (33) in terms of the x and y variables is given by

$$\frac{\dot{H}}{H^2} = -\frac{3}{2}\left[(1+w)(1+y^2 f) - 2wx^2\frac{\partial f}{\partial B}\right]. \tag{37}$$

From this we can extract the effective EoS parameter of the universe as

$$w_{\text{eff}} = w + (w+1)y^2 f - 2wx^2\frac{\partial f}{\partial B}. \tag{38}$$

We can also find the EoS of the scalar field. The energy density and pressure of ϕ are given, respectively, by

$$\rho_\phi = 2X\frac{\partial f}{\partial B} - Vf, \tag{39}$$

$$p_\phi = \mathcal{L}_\phi = Vf. \tag{40}$$

Note that ρ_ϕ coincides with the expression appearing in the Friedmann constraint (32) as expected. To be physically viable at the quantum level ϕ must satisfy $\rho_\phi > 0$. The EoS parameter of the scalar field is then

$$w_\phi = \frac{p_\phi}{\rho_\phi} = \left(2\frac{X}{V}\frac{1}{f}\frac{\partial f}{\partial B} - 1\right)^{-1}. \tag{41}$$

In the canonical case $f = B - 1$ this reduces to (11), while if f is constant, this simply becomes $w_\phi = -1$ describing a cosmological constant. Finally another useful quantity in scalar field cosmology is the so-called[3]speed of sound of adiabatic perturbations [50]. This is defined as

$$c_s^2 = \frac{\partial p_\phi}{\partial X}\Big/\frac{\partial \rho_\phi}{\partial X} = \left(1 + 2\frac{X}{V}\frac{\partial^2 f}{\partial X^2}\Big/\frac{\partial f}{\partial X}\right)^{-1}, \tag{42}$$

and for physically viable cosmological models we must require $c_s^2 > 0$. If this condition is dropped, then instabilities arise at the level of perturbations of the scalar fluid. For the canonical scalar field we find $c_s^2 = 1$ which implies that perturbations propagate at the speed of light.

[3]Strictly speaking c_s^2 as defined in (42) should be called the phase speed of perturbations, not the speed of sound; see [49].

At this point, in order to completely determine the dynamics of a specific model of noncanonical scalar field, we need to choose the form of the function f. Ideally we would like both to find interesting phenomenology at cosmological scales and to satisfy the physical conditions $\rho_\phi > 0$ and $c_s^2 > 0$. A possible attempt could be $f = -\exp(B)$. This choice seems indeed to yield some interesting features as one can realize looking at the EoS parameter for the scalar field which reads

$$w_\phi = \frac{-V}{2X+V} \quad \text{with} \quad \mathcal{L}_\phi = -Ve^{-X/V}. \tag{43}$$

Whenever $X \gg V$ we have $w_\phi \simeq 0$, while if $X \ll V$, we get $w_\phi \simeq -1$. The scalar field (43) can thus be used to characterize a dust fluid at early times and a cosmological constant at late times. Such a field could even be used to build a unified model of dark energy and dark matter, though the effects of the scalar field when $X \gg V$ would result really small since in this limit $\mathcal{L}_\phi \simeq 0$. Another drawback of this model is given by the speed of sound (42) which results to be

$$c_s^2 = \left(1 - \frac{2X}{V}\right)^{-1} \quad \text{with} \quad \mathcal{L}_\phi = -Ve^{-X/V}. \tag{44}$$

As we can note, as soon as $V < 2X$ we obtain $c_s^2 < 0$ which gives rise to instabilities at the level of perturbations. Also when $V = 2X$ the speed of sound diverges. We could overlook this problem for the sake of finding interesting phenomenology for the background evolution of the universe. However, as we shall see in Sec. V, dropping this assumption can actually lead to a much richer cosmology if one chooses a different model.

As we can realize the exponential Lagrangian (43) reduces to the canonical one at first order in X/V, so whenever this quantity is small, which usually happens at late times in cosmology, the exponential model is well approximated by the canonical scalar field. In this case the first corrections at second order would be determined by the term $-X^2/(2V)$. However, as we have seen above, the exponential Lagrangian (43) leads to instabilities at the perturbation level. Of course there could be another form for the function f which does not introduce such problems and which reduces to the canonical case when X/V is small. Corrections to the canonical Lagrangian will then be given by higher order power-law kinetic terms. Thus instead of guessing a specific form for the function f, we can take a starting point based on higher order (kinetic) corrections to the canonical Lagrangian. This will allow us to analyze models which both resemble the canonical scalar field at late times and are sufficiently simple to handle so that one can determine the complete cosmological dynamics of the scalar field.

We will then consider models which gives (kinetic) power-law corrections to the canonical case characterized

by the function $f = B - 1 + \xi B^n$ with ξ and n two real parameters. The corresponding Lagrangian reads

$$\mathcal{L}_\phi = X - V + \xi V \left(\frac{X}{V}\right)^n, \tag{45}$$

which is well defined only considering $n > 0$. The corrections to the canonical case are defined by the parameter n. For example, if $n = 2$, we have that the next-to-first-order corrections are of the square type, while if $n = 3$, these are of the cubic type. If instead $n < 1$, then we get corrections also at late times and the model does not reduce to a canonical scalar field.

The energy density (39) and speed of sound (42) for this model become, respectively,

$$\rho_\phi = V + X + (2n-1)\xi V \left(\frac{X}{V}\right)^n, \tag{46}$$

$$c_s^2 = \frac{X + \xi n V (\frac{X}{V})^n}{X + \xi n (2n-1) V (\frac{X}{V})^n}. \tag{47}$$

If we assume $n > 1/2$ and $\xi \geq 0$, these quantities are always positive and finite and thus physically viable. The case $n = 1/2$ is of particular interest and will be treated in Sec. V, while the value $\xi = 0$ yields back the canonical case. The scalar field EoS parameter is given by

$$w_\phi = \frac{X - V + \xi V (\frac{X}{V})^n}{X + V + \xi (2n-1) V (\frac{X}{V})^n} \tag{48}$$

and reduces to -1 for $V \gg X$ and to $1/(2n-1)$ for $V \ll X$ given $n > 1$. This model allows for a late time cosmological constantlike EoS while the early time value of (48) is determined by the parameter n. Note that for $n > 1$ the scalar field EoS at early times is always positive and smaller than 1.

In the next sections we will focus on the cases $n = 2$ and $n = 1/2$. The first one follows the philosophy of recovering a canonical scalar field at late times and will be studied in Sec. IV. The second one will introduce modifications at both early and late times and the phenomenology at cosmological scales will result much different and richer than the canonical one as we will see in Sec. V.

IV. SQUARE KINETIC CORRECTIONS

This section will be devoted to the dynamical analysis of background cosmologies arising from a scalar field described by Lagrangian (45) with $n = 2$:

$$\mathcal{L}_\phi = X - V + \xi \frac{X^2}{V}. \tag{49}$$

The parameter ξ will be allowed to take any real value. If $\xi = -1/2$, this model approximates the exponential model (43) at second order in the late time small quantity X/V. However ξ must be positive for physically viable models. In fact the energy density (46) and sound speed (47) reduce to, respectively,

$$\rho_\phi = X + V + 3\xi \frac{X^2}{V}, \tag{50}$$

$$c_s^2 = \frac{V + 2\xi X}{V + 6\xi X}. \tag{51}$$

These two quantities are always positive, for all values of X and V, only provided $\xi > 0$. Moreover we notice that the speed of sound of adiabatic perturbations reduces to one when $V \gg X$ and to $1/3$ when $V \ll X$. At early times the perturbations travels at one-third of the speed of light. The EoS parameter of the scalar field (48) becomes

$$w_\phi = \frac{XV - V^2 + \xi X^2}{XV + V^2 + 3\xi X^2}. \tag{52}$$

Interestingly this reduces to -1 when $V \gg X$ and to $1/3$ when $V \ll X$, implying that the scalar field acts as relativistic matter at early times and as an effective cosmological constant at late times. This feature signals that the model we are working with can lead to a physically sensible phenomenology at cosmological scales.

The cosmological equations (32) and (33) for this model are given, respectively, by

$$\frac{3H^2}{\kappa^2} = \rho + V + \frac{1}{2}\dot{\phi}^2 + \frac{3\xi}{4}\frac{\dot{\phi}^4}{V}, \tag{53}$$

$$3H^2 + 2\dot{H} = -\kappa^2 \left(p + \frac{1}{2}\dot{\phi}^2 - V + \frac{\xi}{4}\frac{\dot{\phi}^4}{V}\right), \tag{54}$$

while the scalar field equation (34) becomes

$$\left(1 + 3\xi\frac{\dot{\phi}^2}{V}\right)(\ddot{\phi} + 3H\dot{\phi}) + \left(1 - \frac{3\xi}{4}\frac{\dot{\phi}^4}{V^2}\right)\frac{\partial V}{\partial \phi} = 0. \tag{55}$$

To determine the complete dynamics of these equations, we now employ the dimensionless variables (12). The Friedmann constraint (53) can then be written as

$$\sigma^2 + x^2 + y^2 + 3\xi\frac{x^4}{y^2} = 1, \tag{56}$$

where now the relative scalar field energy density is given by

$$\Omega_\phi = x^2 + y^2 + 3\xi\frac{x^4}{y^4}. \tag{57}$$

The Friedmann constraint (56) can again be used to replace σ^2 in all the other cosmological equations. This will permit

us to write the dynamical equations as an autonomous system in the variable x and y, exactly as we did for the canonical field in Sec. II. In addition, given that $\sigma^2 > 0$ due to the assumption $\rho > 0$, the Friedmann constraint (56) reduces the phase space to be compact and delimited by the close geometric curve defined by $x^2 + y^2 + 3\xi x^4/y^2 = 1$. The boundary of the phase space now depends on the parameter ξ: the larger is ξ, the smaller is the phase space. The shape of the allowed phase space region can be observed in Fig. 5, where the right column shows the phase space for different values of ξ. The boundary of the region always presents an edge in the origin but otherwise is smooth. The phase space becomes the upper-half unit disk if $\xi \to 0$ as expected, while it reduces to the y axis for $\xi \to \infty$.

With the dimensionless variables (12) we can now write Eqs. (54) and (55) as the dynamical system

$$\begin{aligned} x' = \frac{1}{2y^2(6\xi x^2 + y^2)}[&18\xi^2(1-3w)x^7 \\ &- 3xy^4(6\xi x^2(w+1) + (w-1)(x^2-1)) \\ &+ 3\xi x^3 y^2((7-9w)x^2 + 6w - \sqrt{6}\lambda x + 2) \\ &+ y^6(\sqrt{6}\lambda - 3(w+1)x)], \end{aligned} \tag{58}$$

$$\begin{aligned} y' = \frac{1}{2y}[&3y^2(w+1)(1-y^2) + 3\xi(1-3w)x^4 \\ &- xy^2(\sqrt{6}\lambda + 3(w-1)x)]. \end{aligned} \tag{59}$$

Note that this system is invariant under the relation $y \mapsto -y$, which implies that the dynamics on the negative y half plane is symmetric to the one in the upper-half plane, exactly as it happens for the canonical scalar field. This again means that even if one drops the $V > 0$ assumption, the dynamics of the whole system can be determined by just the $y > 0$ analysis. Of course one always has to assume $V \neq 0$ in order for the model to not become singular. Also the transformation (20) leaves the system (58) and (59) unchanged, meaning that opposite values of λ lead to the same dynamics after a reflection over the y axis, again as it was in the canonical case. Note also that given $y > 0$ and $\xi > 0$ the system (58) and (59) is never singular. Moreover the origin can be taken to be part of the phase space since in the limit $x, y \to 0$ the system remains well defined as can be proved in polar coordinates.[4]

From Eq. (54) we can also obtain

$$\begin{aligned} \frac{\dot{H}}{H^2} = \frac{3}{2y^2}[&\xi(3w-1)x^4 + (w-1)x^2y^2 \\ &+ (w+1)y^2(y^2-1)], \end{aligned} \tag{60}$$

[4]Defining $x = r\cos\theta$ and $y = r\sin\theta$ the limit $r \to 0$ always well behaves but for the angles $\theta = 0, \pi$ which however, corresponding to $y = 0$, never happen to be part of the phase space.

TABLE II. Critical points of the system (58) and (59) and their properties. The coordinates of points B and C are given in the Appendix.

Point	x	y	Existence	$w_{\rm eff}$	Acceleration	Ω_ϕ	Stability
O	0	0	$\forall\lambda, \xi, w$	w	No	0	Unstable
B	App.		Fig. 4	w	No	App.	Stable
C	App.		$\forall\lambda, \xi, w$	App.	Fig. 4	1	Fig. 4

from which we can obtain the effective EoS parameter at any critical point (x_*, y_*) as

$$w_{\rm eff} = w - (w-1)x_*^2 - (w+1)y_*^2 - \xi(3w-1)\frac{x_*^4}{y_*^2}. \tag{61}$$

In the origin this reduces to the matter EoS parameter and the scalar field has no effects on the cosmological evolution. On the other side if $x = 0$ and $y = 1$, this becomes $w_{\rm eff} = -1$ and the universe undergoes a de Sitter expansion.

The critical points for the dynamical system (58) and (59), together with their properties, are listed in Table II, while existence and stability are explained in Fig. 4. Assuming the origin is part of the phase space because of the considerations above, there are now only up to three critical points. Because of the high powers in x and y of the system (58) and (59) the coordinate values of the critical points result quite lengthy and complicated. For this reason their explicit expression is given only in the Appendix.

(i) *Point O.*—As we already noticed the origin can be taken to be part of the phase space since the system (58) and (59) is regular at this point, as can be proved in polar coordinates. Of course it represents a matter dominated universe where the effective EoS parameter equals w and $\Omega_m = 1$. Interestingly the origin is now always an unstable node meaning that a completely matter dominated universe results unstable and eventually evolves to other configurations.

(ii) *Point B.*—This point represents again a scaling solutions where $w_{\rm eff} = w_\phi = w$ but the scalar field energy density does not vanish: $0 < \Omega_\phi < 1$. It exists only when the parameters λ and ξ lie inside region III of Fig. 4 and it is always the global attractor of the phase space when it appears. Again since the universe evolves as it was matter dominated, this point will never characterizes an accelerating solution.

(iii) *Point C.*—This point stands again for a completely scalar field dominated universe. In fact it always lies on the border of the phase space where $\Omega_m = \sigma = 0$, $\Omega_\phi = 1$ and $w_{\rm eff} = w_\phi$. However, in contrast with the canonical case, it appears in the phase space for all possible values of λ, ξ and w. For $\lambda \to \pm\infty$ this point moves along the border of the phase space eventually approaching the origin. Regions I and II

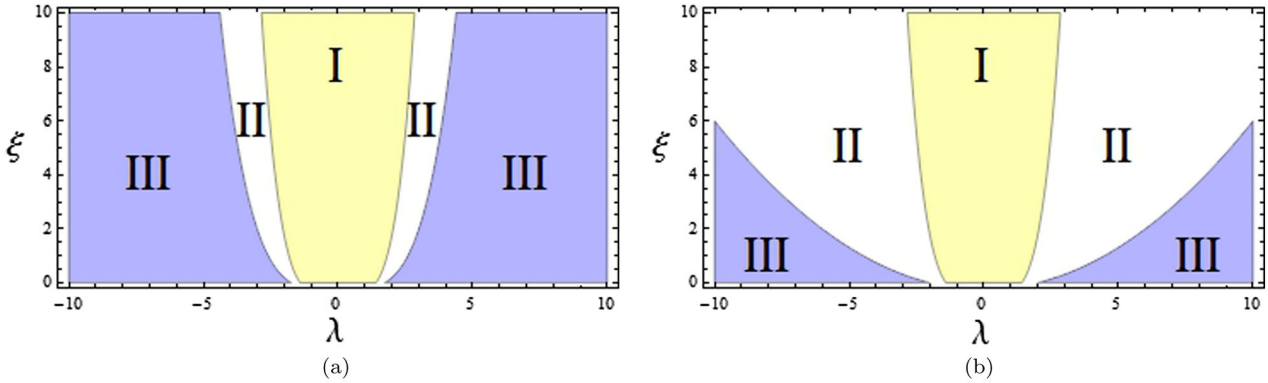

FIG. 4 (color online). Existence and stability in the parameter space (λ, ξ) of the critical points listed in Table II. A matter EoS has been chosen in the left panel (a) $w = 0$, while the corresponding relativistic case is shown in the right panel (b) $w = 1/3$. Region III denotes the existence of point B, while points O and C exist for every values of λ and ξ. In region I point C describes an accelerating universe, while in regions II and III it characterizes a decelerating universe. Point C is the global attractor in regions I and II, while it is a saddle point in region III where the global attractor is point B. The even-parity invariance of the pictures is due to the symmetry (20) of the system (58) and (59).

in Fig. 4 show the values of λ and ξ where point C is the global attractor of the phase space, while in region III it behaves as a saddle point being point B the global attractor. Region I of Fig. 4 represents the area in the (λ, ξ) plane where point C characterizes an inflationary or accelerating universe. In regions II and III instead the effective EoS parameter in point C is bigger than $-1/3$ and the universe undergoes a decelerating expansion.

The first feature that one notices in this model, once a comparison with the canonical case is done, is that the kinetic scalar field dominated solutions appearing as critical points $A_{\pm}$ of the system (18) and (19) now are never part of the phase space. They are replaced by the matter dominated origin which now acts as the early time unstable solution. In this model thus, instead of having a nasty kinetic dominated solution with $w_{\text{eff}} = 1$ at early time, we obtain a much more physical matter universe where $w_{\text{eff}} = w$. In other words, in this model a matter dominated universe results unstable and eventually evolves to a configuration where the energy density of the scalar field does not vanish. Notice also that points B and C reduce to their correspondent canonical ones in the limit $\xi \to 0$.

We can now have a look at the complete phase space dynamics for the three different regions of Fig. 4. This has been drawn in Fig. 5 where (a) and (b) represent region I, (c) and (d) region II and (e) and (f) region III. The left column shows how the dynamics of the phase space changes as the value of λ changes, while the right column shows how it changes as the values of ξ changes. As it is clear from Fig. 5, different values of λ do not change the shape of the phase space, while the value of ξ determines the boundary, and thus the shape, of the phase space. This is of course due to the Friedmann constraint (56) which depends on ξ as we already discussed above. The yellow shaded region represents again the zone of the phase space where the universe undergoes an accelerated expansion.

In Figs. 5(a) and 5(b) the phase spaces for the values $\lambda = 1$, $\xi = 1$ and $\lambda = 2$, $\xi = 4$ have been depicted. The only critical point appearing beside the origin is point C, which, being inside the yellow region, characterizes an accelerating solution. All the trajectories evolve from the unstable matter dominated solution at the origin towards the scalar field dominated solution at point C which acts as the global attractor. This dynamics well suits the phenomenology of our universe since with this parameter choice we can have a decelerated to accelerated transition describing the dominance of dark energy over dark matter at late times and the reverse situation at early times.

The phase space dynamics for region II of Fig. 4 has been drawn in Figs. 5(c) and 5(d) where the values $\lambda = 2$, $\xi = 1$ and $\lambda = 2$, $\xi = 1/2$ have been chosen, respectively. The only two critical points in the phase space are again the origin (early time unstable solution) and point C (late time attractor) which now lies outside the yellow region and thus describes a decelerating scalar field dominated universe. Note that, depending on initial conditions, some trajectories will still experience a stage of accelerated expansion before ending in point C. This particular evolution can thus be used to model universes with a transient inflationary era.

Finally the dynamics characterized by region III of Fig. 4 has been delineated in Figs. 5(e) and 5(f) where the values $\lambda = 4$, $\xi = 1$ and $\lambda = 2$, $\xi = 1/2$ have been chosen, respectively. There are now all three critical points in the phase space. The origin is again the early time unstable node, the global attractor is point B representing a scaling solution and point C is now a saddle point. Depending on initial conditions we can again have a transient acceleration era before ending at point B with a matterlike cosmological

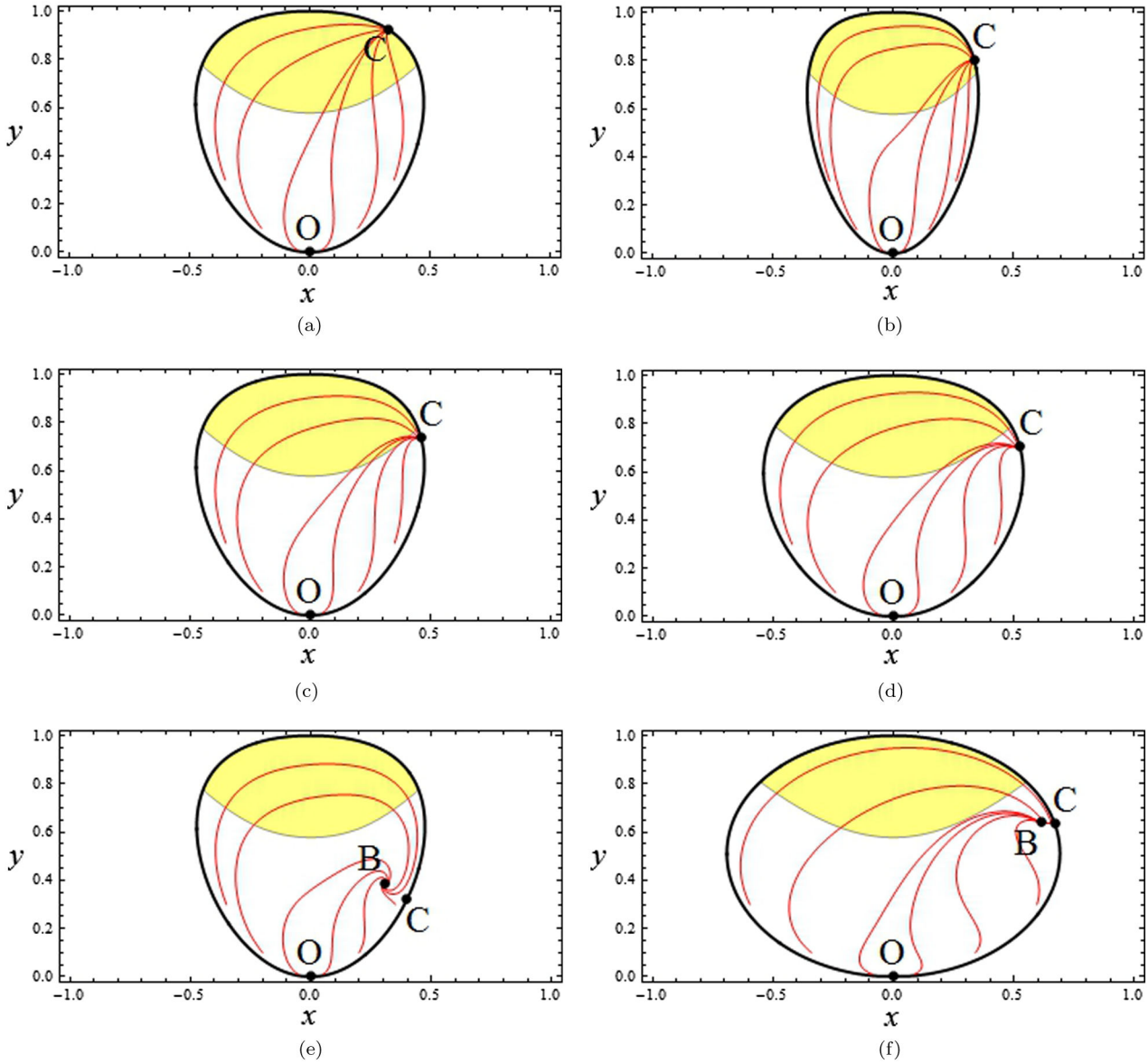

FIG. 5 (color online). Phase space of the dynamical system (58) and (59) with the value $w = 0$. The yellow shaded region represents the zone of the phase space where the universe undergoes an accelerated expansion. In the left column the phase space is shown for different values of λ, while in the right column increasing values of ξ have been displayed. Note how the boundary of the phase space changes for different values of ξ while it remains the same as λ changes. (a) $\lambda = 1$ and $\xi = 1$. (b) $\lambda = 2$ and $\xi = 4$. (c) $\lambda = 2$ and $\xi = 1$. (d) $\lambda = 2$ and $\xi = 1/2$. (e) $\lambda = 4$ and $\xi = 1$. (f) $\lambda = 2$ and $\xi = 1/10$.

evolution. This dynamics can be employed to build models of inflation where after the inflationary phase one obtains a graceful exit to the scaling solution.

To conclude this section we compare this model with the canonical scalar field of Sec. II. Both models present cosmological scaling solutions and late time inflationary attractors. They mainly differ in the early time dynamics where instead of having kinetic scalar field dominated solutions, in the noncanonical case only the matter dominated solution appears. This feature can be used to better motivate the phenomenology of dark energy. In fact with the model presented in this section a matter dominated universe is always unstable and eventually evolves to either a scaling or a scalar field dominated solution. For the right values of the parameters λ and ξ (see Fig. 4) the late time attractor characterizes an accelerated cosmological expansion implying a dynamics describing a transition from matter to dark energy domination in accordance with the current astronomical observations.

Of course, the model (49) being a subclass of (29), we also obtain cosmological scaling solutions, identified with point B in Fig. 5. As we commented in Sec. II these solutions are of great physical interest since they can hide the scalar field effects on the background cosmological

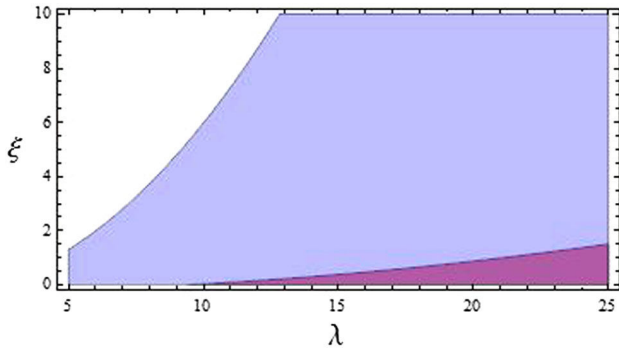

FIG. 6 (color online). Allowed values (purple darker region) for early time cosmological scaling solutions of the scalar field (49) [region III in Fig. 4(b)] permitted by nucleosynthesis observations. The same region appears for negative values of λ due to symmetry (20).

evolution. In the canonical case however there are strong constraints on the scalar field energy density obtained from nucleosynthesis observations which eventually impose $\lambda \gtrsim 9$. One could hope that for the scalar field (49) the constraint on λ would relax. Unfortunately the introduction of the square kinetic corrections, parameterized by ξ, does not help in this situation. As can be realized from Fig. 6, the allowed region of the (λ, ξ) space for a viable scaling solution at early times, when $w = 1/3$, is well separated from the late time acceleration region. The model (49) thus presents the same difficulties of the canonical case for hiding a scalar field at early times which eventually becomes relevant for dark energy phenomenology at late times.

The addition of the square kinetic correction (49) to the canonical Lagrangian complicates the resulting cosmological background equations. As a consequence the autonomous system of equations (58) and (59) contains power-law terms in x and y up to fifth order, in contrast with (18) and (19) where the highest order is the third. This implies that the critical points of the system are much more complex and difficult to find as it is shown in the Appendix. If one considers cubic or higher order kinetic corrections to the canonical scalar field Lagrangian, the corresponding cosmological dynamical system becomes almost impossible to analyze even with numerical techniques. The model (49) with square kinetic corrections is sufficiently simple to study and sufficiently different from the canonical case to present new phenomenology at cosmic distances, especially at early times where the scalar field kinetic dominated solutions no longer appear. If $\xi \ll 1$, the dynamics of the scalar field (49) approaches the corresponding canonical one. However as long as $\xi \neq 0$ the kinetic dominated solutions, corresponding to $x = \pm 1$ and $y = 0$, will never appear in the phase space. Interestingly if ξ is almost zero, these points effectively behave as saddle points, but for a nonvanishing ξ, no matter how small, they never characterize kinetic dominated solutions because we obtain $w_\phi = 1/3$ at that point. This implies a radiationlike evolution meaning that the scalar field behaves as relativistic matter.

V. SQUARE ROOT KINETIC CORRECTIONS

In this section we will consider square root kinetic corrections to the canonical scalar field Lagrangian. In other words we will study the model (45) with $n = 1/2$, which is simple to analyze and capable of providing interesting phenomenology at cosmological scales. The scalar field Lagrangian of this model is then

$$\mathcal{L}_\phi = X - V + \xi\sqrt{XV}, \tag{62}$$

where ξ is again a free parameter. Recall that V has been assumed to be positive and of the exponential form (16), which means there are no inconsistencies with the square root appearing in (62).

Before one proceeds with the analysis of the dynamical equations, a subtlety must be taken into account. The square root in (62) will provide terms containing $\sqrt{\dot\phi^2}$, or equivalently $\sqrt{x^2}$. This are strictly positive quantities which should be replaced by $|\dot\phi|$ or $|x|$. However this would prevent the autonomous system of equations from being differentiable in $x = 0$ and the whole dynamical system analysis would be impossible since the function f_x and f_y of (27) must be differentiable. For this reason we will replace $\sqrt{\dot\phi^2}$ with $\dot\phi$ in what follows, or equivalently $\sqrt{x^2} \mapsto x$. This operation can be made mathematically rigorous assuming that $\xi \mapsto s\xi$ with s the sign of $\dot\phi$, i.e. $s = 1$ if $\dot\phi > 0$ and $s = -1$ if $\dot\phi < 0$. Note that we could have choose the opposite branch, i.e. $\sqrt{\dot\phi^2} \mapsto -\dot\phi$ or $\sqrt{x^2} \mapsto -x$; however due to the symmetry (71) of the resulting dynamical system both the choices would result in the same cosmological dynamics.

With the scalar field (62), the energy density (46) and speed of sound (47) reduce, respectively, to

$$\rho_\phi = X + V, \tag{63}$$

$$c_s^2 = 1 + s\frac{\xi}{2}\sqrt{\frac{V}{X}} = 1 + \frac{\xi}{2}\frac{y}{x}. \tag{64}$$

Of course the energy density (63) corresponds to the canonical energy density (9). As we already noticed in Sec. III, we can always add a $\sqrt{B}$ term to the function f on the noncanonical scalar field (29) leaving the Friedmann constraint unmodified. For this reason the choice (62) yields nothing but the Friedmann constraint

$$1 = \sigma^2 + x^2 + y^2, \tag{65}$$

which corresponds to the one arising in the canonical case, i.e. (13). This equals saying that the (gravitating) energy density of the scalar field (62) is the same as the canonical one and that the square root term does not give any energy contribution. The scalar field relative energy density will thus be

$$\Omega_\phi = x^2 + y^2, \tag{66}$$

which equals (14).

The speed of sound (64) prevents the scalar field (62) from being physically viable. In fact it is easy to see that whenever $X = 0$, or $x = 0$, the speed of sound (64) diverges giving an infinite velocity of propagation for adiabatic perturbations. Moreover if $\xi x < 0$, we always obtain $c_s^2 < 0$ in some region of the phase space in which the scalar field will present instabilities at the perturbation level. The model (62) results thus to be theoretically instable and nonviable. However, despite all these drawbacks, in what follows we will ignore all the problems arising from Eq. (64). We will go on in analyzing the cosmological background dynamics implied by the scalar field (62) showing that it is capable of producing phenomenology which cannot be obtained with the canonical scalar field and which is slightly favored by astronomical observations.

The cosmological equations (33) and (34) now become, respectively,

$$2\dot{H} + 3H^2 = -\kappa^2\left(p + \frac{1}{2}\dot{\phi}^2 - V + \xi\dot{\phi}\sqrt{V}\right), \tag{67}$$

$$\ddot{\phi} + 3H\dot{\phi} + 3H\xi\sqrt{V} + \frac{\partial V}{\partial \phi} = 0. \tag{68}$$

Notice that though the scalar field energy density is the same, its pressure changes due to the ξ term. This is a peculiar feature of the square root term (62) which, despite having no gravitating energy, yields a nonzero pressure term into the acceleration equation (67). Moreover in the scalar field equation of motion the only modification due to ξ is a new term directly coupling H and the potential V. From these equations we obtain the following dynamical system:

$$x' = \frac{1}{2}[-3(w-1)x^3 - 3x[(w+1)y^2 - w + 1] + 3\sqrt{2}\xi x^2 y + \sqrt{2}y(\sqrt{3}\lambda y - 3\xi)], \tag{69}$$

$$y' = -\frac{1}{2}y[3(w-1)x^2 + 3(w+1)(y^2-1) + x(\sqrt{6}\lambda - 3\sqrt{2}\xi y)], \tag{70}$$

which generalizes the system (18) and (19) with the terms containing ξ. Note that Eqs. (69) and (70) are invariant under the simultaneous replacement

$$\lambda \mapsto -\lambda, \qquad \xi \mapsto -\xi, \qquad x \mapsto -x, \tag{71}$$

which implies that the phase space is symmetric around the y axis for opposite values of the parameters λ and ξ. In the $\xi \to 0$ limit the symmetry (71) becomes (20). The system is also invariant under the following transformation:

$$\xi \mapsto -\xi, \qquad y \mapsto -y, \tag{72}$$

which tells us that the dynamics in the $y < 0$ half phase space equals the one in the upper-half space after a redefinition of ξ. In the $\xi \to 0$ limit this reduces to the $y \mapsto -y$ symmetry of the canonical case. Equation (37) now reduces to

$$\frac{\dot{H}}{H^2} = \frac{3}{2}[(w-1)x^2 + (w+1)(y^2-1) - \sqrt{2}\xi xy] \tag{73}$$

and implies the following effective EoS parameter at any critical point (x_*, y_*):

$$w_{\text{eff}} = x_*^2 - y_*^2 + w(1 - x_*^2 - y_*^2) + \sqrt{2}\xi x_* y_*. \tag{74}$$

Exactly as in (61), the fact that now the parameter ξ is nonzero leads to new interesting phenomenology in comparison with the cosmology of the standard scalar field. The EoS parameter of the scalar field now reads

$$w_\phi = \frac{x^2 - y^2 + \sqrt{2}\xi xy}{x^2 + y^2} \tag{75}$$

and differs from the canonical (25) only by the ξ term in the numerator.

The critical points of the system (69) and (70) are listed in Table III, while their existence and stability properties are explained in Fig. 7. There are now seven possible critical points and up to six of them can appear in the phase space at the same time.

(i) *Point O.*—Again the origin of the phase space formally corresponds to a matter dominated universe where $w_{\text{eff}} = w$ and $\Omega_m = 1$. Its properties are unmodified being always a saddle point and existing for all values of the parameters.

(ii) *Points $A_\pm$.*—Also the two kinetic dominated solutions ($w_{\text{eff}} = w_\phi = 1$ and $\Omega_\phi = 1$), labeled by points $A_\pm$, still appear in the phase space presenting their standard behavior. In particular they are always saddle or unstable nodes depending on the absolute value of λ being smaller or greater than $\sqrt{6}$.

(iii) *Points $B_\pm$.*—These two points describe scaling solutions since in both of them $w_{\text{eff}} = w_\phi = w$ and the scalar field energy density does not vanish. In fact the relative energy density of the scalar field is

TABLE III. Critical points of the system (69) and (70) and their properties. The definitions of Ω_ϕ^B and $Q_\pm$ are given in (76) and (77), respectively.

Point	x	y	Existence	$w_{\rm eff}$	Acceleration	Ω_ϕ	Stability
O	0	0	$\forall\lambda,\xi,w$	w	No	0	Saddle
A_-	-1	0	$\forall\lambda,\xi,w$	1	No	1	Unstable if $\lambda \geq -\sqrt{6}$ Saddle if $\lambda < -\sqrt{6}$
A_+	1	0	$\forall\lambda,\xi,w$	1	No	1	Unstable if $\lambda \leq \sqrt{6}$ Saddle if $\lambda > \sqrt{6}$
$B_\pm$	$\sqrt{\frac{3}{2}\frac{(w+1)}{\lambda}}$	$\frac{\sqrt{3}}{2\lambda}(\xi \pm \sqrt{\xi^2-2w^2+2})$	Fig. 7	w	No	Ω_ϕ^B	Stable
C_-	$\frac{\sqrt{2}\lambda-\xi\sqrt{3\xi^2+6-\lambda^2}}{\sqrt{3}(\xi^2+2)}$	$\frac{\lambda\xi+\sqrt{6\xi^2+12-2\lambda^2}}{\sqrt{3}(\xi^2+2)}$	Fig. 7	Q_-	Fig. 7	1	Fig. 7
C_+	$\frac{\sqrt{2}\lambda+\xi\sqrt{3\xi^2+6-\lambda^2}}{\sqrt{3}(\xi^2+2)}$	$\frac{\lambda\xi-\sqrt{6\xi^2+12-2\lambda^2}}{\sqrt{3}(\xi^2+2)}$	Fig. 7	Q_+	No	1	Unstable

$$\Omega_\phi^B = \frac{3}{2\lambda^2}(\xi^2 \pm \xi\sqrt{\xi^2-2w^2+2}+2w+2), \quad (76)$$

which is always between 0 and 1 when point B exists. Their existence is given by regions $\mathrm{III}_\pm$ in Fig. 7 and depends also on the matter EoS parameter. The smaller the value of w, the bigger the existence region in the (λ,ξ) parameter space, as can be seen comparing the left and right panels of Fig. 7. Whenever these points are present they always represent the global attractor of the phase space, but never describe accelerating solutions.

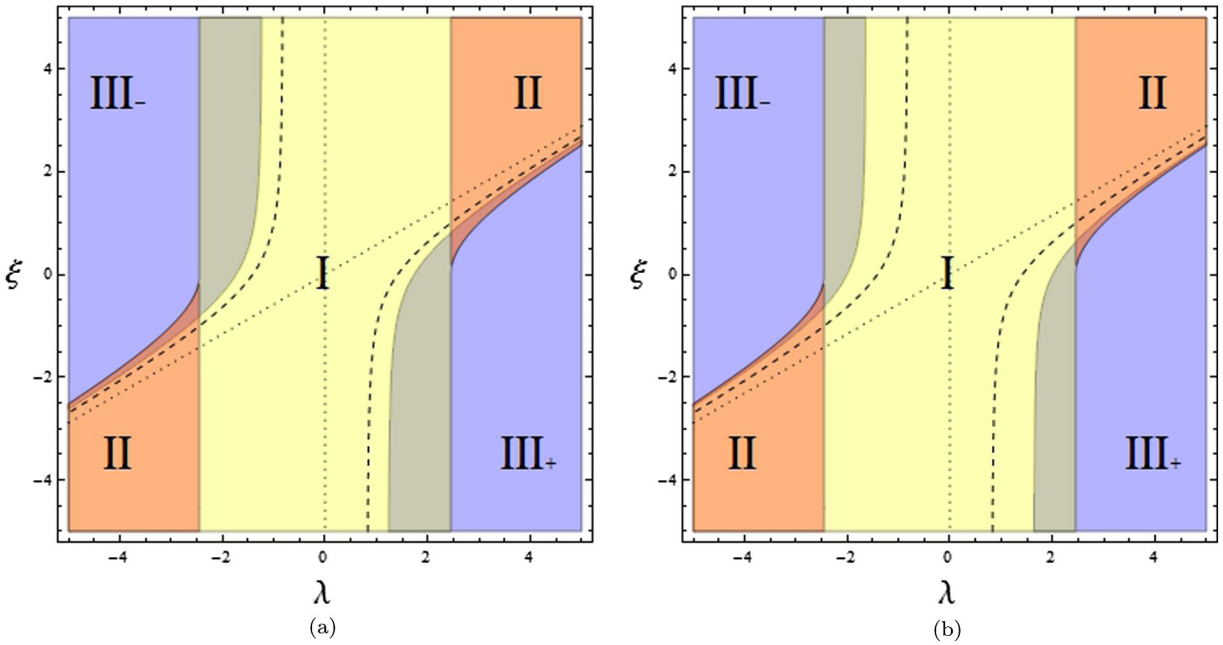

FIG. 7 (color online). Existence in the parameter space (λ,ξ) of the critical points $B_\pm$ and $C_\pm$ listed in Table III. A pressureless matter EoS ($w=0$) has been chosen in the left panel (a), while the relativistic case ($w=1/3$) is drawn in the right panel (b). In both cases we can identify four distinct zones. Inside zone I the only critical point appearing in the phase space, together with points $A_\pm$ and O, is point C_-, which behaves as the global attractor. Inside the disconnected zone II both points $C_\pm$ appear in the phase space, but point C_+ is always an unstable node and point C_- again acts as the global attractor. In zone III_- we find only points B_- and in zone III_+ we only have point B_+. They both represent the global attractor in their respective zone. In the cross regions $I/\mathrm{III}_\pm$ both points $B_\pm$ and C_- are present, but points $B_\pm$ represent the global attractors, while point C_- behaves as a saddle point. The same situation happens in the crossing regions $\mathrm{II}/\mathrm{III}_\pm$, but now also point C_+ is present and still acts as an unstable node. The connected region inside zones I and II delimited by the dashed lines identifies the region where point C_- represents an accelerating solution, while in the remaining parts of zones I and II point C_- represents a decelerating universe. As is clear from the picture the accelerated region of point C_- never overlaps zones $\mathrm{III}_\pm$, meaning that both accelerated and scaling solutions cannot exist together. Moreover the dotted lines inside the acceleration region identify the phantom regimes. The top right and bottom left parts represent a region where point C_- gives $w_{\rm eff} < -1$, while in the rest of the acceleration zone it gives $-1 < w_{\rm eff} < -1/3$. Finally the odd-parity invariance of the picture is due to the transformation (71) which leaves the dynamical system unchanged.

(iv) *Points $C_\pm$.*—These two points represent scalar field dominated solutions and thus always lie on the unit circle being $\Omega_\phi = 1$. In Fig. 7 the existence of point C_+ is given by the disconnected region II, while point C_- exists in both zones I and II. Point C_+ is always an unstable node, while point C_+ is always the global attractor but inside the cross regions $\mathrm{I}/\mathrm{III}_\pm$ and $\mathrm{II}/\mathrm{III}_\pm$ where it behaves as a saddle point. The effective EoS is given by $w_{\mathrm{eff}} = w_\phi = Q_\pm$, where

$$Q_\pm = \frac{2\lambda^2 - 3(\xi^2+2) \pm \lambda\xi\sqrt{6\xi^2 + 12 - 2\lambda^2}}{3(\xi^2+2)}. \quad (77)$$

This describes an inflationary solution in the connected region delineated by the dashed lines as drawn in Fig. 7. Unfortunately, for positive values of w, this accelerating region never overlaps the existence zones of points $B_\pm$ meaning that inflating and scaling solutions cannot live in the same phase space. These features appeared also in the standard case. Whenever both points B and C were present, the latter never described an inflationary solution as one can see from Fig. 2. Finally note that, depending on the choice of parameters λ and ξ, point C_- can also describe a phantom dominated universe where $w_{\mathrm{eff}} = w_\phi < -1$. The regions in the parameter space where this happens are delimited by the two dotted line crossing the origin in Fig. 7. The top right and bottom left parts denotes phantom solutions for point C_-, while in the rest of zones I and II we always find $w_{\mathrm{eff}} > -1$.

Note that critical points $B_\pm$ and $C_\pm$ reduce to points B and C of the canonical case of Sec. II in the limit $\xi \to 0$.

We will now have a look at the dynamics of the phase space for values of the parameters λ and ξ representing the different zones in Fig. 7. We will restrict our analysis to $w = 0$ since the qualitative dynamical features do not change with other values of the matter EoS parameter. Moreover because of the symmetry (71) we need only to study half of the parameter space, say $\lambda > 0$. The remaining half will describe identical phase spaces but for a reflection $x \mapsto -x$. In Figs. 8–12 the yellow shaded region identifies the part of the phase space where the EoS parameter of stationary points is smaller than $-1/3$, implying an accelerated cosmological solution. The blue (dark) part inside the yellow (shaded) region delimits the zone where the universe undergoes a phantom acceleration, i.e. where $w_{\mathrm{eff}} < -1$. Finally the green (shaded) region denotes the area of the phase space where the effective equations of state takes superstiff values, i.e. where $w_{\mathrm{eff}} > 1$.

We start considering zone I. If we choose $\lambda = 1$ and $\xi = 1$, the phase space looks like the one drawn in Fig. 8. Points $A_\pm$ are unstable nodes while the origin O represents the matter dominated saddle point. The global attractor is point C_- which happens to be inside the accelerated region

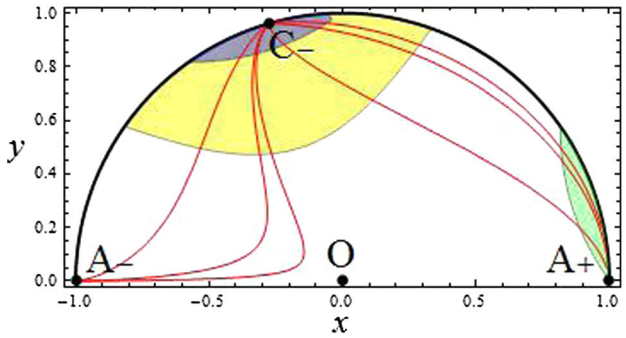

FIG. 8 (color online). Phase space with $w = 0$, $\lambda = 1$ and $\xi = 1$ (region I in Fig. 7). Point C_- is the global attractor describing a phantom accelerating solution.

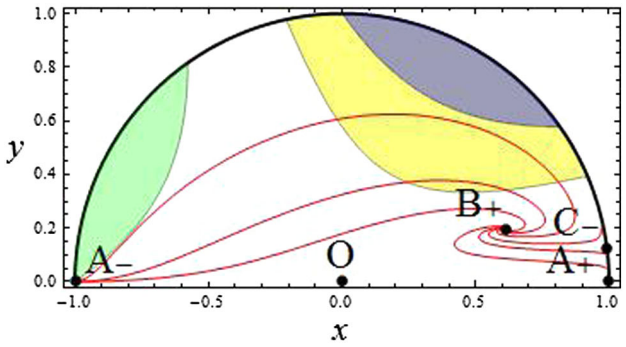

FIG. 9 (color online). Phase space with $w = 0$, $\lambda = 2$ and $\xi = -2$ (cross region $\mathrm{I}/\mathrm{III}_\pm$ in Fig. 7). Point C_- is a saddle point while point B_+ represents the global attractor describing a scaling solution with $w_{\mathrm{eff}} = w$.

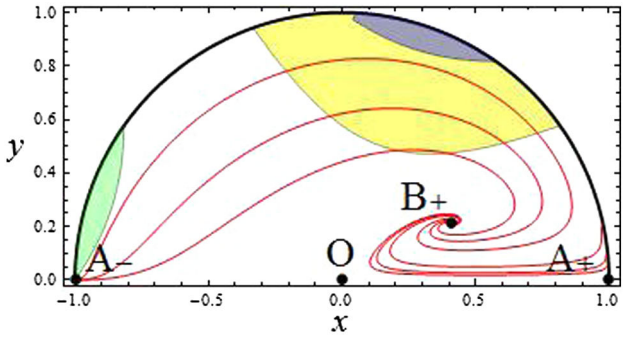

FIG. 10 (color online). Phase space with $w=0$, $\lambda=3$ and $\xi = -1$ (region III_+ in Fig. 7). Point B_+ is the global attractor describing a scaling solution with $w_{\mathrm{eff}} = w$.

and thus describes an inflationary solution with $w_{\mathrm{eff}} = -11/9$. Being also inside the phantom region this value is clearly smaller than -1. Moreover since it lies on the unit circle it characterizes a universe completely dominated by the scalar field. If we had chosen the parameters λ and ξ to be outside the connected region delimited by the dashed lines in Fig. 4 but still inside zone I,

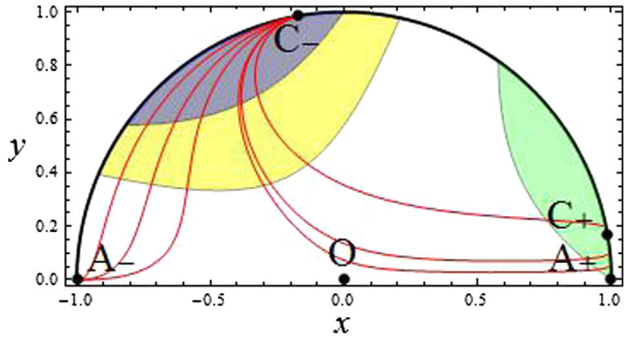

FIG. 11 (color online). Phase space with $w = 0$, $\lambda = 3$ and $\xi = 2$ (region II in Fig. 7). Point C_- is the global attractor and represents a phantom accelerated solution. Point C_+ is an unstable node characterizing a superstiff ($w_{\rm eff} > 1$) solution.

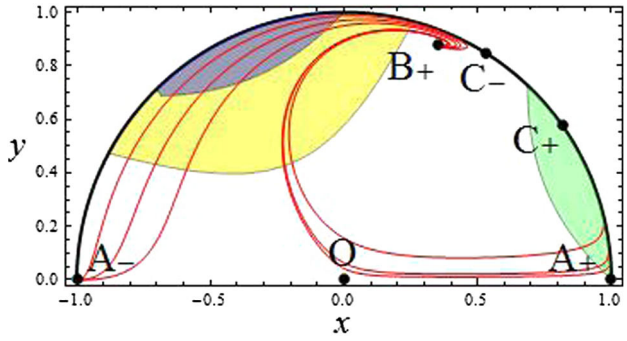

FIG. 12 (color online). Phase space with $w = 0$, $\lambda = 3.5$ and $\xi = 1.5$ (cross region II/III$_+$ in Fig. 7). Point B_+ is the global attractor scaling solution, while points $C_\pm$ represent a saddle and unstable node, respectively.

then point C_- would have been outside the accelerated region, though still on the circle. In that case it would have described a decelerating universe dominated by the scalar field. On the other hand if we had chosen parameters inside the acceleration region, but outside the phantom region, then we would have obtained an acceleration with $w_{\rm eff} > -1$. Note how the accelerated region is now different from the one in the standard case, Figs. 1–3. This is due to the difference between the two EoS parameters (24) and (74). Moreover because in Eq. (74) there is a dependence on ξ, the acceleration region will change whenever ξ is different, as in the next examples.

The second zone we analyze in Fig. 7 is the superposition region between zone I and zone III$_+$. Choosing the values $\lambda = 2$ and $\xi = -2$ the phase space can be depicted as in Fig. 9. Points $A_\pm$ and O are again unstable nodes and a saddle point, respectively. Point C_- is now a saddle point and the global attractor is point B_+ describing a cosmological scaling solution with effective EoS parameter matching the matter one. Point B_+ clearly lies outside the accelerated region which happens to be modified with respect to the one in Fig. 8, as we discussed above.

The phase space characterized by zone III$_+$ of Fig. 7 is depicted in Fig. 10 where the values $\lambda = 3$ and $\xi = -1$ have been chosen. Point B_+ is again the global attractor representing a cosmological scaling solution. Point A_- is still an unstable node, while point A_+ is now a saddle point exactly as the origin O.

In Fig. 11 the portrait of the phase space for zone II has been drawn. Now both points $C_\pm$ appear, one describing an unstable node (C_+) and the other one representing the global attractor (C_-) which can lie inside the phantom ($w_{\rm eff} < -1$), accelerated ($-1 < w_{\rm eff} < -1/3$) or decelerated ($w_{\rm eff} > -1/3$) regions depending on the values of λ and ξ. Points $A_\pm$ are unstable nodes and point O is a saddle point.

Finally the phase space of the region where zones II and III$_+$ superpose has been depicted in Fig. 12. Now points $C_\pm$ appear together with point B_+ representing a scaling solution. The situation is now similar to the one in Fig. 9 (crossing zone I/III$_+$): point B_+ is always the global attractor while point C_- is a saddle point. The only difference is now point C_+ which acts as an unstable node. Points $C_\pm$, representing the scalar field dominated solutions, always lie outside the accelerated region and thus never describe an inflationary solution. However, as it is clear from Fig. 12, before ending in point B_+ several trajectories pass through the accelerated (phantom) region, meaning that the universe undergoes a stage of accelerated (phantom) expansion before scaling as a matter dominated solution.

It is now interesting to compare the results we obtain from the model (62) with the ones following from the canonical scalar field of Sec. II. The square root term in (62) leads to a much richer phenomenology at cosmic distances which includes phantom late time solutions, scaling solutions, new early time unstable solutions, superstiff behavior and dynamical crossing of the phantom barrier at $w_{\rm eff} = -1$. Within this model one can not only achieve a matter to phantom transition at late times, but also phantom and superstiff transient eras. This can be easily seen from Figs. 8–12 where, depending on initial conditions, some trajectories of the phase space will cross the blue and green regions representing phantom and superstiff behavior, respectively. Thus the scalar field (62) can describe a universe which is phantom dominated at late times instead of being only dark energy dominated as it happens in the canonical case. Despite the problems at the level of cosmological perturbations arising from Eq. (64), the scalar field model (62) is actually better in agreement with the latest astronomical observations which favor a value $w_\phi < -1$ at present, though the minus one value still lies inside the two-sigma confidence limit [15,16]. The scalar field (62) can thus characterize a quintom scenario where the crossing of the phantom barrier happens at late times with the universe being nowadays dark energy dominated ($w_{\rm eff} > -1$) but evolving through a final

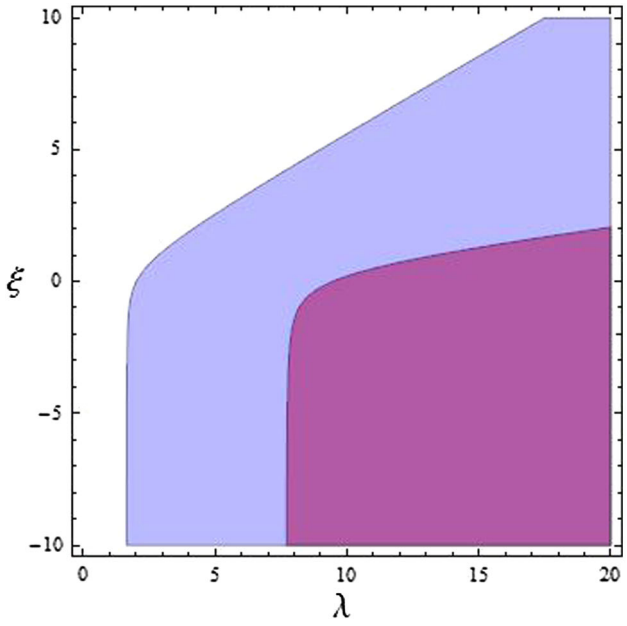

FIG. 13 (color online). Allowed values (purple darker region) for early time cosmological scaling solutions of the scalar field (62) [region III_+ in Fig. 7(b)] permitted by nucleosynthesis observations.

phantom era ($w_{\rm eff} < -1$). However in order to render this a viable model of our Universe one must first solve the problems arising at the level of cosmological perturbations.

Finally, the scalar field (62) being a subclass of (29), we obtain again cosmological scaling solutions (points $B_\pm$) which, as we said, can be of great phenomenological interest. The scalar field can in fact hide its presence at early times letting the cosmological evolution scale as a matter dominated universe. For this to happen however we need to satisfy the constraints derived from nucleosynthesis observations [46]. In Fig. 13 the region allowed by these constraints for point B_+ in the (λ, ξ) space is shown. For point B_- the same region appears at opposite values of λ and ξ due to the symmetry (71). The introduction of the square root term in (62) does not help in relaxing the $\lambda \gtrsim 9$ constraint of the canonical case. In fact, as can be realized from Fig. 13, the allowed region is well separated from the acceleration region of point C_-, meaning that scaling and late time accelerated solution cannot appear in the same phase space. The same happens in both the canonical case and the model of Sec. IV where the allowed region results to be much more constrained as can be understood comparing Figs. 13 and 6.

VI. CONCLUSION

In the present work the cosmological background evolution characterized by different scalar field models has been studied. The use of dynamical system techniques has allowed us to completely determine the cosmological features of canonical and noncanonical scalar fields. After the canonical model has been reviewed in Sec. II, extended scalar field Lagrangians have been presented and discussed in Sec. III. The analysis has then focused to models whose dynamics can be completely parameterized by the dimensionless variable (12) and which always lead to scaling solutions.

In Sec. IV a scalar field with square kinetic corrections to the canonical Lagrangian has been examined. The late time dynamics of the system results similar to the late time dynamics of the canonical case with the appearance of dark energy and scaling solutions. However the early time dynamics is completely different from the canonical one. In particular the scalar field kinetic dominated solutions no longer appear in the phase space of this model. The early time behavior is now characterized by a matter dominated solution, which is better in agreement with a radiation or dark matter dominated epoch as required by observations. The model can thus be used to describe a universe where dark energy becomes important only at late times while dark matter dominates at early times. It also happens to be safe at the level of perturbations once the condition $\xi > 0$ is assumed. Furthermore the phase space boundaries of the model presented in Sec. IV differ from the canonical ones. The phase space ceases to be the upper-half unit disk in the (x, y) plane and, remaining compact, assumes a form depending on the parameter ξ as can be seen from Fig. 5. This is an interesting mathematical feature which implies that the variables (12) can lead to different phase space boundaries depending on the scalar field Lagrangian one chooses.

Section V has been devoted to the study of the cosmological consequences of scalar field models with square root kinetic corrections to the canonical Lagrangian. The background dynamics of this model presents a richer phenomenology with respect to the canonical case. The early time behavior results similar to the canonical one, though superstiff ($w_{\rm eff} > 1$) transient regions always appear in the phase space. What changes more is the late time evolution where phantom dominated solutions, dynamical crossings of the phantom barrier and new scaling solutions emerge in the phase space. This model can thus be used to describe a late time dark energy dominated universe capable of dynamically crossing the phantom barrier ($w_{\rm eff} = -1$) as the astronomical observations slightly favor. Moreover we can achieve transient periods of superacceleration ($\dot{H} > 0$) where the universe expands only for a finite amount of time. These solutions are characterized by the trajectories that cross the phantom region in Figs. 8–12 and can be employed to build phantom models of inflation. The drawbacks arise of course at the level of perturbations where instabilities of the scalar field always appear. Until these problems are resolved the scalar field model of Sec. V cannot be seriously employed to describe physical universes.

Finally a comment on the choice of the potential $V(\phi)$. In this work the potential of the scalar field has always been assumed to be of the exponential type. Different choices of

$V(\phi)$ can be analyzed adding the variable (17) which will increase the dimensions of the phase space also in the noncanonical cases. If the potential is of the power-law type, then the phase space will always be three dimensional, but for different choices it is possible that more dimensions will be required. It is expected that the analysis of the noncanonical models with exponential potential considered in this work can be extended to other kinds of potentials in exactly the same way the canonical case has been generalized. For example one should be able to find the so-called tracker solutions in the inverse power-law potential case where the universe evolves as a scaling solution at early times and then approaches the dark energy dominated solution at late times [6]. Note that in the case studied in Sec. V one could also expect to find tracker solutions which let the universe evolve towards a phantom, rather than simple dark energy, dominated epoch at late times. It will be the task of future work to study and analyze the possible outcomes of the noncanonical models considered in this paper with potentials $V(\phi)$ different from the exponential one.

ACKNOWLEDGMENTS

The author would like to thank Christian Böhmer, Marco Bruni, Emmanuel Saridakis and David Wands for useful discussions and comments on the paper.

APPENDIX A

In this Appendix we will provide the coordinate values of the critical points of the system (58) and (59). For the sake of simplicity we will assume $w = 0$ in what follows.

Point B is identified by the coordinates

$$x_B = \frac{1}{\lambda}\sqrt{\frac{3}{2}}, \tag{A1}$$

$$y_B = \frac{\sqrt{3}}{4|\lambda|}(1+\sqrt{4\xi+1})^{1/2}, \tag{A2}$$

while point C assumes the complicated values

$$x_C = \frac{\Delta^{2/3} + 4\lambda\Delta^{1/3} - 36\xi(\lambda^2+4) + 7\lambda^2 - 36}{3\sqrt{6}(4\xi+1)\Delta^{1/3}}, \tag{A3}$$

$$y_C = \frac{1}{\sqrt{6}}[3(x_C^2+1) - \sqrt{6}\lambda x_C + \sqrt{36\xi x_C^4 + (3x_C^2 - \sqrt{6}\lambda x_C + 3)^2}]^{1/2}, \tag{A4}$$

where

$$\Delta = 54(48\xi^2 + 8\xi - 1)\lambda + (10 - 216\xi)\lambda^3 + 9(4\xi+1)[36\xi(\lambda^6 - 12\lambda^4 + 24\lambda^2 + 64) + 5184\xi^2\lambda^2 - (\lambda^2-6)^2(3\lambda^2-16)]^{1/2}. \tag{A5}$$

Note the complexity of the coordinates of point C where the best expression one can obtain for y_C is only in terms of x_C. Finally to obtain the effective EoS parameter and Ω_ϕ for point C one should insert expressions (A3) and (A4) into (61) and (57), respectively. These values have not been displayed due to their length.

[1] A. G. Riess *et al.* (Supernova Search Team Collaboration), Astron. J. **116**, 1009 (1998).
[2] S. Perlmutter *et al.* (Supernova Cosmology Project Collaboration), Astrophys. J. **517**, 565 (1999).
[3] S. Weinberg, Rev. Mod. Phys. **61**, 1 (1989).
[4] J. Martin, C. R. Phys. **13**, 566 (2012).
[5] I. Zlatev, L.-M. Wang, and P. J. Steinhardt, Phys. Rev. Lett. **82**, 896 (1999).
[6] E. J. Copeland, M. Sami, and S. Tsujikawa, Int. J. Mod. Phys. D **15**, 1753 (2006).
[7] S. Tsujikawa, Classical Quantum Gravity **30**, 214003 (2013).
[8] A. R. Liddle and D. H. Lyth, *Cosmological Inflation and Large Scale Structure* (Cambridge University Press, Cambridge, England, 2000).
[9] J. Magana and T. Matos, J. Phys. Conf. Ser. **378**, 012012 (2012).
[10] D. Bertacca, N. Bartolo, and S. Matarrese, Adv. Astron. **2010**, 1 (2010).
[11] C. Armendariz-Picon, V. F. Mukhanov, and P. J. Steinhardt, Phys. Rev. D **63**, 103510 (2001).
[12] A. Vikman, Phys. Rev. D **71**, 023515 (2005).
[13] G.-B. Zhao, J.-Q. Xia, M. Li, B. Feng, and X. Zhang, Phys. Rev. D **72**, 123515 (2005).
[14] R. R. Caldwell and M. Doran, Phys. Rev. D **72**, 043527 (2005).
[15] J.-Q. Xia, H. Li, and X. Zhang, Phys. Rev. D **88**, 063501 (2013).
[16] B. Novosyadlyj, O. Sergijenko, R. Durrer, and V. Pelykh, arXiv:1312.6579.
[17] R. R. Caldwell, Phys. Lett. B **545**, 23 (2002).
[18] Y.-F. Cai, E. N. Saridakis, M. R. Setare, and J.-Q. Xia, Phys. Rep. **493**, 1 (2010).
[19] E. J. Copeland, A. R. Liddle, and D. Wands, Phys. Rev. D **57**, 4686 (1998).
[20] L. Amendola, Phys. Rev. D **60**, 043501 (1999).
[21] O. Hrycyna and M. Szydowski, J. Cosmol. Astropart. Phys. 12 (2013) 016.

[22] H. Wei, Phys. Lett. B **712**, 430 (2012).
[23] C. Xu, E. N. Saridakis, and G. Leon, J. Cosmol. Astropart. Phys. 07 (2012) 005.
[24] J. M. Aguirregabiria and R. Lazkoz, Phys. Rev. D **69**, 123502 (2004).
[25] G. Leon and E. N. Saridakis, J. Cosmol. Astropart. Phys. 03 (2013) 025.
[26] X.-m. Chen, Y.-g. Gong, and E. N. Saridakis, J. Cosmol. Astropart. Phys. 04 (2009) 001.
[27] R. Lazkoz and G. Leon, Phys. Lett. B **638**, 303 (2006).
[28] Z.-K. Guo and N. Ohta, J. Cosmol. Astropart. Phys. 04 (2008) 035.
[29] C. Ahn, C. Kim, and E. V. Linder, Phys. Rev. D **80**, 123016 (2009).
[30] C. Kaeonikhom, D. Singleton, S. V. Sushkov, and N. Yongram, Phys. Rev. D **86**, 124049 (2012).
[31] T. Koivisto, D. Wills, and I. Zavala, arXiv:1312.2597.
[32] R.-J. Yang and G. Xiang-Ting, Classical Quantum Gravity **28**, 065012 (2011).
[33] J. De-Santiago, J. L. Cervantes-Cota, and D. Wands, Phys. Rev. D **87**, 023502 (2013).
[34] N. Tamanini and C. G. Böhmer, Phys. Rev. D **87**, 084031 (2013).
[35] T. S. Koivisto and N. J. Nunes, Phys. Rev. D **80**, 103509 (2009).
[36] C. G. Boehmer, N. Chan, and R. Lazkoz, Phys. Lett. B **714**, 11 (2012).
[37] N. Frusciante, M. Raveri, and A. Silvestri, J. Cosmol. Astropart. Phys. 02 (2014) 026.
[38] A. P. Billyard and A. A. Coley, Phys. Rev. D **61**, 083503 (2000).
[39] C. G. Boehmer, G. Caldera-Cabral, R. Lazkoz, and R. Maartens, Phys. Rev. D **78**, 023505 (2008).
[40] C. G. Boehmer, G. Caldera-Cabral, N. Chan, R. Lazkoz, and R. Maartens, Phys. Rev. D **81**, 083003 (2010).
[41] S. C. C. Ng, N. J. Nunes, and F. Rosati, Phys. Rev. D **64**, 083510 (2001).
[42] L. A. Urena-Lopez and M. J. Reyes-Ibarra, Int. J. Mod. Phys. D **18**, 621 (2009).
[43] V. V. Kiselev and S. A. Timofeev, Gen. Relativ. Gravit. **42**, 183 (2010).
[44] A. Nunes and J. P. Mimoso, Phys. Lett. B **488**, 423 (2000).
[45] J. P. Mimoso, A. Nunes, and D. Pavon, Phys. Rev. D **73**, 023502 (2006).
[46] R. Bean, S. H. Hansen, and A. Melchiorri, Phys. Rev. D **64**, 103508 (2001).
[47] F. Piazza and S. Tsujikawa, J. Cosmol. Astropart. Phys. 07 (2004) 004.
[48] S. Tsujikawa and M. Sami, Phys. Lett. B **603**, 113 (2004).
[49] A. J. Christopherson and K. A. Malik, Phys. Lett. B **675**, 159 (2009).
[50] J. Garriga and V. F. Mukhanov, Phys. Lett. B **458**, 219 (1999).

Appendix B

Generalized hybrid metric-Palatini gravity

N. Tamanini and C. G. Böhmer,
Generalized hybrid metric-Palatini gravity,
Phys. Rev. D **87** (2013) 8, 084031 [arXiv:1302.2355 [gr-qc]].

PHYSICAL REVIEW D **87,** 084031 (2013)

Generalized hybrid metric-Palatini gravity

N. Tamanini* and C. G. Böhmer†

Department of Mathematics, University College London, Gower Street, London WC1E 6BT, United Kingdom

(Received 6 March 2013; published 11 April 2013)

We introduce a new approach to modified gravity which generalizes the recently proposed hybrid metric-Palatini gravity. The gravitational action is taken to depend on a general function of both the metric and Palatini curvature scalars. The dynamical equivalence with a nonminimally coupled biscalar field gravitational theory is proved. The evolution of cosmological solutions is studied using dynamical systems techniques.

DOI: 10.1103/PhysRevD.87.084031 PACS numbers: 04.50.Kd, 98.80.−k

I. INTRODUCTION

In order to explain the present and initial accelerated expansions of the universe, a large variety of modified theories of gravity has been proposed in recent years. Among them, one of the most popular is $f(R)$ modified gravity, where the gravitational action depends on a general function of the curvature scalar R; see Ref. [1] for two reviews. To derive the gravitational field equations from those modified actions, two approaches are extensively used in the literature: the metric and the Palatini variational principles (see Ref. [2] for recent extensions of the Palatini variational method in modify gravity). In the so-called metric approach, one takes the metric $g_{\mu\nu}$ as the only dynamical variable and considers only variations of the action with respect to it. The so-called Palatini approach is based on the idea of considering the connection defining the Riemann curvature tensor to be *a priori* independent of the metric. As such, one performs variations of the action with respect to the metric and the connection independently. Both approaches have been used extensively to build cosmological models, many of which contain an era of accelerated expansion.

It is well known that $f(R)$ theories are dynamically equivalent to Brans-Dicke (BD) theories. In fact, metric $f(R)$ gravity has been shown to be dynamically equivalent to Brans-Dicke theories with vanishing BD parameter, while Palatini $f(R)$ gravity presents the same equivalence if the BD parameter equals $-3/2$ (see again Ref. [1]). The value $-3/2$ for the BD parameter is a peculiar one since it implies no dynamics for the scalar field in BD theories. Consequently, Palatini $f(R)$ gravity has the same number of dynamical degrees of freedom as general relativity; see Ref. [3] for a very different model that also does not introduce new dynamical degrees of freedom.

More recently, a novel approach to modified gravity has been introduced, where a Palatini-like $f(\mathcal{R})$ term is added to the metric Einstein-Hilbert action [4]. In this context cosmological and astrophysical applications together with wormhole geometries have been studied in Ref. [5], where it has also been shown that viable accelerating cosmological solutions are allowed by some specific models. The theory is dynamically equivalent to a scalar-tensor theory with nonminimal coupling to gravity given by $(1 + \phi)R$, where R is the metric curvature scalar and ϕ is the scalar field. This is done in strict analogy with Palatini $f(R)$ gravity and, indeed, the BD parameter for this theory is still $-3/2$. However, because of the different coupling to R compared with BD theories, in this theory the scalar field is dynamical and represents a new dynamical degree of freedom.

In the present paper, we analyze a natural extension of the theory introduced in Ref. [4]. We introduce a general function that depends on both the metric and Palatini curvature scalars. We show that this new generalization can be considered as dynamically equivalent to a gravitational theory with two scalar fields. Only one of these scalar fields is nonminimally coupled to R, and in general an interaction between the two appears in the action. The cosmological features of the theory are then studied using dynamical system techniques.

Let us define $\kappa^2 = 8\pi G/c^4$ and start from the action

$$S_f = \frac{1}{2\kappa^2}\int d^4x\sqrt{-g}f(R,\mathcal{R}), \tag{1}$$

which generalizes the so-called hybrid metric-Palatini action of Ref. [4]; see also Ref. [6] for a similar study. In action (1) R is the Ricci curvature scalar formed with the Levi-Civita connection,

$$\Gamma^{\lambda}_{\mu\nu} = \frac{1}{2}g^{\lambda\sigma}(\partial_\mu g_{\nu\sigma} + \partial_\nu g_{\mu\sigma} - \partial_\sigma g_{\mu\nu}), \tag{2}$$

while $\mathcal{R}$ is the curvature scalar of an independent torsionless connection $\hat{\Gamma}^{\lambda}_{\mu\nu}$, in analogy with the Palatini approach. The variation of the action (1) with respect to the independent connection $\hat{\Gamma}^{\lambda}_{\mu\nu}$ leads to

$$\hat{\nabla}_\lambda\left(\sqrt{-g}\frac{\partial f}{\partial\mathcal{R}}g^{\mu\nu}\right) = 0, \tag{3}$$

whose solution is a Levi-Civita connection in terms of the conformal metric $h_{\mu\nu} = \frac{\partial f}{\partial\mathcal{R}}g_{\mu\nu}$,

*n.tamanini.11@ucl.ac.uk
†c.boehmer@ucl.ac.uk

$$\hat{\Gamma}^{\lambda}_{\mu\nu} = \frac{1}{2}h^{\lambda\sigma}(\partial_\mu h_{\nu\sigma} + \partial_\nu h_{\mu\sigma} - \partial_\sigma h_{\mu\nu}). \tag{4}$$

The variation with respect to the metric yields

$$\frac{\partial f}{\partial R}R_{\mu\nu} - \frac{1}{2}g_{\mu\nu}f - (\nabla_\mu\nabla_\nu - g_{\mu\nu}\Box)\frac{\partial f}{\partial R} + \frac{\partial f}{\partial \mathcal{R}}\mathcal{R}_{\mu\nu} = 8\pi T_{\mu\nu}, \tag{5}$$

where also the matter action has been considered in the variation. Because of (4), $\mathcal{R}_{\mu\nu}$ can be related to $R_{\mu\nu}$ and terms involving (derivatives of) $\partial f/\partial\mathcal{R}$ as in Palatini $f(R)$. However, the trace of (5) now relates $\mathcal{R}$ and its derivatives to T and $g_{\mu\nu}$, meaning that it is not possible, in general, to solve for $\mathcal{R}$. However, this can be avoided by requiring $\partial^2 f/\partial R\partial\mathcal{R} = 0$. In this particular case, the trace of (5) becomes an algebraic equation in $\mathcal{R}$, which can be solved for T and (derivatives of) $g_{\mu\nu}$. Note that in the following we will keep the function f completely arbitrary as it turns out that all results we will obtain hold for any (sufficiently smooth) function f.

II. DYNAMICALLY EQUIVALENT ACTIONS AND CONFORMAL TRANSFORMATIONS

Let us start by considering the action

$$S = \frac{1}{2\kappa^2}\int d^4x\sqrt{-g}\Big[f(\alpha,\beta) + \frac{\partial f(\alpha,\beta)}{\partial\alpha}(R-\alpha) + \frac{\partial f(\alpha,\beta)}{\partial\beta}(\mathcal{R}-\beta)\Big], \tag{6}$$

where α and β are two scalar fields. Variation with respect to α and β gives the system

$$\frac{\partial^2 f}{\partial\alpha^2}(R-\alpha) + \frac{\partial^2 f}{\partial\alpha\partial\beta}(\mathcal{R}-\beta) = 0, \tag{7}$$

$$\frac{\partial^2 f}{\partial\alpha\partial\beta}(R-\alpha) + \frac{\partial^2 f}{\partial\beta^2}(\mathcal{R}-\beta) = 0, \tag{8}$$

whose only solution is given by $\alpha = R$ and $\beta = \mathcal{R}$, provided that

$$\frac{\partial^2 f}{\partial\alpha^2}\frac{\partial^2 f}{\partial\beta^2} \neq \left(\frac{\partial^2 f}{\partial\alpha\partial\beta}\right)^2. \tag{9}$$

This condition follows simply from requiring that this matrix-type equation is nondegenerate. It is interesting to note that the matrix involved is in fact the Hessian of f. Since our theory is based on an action principle, a nondegenerate Hessian in this context means nothing but that solutions of the field equations derived from the action are indeed stationary points of the action.

It is now clear that substituting this solution back into action (6) immediately produces action (1). The two actions are thus dynamically equivalent. Constraint (9) excludes from our analysis the cases when the function f is linear in either α (i.e. R) or β (i.e. $\mathcal{R}$). However, the first case is nothing but the hybrid metric-Palatini theory studied in Refs. [4,5], while the second is equivalent to usual metric $f(R)$ theories. Moreover, constraint (9) also excludes some particular models such as $f = \exp(R+\mathcal{R})$ or $f = \sqrt{R\mathcal{R}}$. We have thus to reduce the results of this section to the models satisfying (9).

Let us define two new scalar fields as

$$\chi = \frac{\partial f(\alpha,\beta)}{\partial\alpha} \quad \text{and} \quad \xi = -\frac{\partial f(\alpha,\beta)}{\partial\beta}. \tag{10}$$

The minus sign in the definition of ξ is required in order not to allow for a negative kinetic energy of the field. Action (6) can be rewritten as

$$S = \frac{1}{2\kappa^2}\int d^4x\sqrt{-g}[\chi R - \xi\mathcal{R} - V(\chi,\xi)], \tag{11}$$

where the interaction potential is defined as

$$V(\chi,\xi) = -f(\alpha(\chi),\beta(\xi)) + \chi\alpha(\chi) - \xi\beta(\xi). \tag{12}$$

Due to solution (4) (which can also be obtained varying action (11) with respect to $\hat{\Gamma}^{\lambda}_{\mu\nu}$), we can expand $\mathcal{R}$ and find (up to boundary terms)

$$S = \frac{1}{2\kappa^2}\int d^4x\sqrt{-g}\Big[(\chi-\xi)R - \frac{3}{2\xi}(\partial\xi)^2 - V(\chi,\xi)\Big]. \tag{13}$$

We can shift χ by ξ defining a new scalar field as $\phi = \chi - \xi$. In this way the action becomes

$$S = \frac{1}{2\kappa^2}\int d^4x\sqrt{-g}\Big[\phi R - \frac{3}{2\xi}(\partial\xi)^2 - W(\phi,\xi)\Big]. \tag{14}$$

It is possible to think of action (14) as a Brans-Dicke theory with vanishing BD parameter and a potential interacting with another minimally coupled scalar field.

At this point we can perform a conformal transformation in order to switch from the Jordan to the Einstein frame. The transformation

$$g_{\mu\nu} \mapsto \tilde{g}_{\mu\nu} = \phi g_{\mu\nu} \tag{15}$$

allows us then, up to surface terms, to rewrite action (14) as

$$S = \frac{1}{2\kappa^2}\int d^4x\sqrt{-\tilde{g}}\Big[\tilde{R} - \frac{3}{2\phi^2}(\partial\phi)^2 - \frac{3}{2\phi\xi}(\partial\xi)^2 - \frac{W(\phi,\xi)}{\phi^2}\Big]. \tag{16}$$

Finally, we redefine the two scalar fields as

$$\tilde{\phi} = \sqrt{\frac{3}{2}}\frac{\ln\phi}{\kappa} \quad \text{and} \quad \tilde{\xi} = \frac{2\sqrt{2}}{\kappa}\sqrt{\xi}, \tag{17}$$

and the action becomes

$$S = \int d^4x\sqrt{-\tilde{g}}\Big[\frac{1}{2\kappa^2}\tilde{R} - \frac{1}{2}(\tilde{\nabla}\tilde{\phi})^2 - \frac{1}{2}e^{-\sqrt{2}\kappa\tilde{\phi}/\sqrt{3}}(\tilde{\nabla}\tilde{\xi})^2 - \tilde{W}(\tilde{\phi},\tilde{\xi})\Big], \quad (18)$$

where the new potential is defined as

$$\tilde{W}(\tilde{\phi},\tilde{\xi}) = \frac{1}{2\kappa^2}e^{-2\sqrt{2}\kappa\tilde{\phi}/\sqrt{3}}W(e^{\sqrt{2}\kappa\tilde{\phi}/\sqrt{3}}, \kappa^2\tilde{\xi}^2/8). \quad (19)$$

Action (18) is well known within the context of the so-called Brans-Dicke or two-field inflation [7–9], where the scalar field ϕ represents the Brans-Dicke field, while ξ denotes the inflaton. Usually these studies start from a more general action than (14), where a kinetic term for ϕ is also considered, but do not allow for a coupling between the two scalar fields in the potential [7]. A more general coupling between the scalar ϕ and R was considered in Ref. [8]. In the Einstein frame this leads to a general function of $\tilde{\phi}$ in the exponential coupling to the kinetic term of $\tilde{\xi}$. In general, we can address action (18) as a specific model of Brans-Dicke inflation with vanishing BD parameter. This means that from hybrid metric-Palatini gravity we have a natural explanation for introducing both the inflaton and the Brans-Dicke scalar fields. We refer to Ref. [9] for recent developments in the context of two-field inflation.

In the next section we will analyze the general cosmological dynamics of the theory in the Einstein frame.

III. COSMOLOGICAL DYNAMICS IN THE EINSTEIN FRAME

For the sake of simplicity, from now on we will omit the tildes in action (18). In other words, in what follows we will denote with $g_{\mu\nu}$, ϕ, ξ and W the quantities in the Einstein frame. The field equations can be obtained by varying action (18) with respect to the dynamical variables $g_{\mu\nu}$, ϕ and ξ. The gravitational field equations in the Einstein frame are thus given by

$$G_{\mu\nu} = \kappa^2(T^{(\phi)}_{\mu\nu} + e^{-\kappa\phi\sqrt{2/3}}T^{(\xi)}_{\mu\nu} - g_{\mu\nu}W), \quad (20)$$

where we define

$$T^{(\phi)}_{\mu\nu} = \nabla_\mu\phi\nabla_\nu\phi - \frac{1}{2}g_{\mu\nu}(\nabla\phi)^2, \quad (21)$$

$$T^{(\xi)}_{\mu\nu} = \nabla_\mu\xi\nabla_\nu\xi - \frac{1}{2}g_{\mu\nu}(\nabla\xi)^2. \quad (22)$$

For the moment we assume that every other form of matter is negligible in comparison to the two scalar fields. The equations for the two scalar fields are given by

$$\Box\phi + \frac{\kappa}{\sqrt{6}}e^{-\kappa\phi\sqrt{2/3}}(\nabla\xi)^2 - W_\phi = 0, \quad (23)$$

$$\Box\xi + \frac{\kappa\sqrt{2}}{\sqrt{3}}\nabla_\mu\phi\nabla^\mu\xi - e^{\kappa\phi\sqrt{2/3}}W_\xi = 0, \quad (24)$$

where W_ϕ and W_ξ are the derivatives of the potential with respect to ϕ and ξ.

We consider a cosmological Friedmann-Leimatre-Robertson-Walker metric

$$ds^2 = -dt^2 + a(t)^2\Big(\frac{dr^2}{1-kr^2} + r^2d\Omega^2\Big), \quad (25)$$

where $a(t)$ is the scale factor. From the gravitational field equations (20), we obtain the following cosmological equations:

$$3\frac{k}{a^2} + 3H^2 = \frac{\kappa^2}{2}e^{-\sqrt{2/3}\kappa\phi}\dot{\xi}^2 + \frac{\kappa^2}{2}\dot{\phi}^2 + \kappa^2W, \quad (26)$$

$$\frac{k}{a^2} + 2\dot{H} + 3H^2 = -\frac{\kappa^2}{2}e^{-\sqrt{2/3}\kappa\phi}\dot{\xi}^2 - \frac{\kappa^2}{2}\dot{\phi}^2 + \kappa^2W. \quad (27)$$

The scalar fields equations (23) and (24) give the following evolution equations:

$$\ddot{\phi} + 3H\dot{\phi} + \frac{\kappa}{\sqrt{6}}e^{-\sqrt{2/3}\kappa\phi}\dot{\xi}^2 + W_\phi = 0, \quad (28)$$

$$\ddot{\xi} + 3H\dot{\xi} - \frac{\kappa\sqrt{2}}{\sqrt{3}}\dot{\xi}\,\dot{\phi} + e^{\sqrt{2/3}\kappa\phi}W_\xi = 0. \quad (29)$$

In what follows we will consider only spatially flat ($k = 0$) cosmological models. In order to recast the cosmological equations (26)–(29) into a dynamical system, we will make use of the following dimensionless variable:

$$x^2 = \frac{\kappa^2\dot{\phi}^2}{6H^2}, \qquad y^2 = \frac{\kappa^2W}{3H^2}, \qquad s^2 = \frac{\kappa^2\dot{\xi}^2}{6H^2}e^{-\sqrt{2/3}\kappa\phi}. \quad (30)$$

The definitions of the x and y variables have been extensively considered to study the cosmological dynamics in both uncoupled and coupled dark energy–dark matter models [10]. With (30) the Friedmann constraint (26) reads

$$x^2 + y^2 = 1 - s^2, \quad (31)$$

impliying that

$$0 \le x^2 + y^2 \le 1, \quad (32)$$

since $0 \le s^2 \le 1$. Moreover, because of the positiveness of the potential energy, we must have $y \ge 0$, which implies that x and y can only take values within half a unit disc.

In order to complete the autonomous system of equations coming from the cosmological equations (27)–(29), we must specify the potential W. In the following we will consider three possible cases for W and will analyze the resulting phase spaces.

A. Model 1: $W = W_0 e^{-\lambda\kappa\phi/\sqrt{6}}$

First we will consider the usual quintessence exponential potential given by

$$W = W_0 e^{-\lambda\kappa\phi/\sqrt{6}}, \tag{33}$$

where W_0 and λ are both positive constants. In this model the only interaction between ϕ and ξ is given by the kinetic coupling because the potential W depends on ϕ only. The scalar field ϕ plays the role of the usual quintessence dark energy field, while we can consider ξ as representing dark matter. Both dark matter and dark energy have thus a geometrical origin in this model, and no particles have to be opportunely introduced.

In terms of the variables (30), Eq. (27) becomes

$$\frac{\dot{H}}{H^2} = 3(y^2 - 1), \tag{34}$$

which always gives a scaling solution for $a(t)$ in terms of the value of y. If $y = 1$ we have $\dot{H} = 0$, and the universe undergoes an exponential expansion, while if $y > \sqrt{2/3}$ the universe undergoes a scaling accelerated expansion. From (34) we can read off the effective equation of state parameter of the total energy content of the universe as

$$w_{\text{eff}} = 1 - 2y^2. \tag{35}$$

The autonomous system of equation is in this case two dimensional, and it is given by Eqs. (28) and (29) as

$$x' = x^2 - 3xy^2 + \frac{1}{2}(\lambda + 2)y^2 - 1, \tag{36}$$

$$y' = -\frac{1}{2}y(\lambda x + 6y^2 - 6), \tag{37}$$

where a prime denotes differentiation with respect to $N = \ln a$. There are up to four critical points for this system. The points and their properties are shown in Table I. There are three possible qualitative behaviors of the phase space, depending on the following three ranges for λ: $0 < \lambda \leq \sqrt{37} - 1$, $\sqrt{37} - 1 \leq \lambda \leq 6$ and $\lambda > 6$.

From Table I we see that in order to have a stable accelerated attractor, we must have $\lambda < 2\sqrt{3}$, so the most interesting solutions will belong to the first range whose phase space is shown in Fig. 1. Points A_- and A_+ are, respectively, a saddle and unstable point and represent early time solutions with a stiff fluid effective equation of state. Every solution evolves eventually, reaching point C, which always lies on the unit circle and acts as a global attractor. If $\lambda < 2\sqrt{3}$, point C belongs to the region above the dashed/red line where the universe is accelerating. If instead $2\sqrt{3} \leq \lambda \leq \sqrt{37} - 1$, point C will be below the dashed/red line and the universe will end in a decelerating solution. However, we can still have a period of accelerated expansion because, for a wide range of initial conditions, the evolution still passes through the accelerated region for some time as is shown in Fig. 2. If $\lambda = 3\sqrt{2}$ the global attractor will represent a matter-dominated universe with vanishing effective equation of state parameter, while for $\lambda = 2\sqrt{6}$ the final state will be a radiationlike dominated universe, which suggests that this model could be of interest in early time inflationary dynamics.

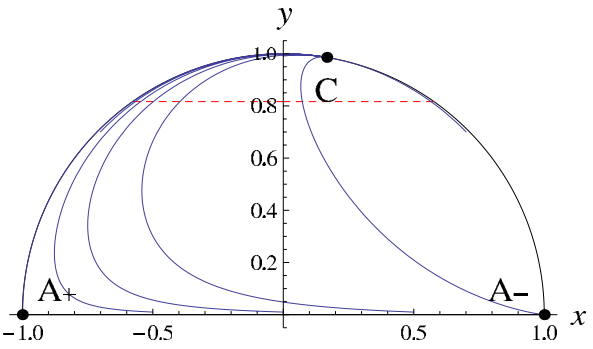

FIG. 1 (color online). Phase space for model 1 with $\lambda = 1$. The global attractor represents an accelerating solution because it lies in the region above the dashed/red line.

The phase space for the range $\sqrt{37} - 1 \leq \lambda \leq 6$ has been drawn in Fig. 3. Point B is now the global attractor and always represents a decelerating solution since it can only appear below the dashed/red line. Point C is now a saddle point, which attracts all the trajectories before they turn to point B. Again, depending on the initial conditions, the universe can still undergo a phase of accelerated expansion since several trajectories pass through the accelerated region above the dashed/red line.

The last range for which the dynamics of model 1 is different is given for $\lambda > 6$. Its phase space is depicted in

TABLE I. Critical points and their properties for model 1.

Point	x	y	Existence	w_{eff}	Acceleration	Stability
A_-	-1	0	$\forall\ \lambda$	1	No	Saddle
A_+	1	0	$\forall\ \lambda$	1	No	Unstable if $\lambda \leq 6$ Saddle if $\lambda > 6$
B	$\frac{6}{\lambda+2}$	$\frac{\sqrt{2}}{\sqrt{\lambda+2}}$	$\lambda \geq \sqrt{37} - 1$	$\frac{\lambda-2}{\lambda+2}$	No	Saddle if $\lambda = \sqrt{37} - 1$ Stable spiral if $\lambda > \sqrt{37} - 1$
C	$\frac{\lambda}{6}$	$\frac{\sqrt{36-\lambda^2}}{6}$	$\lambda \leq 6$	$\frac{\lambda^2}{18} - 1$	$\lambda < 2\sqrt{3}$	Stable if $\lambda < \sqrt{37} - 1$ Saddle if $\sqrt{37} - 1 \leq \lambda \leq 6$

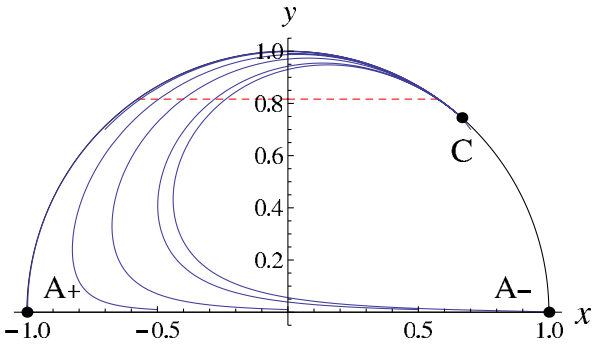

FIG. 2 (color online). Phase space for model 1 with $\lambda = 4$. The global attractor does not represent an accelerating solution because it lies in the region below the dashed/red line.

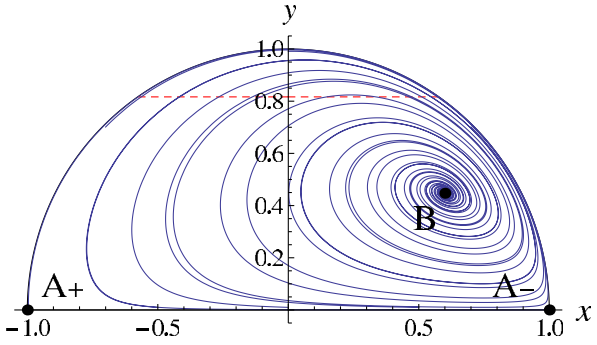

FIG. 4 (color online). Phase space for model 1 with $\lambda = 8$. The global attractor is point B, while A_+ is now a saddle point.

Fig. 4. Point A_+ is now a saddle point and attracts all the trajectories along the y direction. The global attractor is still point B and the cosmological evolution can experience more than one eras of accelerated expansion before ending eventually in the final decelerating solution.

In conclusion we have seen that in model 1 the universe can undergo phases of accelerated expansion for all the possible ranges of λ. If $\lambda < 2\sqrt{3}$ the cosmic evolution will end in an accelerated state, while for all the other values of λ, it eventually reaches a stable decelerating solution.

B. Model 2: $W = \alpha(\kappa\xi)^{\lambda} e^{-\lambda\kappa\phi/\sqrt{6}}$

In this section we will consider the potential given by

$$W(\phi, \xi) = \alpha(\kappa\xi)^{\lambda} e^{-\lambda\kappa\phi/\sqrt{6}}, \tag{38}$$

where α and λ are two dimensionless positive parameters. This potential allows for a direct coupling between the two scalar fields ϕ and ξ. Unfortunately, we cannot recast the cosmological evolution equations (27)–(29) into a two- dimensional dynamical system. However, defining in addition to (30) the new variable

$$z = \frac{H_0}{H + H_0}, \tag{39}$$

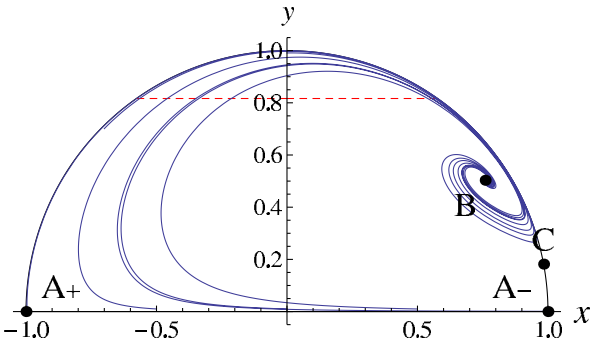

FIG. 3 (color online). Phase space for model 1 with $\lambda = 5.9$. The global attractor is now point B, while C is a saddle point.

we can obtain a three-dimensional system. The new variable z has been chosen in such a way to maintain the phase space compact [11]. It takes values between 0 and 1, meaning that the phase space is now represented by a half cylinder with radius and height equal to one. Equations (27) can still be rewritten as (34), implying that at every point of the phase space, the effective equation of state is again given by (35). The accelerated region is now the part of the half cylinder corresponding to $y > \sqrt{2/3}$ for all the possible values of z.

The cosmological equations (27)–(29) give the following three-dimensional dynamical system

$$x' = \frac{y^2}{2}(\lambda + 2 - 6x) + x^2 - 1, \tag{40}$$

$$y' = y\left[3 - 3y^2 - \frac{\lambda}{2}x + \beta\sqrt{1 - x^2 - y^2}\left(\frac{z}{y(1-z)}\right)^{2/\lambda}\right], \tag{41}$$

$$z' = 3(y^2 - 1)(z - 1)z, \tag{42}$$

where again a prime denotes a derivative with respect to $N = \ln a$, and we have to redefine the parameter α as

$$\beta = \frac{\lambda}{\sqrt{2}} 3^{\frac{\lambda-2}{2\lambda}} \alpha^{1/\lambda}\left(\frac{\kappa}{H_0}\right)^{2/\lambda}. \tag{43}$$

In the above system of equations, the term with β in (41) becomes singular as $y \to 0$ or $z \to 1$, and one must be rather careful when investigating the equations for those values. The critical points are given in Table II and, according to the value of λ, there can be up to seven critical points. However, when considering the critical points with $z = 1$, we have assumed that the term proportional to β approaches zero when $z \to 1$. This issue is very difficult to settle analytically; however, the numerical solutions and the resulting phase space confirm that this assumption is valid.

Again the three ranges $\lambda < \sqrt{37} - 1$, $\sqrt{37} - 1 \le \lambda \le 6$ and $\lambda > 6$ give the three qualitatively different behaviors of the phase space. The four points $A_\pm$ and $B_\pm$ always

TABLE II. Critical points and their properties for model 2.

Point	x	y	z	Existence	w_{eff}	Acceleration
A_-	-1	0	0	$\forall\ \lambda$	1	No
A_+	1	0	0	$\forall\ \lambda$	1	No
B_-	-1	0	1	$\forall\ \lambda$	1	No
B_+	1	0	1	$\forall\ \lambda$	1	No
C_0	$\frac{6}{\lambda+2}$	$\frac{\sqrt{2}}{\sqrt{\lambda+2}}$	0	$\lambda \geq \sqrt{37}-1$	$\frac{\lambda-2}{\lambda+2}$	No
D_0	$\frac{\lambda}{6}$	$\frac{\sqrt{36-\lambda^2}}{6}$	0	$\lambda \leq 6$	$\frac{\lambda^2}{18}-1$	$\lambda < 2\sqrt{3}$
D_1	$\frac{\lambda}{6}$	$\frac{\sqrt{36-\lambda^2}}{6}$	1	$\lambda \leq 6$	$\frac{\lambda^2}{18}-1$	$\lambda < 2\sqrt{3}$

represent universes evolving with a stiff matter effective equation of state. However, they are expected to be relevant only at early time and not to be stable solutions.

The phase space for the first range is shown in Fig. 5. Points A_+ and D_0 act as saddle points attracting the early time solutions before these turn towards greater values of z. The trajectories always evolve towards point D_1, which represents the global attractor. A few more remarks are required about this point. First, one of the eigenvalues approaches $-\infty$ as $z \to 1$. The term responsible for this is $\beta\sqrt{1-x^2-y^2}(\frac{z}{y(1-z)})^{2/\lambda}$, which we assumed to approach zero. The linear stability matrix (Jacobian) contains the inverse of this term which in turn can yield an eigenvalue which formally is $-\infty$ (see Table III). This explains why this point acts as the global attractor to the system. There is a λ range where one of the eigenvalues of D_1 is positive, and this point will still attract all trajectories. While there is a direction in which the point repels trajectories, the nonlinearities of the system will move any trajectory away from this exact direction and the attractive behavior in the other directions will dominate. This behavior can be seen quite clearly in the phase space plots.

If $\lambda < 2\sqrt{3}$, this characterizes an accelerating scaling solution, while if $\lambda > 2\sqrt{3}$, the universes undergo deceleration. Again, this represents the cosmologically interesting case, where the global attractor of the phase space could represent an accelerating universe.

The phase space for the second qualitative range $\sqrt{37}-1 \leq \lambda \leq 6$ is depicted in Fig. 6. Points A_+, C_0 and D_0 represent saddle points which attract the early time solutions. Point D_1 still represents the global attractor but does not characterize an accelerating solution, being always outside the accelerated region.

We have identified another interesting point, C_1 with coordinates $x = \frac{6}{\lambda+2}$, $y = \frac{\sqrt{2}}{\sqrt{\lambda+2}}$, $z = 1$, which is not a critical point to the dynamical system. However, when evaluating Eqs. (40) and (42), we note that both right-hand sides vanish. The remaining Eq. (41) at this point is

$$y'_{C_1} = \frac{\beta}{2}\left(\frac{\lambda}{2}+1\right)^{1/\lambda-3/2}\sqrt{\lambda^2+2\lambda-36}\left(\frac{z}{1-z}\right)^{2/\lambda} = \beta C(\lambda)\left(\frac{z}{1-z}\right)^{2/\lambda}, \tag{44}$$

where $C(\lambda)$ is a constant depending on λ. We can now understand the phase space at this point; see Fig. 7. If β is chosen to be small, then the solution behaves as if C_1 were a critical point. The smaller the value of β, the better C_1 acts as an attracting point. However, when z gets sufficiently close to 1, the trajectories will get repelled from this point eventually. If $\lambda > 6$, none of the critical points is stable, and the solution will keep evolving without a determined late time behavior. As can be seen in Fig. 7, all trajectories reach the $z \to 1$ surface and then stay there.

C. Model 3: $W = W_0 e^{-\lambda\kappa\phi/\sqrt{6}}$ + matter

In this final section we reconsider model 1 with the potential (33) and add a standard matter perfect fluid energy-momentum tensor to the gravitational field equations (20),

TABLE III. Critical points and their stability properties for model 2.

Point	Eigenvalues	Stability
A_-	$3,\ -2,\ 3+\lambda/2$	Saddle point
A_+	$3,\ 2,\ 3-\lambda/2$	Saddle point
B_-	$-3,\ -2,\ 3+\lambda/2$	Saddle point
B_+	$-3,\ 2,\ 3-\lambda/2$	Saddle point
C_0	$3\lambda/(2+\lambda),\ (-3 \pm \sqrt{81+32\lambda-4\lambda^2-\lambda^3})/(2+\lambda)$	Saddle point
D_0	$\lambda^2/12,\ -3+\lambda^2/12,\ -6+\lambda/3+\lambda^2/12$	Saddle point
D_1	$-\lambda^2/12,\ -9/2+\lambda/6+\lambda^2/8,\ -\infty$	Stable if $\lambda < 2(\sqrt{82}-1)/3$ 'Saddle' if $(2\sqrt{82}-2)/3 < \lambda$

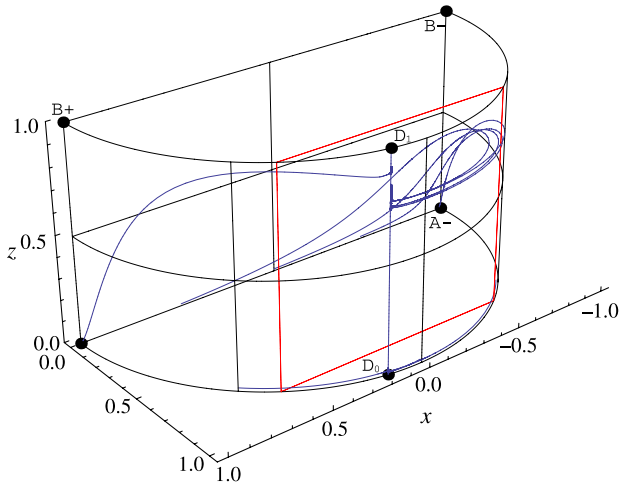

FIG. 5 (color online). Phase space for model 2 with $\lambda = 1$ and $\beta = 0.01$. The global attractor is point D_1, representing an accelerating solution whenever $\lambda < 2\sqrt{3}$ because it lies in the region marked by the dashed/red line.

$$G_{\mu\nu} = \kappa^2(T^{(\phi)}_{\mu\nu} + e^{-\kappa\phi\sqrt{2/3}}T^{(\xi)}_{\mu\nu} - g_{\mu\nu}W + T^{(M)}_{\mu\nu}), \tag{45}$$

where

$$T^{(M)}_{\mu\nu} = pg_{\mu\nu} + (p + \rho)U_\mu U_\nu, \tag{46}$$

with U^μ the comoving four-velocity of the fluid, ρ its energy density and p its pressure. We will consider a linear equation of state given by

$$p = w\rho \tag{47}$$

and assume that standard matter is covariantly conserved,

$$\nabla^\mu T^{(M)}_{\mu\nu} = 0. \tag{48}$$

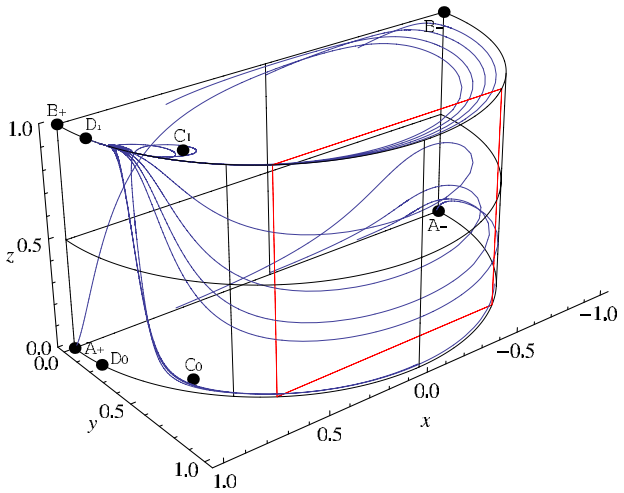

FIG. 6 (color online). Phase space for model 2 with $\lambda = 5.9$ and $\beta = 0.01$. The global attractor is still point D_1 but now the trajectories are first attracted by point C_1, which is not a critical point.

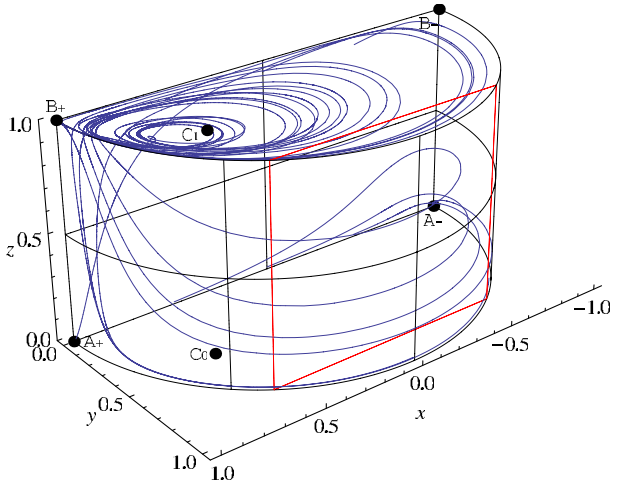

FIG. 7 (color online). Phase space for model 2 with $\lambda = 8$ and $\beta = 0.01$.

We will also consider only the physical range $0 \leq z \leq 1/3$, meaning that we cannot have cosmic acceleration from matter alone. In this model, dark matter is included in the standard matter sector, while both the scalar fields ϕ and ξ act as dark energy. Note that we are adding a matter action to (18) and thus assuming that the matter fields couple with the Einstein frame metric $\tilde{g}_{\mu\nu}$. This procedure is different to adding a matter action directly to (1) but has largely been considered in literature without entering into deep philosophical issues (see Ref. [12] for a discussion).

The new cosmological field equations derived from (45), with $k = 0$, read

$$3H^2 = \kappa^2\rho + \frac{\kappa^2}{2}e^{-\sqrt{2/3}\kappa\phi}\dot{\xi}^2 + \frac{\kappa^2}{2}\dot{\phi}^2 + \kappa^2 W, \tag{49}$$

$$2\dot{H} + 3H^2 = -\kappa^2 p - \frac{\kappa^2}{2}e^{-\sqrt{2/3}\kappa\phi}\dot{\xi}^2 - \frac{\kappa^2}{2}\dot{\phi}^2 + \kappa^2 W, \tag{50}$$

while the two evolution equations for the scalar fields still coincide with (28) and (29). These equations can be recast in a three-dimensional autonomous system of equations defining, in addition to (30), the new adimensional variable,

$$z^2 = \frac{\kappa^2\rho}{3H^2}. \tag{51}$$

The Friedmann constraint (49) reduces to

$$x^2 + y^2 + z^2 = 1 - s^2, \tag{52}$$

implying that the phase space is now the quarter of a unit sphere because, thanks to (52) and the positiveness of ρ and W, we must have $y \geq 0$, $z \geq 0$ and

$$0 \leq x^2 + y^2 + z^2 \leq 1. \tag{53}$$

Equation (50) becomes

$$\frac{\dot{H}}{H^2} = \frac{3}{2}[-2 + 2y^2 + (1 - w)z^2], \tag{54}$$

from which we can read off the new effective equation of state parameter,

$$w_{\text{eff}} = 1 - 2y^2 + (w - 1)z^2. \tag{55}$$

The three-dimensional dynamical system is given by equations (48)–(50) as

$$x' = -\frac{3}{2}x[2y^2 - (w - 1)z^2] + \frac{1}{2}(\lambda + 2)y^2 + x^2 + z^2 - 1, \tag{56}$$

$$y' = -\frac{1}{2}y[-3(w - 1)z^2 + \lambda x + 6y^2 - 6], \tag{57}$$

$$z' = \frac{3}{2}z[(w - 1)(z^2 - 1) - 2y^2], \tag{58}$$

and the critical points together with their properties are listed in Table IV. If we compare this with Table I, we see that we now have two more critical points (D and E) corresponding to a universe evolving in accordance with the matter equation of state parameter. Point D corresponds to a universe completely dominated by the matter sector with no dark energy affecting the evolution. Point E presents instead both matter and dark energy, but the total outcome on the universe's evolution is still completely equivalent to a matter-dominated universe. The other points, belonging to the $z = 0$ plane, have the same properties of model 1, with point C being the cosmic accelerated stable attractor solution for $\lambda < 2\sqrt{3}$. We now have four qualitative behaviors for the dynamics of the phase space, depending again on the possible values of λ: $\lambda < 3\sqrt{2(w + 1)}$, $3\sqrt{2(w + 1)} \leq \lambda < \sqrt{37} - 1$, $\sqrt{37} - 1 \leq \lambda \leq 6$ and $\lambda > 6$. Note that because $0 \leq z \leq 1/3$, we always have $3\sqrt{2(w + 1)} < \sqrt{37} - 1$.

The first range is again the more interesting, since we can have a late time attractor where the universe is accelerating its expansion. The dynamics of the phase space is depicted in Fig. 8. The late time attractor is point C, which results in an accelerating solution whenever $\lambda < 2\sqrt{3}$. Point D represents a saddle point where the universe is completely dominated by the matter sector and expands according to radiation/dust solutions. It is then clear that every trajectory passing nearby point D and eventually ending in point C describes a possible physical universe. In fact, all these solutions will allow the universe to undergo the standard radiation and matter eras before the transition to the dark energy accelerating solution.

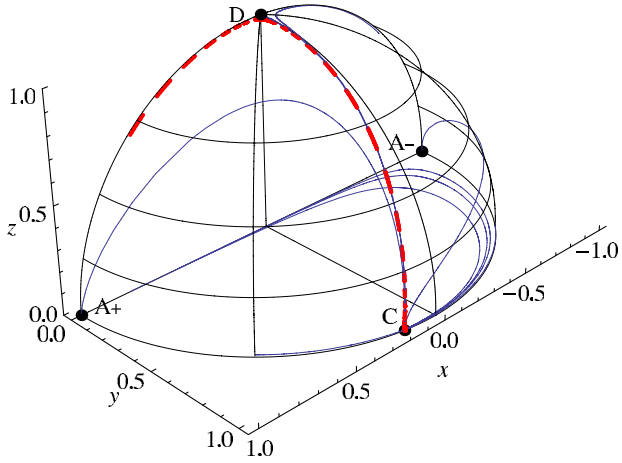

FIG. 8 (color online). Phase space for model 3 with $\lambda = 1$ and $w = 0$. The global attractor is point C, which represents an accelerating solution when $\lambda < 2\sqrt{3}$, while point D is a matter-dominated saddle point.

As an example we can look at the dashed/red solution in Fig. 8 and see how the effective equation of state parameter evolves. This is plotted in Fig. 9. We see that the universe immediately reaches a matter-dominated expansion and keeps this evolution for some time unperturbed. Of course, if the matter equation of state parameter w changed during this period, from radiation to dust in a physical situation, w_{eff} also would change according to w. This means that during this period the universe has the time to undergo the standard cosmological eras in agreement with the

TABLE IV. Critical points and their properties for model 3.

Point	x	y	z	Existence	w_{eff}	Acceleration	Stability
A_-	-1	0	0	$\forall\ \lambda$	1	No	Saddle
A_+	1	0	0	$\forall\ \lambda$	1	No	Unstable if $\lambda \leq 6$ Saddle if $\lambda > 6$
B	$\frac{6}{\lambda+2}$	$\frac{\sqrt{2}}{\sqrt{\lambda+2}}$	0	$\lambda \geq \sqrt{37} - 1$	$\frac{\lambda-2}{\lambda+2}$	No	Saddle
C	$\frac{\lambda}{6}$	$\frac{\sqrt{36-\lambda^2}}{6}$	0	$\lambda \leq 6$	$\frac{\lambda^2}{18} - 1$	$\lambda < 2\sqrt{3}$	Stable if $\lambda < 3\sqrt{2(w + 1)}$ Saddle otherwise
D	0	0	1	$\forall\ \lambda$	w	No	Saddle
E	$\frac{3(w+1)}{\lambda}$	$\frac{3\sqrt{1-w^2}}{\lambda}$	$\frac{\sqrt{\lambda^2-18(w+1)}}{\lambda}$	$\lambda \geq 3\sqrt{2(w + 1)}$	w	No	Stable if $3\sqrt{2(w + 1)} \leq \lambda$ Saddle otherwise

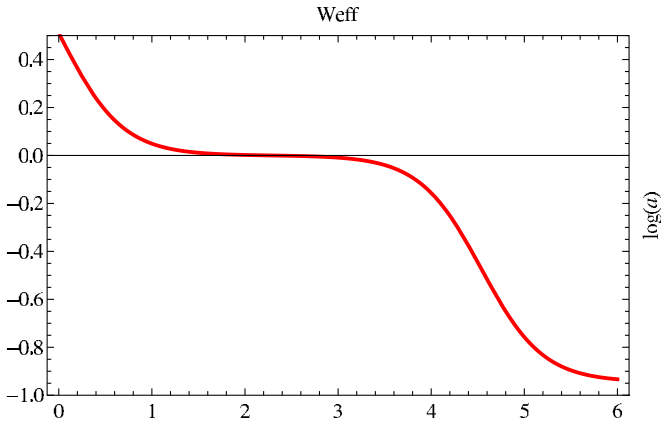

FIG. 9 (color online). Evolution of the effective equation of state parameter for the dashed/red trajectories in Fig. 8. After reaching a long-lasting matter-dominated evolution according to observations, the universe eventually ends in an accelerated expansion, representing the final cosmological stage.

observations. Depending on the initial conditions, this stage can last for the time needed to produce the nucleosynthesis and create the cosmological structures. Eventually, we will have the transition to the accelerated phase, which represents the final phase of the universe where the effective equation of state parameter assumes the value $\lambda^2/18 - 1$. The situation is completely equivalent to quintessence plus dark matter, with ϕ playing the role of the dark energy scalar field. In fact the trajectories confined to the border of the sphere, such as the dashed/red one in Fig. 8, must have $s = 0$, meaning that ξ does not influence the dynamics of this solution.

We can now look at the second range $3\sqrt{2(w+1)} \leq \lambda < \sqrt{37} - 1$, whose phase space is drawn in Fig. 10. The global attractor is now point E, where the universe expands according to the matter equation of state. Depending on the initial conditions, the trajectories can either pass nearby saddle point D, where we also have $w_{\text{eff}} = w$, or pass through the region surrounding the point (0, 1, 0), where the universe accelerates its expansion and eventually approaches saddle point C before ending in point E. This shows how this model can be useful in early inflationary dynamics, since we can have an accelerated period before the universe starts to be radiation/dust dominated.

This feature is presented also in the third possible range, $\sqrt{37} - 1 \leq \lambda \leq 6$, as Fig. 11 shows. For this reason and because the phase space properties are more evident, we chose to show the dynamics in the $w = 1/3$ case. We still have point E as the global attractor, but now, besides point C, point B also acts as a saddle point influencing trajectories starting from the $z = 0$ plane. The dynamics is similar to the second λ range, with several solutions experiencing

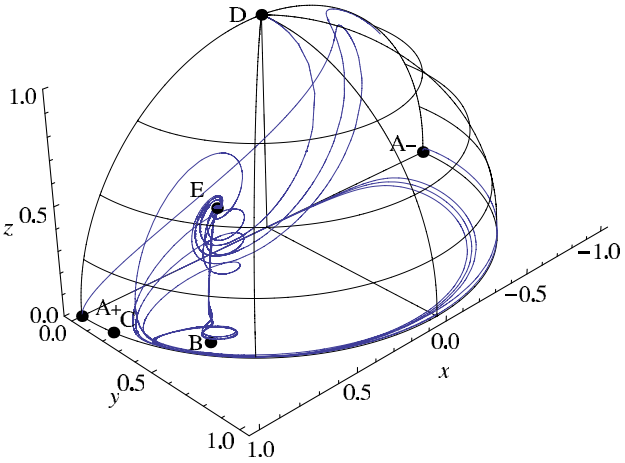

FIG. 11 (color online). Phase space for model 3 with $\lambda = 5.9$ and $w = 1/3$. The global attractor is still point E, but now the trajectories starting from the $z = 0$ plane are first attracted by saddle point B.

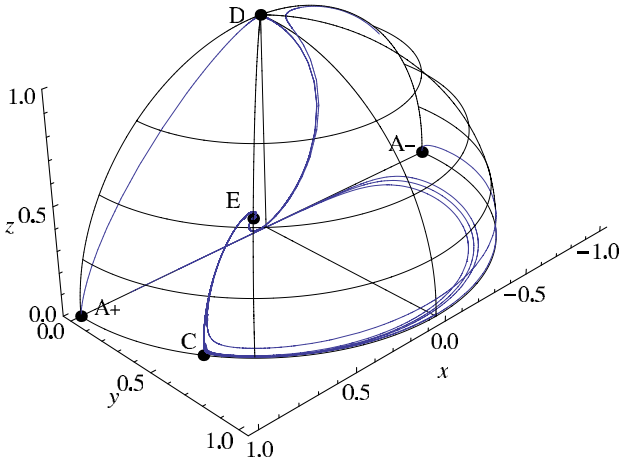

FIG. 10 (color online). Phase space for model 3 with $\lambda = 5$ and $w = 0$. The global attractor is now point E, where the universe evolves according to the matter equation of state.

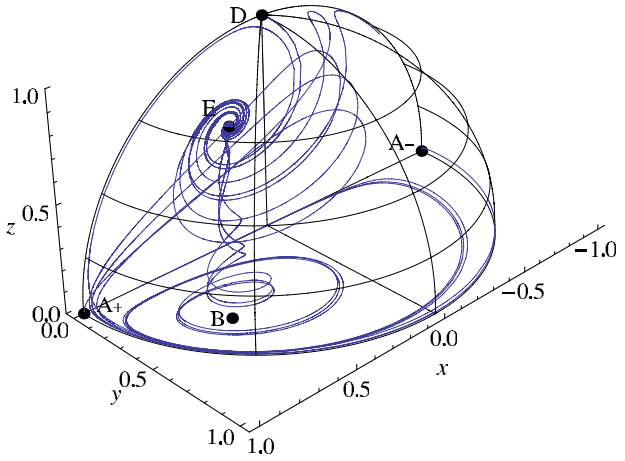

FIG. 12 (color online). Phase space for model 3 with $\lambda = 8$ and $w = 1/3$. The global attractor is point E, but now A_+ is a saddle point attracting the $z = 0$ trajectories.

an accelerated phase before ending in the matter-dominated final evolution.

Finally the phase space for the last range, $\lambda > 6$, is presented in Fig. 12. Point C is now gone and point A_+ plays its role attracting the $z = 0$ trajectories. The dynamics is again similar to the previous ranges, with point E being the global attractor and solutions having a possible era of cosmic-accelerated expansion depending on the initial conditions.

IV. CONCLUSIONS

In this paper we have studied a natural generalization of the so-called hybrid metric-Palatini gravity introduced in Ref. [4]. A completely arbitrary function of both the metric and Palatini curvature scalars was considered as the Lagrangian density in the action. Using dynamically equivalent actions and conformal transformation techniques, we have shown that this new theory can be recast into general relativity plus two scalar fields coupled with each other. Therefore, using this approach one arrives naturally at theories where the different matter components couple to each other. It should be emphasized that there are no theoretical restrictions when it comes to coupling different matter components; all that is required by general relativity and its generalization is that the total energy-momentum tensor is conserved.

We analyzed the possible applications to cosmology considering a FLRW universe and employing dynamical system methods. Three specific models specified by their potentials were studied in detail, and in each case a late time cosmological accelerated solution has been found. Depending on the model parameters, these can represent global attractor solutions. We also encountered a rather peculiar parameter choice (Fig. 7), where the dynamical system has no global attractor and the cosmological solution would never stop evolving.

The first model has a potential without coupling the two scalar fields and shows several similarities with usual quintessence models. The second model considers a direct coupling between the two scalars in the potential, and it is characterized by more mathematical complexity. Its evolution is easily understood. Finally, in the third and most interesting model, we add standard (dark) matter to the theory and show that the universe can undergo an ''extended period'' of matter domination followed by an accelerating dark-energy-dominated era. This would in principle allow for structure formation in this model. It would be interesting to study such models in more detail, studying not only the background evolution but also the evolution of perturbation on this background and, in particular, structure formation. This would eventually allow us to compare such models with experimental data.

[1] T. P. Sotiriou and V. Faraoni, Rev. Mod. Phys. **82**, 451 (2010); A. De Felice and S. Tsujikawa, Living Rev. Relativity **13**, 3 (2010).

[2] L. Amendola, K. Enqvist, and T. Koivisto, Phys. Rev. D **83**, 044016 (2011); T. S. Koivisto, Phys. Rev. D **83**, 101501 (2011); **84**, 121502 (2011); N. Tamanini, Phys. Rev. D **86**, 024004 (2012).

[3] C. G. Boehmer and N. Tamanini, arXiv:1301.5471.

[4] T. Harko, T. S. Koivisto, F. S. N. Lobo, and G. J. Olmo, Phys. Rev. D **85**, 084016 (2012); S. Capozziello, T. Harko, T. S. Koivisto, F. S. N. Lobo, and G. J. Olmo, arXiv:1301.2209.

[5] S. Capozziello, T. Harko, T. S. Koivisto, F. S. N. Lobo, and G. J. Olmo, arXiv:1209.2895; Phys. Rev. D **86**, 127504 (2012); arXiv:1212.5817.

[6] E. E. Flanagan, Classical Quantum Gravity **21**, 417 (2004).

[7] A. L. Berkin and K.-I. Maeda, Phys. Rev. D **44**, 1691 (1991); A. A. Starobinsky and J.'i. Yokoyama, arXiv:gr-qc/9502002; A. A. Starobinsky, S. Tsujikawa, and J.'i. Yokoyama, Nucl. Phys. **B610**, 383 (2001).

[8] J. Garcia-Bellido and D. Wands, Phys. Rev. D **52**, 6739 (1995); **53**, 5437 (1996); F. Di Marco, F. Finelli, and R. Brandenberger, Phys. Rev. D **67**, 063512 (2003); F. Di Marco and F. Finelli, Phys. Rev. D **71**, 123502 (2005).

[9] A. Cid and S. del Campo, J. Cosmol. Astropart. Phys. 01 (2011) 013; S. Cremonini, Z. Lalak, and K. Turzynski, J. Cosmol. Astropart. Phys. 03 (2011) 016; Phys. Rev. D **82**, 047301 (2010); Z. Lalak, D. Langlois, S. Pokorski, and K. Turzynski, J. Cosmol. Astropart. Phys. 07 (2007) 014; K.-Y. Choi, L. M. H. Hall, and C. van de Bruck, J. Cosmol. Astropart. Phys. 02 (2007) 029; T. Wang, Phys. Rev. D **82**, 123515 (2010).

[10] C. Wetterich, Astron. Astrophys. **301**, 321 (1995); E. J. Copeland, A. R. Liddle, and D. Wands, Phys. Rev. D **57**, 4686 (1998); L. Amendola, Phys. Rev. D **60**, 043503 (1999); A. P. Billyard and A. A. Coley, Phys. Rev. D **61**, 083503 (2000); W. Zimdahl and D. Pavon, Phys. Lett. B **521**, 133 (2001); G. R. Farrar and P. J. E. Peebles, Astrophys. J. **604**, 1 (2004); L. P. Chimento, A. S. Jakubi, D. Pavon, and W. Zimdahl, Phys. Rev. D **67**, 083513 (2003); G. Olivares, F. Atrio-Barandela, and D. Pavon, Phys. Rev. D **71**, 063523 (2005); H. M. Sadjadi and M. Alimohammadi, Phys. Rev. D **74**, 103007 (2006); Z.-K. Guo, N. Ohta, and S. Tsujikawa, Phys. Rev. D **76**, 023508 (2007); K. Y. Kim, H. W. Lee, and Y. S. Myung, Mod. Phys. Lett. A **22**, 2631 (2007); J.-H. He and B. Wang, J. Cosmol. Astropart. Phys. 06 (2008) 010; S. Chen, B. Wang, and J. Jing, Phys. Rev. D **78**, 123503 (2008); M. Quartin, M. O. Calvao, S. E. Joras, R. R. R. Reis, and I. Waga, J. Cosmol. Astropart. Phys. 05 (2008)

007; S. H. Pereira and J. F. Jesus, Phys. Rev. D **79**, 043517 (2009); C. Quercellini, M. Bruni, A. Balbi, and D. Pietrobon, Phys. Rev. D **78**, 063527 (2008); G. Caldera-Cabral, R. Maartens, and L. A. Urena-Lopez, Phys. Rev. D **79**, 063518 (2009); J. Valiviita, R. Maartens, and E. Majerotto, Mon. Not. R. Astron. Soc. **402**, 2355 (2010); C. G. Böhmer, G. Caldera-Cabral, N. Chan, R. Lazkoz, and R. Maartens, Phys. Rev. D **81**, 083003 (2010); T. S. Koivisto and N. J. Nunes, Phys. Rev. D **80**, 103509 (2009); Phys. Lett. B **685**, 105 (2010); T. Ngampitipan and P. Wongjun, J. Cosmol. Astropart. Phys. 11 (2011) 036; E. J. Copeland, M. Sami, and S. Tsujikawa, Int. J. Mod. Phys. D **15**, 1753 (2006); G. Leon and E. N. Saridakis, Phys. Lett. B **693**, 1 (2010);

[11] C. G. Böhmer, G. Caldera-Cabral, R. Lazkoz, and R. Maartens, Phys. Rev. D **78**, 023505 (2008).

[12] V. Faraoni, *Cosmology in Scalar Tensor Gravity* (Kluwer Academic Publishers, Dordrecht, The Netherlands, 2004).

Bibliography

Abdelwahab, M., Carloni, S., & Dunsby, P. K. (2008). Cosmological dynamics of exponential gravity. *Class.Quant.Grav.*, *25*, 135002. arXiv: 0706.1375

Acquaviva, G., & Beesham, A. (2014). Nonlinear bulk viscosity and the stability of accelerated expansion in FRW spacetime. arXiv: 1405.3459

Ade, P., et al. (2013). Planck 2013 results. XVI. Cosmological parameters. arXiv: 1303.5076

Agarwal, N., & Bean, R. (2008). The Dynamical viability of scalar-tensor gravity theories. *Class.Quant.Grav.*, *25*, 165001. arXiv: 0708.3967

Aguirregabiria, J., & Lazkoz, R. (2004). Tracking solutions in tachyon cosmology. *Phys.Rev.*, *D69*, 123502. arXiv: hep-th/0402190

Ahn, C., Kim, C., & Linder, E. V. (2009). Dark Energy Properties in DBI Theory. *Phys.Rev.*, *D80*, 123016. arXiv: 0909.2637

Ahn, C., Kim, C., & Linder, E. V. (2010). Cosmological Constant Behavior in DBI Theory. *Phys.Lett.*, *B684*, 181–184. arXiv: 0904.3328

Alho, A., & Uggla, C. (2014). Global dynamics and inflationary center manifold and slow-roll approximants. arXiv: 1406.0438

Alimohammadi, M., & Ghalee, A. (2009). The Phase-space of generalized Gauss-Bonnet dark energy. *Phys.Rev.*, *D80*, 043006. arXiv: 0908.1150

Alimohammadi, M., & Mohseni Sadjadi, H. (2006). Attractor solutions for general hessence dark energy. *Phys.Rev.*, *D73*, 083527. arXiv: hep-th/0602268

Amendola, L. (1999). Scaling solutions in general nonminimal coupling theories. *Phys.Rev.*, *D60*, 043501. arXiv: astro-ph/9904120

Amendola, L. (2000). Coupled quintessence. *Phys.Rev.*, *D62*, 043511. arXiv: astro-ph/9908023

Amendola, L., Gannouji, R., Polarski, D., & Tsujikawa, S. (2007a). Conditions for the cosmological viability of $f(R)$ dark energy models. *Phys.Rev.*, *D75*, 083504. arXiv: gr-qc/0612180

Amendola, L., Polarski, D., & Tsujikawa, S. (2007b). Power-laws $f(R)$ theories are cosmologically unacceptable. *Int.J.Mod.Phys.*, *D16*, 1555–1561. arXiv: astro-ph/0605384

Amendola, L., Quartin, M., Tsujikawa, S., & Waga, I. (2006). Challenges for scaling cosmologies. *Phys.Rev.*, *D74*, 023525. arXiv: astro-ph/0605488

Amendola, L., & Tsujikawa, S. (2008). Phantom crossing, equation-of-state singularities, and local gravity constraints in $f(R)$ models. *Phys.Lett.*, *B660*, 125–132. arXiv: 0705.0396

Armendariz-Picon, C. (2004). Could dark energy be vector-like? *JCAP*, *0407*, 007. arXiv: astro-ph/0405267

Armendariz-Picon, C., Mukhanov, V. F., & Steinhardt, P. J. (2000). A Dynamical solution to the problem of a small cosmological constant and late time cosmic acceleration. *Phys.Rev.Lett.*, *85*, 4438–4441. arXiv: astro-ph/0004134

Armendariz-Picon, C., Mukhanov, V. F., & Steinhardt, P. J. (2001). Essentials of k essence. *Phys.Rev.*, *D63*, 103510. arXiv: astro-ph/0006373

Arrowsmith, D. K., & Place, C. M. (1990). *An introduction to dynamical systems*. Cambridge University Press.

Astier, P., & Pain, R. (2012). Observational Evidence of the Accelerated Expansion of the Universe. *Comptes Rendus Physique*, *13*, 521–538. arXiv: 1204.5493

Aulbach, B. (1984). *Continuous and discrete dynamics near manifolds of equilibria*. Lecture notes in mathematics, 1058, Springer-Verlag, 2nd ed.

Auslander, J., Bhatia, N. P., & Seibert, P. (1964). Attractors in dynamical systems.

Avelino, A., Leyva, Y., & Urena-Lopez, L. A. (2013). Interacting viscous dark fluids. *Phys.Rev.*, *D88*, 123004. arXiv: 1306.3270

Azreg-Anou, M. (2013). Phase-space analysis of the cosmological 3-fluid problem: Families of attractors and repellers. *Class.Quant.Grav.*, *30*, 205001. arXiv: 1304.7470

Bagla, J., Jassal, H. K., & Padmanabhan, T. (2003). Cosmology with tachyon field as dark energy. *Phys.Rev.*, *D67*, 063504. arXiv: astro-ph/0212198

Barbour, J., & Pfister, H. (1995). Mach's principle: From Newton's bucket to quantum gravity. Proceedings, Conference, Tuebingen, Germany, July 26-30, 1993.

Barreiro, T., Copeland, E. J., & Nunes, N. (2000). Quintessence arising from exponential potentials. *Phys.Rev.*, *D61*, 127301. arXiv: astro-ph/9910214

Basak, A., Bhatt, J. R., Shankaranarayanan, S., & Prasantha Varma, K. (2013). Attractor behaviour in ELKO cosmology. *JCAP*, *1304*, 025. arXiv: 1212.3445

Bassett, B. A., Tsujikawa, S., & Wands, D. (2006). Inflation dynamics and reheating. *Rev.Mod.Phys.*, *78*, 537–589. arXiv: astro-ph/0507632

Bento, M., Bertolami, O., Moniz, P., Mourao, J., & Sa, P. (1993). On the cosmology of massive vector fields with SO(3) global symmetry. *Class.Quant.Grav.*, *10*, 285–298. arXiv: gr-qc/9302034

Billyard, A. P., & Coley, A. A. (2000). Interactions in scalar field cosmology. *Phys.Rev.*, *D61*, 083503. arXiv: astro-ph/9908224

Boehmer, C. G., Burnett, J., Mota, D. F., & Shaw, D. J. (2010a). Dark spinor models in gravitation and cosmology. *JHEP*, *1007*, 053. arXiv: 1003.3858

Boehmer, C. G., Caldera-Cabral, G., Chan, N., Lazkoz, R., & Maartens, R. (2010b). Quintessence with quadratic coupling to dark matter. *Phys.Rev.*, *D81*, 083003. arXiv: 0911.3089

Boehmer, C. G., Caldera-Cabral, G., Lazkoz, R., & Maartens, R. (2008). Dynamics of dark energy with a coupling to dark matter. *Phys.Rev.*, *D78*, 023505. arXiv: 0801.1565

Boehmer, C. G., Chan, N., & Lazkoz, R. (2012a). Dynamics of dark energy models and centre manifolds. *Phys.Lett.*, *B714*, 11–17. arXiv: 1111.6247

Boehmer, C. G., Harko, T., & Sabau, S. (2012b). Jacobi stability analysis of dynamical systems: Applications in gravitation and cosmology. *Adv.Theor.Math.Phys.*, *16*, 1145–1196. arXiv: 1010.5464

Bogoyavlensky, O. (1985). *Methods in the qualitative theory of dynamical systems in astrophysics and gas dynamics*. Springer-Verlag.

Bolotin, Y. L., Kostenko, A., Lemets, O., & Yerokhin, D. (2013). Cosmological Evolution With Interaction Between Dark Energy And Dark Matter. arXiv: 1310.0085

Brans, C., & Dicke, R. (1961). Mach's principle and a relativistic theory of gravitation. *Phys.Rev.*, *124*, 925–935.

Burd, A., & Barrow, J. D. (1988). Inflationary Models with Exponential Potentials. *Nucl.Phys.*, *B308*, 929–945.

Cai, Y.-F., Saridakis, E. N., Setare, M. R., & Xia, J.-Q. (2010). Quintom Cosmology: Theoretical implications and observations. *Phys.Rept.*, *493*, 1–60. arXiv: 0909.2776

Caldera-Cabral, G., Maartens, R., & Urena-Lopez, L. A. (2009). Dynamics of interacting dark energy. *Phys.Rev.*, *D79*, 063518. arXiv: 0812.1827

Caldwell, R. (2002). A Phantom menace? *Phys.Lett.*, *B545*, 23–29. arXiv: astro-ph/9908168

Caldwell, R., Dave, R., & Steinhardt, P. J. (1998). Cosmological imprint of an energy component with general equation of state. *Phys.Rev.Lett.*, *80*, 1582–1585. arXiv: astro-ph/9708069

Caldwell, R. R., Kamionkowski, M., & Weinberg, N. N. (2003). Phantom energy and cosmic doomsday. *Phys.Rev.Lett.*, *91*, 071301. arXiv: astro-ph/0302506

Carloni, S., Capozziello, S., Leach, J., & Dunsby, P. (2008). Cosmological dynamics of scalar-tensor gravity. *Class.Quant.Grav.*, *25*, 035008. arXiv: gr-qc/0701009

Carloni, S., Dunsby, P. K., Capozziello, S., & Troisi, A. (2005). Cosmological dynamics of R**n gravity. *Class.Quant.Grav.*, *22*, 4839–4868. arXiv: gr-qc/0410046

Carloni, S., Troisi, A., & Dunsby, P. (2009). Some remarks on the dynamical systems approach to fourth order gravity. *Gen.Rel.Grav.*, *41*, 1757–1776. arXiv: 0706.0452

Carr, J. (1981). *Applications of centre manifold theory*. Springer-Verlag.

Carroll, S. M. (2001). The Cosmological constant. *Living Rev.Rel.*, *4*, 1. arXiv: astro-ph/0004075

Carroll, S. M., De Felice, A., Duvvuri, V., Easson, D. A., Trodden, M., et al. (2005). The Cosmology of generalized modified gravity models. *Phys.Rev.*, *D71*, 063513. arXiv: astro-ph/0410031

Carroll, S. M., Hoffman, M., & Trodden, M. (2003). Can the dark energy equation-of-state parameter w be less than -1? *Phys.Rev.*, *D68*, 023509. arXiv: astro-ph/0301273

Cervantes-Cota, J. L., de Putter, R., & Linder, E. V. (2010). Induced Gravity and the Attractor Dynamics of Dark Energy/Dark Matter. *JCAP*, *1012*, 019. arXiv: 1010.2237

Chang, B.-R., Liu, H.-Y., Liu, H.-Y., & Xu, L.-X. (2005). Five-dimensional cosmological scaling solution. *Mod.Phys.Lett.*, *A20*, 923–928. arXiv: astro-ph/0405084

Chen, S., & Jing, J. (2009). Dark energy interacting with dark matter and unparticle. *Class.Quant.Grav.*, *26*, 155006. arXiv: 0903.0120

Chen, S., Wang, B., & Jing, J. (2008). Dynamics of interacting dark energy model in Einstein and Loop Quantum Cosmology. *Phys.Rev.*, *D78*, 123503. arXiv: 0808.3482

Chen, X.-m., & Gong, Y. (2009). Fixed points in interacting dark energy models. *Phys.Lett.*, *B675*, 9–13. arXiv: 0811.1698

Chen, X.-m., Gong, Y.-g., & Saridakis, E. N. (2009). Phase-space analysis of interacting phantom cosmology. *JCAP*, *0904*, 001. arXiv: 0812.1117

Chiba, T., De Felice, A., & Tsujikawa, S. (2014). Cosmological Scaling Solutions for Multiple Scalar Fields. arXiv: 1403.7604

Chiba, T., Okabe, T., & Yamaguchi, M. (2000). Kinetically driven quintessence. *Phys.Rev.*, *D62*, 023511. arXiv: astro-ph/9912463

Chingangbam, P., & Qureshi, T. (2005). Dynamics of rolling massive scalar field cosmology. *Int.J.Mod.Phys.*, *A20*, 6083. arXiv: hep-th/0409015

Chueshov, I. D. (1999). *Introduction to the theory of infinite-dimensional dissipative systems*. ACTA Scientific Publishing House.

Cicoli, M., Pedro, F. G., & Tasinato, G. (2012). Natural Quintessence in String Theory. *JCAP*, *1207*, 044. arXiv: 1203.6655

Clifton, T. (2008). Higher Powers in Gravitation. *Phys.Rev.*, *D78*, 083501. arXiv: 0807.4682

Clifton, T., & Barrow, J. D. (2005). The Power of general relativity. *Phys.Rev.*, *D72*, 103005. arXiv: gr-qc/0509059

Cline, J. M., Jeon, S., & Moore, G. D. (2004). The Phantom menaced: Constraints on low-energy effective ghosts. *Phys.Rev.*, *D70*, 043543. arXiv: hep-ph/0311312

Clowe, D., et al. (2006). A direct empirical proof of the existence of dark matter. *Astrophys.J.*, *648*, L109–L113. arXiv: astro-ph/0608407

Coble, K., Dodelson, S., & Frieman, J. A. (1997). Dynamical Lambda models of structure formation. *Phys.Rev.*, *D55*, 1851–1859. arXiv: astro-ph/9608122

Coley, A. (2003). *Dynamical systems and cosmology*. Astrophysic and space science library, 291, Kluwer Academic Publishers.

Coley, A., Ibanez, J., & van den Hoogen, R. (1997). Homogeneous scalar field cosmologies with an exponential potential. *J.Math.Phys.*, *38*, 5256–5271.

Coley, A., & van den Hoogen, R. (2000). The Dynamics of multiscalar field cosmological models and assisted inflation. *Phys.Rev.*, *D62*, 023517. arXiv: gr-qc/9911075

Collinucci, A., Nielsen, M., & Van Riet, T. (2005). Scalar cosmology with multi-exponential potentials. *Class.Quant.Grav.*, *22*, 1269–1288. arXiv: hep-th/0407047

Copeland, E. J., Garousi, M. R., Sami, M., & Tsujikawa, S. (2005a). What is needed of a tachyon if it is to be the dark energy? *Phys.Rev.*, *D71*, 043003. arXiv: hep-th/0411192

Copeland, E. J., Lee, S.-J., Lidsey, J. E., & Mizuno, S. (2005b). Generalised cosmological scaling solutions. *Phys.Rev.*, *D71*, 023526. arXiv: astro-ph/0410110

Copeland, E. J., Liddle, A. R., & Wands, D. (1998). Exponential potentials and cosmological scaling solutions. *Phys.Rev.*, *D57*, 4686–4690. arXiv: gr-qc/9711068

Copeland, E. J., Mizuno, S., & Shaeri, M. (2009). Dynamics of a scalar field in Robertson-Walker spacetimes. *Phys.Rev.*, *D79*, 103515. arXiv: 0904.0877

Copeland, E. J., Mizuno, S., & Shaeri, M. (2010). Cosmological Dynamics of a Dirac-Born-Infeld field. *Phys.Rev.*, *D81*, 123501. arXiv: 1003.2881

Copeland, E. J., Sami, M., & Tsujikawa, S. (2006). Dynamics of dark energy. *Int.J.Mod.Phys.*, *D15*, 1753–1936. arXiv: hep-th/0603057

Cruz, N., Lepe, S., Leyva, Y., Pea, F., & Saavedra, J. (2014). No stable dissipative phantom scenario in the framework of a complete cosmological dynamics. arXiv: 1406.7348

De Felice, A., & Tsujikawa, S. (2010). $f(R)$ theories. *Living Rev.Rel.*, *13*, 3. arXiv: 1002.4928

de la Macorra, A., & Filobello, U. (2008). Interacting Tachyon: Generic cosmological evolution for a tachyon and a scalar field. *Phys.Rev.*, *D77*, 023531. arXiv: 0705.2059

de la Macorra, A., & Piccinelli, G. (2000). General scalar fields as quintessence. *Phys.Rev.*, *D61*, 123503. arXiv: hep-ph/9909459

de la Macorra, A., & Stephan-Otto, C. (2001). Natural quintessence with gauge coupling unification. *Phys.Rev.Lett.*, *87*, 271301. arXiv: astro-ph/0106316

De-Santiago, J., & Cervantes-Cota, J. L. (2014). Phase space analysis of the $F(X)$ $V(\phi)$ scalar field Lagrangian and scaling solutions in flat cosmology. *J.Phys.Conf.Ser.*, *485*, 012017. arXiv: 1404.0946

De-Santiago, J., Cervantes-Cota, J. L., & Wands, D. (2013). Cosmological phase space analysis of the $F(X) - V(phi)$ scalar field and bouncing solutions. *Phys.Rev.*, *D87*, 023502. arXiv: 1204.3631

de Souza, J. C., & Faraoni, V. (2007). The Phase space view of $f(R)$ gravity. *Class.Quant.Grav.*, *24*, 3637–3648. arXiv: 0706.1223

de Souza, J. C., & Saa, A. (2005). Phase space solutions in scalar-tensor cosmological models. *Braz.J.Phys.*, *35*, 1041–1043. arXiv: gr-qc/0510128

del Campo, S., Fadragas, C. R., Herrera, R., Leiva, C., Leon, G., et al. (2013). Thawing models in the presence of a generalized Chaplygin gas. *Phys.Rev.*, *D88*, 023532. arXiv: 1303.5779

Dodelson, S. (2003). *Modern cosmology*. Academic Press.

Escobar, D., Fadragas, C. R., Leon, G., & Leyva, Y. (2014). Asymptotic behavior of a scalar field with an arbitrary potential trapped on a Randall-Sundrum‘s braneworld: the effect of a negative dark radiation term on a Bianchi I brane. *Astrophys.Space Sci.*, *349*, 575–602. arXiv: 1301.2570

Fadragas, C. R., & Leon, G. (2014). Some remarks about non-minimally coupled scalar field models. arXiv: 1405.2465

Fadragas, C. R., Leon, G., & Saridakis, E. N. (2014). Dynamical analysis of anisotropic scalar-field cosmologies for a wide range of potentials. *Class.Quant.Grav.*, *31*, 075018. arXiv: 1308.1658

Fang, W., Li, Y., Zhang, K., & Lu, H.-Q. (2009). Exact Analysis of Scaling and Dominant Attractors Beyond the Exponential Potential. *Class.Quant.Grav.*, *26*, 155005. arXiv: 0810.4193

Fang, W., Lu, H., Huang, Z., & Zhang, K. (2006). The evolution of the universe with the B-I type phantom scalar field. *Int.J.Mod.Phys.*, *D15*, 199–214. arXiv: hep-th/0409080

Fang, W., & Lu, H.-Q. (2010). Dynamics of tachyon and phantom field beyond the inverse square potentials. *Eur.Phys.J.*, *C68*, 567–572. arXiv: 1007.2330

Fang, W., Tu, H., Huang, J., & Shu, C. (2014a). Dynamical System of Scalar Field from 2-Dimension to 3-D and its Cosmological Implication. arXiv: 1402.4045

Fang, W., Tu, H., Li, Y., Huang, J., & Shu, C. (2014b). Full Investigation on the Dynamics of Power-Law Kinetic Quintessence. arXiv: 1406.0128

Farajollahi, H., & Salehi, A. (2011a). A New approach in stability analysis: case study: tachyon cosmology with non-minimally coupled scalar field-matter. *Phys.Rev.*, *D83*, 124042. arXiv: 1106.0091

Farajollahi, H., & Salehi, A. (2011b). Stability analysis and observational measurement in chameleonic generalised Brans-Dicke cosmology. *JCAP*, *1107*, 036. arXiv: 1109.6358

Farajollahi, H., Salehi, A., Tayebi, F., & Ravanpak, A. (2011). Stability Analysis in Tachyonic Potential Chameleon cosmology. *JCAP*, *1105*, 017. arXiv: 1105.4045

Faraoni, V. (2004). *Cosmology in scalar tensor gravity*. Springer.

Faraoni, V., Jensen, M., & Theuerkauf, S. (2006). Non-chaotic dynamics in general-relativistic and scalar-tensor cosmology. *Class.Quant.Grav.*, *23*, 4215–4230. arXiv: gr-qc/0605050

Faraoni, V., & Protheroe, C. S. (2013). Scalar field cosmology in phase space. *Gen.Rel.Grav.*, *45*, 103–123. arXiv: 1209.3726

Fay, S., Tavakol, R., & Tsujikawa, S. (2007). $f(R)$ gravity theories in Palatini formalism: Cosmological dynamics and observational constraints. *Phys.Rev.*, *D75*, 063509. arXiv: astro-ph/0701479

Felder, G. N., Frolov, A. V., Kofman, L., & Linde, A. D. (2002). Cosmology with negative potentials. *Phys.Rev.*, *D66*, 023507. arXiv: hep-th/0202017

Feng, B., Wang, X.-L., & Zhang, X.-M. (2005). Dark energy constraints from the cosmic age and supernova. *Phys.Lett.*, *B607*, 35–41. arXiv: astro-ph/0404224

Ferreira, P. G., & Joyce, M. (1997). Structure formation with a selftuning scalar field. *Phys.Rev.Lett.*, *79*, 4740–4743. arXiv: astro-ph/9707286

Ferreira, P. G., & Joyce, M. (1998). Cosmology with a primordial scaling field. *Phys.Rev.*, *D58*, 023503. arXiv: astro-ph/9711102

Frieman, J. A., Hill, C. T., Stebbins, A., & Waga, I. (1995). Cosmology with ultralight pseudo Nambu-Goldstone bosons. *Phys.Rev.Lett.*, *75*, 2077–2080. arXiv: astro-ph/9505060

Fujii, Y., & Maeda, K. (2003). *The scalar-tensor theory of gravitation*. Cambridge University Press.

Gao, C., Kunz, M., Liddle, A. R., & Parkinson, D. (2010). Unified dark energy and dark matter from a scalar field different from quintessence. *Phys.Rev.*, *D81*, 043520. arXiv: 0912.0949

Garcia-Salcedo, R., Gonzalez, T., Moreno, C., Napoles, Y., Leyva, Y., et al. (2010). Asymptotic Properties of a Supposedly Regular (Dirac-Born-Infeld) Modification of General Relativity. *JCAP*, *1002*, 027. arXiv: 0912.5048

Garriga, J., & Mukhanov, V. F. (1999). Perturbations in k-inflation. *Phys.Lett.*, *B458*, 219–225. arXiv: hep-th/9904176

Georgi, H. (2007). Unparticle physics. *Phys.Rev.Lett.*, *98*, 221601. arXiv: hep-ph/0703260

Gibbons, G. (2003). Thoughts on tachyon cosmology. *Class.Quant.Grav.*, *20*, S321–S346. arXiv: hep-th/0301117

Gibbons, G. W. (2002). Cosmological evolution of the rolling tachyon. *Phys.Lett.*, *B537*, 1–4. arXiv: hep-th/0204008

Goheer, N., Goswami, R., & Dunsby, P. K. (2009). Dynamics of $f(R)$-cosmologies containing Einstein static models. *Class.Quant.Grav.*, *26*, 105003. arXiv: 0809.5247

Goheer, N., Leach, J. A., & Dunsby, P. K. (2007). Dynamical systems analysis of anisotropic cosmologies in R**n-gravity. *Class.Quant.Grav.*, *24*, 5689–5708. arXiv: 0710.0814

Goheer, N., Leach, J. A., & Dunsby, P. K. (2008). Compactifying the state space for alternative theories of gravity. *Class.Quant.Grav.*, *25*, 035013. arXiv: 0710.0819

Gomes, A., & Amendola, L. (2014). Towards scaling cosmological solutions with full coupled Horndeski Lagrangian: the KGB model. *JCAP*, *1403*, 041. arXiv: 1306.3593

Gong, Y. (2014). The general property of dynamical quintessence field. *Phys.Lett.*, *B731*, 342–349. arXiv: 1401.1959

Gong, Y., Wang, A., & Zhang, Y.-Z. (2006). Exact scaling solutions and fixed points for general scalar field. *Phys.Lett.*, *B636*, 286–292. arXiv: gr-qc/0603050

Gonzalez, T., Leon, G., & Quiros, I. (2006). Dynamics of quintessence models of dark energy with exponential coupling to dark matter. *Class.Quant.Grav.*, *23*, 3165–3179. arXiv: astro-ph/0702227

Gorini, V., Kamenshchik, A. Y., Moschella, U., & Pasquier, V. (2004). Tachyons, scalar fields and cosmology. *Phys.Rev.*, *D69*, 123512. arXiv: hep-th/0311111

Gubser, S. S., & Khoury, J. (2004). Scalar self-interactions loosen constraints from fifth force searches. *Phys.Rev.*, *D70*, 104001. arXiv: hep-ph/0405231

Gumjudpai, B., Naskar, T., Sami, M., & Tsujikawa, S. (2005). Coupled dark energy: Towards a general description of the dynamics. *JCAP*, *0506*, 007. arXiv: hep-th/0502191

Gumjudpai, B., & Ward, J. (2009). Generalised DBI-Quintessence. *Phys.Rev.*, *D80*, 023528. arXiv: 0904.0472

Gunzig, E., Faraoni, V., Figueiredo, A., Rocha, T., & Brenig, L. (2000). The dynamical system approach to scalar field cosmology. *Class.Quant.Grav.*, *17*, 1783–1814.

Guo, J.-Q., & Frolov, A. V. (2013). Cosmological dynamics in $f(R)$ gravity. *Phys.Rev.*, *D88*, 124036. arXiv: 1305.7290

Guo, Z.-K., Cai, R.-G., & Zhang, Y.-Z. (2005a). Cosmological evolution of interacting phantom energy with dark matter. *JCAP*, *0505*, 002. arXiv: astro-ph/0412624

Guo, Z.-K., & Ohta, N. (2008). Cosmological Evolution of Dirac-Born-Infeld Field. *JCAP*, *0804*, 035. arXiv: 0803.1013

Guo, Z.-K., Piao, Y.-S., Cai, R.-G., & Zhang, Y.-Z. (2003a). Cosmological scaling solutions and cross coupling exponential potential. *Phys.Lett.*, *B576*, 12–17. arXiv: hep-th/0306245

Guo, Z.-K., Piao, Y.-S., Cai, R.-G., & Zhang, Y.-Z. (2003b). Inflationary attractor from tachyonic matter. *Phys.Rev.*, *D68*, 043508. arXiv: hep-ph/0304236

Guo, Z.-K., Piao, Y.-S., Zhang, X.-M., & Zhang, Y.-Z. (2005b). Cosmological evolution of a quintom model of dark energy. *Phys.Lett.*, *B608*, 177–182. arXiv: astro-ph/0410654

Guo, Z. K., Piao, Y.-S., & Zhang, Y.-Z. (2003c). Cosmological scaling solutions and multiple exponential potentials. *Phys.Lett.*, *B568*, 1–7. arXiv: hep-th/0304048

Guo, Z.-K., & Zhang, Y.-Z. (2004). Cosmological scaling solutions of the tachyon with multiple inverse square potentials. *JCAP*, *0408*, 010. arXiv: hep-th/0403151

Halliwell, J. (1987). Scalar Fields in Cosmology with an Exponential Potential. *Phys.Lett.*, *B185*, 341.

Hao, J.-g., & Li, X.-z. (2003a). An Attractor solution of phantom field. *Phys.Rev.*, *D67*, 107303. arXiv: gr-qc/0302100

Hao, J.-g., & Li, X.-z. (2003b). Constructing dark energy models with late time de Sitter attractor. *Phys.Rev.*, *D68*, 083514. arXiv: hep-th/0306033

Hao, J.-G., & Li, X.-z. (2004). Phantom cosmic dynamics: Tracking attractor and cosmic doomsday. *Phys.Rev.*, *D70*, 043529. arXiv: astro-ph/0309746

Hartman, P. (1982). *Ordinary differential equations*. Birkhauser.

Hartong, J., Ploegh, A., Van Riet, T., & Westra, D. B. (2006). Dynamics of generalized assisted inflation. *Class.Quant.Grav.*, *23*, 4593–4614. arXiv: gr-qc/0602077

Heard, I. P., & Wands, D. (2002). Cosmology with positive and negative exponential potentials. *Class.Quant.Grav.*, *19*, 5435–5448. arXiv: gr-qc/0206085

Hinshaw, G., et al. (2013). Nine-Year Wilkinson Microwave Anisotropy Probe (WMAP) Observations: Cosmological Parameter Results. *Astrophys.J.Suppl.*, *208*, 19. arXiv: 1212.5226

Hirsch, M. W., & Smale, S. (1974). *Differential equations, dynamical systems, and linear algebra*. Academic Press.

Holden, D. J., & Wands, D. (2000). Selfsimilar cosmological solutions with a nonminimally coupled scalar field. *Phys.Rev.*, *D61*, 043506. arXiv: gr-qc/9908026

Hossain, M. W., Myrzakulov, R., Sami, M., & Saridakis, E. N. (2014). Variable gravity: A suitable framework for quintessential inflation. arXiv: 1402.6661

Hrycyna, O., Kamionka, M., & Szydlowski, M. (2014). Dynamics and cosmological constraints on Brans-Dicke cosmology. arXiv: 1404.7112

Hrycyna, O., & Szydlowski, M. (2010). Uniting cosmological epochs through the twister solution in cosmology with non-minimal coupling. *JCAP*, *1012*, 016. arXiv: 1008.1432

Hrycyna, O., & Szydlowski, M. (2013a). Brans-Dicke theory and the emergence of ΛCDM model. *Phys.Rev.*, *D88*(6), 064018. arXiv: 1304.3300

Hrycyna, O., & Szydlowski, M. (2013b). Dynamical complexity of the Brans-Dicke cosmology. *JCAP*, *1312*, 016. arXiv: 1310.1961

Huey, G., & Tavakol, R. K. (2002). Robustness of the quintessence scenario in particle cosmologies. *Phys.Rev.*, *D65*, 043504. arXiv: astro-ph/0108517

Ishak, M., & Moldenhauer, J. (2009). A minimal set of invariants as a systematic approach to higher order gravity models. *JCAP*, *0901*, 024. arXiv: 0808.0951

Jarv, L., Kuusk, P., & Saal, M. (2010). Potential dominated scalar-tensor cosmologies in the general relativity limit: phase space view. *Phys.Rev.*, *D81*, 104007. arXiv: 1003.1686

Jarv, L., Mohaupt, T., & Saueressig, F. (2004). Quintessence cosmologies with a double exponential potential. *JCAP*, *0408*, 016. arXiv: hep-th/0403063

Kaeonikhom, C., Singleton, D., Sushkov, S. V., & Yongram, N. (2012). Dynamics of Dirac-Born-Infeld dark energy interacting with dark matter. *Phys.Rev.*, *D86*, 124049. arXiv: 1209.5219

Kamenshchik, A. Y., Moschella, U., & Pasquier, V. (2001). An Alternative to quintessence. *Phys.Lett.*, *B511*, 265–268. arXiv: gr-qc/0103004

Karthauser, J. L., & Saffin, P. (2006). Scaling solutions and geodesics in moduli space. *Class.Quant.Grav.*, *23*, 4615–4624. arXiv: hep-th/0604046

Khoury, J., & Weltman, A. (2004). Chameleon fields: Awaiting surprises for tests of gravity in space. *Phys.Rev.Lett.*, *93*, 171104. arXiv: astro-ph/0309300

Kim, E. J., & Kawai, S. (2013). Chaotic dynamics of the Bianchi IX universe in Gauss-Bonnet gravity. *Phys.Rev.*, *D87*(8), 083517. arXiv: 1301.6853

Kim, S. A., Liddle, A. R., & Tsujikawa, S. (2005). Dynamics of assisted quintessence. *Phys.Rev.*, *D72*, 043506. arXiv: astro-ph/0506076

Kiselev, V. (2008). Scaling attractors for quintessence in flat universe with cosmological term. *JCAP*, *0801*, 019. arXiv: gr-qc/0611064

Koivisto, T., & Mota, D. F. (2008). Vector Field Models of Inflation and Dark Energy. *JCAP*, *0808*, 021. arXiv: 0805.4229

Koivisto, T. S. (2010). Cosmology of modified (but second order) gravity. *AIP Conf.Proc.*, *1206*, 79–96. arXiv: 0910.4097

Koivisto, T. S., & Nunes, N. J. (2009). Inflation and dark energy from three-forms. *Phys.Rev.*, *D80*, 103509. arXiv: 0908.0920

Kolitch, S. J. (1996). Qualitative analysis of Brans-Dicke universes with a cosmological constant. *Annals Phys.*, *246*, 121–132. arXiv: gr-qc/9409002

Lazkoz, R., & Leon, G. (2006). Quintom cosmologies admitting either tracking or phantom attractors. *Phys.Lett.*, *B638*, 303–309. arXiv: astro-ph/0602590

Lazkoz, R., Leon, G., & Quiros, I. (2007). Quintom cosmologies with arbitrary potentials. *Phys.Lett.*, *B649*, 103–110. arXiv: astro-ph/0701353

Leach, J. A., Carloni, S., & Dunsby, P. K. (2006). Shear dynamics in Bianchi I cosmologies with R**n-gravity. *Class.Quant.Grav.*, *23*, 4915–4937. arXiv: gr-qc/0603012

Lefschetz, S. (1957). *Differential equations: geometric theory*. John Wiley and Sons.

Leon, G. (2009). On the Past Asymptotic Dynamics of Non-minimally Coupled Dark Energy. *Class.Quant.Grav.*, *26*, 035008. arXiv: 0812.1013

Leon, G., Cardenas, R., & Morales, J. L. (2008). Equilibrium sets in quintom cosmologies: the past asymptotic dynamics. arXiv: 0812.0830

Leon, G., Leyva, Y., Saridakis, E. N., Martin, O., & Cardenas, R. (2009). Falsifying Field-based Dark Energy Models. arXiv: 0912.0542

Leon, G., Leyva, Y., & Socorro, J. (2014). Quintom phase-space: beyond the exponential potential. *Phys.Lett.*, *B732*, 285–297. arXiv: 1208.0061

Leon, G., & Roque, A. A. (2014). Qualitative analysis of Kantowski-Sachs metric in a generic class of $f(R)$ models. *JCAP*, *1405*, 032. arXiv: 1308.5921

Leon, G., & Saridakis, E. N. (2010). Phantom dark energy with varying-mass dark matter particles: acceleration and cosmic coincidence problem. *Phys.Lett.*, *B693*, 1–10. arXiv: 0904.1577

Leon, G., & Saridakis, E. N. (2011). Dynamics of the anisotropic Kantowsky-Sachs geometries in R^n gravity. *Class.Quant.Grav.*, *28*, 065008. arXiv: 1007.3956

Leon, G., & Saridakis, E. N. (2013). Dynamical analysis of generalized Galileon cosmology. *JCAP*, *1303*, 025. arXiv: 1211.3088

Leon, G., Silveira, P., & Fadragas, C. R. (2010). Phase-space of flat Friedmann-Robertson-Walker models with both a scalar field coupled to matter and radiation. arXiv: 1009.0689

Li, B., & Barrow, J. D. (2007). The Cosmology of $f(R)$ gravity in metric variational approach. *Phys.Rev.*, *D75*, 084010. arXiv: gr-qc/0701111

Li, J.-L., & Wu, J.-P. (2010). Dynamics of tachyon field in spatially curved FRW universe. *Phys.Lett.*, *B686*, 221–226. arXiv: 1003.1870

Li, M., Li, X.-D., Wang, S., & Wang, Y. (2011). Dark Energy. *Communications in Theoretical Physics*, *56*, 525–604. arXiv: 1103.5870

Li, S., & Ma, Y. (2010). Dark Energy Interacting with Dark Matter in Classical Einstein and Loop Quantum Cosmology. *Eur.Phys.J.*, *C68*, 227–239. arXiv: 1004.4350

Li, S., Ma, Y., & Chen, Y. (2009). Dynamical Evolution of Interacting Modified Chaplygin Gas. *Int.J.Mod.Phys.*, *D18*, 1785–1800. arXiv: 0809.0617

Li, X.-z., & Hao, J.-g. (2004). Phantom field with o(n) symmetry in an exponential potential. *Phys.Rev.*, *D69*, 107303. arXiv: hep-th/0303093

Li, X.-Z., Zhao, Y.-B., & Sun, C.-B. (2005). Heteroclinic orbit and tracking attractor in cosmological model with a double exponential potential. *Class.Quant.Grav.*, *22*, 3759–3766. arXiv: astro-ph/0508019

Li, Y.-H., Zhang, J.-F., & Zhang, X. (2014). Exploring the full parameter space for an interacting dark energy model with recent observations including redshift-space distortions: application of the parametrized post-Friedmann approach. arXiv: 1409.7205

Liddle, A. R., Mazumdar, A., & Schunck, F. E. (1998). Assisted inflation. *Phys.Rev.*, *D58*, 061301. arXiv: astro-ph/9804177

Liddle, A. R., & Scherrer, R. J. (1999). A Classification of scalar field potentials with cosmological scaling solutions. *Phys.Rev.*, *D59*, 023509. arXiv: astro-ph/9809272

Linde, A. D. (1990). Particle physics and inflationary cosmology. *Contemp.Concepts Phys.*, *5*, 1–362. arXiv: hep-th/0503203

Liu, D.-J., & Li, X.-Z. (2005). Dynamics of quintessence with thermal interactions. *Phys.Lett.*, *B611*, 8–14. arXiv: astro-ph/0501596

Liu, X.-M., Zhai, Z.-X., Xiao, K., & Liu, W.-B. (2012). The accelerated scaling attractor solution of the interacting agegraphic dark energy in Brans-Dicke theory. *Eur.Phys.J.*, *C72*, 2057. arXiv: 1206.1911

Lopez Honorez, L., Mena, O., & Panotopoulos, G. (2010). Higher-order coupled quintessence. *Phys.Rev.*, *D82*, 123525. arXiv: 1009.5263

Lynch, S. (2007). *Dynamical systems with applications using Mathematica*. Birkhauser.

Maeda, K.-i., & Fujii, Y. (2009). Attractor Universe in the Scalar-Tensor Theory of Gravitation. *Phys.Rev.*, *D79*, 084026. arXiv: 0902.1221

Malik, K. A., & Wands, D. (1999). Dynamics of assisted inflation. *Phys.Rev.*, *D59*, 123501. arXiv: astro-ph/9812204

Malquarti, M., Copeland, E. J., & Liddle, A. R. (2003a). K-essence and the coincidence problem. *Phys.Rev.*, *D68*, 023512. arXiv: astro-ph/0304277

Malquarti, M., Copeland, E. J., Liddle, A. R., & Trodden, M. (2003b). A New view of k-essence. *Phys.Rev.*, *D67*, 123503. arXiv: astro-ph/0302279

Marsh, D. J., Tarrant, E. R., Copeland, E. J., & Ferreira, P. G. (2012). Cosmology of Axions and Moduli: A Dynamical Systems Approach. *Phys.Rev.*, *D86*, 023508. arXiv: 1204.3632

Martin, J. (2012). Everything You Always Wanted To Know About The Cosmological Constant Problem (But Were Afraid To Ask). *Comptes Rendus Physique*, *13*, 566–665. arXiv: 1205.3365

Matos, T., Luevano, J.-R., Quiros, I., Urena-Lopez, L. A., & Vazquez, J. A. (2009). Dynamics of Scalar Field Dark Matter With a Cosh-like Potential. *Phys.Rev.*, *D80*, 123521. arXiv: 0906.0396

Mazumdar, A., Panda, S., & Perez-Lorenzana, A. (2001). Assisted inflation via tachyon condensation. *Nucl.Phys.*, *B614*, 101–116. arXiv: hep-ph/0107058

Mimoso, J. P., Nunes, A., & Pavon, D. (2006). Asymptotic behavior of the warm inflation scenario with viscous pressure. *Phys.Rev.*, *D73*, 023502. arXiv: gr-qc/0512057

Miritzis, J. (2003a). Dynamical system approach to FRW models in higher order gravity theories. *J.Math.Phys.*, *44*, 3900–3910. arXiv: gr-qc/0305062

Miritzis, J. (2003b). Scalar field cosmologies with an arbitrary potential. *Class.Quant.Grav.*, *20*, 2981–2990. arXiv: gr-qc/0303014

Morris, S. C. F., Green, A. M., Padilla, A., & Tarrant, E. R. M. (2013). Cosmological effects of coupled dark matter. *Phys.Rev.*, *D88*, 083522. arXiv: 1304.2196

Mukhanov, V. (2005). *Physical fundations of cosmology*. Cambridge University Press.

Ng, S., Nunes, N., & Rosati, F. (2001). Applications of scalar attractor solutions to cosmology. *Phys.Rev.*, *D64*, 083510. arXiv: astro-ph/0107321

Ng, S. C., & Wiltshire, D. L. (2001). Properties of cosmologies with dynamical pseudo Nambu-Goldstone bosons. *Phys.Rev.*, *D63*, 023503. arXiv: astro-ph/0004138

Ngampitipan, T., & Wongjun, P. (2011). Dynamics of three-form dark energy with dark matter couplings. *JCAP*, *1111*, 036. arXiv: 1108.0140

Nojiri, S., Odintsov, S. D., & Tsujikawa, S. (2005). Properties of singularities in (phantom) dark energy universe. *Phys.Rev.*, *D71*, 063004. arXiv: hep-th/0501025

Nunes, A., & Mimoso, J. P. (2000). On the potentials yielding cosmological scaling solutions. *Phys.Lett.*, *B488*, 423–427. arXiv: gr-qc/0008003

Ohashi, J., & Tsujikawa, S. (2009). Assisted dark energy. *Phys.Rev.*, *D80*, 103513. arXiv: 0909.3924

Olivares, G., Atrio-Barandela, F., & Pavon, D. (2008). Dynamics of Interacting Quintessence Models: Observational Constraints. *Phys.Rev.*, *D77*, 063513. arXiv: 0706.3860

Padmanabhan, T. (2002). Accelerated expansion of the universe driven by tachyonic matter. *Phys.Rev.*, *D66*, 021301. arXiv: hep-th/0204150

Padmanabhan, T., & Choudhury, T. R. (2002). Can the clustered dark matter and the smooth dark energy arise from the same scalar field? *Phys.Rev.*, *D66*, 081301. arXiv: hep-th/0205055

Peebles, P., & Ratra, B. (1988). Cosmology with a Time Variable Cosmological Constant. *Astrophys.J.*, *325*, L17.

Pereira, S., Pinho S.S., A., & Hoff da Silva, J. M. (2014). Some remarks on the attractor behaviour in ELKO cosmology. arXiv: 1402.6723

Perez, J., Fzfa, A., Carletti, T., Mlot, L., & Guedezounme, L. (2013). The Jungle Universe. arXiv: 1306.1037

Perko, L. (2001). *Differential equations and dynamical systems*. Springer-Verlag, 3rd ed.

Perlmutter, S., et al. (1999). Measurements of Omega and Lambda from 42 high redshift supernovae. *Astrophys.J.*, *517*, 565–586. arXiv: astro-ph/9812133

Piazza, F., & Tsujikawa, S. (2004). Dilatonic ghost condensate as dark energy. *JCAP*, *0407*, 004. arXiv: hep-th/0405054

Quartin, M., Calvao, M. O., Joras, S. E., Reis, R. R., & Waga, I. (2008). Dark Interactions and Cosmological Fine-Tuning. *JCAP*, *0805*, 007. arXiv: 0802.0546

Quercellini, C., Bruni, M., Balbi, A., & Pietrobon, D. (2008). Late universe dynamics with scale-independent linear couplings in the dark sector. *Phys.Rev.*, *D78*, 063527. arXiv: 0803.1976

Quiros, I., Gonzalez, T., Gonzalez, D., & Napoles, Y. (2010). Study Of Tachyon Dynamics For Broad Classes of Potentials. *Class.Quant.Grav.*, *27*, 215021. arXiv: 0906.2617

Ratra, B., & Peebles, P. (1988). Cosmological Consequences of a Rolling Homogeneous Scalar Field. *Phys.Rev.*, *D37*, 3406.

Ribas, M., Devecchi, F., & Kremer, G. (2005). Fermions as sources of accelerated regimes in cosmology. *Phys.Rev.*, *D72*, 123502. arXiv: gr-qc/0511099

Riess, A. G., et al. (1998). Observational evidence from supernovae for an accelerating universe and a cosmological constant. *Astron.J.*, *116*, 1009–1038. arXiv: astro-ph/9805201

Riotto, A. (2002). Inflation and the theory of cosmological perturbations. *Astroparticle physics and cosmology. Proceedings: Summer School, Trieste, Italy, Jun 17-Jul 5 2002*, (pp. 317–413). arXiv: hep-ph/0210162

Roy, N., & Banerjee, N. (2014a). Quintessence Scalar Field: A Dynamical Systems Study. arXiv: 1402.6821

Roy, N., & Banerjee, N. (2014b). Tracking quintessence: a dynamical systems study. *Gen.Rel.Grav.*, *46*, 1651. arXiv: 1312.2670

Sadjadi, H. M. (2012). On coincidence problem and attractor solutions in ELKO dark energy model. *Gen.Rel.Grav.*, *44*, 2329–2336. arXiv: 1109.1961

Saridakis, E. N., & Weller, J. M. (2010). A Quintom scenario with mixed kinetic terms. *Phys.Rev.*, *D81*, 123523. arXiv: 0912.5304

Sawicki, I., & Hu, W. (2007). Stability of Cosmological Solution in $f(R)$ Models of Gravity. *Phys.Rev.*, *D75*, 127502. arXiv: astro-ph/0702278

Scherrer, R. J., & Sen, A. (2008). Thawing quintessence with a nearly flat potential. *Phys.Rev.*, *D77*, 083515. arXiv: 0712.3450

Schutz, B. F. (1985). *A first course in general relativity*. Cambridge University Press.

Sen, A. (2002a). Field theory of tachyon matter. *Mod.Phys.Lett.*, *A17*, 1797–1804. arXiv: hep-th/0204143

Sen, A. (2002b). Rolling tachyon. *JHEP*, *0204*, 048. arXiv: hep-th/0203211

Sen, A. (2002c). Tachyon matter. *JHEP*, *0207*, 065. arXiv: hep-th/0203265

Setare, M., & Saridakis, E. (2008). Quintom model with O(N) symmetry. *JCAP*, *0809*, 026. arXiv: 0809.0114

Setare, M., & Saridakis, E. (2009). Quintom Cosmology with General Potentials. *Int.J.Mod.Phys.*, *D18*, 549–557. arXiv: 0807.3807

Shi, S.-G., Piao, Y.-S., & Qiao, C.-F. (2009). Cosmological Evolution of a Tachyon-Quintom Model of Dark Energy. *JCAP*, *0904*, 027. arXiv: 0812.4022

Silverstein, E., & Tong, D. (2004). Scalar speed limits and cosmology: Acceleration from D-cceleration. *Phys.Rev.*, *D70*, 103505. arXiv: hep-th/0310221

Skugoreva, M. A., Toporensky, A. V., & Vernov, S. Y. (2014). Global stability analysis for cosmological models with non-minimally coupled scalar fields. arXiv: 1404.6226

Sotiriou, T. P., & Faraoni, V. (2010). $f(R)$ Theories Of Gravity. *Rev.Mod.Phys.*, *82*, 451–497. arXiv: 0805.1726

Steinhardt, P. J., Wang, L.-M., & Zlatev, I. (1999). Cosmological tracking solutions. *Phys.Rev.*, *D59*, 123504. arXiv: astro-ph/9812313

Szydlowski, M., & Hrycyna, O. (2009). Scalar field cosmology in the energy phase-space – unified description of dynamics. *JCAP*, *0901*, 039. arXiv: 0811.1493

Szydlowski, M., Hrycyna, O., & Stachowski, A. (2014). Scalar field cosmology - geometry of dynamics. *Int.J.Geom.Meth.Mod.Phys.*, *11*, 1460012. arXiv: 1308.4069

Tamanini, N. (2014). Dynamics of cosmological scalar fields. *Phys.Rev.*, *D89*, 083521. arXiv: 1401.6339

Tamanini, N., & Boehmer, C. G. (2013). Generalized hybrid metric-Palatini gravity. *Phys.Rev.*, *D87*(8), 084031. arXiv: 1302.2355

Tocchini-Valentini, D., & Amendola, L. (2002). Stationary dark energy with a baryon dominated era: Solving the coincidence problem with a linear coupling. *Phys.Rev.*, *D65*, 063508. arXiv: astro-ph/0108143

Tsujikawa, S. (2006). General analytic formulae for attractor solutions of scalar-field dark energy models and their multi-field generalizations. *Phys.Rev.*, *D73*, 103504. arXiv: hep-th/0601178

Tsujikawa, S., & Sami, M. (2004). A Unified approach to scaling solutions in a general cosmological background. *Phys.Lett.*, *B603*, 113–123. arXiv: hep-th/0409212

Tsujikawa, S., & Sami, M. (2007). String-inspired cosmology: Late time transition from scaling matter era to dark energy universe caused by a Gauss-Bonnet coupling. *JCAP*, *0701*, 006. arXiv: hep-th/0608178

Tzanni, K., & Miritzis, J. (2014). Coupled quintessence with double exponential potentials. arXiv: 1403.6618

Uddin, K., Lidsey, J. E., & Tavakol, R. (2009). Cosmological scaling solutions in generalised Gauss-Bonnet gravity theories. *Gen.Rel.Grav.*, *41*, 2725–2736. arXiv: 0903.0270

Urena-Lopez, L. A. (2005). Scalar phantom energy as a cosmological dynamical system. *JCAP*, *0509*, 013. arXiv: astro-ph/0507350

Urena-Lopez, L. A. (2012). Unified description of the dynamics of quintessential scalar fields. *JCAP*, *1203*, 035. arXiv: 1108.4712

Urena-Lopez, L. A., & Reyes-Ibarra, M. J. (2009). On the dynamics of a quadratic scalar field potential. *Int.J.Mod.Phys.*, *D18*, 621–634. arXiv: 0709.3996

Uzan, J.-P. (1999). Cosmological scaling solutions of nonminimally coupled scalar fields. *Phys.Rev.*, *D59*, 123510. arXiv: gr-qc/9903004

van de Bruck, C., & Weller, J. M. (2009). Quintessence dynamics with two scalar fields and mixed kinetic terms. *Phys.Rev.*, *D80*, 123014. arXiv: 0910.1934

van den Hoogen, R., & Filion, L. (2000). Stability analysis of multiple scalar field cosmologies with matter. *Class.Quant.Grav.*, *17*, 1815–1825.

Wainwright, J., & Ellis, G. F. R. (1997). *Dynamical systems in cosmology*. Cambridge University Press.

Wald, R. (1983). *General relativity*. The University of Chicago Press.

Wands, D., Copeland, E. J., & Liddle, A. R. (1993). Exponential Potentials, Scaling Solutions, and Inflation. *688*, 647.

Wang, L.-M., Caldwell, R., Ostriker, J., & Steinhardt, P. J. (2000). Cosmic concordance and quintessence. *Astrophys.J.*, *530*, 17–35. arXiv: astro-ph/9901388

Wang, Y., Wands, D., Zhao, G.-B., & Xu, L. (2014). Post-*Planck* constraints on interacting vacuum energy. *Phys.Rev.*, *D90*, 023502. arXiv: 1404.5706

Wei, H. (2011a). Cosmological Evolution of Quintessence and Phantom with a New Type of Interaction in Dark Sector. *Nucl.Phys.*, *B845*, 381–392. arXiv: 1008.4968

Wei, H. (2011b). Spinor Dark Energy and Cosmological Coincidence Problem. *Phys.Lett.*, *B695*, 307–311. arXiv: 1002.4230

Wei, H., & Cai, R.-G. (2005). Cosmological evolution of hessence dark energy and avoidance of big rip. *Phys.Rev.*, *D72*, 123507. arXiv: astro-ph/0509328

Wei, H., & Cai, R.-G. (2006). Interacting vector-like dark energy, the first and second cosmological coincidence problems. *Phys.Rev.*, *D73*, 083002. arXiv: astro-ph/0603052

Wei, H., & Cai, R.-G. (2007). Cheng-Weyl Vector Field and its Cosmological Application. *JCAP*, *0709*, 015. arXiv: astro-ph/0607064

Weinberg, S. (1972). *Gravitation and cosmology*. John Wiley and Sons.

Weinberg, S. (1989). The Cosmological Constant Problem. *Rev.Mod.Phys.*, *61*, 1–23.

Weinberg, S. (2000). The Cosmological constant problems. *Sources and detection of dark matter and dark energy in the universe. Proceedings, 4th International Symposium, DM 2000, Marina del Rey, USA, February 23-25, 2000*, (pp. 18–26). arXiv: astro-ph/0005265

Weinberg, S. (2008). *Cosmology*. Oxford University Press.

Wetterich, C. (1995). The Cosmon model for an asymptotically vanishing time dependent cosmological 'constant'. *Astron.Astrophys.*, *301*, 321–328. arXiv: hep-th/9408025

Wiggins, S. (1990). *Introduction to applied nonlinear dynamical systems and chaos*. Springer-Verlag.

Will, C. M. (2014). The Confrontation between General Relativity and Experiment. *Living Rev.Rel.*, *17*, 4. arXiv: 1403.7377

Wu, P., & Yu, H. W. (2007). Interacting generalized Chaplygin gas. *Class.Quant.Grav.*, *24*, 4661–4668.

Yang, R.-J., & Xiang-Ting, G. (2011). Phase-space analysis of a class of k-essence cosmology. *Class.Quant.Grav.*, *28*, 065012. arXiv: 1006.4986

Yang, W., & Xu, L. (2014). Testing coupled dark energy with large scale structure observation. *JCAP*, *1408*, 034. arXiv: 1401.5177

Zhai, X.-h., & Zhao, Y.-b. (2006). Dynamics of quintessential inflation. *Chin.Phys.*, *15*, 2465. arXiv: astro-ph/0511512

Zhang, X.-F., Li, H., Piao, Y.-S., & Zhang, X.-M. (2006). Two-field models of dark energy with equation of state across -1. *Mod.Phys.Lett.*, *A21*, 231–242. arXiv: astro-ph/0501652

Zhang, Y., Xia, T., & Zhao, W. (2007). Yang-Mills condensate dark energy coupled with matter and radiation. *Class.Quant.Grav.*, *24*, 3309–3338. arXiv: gr-qc/0609115

Zhao, W. (2009). Attractor Solution in Coupled Yang-Mills Field Dark Energy Models. *International Journal of Modern Physics D*, *18*, 1331–1342. arXiv: 0810.5506

Zhou, S.-Y. (2008). A New Approach to Quintessence and Solution of Multiple Attractors. *Phys.Lett.*, *B660*, 7–12. arXiv: 0705.1577

Zlatev, I., Wang, L.-M., & Steinhardt, P. J. (1999). Quintessence, cosmic coincidence, and the cosmological constant. *Phys.Rev.Lett.*, *82*, 896–899. arXiv: astro-ph/9807002